LOS ANGELES PUBLIC LIBRARY
JUN 20 1956
SCIENCE AND TECHNOLOGY

JET PROPULSION

Journal of the
AMERICAN ROCKET SOCIETY
Rocketry . . . . Jet Propulsion Sciences . . . . Astron

VOLUME 26 JUNE 1956 NUMBER 6

Generalized Theory of the Optimum Thrust Programming for the Level Flight of a Rocket-Powered Aircraft . . . . . *Placido Cicala and Angelo Miele* 443

A Mechanism for High-Frequency Oscillation in Ramjet Combustors and Afterburners . . . . . *Don E. Rogers and Frank E. Marble* 456

On the Motion of a Missile Under Water . . . . . *Walter P. Reid* 463

Optimalizing Control in the Presence of Noise Interference . . . *Sedat Serdengecti* 465

Ground Handling and Launching Procedures for an Alcohol-Oxygen Rocket Missile . . . . . *T. M. Pettey, Jr.* 474

Combustion in Turbulent Flow, *Proceedings of a Symposium at the Applied Physics Laboratory* 480

Technical Notes

Instrumenting Unmanned Satellites . . . . . *H. E. Lagow* 496

Methods of Calculating the Equilibrium Laminar Heat Transfer Rate at Hypersonic Flight Speeds . . . . . *Ronald F. Probstein* 497

Flame Generated Turbulence . . . . . *W. Paul Jensen* 499

Hazards Associated With 90 Per Cent Hydrogen Peroxide Aerosols . . . . . *Charles L. Punte, Leon Z. Saunders, and Eugene H. Krackow* 500

Study of Premixed Flames Using Radioactive Tracers . . . . . *Vadim Kopytoff, Carlos G. Bell, and Ali Bulent Cambel* 501



Bell X-2 rocket-powered supersonic aircraft designed to investigate high speed heating

Jet Propulsion News 505

ARS News 509

New Patents 517

New Equipment and Processes . . 518

Book Reviews 526

Technical Literature Digest . . . 530



for Pushbutton Marksmen

Realistic targets for today's advanced weapons systems must be as fleet and maneuverable as the potential opponents they simulate. Small, speedy, remotely controlled drones can give pilots and gunnery crews the combat training they require.

Powerplants to propel drones at transonic and supersonic speeds represent another important area for the application of the advanced technology resulting from *RMI POWER ENGINEERING.*

Rocket power to drive missiles and piloted aircraft higher and faster has been the prime product of RMI since its inception 15 years ago. Today, as the oldest company in the rocket engine field, Reaction Motors has a wealth of experience gained in the design and production of engines for record-holding vehicles of both types.

Engineers and Scientists: creative and rewarding opportunities exist for all types of technical specialists in the research, development and production of rocket power devices. Send complete resume and salary requirements to employment manager.

PRIMARY AND AUXILIARY ROCKET POWER FOR: Missile Boosters and Sustainers, Aircraft, Target Drones, Ordnance Rockets, Ejection Systems, Launching Devices.

Power for Progress

RMI

REACTION MOTORS, INC.

A MEMBER OF THE OMAR TEAM

DENVILLE, NEW JERSEY

Scope of JET PROPULSION

JET PROPULSION, the Journal of the American Rocket Society, is devoted to the advancement of the field of jet propulsion through the publication of original papers disclosing new knowledge and new developments. The term "jet propulsion" as used herein is understood to embrace all engines that develop thrust by rearward discharge of a jet through a nozzle or duct; and thus it includes systems utilizing atmospheric air and underwater systems, as well as rocket engines. JET PROPULSION is open to contributions, either fundamental or applied, dealing with specialized aspects of jet and rocket propulsion, such as fuels and propellants, combustion, heat transfer, high temperature materials, mechanical design analyses, flight mechanics of jet-propelled vehicles, astronautics, and so forth. JET PROPULSION endeavors, also, to keep its subscribers informed of the affairs of the Society and of outstanding events in the rocket and jet propulsion field.

Limitation of Responsibility

Statements and opinions expressed in JET PROPULSION are to be understood as the individual expressions of the authors and do not necessarily reflect the views of the Editors or the Society.

Subscription Rates

One year (twelve monthly issues)	$12.50
Foreign countries, additional postage	add .50
Single copies	1.25
Special issues, single copies	2.50
Back numbers	2.00

Change of Address

Notices of change of address should be sent to the Secretary of the Society at least 30 days prior to the date of publication.

Information for Authors

Preparation of Manuscripts

Manuscripts must be double spaced on one side of paper only with wide margins to allow for instructions to printer. Submit two copies: original and first carbon. Include a 100–200 word abstract of paper. The title of the paper should be brief to simplify indexing. The author's name should be given without title, degree, or honor. A footnote on the first page should indicate the author's position and affiliation. Include only essential illustrations, tables, and mathematics. References should be grouped at the end of the manuscript; footnotes are reserved for comments on the text. Use American Standard symbols and abbreviations published by the American Standards Association. Greek letters should be identified clearly for the printer. References should be given as follows: For Journal Articles: Authors, Title, Journal, Volume, Year, Page Numbers. For Books: Author, Title, Publisher, City, Edition, Year, Page Numbers. Line drawings must be made with India ink on white paper or tracing cloth. Lettering on drawings should be large enough to permit reduction to standard one-column width, except for unusually complex drawings where such reduction would be prohibitive. Photographs should be clear, glossy prints. Legends must accompany each illustration submitted and should be listed in order on a separate sheet of paper.

Security Clearance

Manuscripts must be accompanied by written assurance as to security clearance in the event the subject matter of the manuscript is considered to lie in a classified area. Alternatively, written assurance that clearance is unnecessary should be submitted. Full responsibility for obtaining authoritative clearance rests with the author.

Submission of Manuscripts

Manuscripts should be submitted in duplicate to the Editor-in-Chief, Martin Summerfield, Professor of Aeronautical Engineering, Princeton University, Princeton, N. J.

Manuscripts Presented at ARS Meetings

A manuscript submitted to the ARS Program Chairman and accepted for presentation at a national meeting will automatically be referred to the Editors for consideration for publication in JET PROPULSION, unless a contrary request is made by the author.

To Order Reprints

Prices for reprints will be sent to the author with the galley proof, and orders should accompany the corrected galley when it is returned to the Assistant Editor.

JET PROPULSION

Journal of the
AMERICAN ROCKET SOCIETY

EDITOR-IN-CHIEF
MARTIN SUMMERFIELD
Princeton University

ASSISTANT EDITOR
H. K. WILGUS

ART EDITOR
N. KOCHANSKY

ASSOCIATE EDITORS
ALI BULENT CAMBEL
Northwestern University
IRVIN GLASSMAN
Princeton University
M. H. SMITH
Princeton University
A. J. ZAEHRINGER
American Rocket Company

CONTRIBUTORS
NORMAN L. BAKER
Indiana Technical College
MARSHALL FISHER
Princeton University
G. F. McLAUGHLIN
K. R. STEHLING
Naval Research Laboratory

EDITORIAL BOARD
D. ALTMAN
California Institute of Technology
L. CROCCO
Princeton University
P. DUWEZ
California Institute of Technology
R. D. GECKLER
Aerojet-General Corporation
C. A. CONGWER
Aerojet-General Corporation
C. A. MEYER
Westinghouse Electric Corporation
P. F. WINTERNITZ
New York University
K. WOHL
University of Delaware
M. J. ZUCROW
Purdue University

ADVISORS ON PUBLICATION POLICY
L. G. DUNN
Ramo-Wooldridge Corporation
Los Angeles, California
R. G. FOLSOM
Director, Engineering Research Institute
University of Michigan
R. E. GIBSON
Director, Applied Physics Laboratory
Johns Hopkins University
H. F. GUGGENHEIM
President, The Daniel and Florence Guggenheim Foundation
R. P. KROON
Director of Research, AGT Div.
Westinghouse Electric Corporation
ABE SILVERSTEIN
Associate Director, Lewis Laboratory
National Advisory Committee for Aeronautics
T. VON KÁRMÁN
Chairman, Advisory Group for Aeronautical Research and Development, NATO
W. E. ZISCH
Vice-President and General Manager
Aerojet-General Corporation

OFFICERS

President	Noah S. Davis
Vice-President	Robert C. Truax
Executive Secretary	James J. Harford
Secretary	A. C. Slade
Treasurer	Robert M. Lawrence
General Counsel	Andrew G. Haley

BOARD OF DIRECTORS
Terms expiring on dates indicated

J. B. Cowen, 1956	Milton W. Rosen, 1957
Andrew G. Haley, 1957	H. S. Seifert, 1958
S. K. Hoffman, 1958	K. R. Stehling, 1958
H. W. Ritchey, 1956	George P. Sutton, 1956

Wernher von Braun, 1957

Advertising Representatives

EMERY-HARFORD
155 East 42 St., New York, N. Y.
Telephone: Mu 4-7232

J. C. GALLOWAY & J. W. HARBISON
6535 Wilshire Blvd., Los Angeles, Calif.
Telephone: Olive 3-3223

JIM SUMMERS
400 N. Michigan Ave.
Chicago, Ill.
Telephone: Su 7-1641

R. F. PICKRELL AND ASSOCIATES
318 Stephenson Bldg.
Detroit, Mich.
Telephone: Trinity 1-0790

HAROLD SHORT
Holt Rd., Andover, Mass.
Telephone: Andover 2212

JET PROPULSION, the Journal of the American Rocket Society, published monthly by the American Rocket Society at 20th and Northampton Streets, Easton, Pa., U.S.A. The Editorial Office is located at 500 5th Ave., New York 36, N. Y. Price $1.25 per copy, $12.50 per year: Entered as second-class matter at the Post Office at Easton, Pa., under the Act of March 3, 1879.

© Copyright, 1956, by the American Rocket Society, Inc. Permission for reprinting may be obtained by written application to the Assistant Editor.

NIAFRAX nozzles last the full burning time... *without cooling*

Even under extreme temperatures, heat shock and erosion, these NIAFRAX® silicon-nitride-bonded silicon carbide refractories stand up for the full burning time. In fact, NIAFRAX nozzles and liners in some motors will last *through numerous firings* when used in place of regeneratively cooled alloy nozzles. They are equally adaptable to liquid and solid propellant motors.

NIAFRAX parts are available in intricate shapes ranging from ½" to more than 30" in diameter and can be produced to extremely close tolerances. For details write Department T-26, Refractories Division, The Carborundum Company, Perth Amboy, New Jersey.

CARBORUNDUM

Registered Trade Mark



A section of the Nike guided missile system. Western Electric Co., Prime Contractor.

★ **AIRCRAFT PUMPS**

Precision-built to rigid government specifications, a broad selection among Eastern pumps offers flexibility to your choice. Modifications can be made, or custom-made units designed to suit your project. Trim in size, light in weight, Eastern Aircraft Pumps give reliable long-term service.





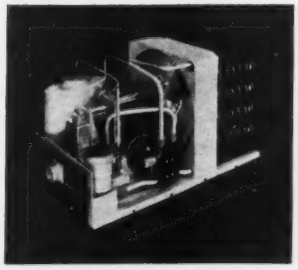
PRESSURIZATION

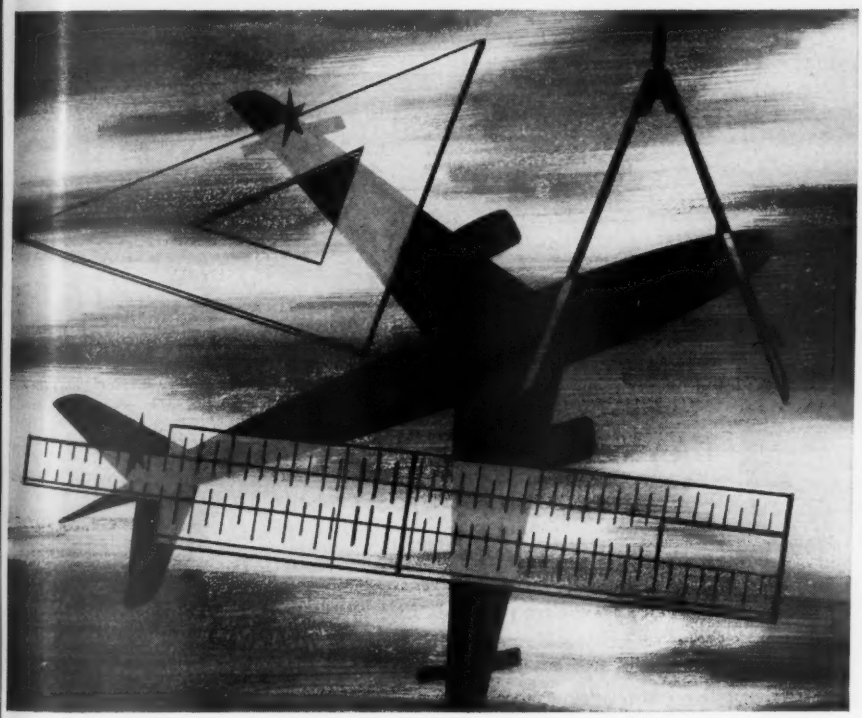
Eastern pressurization units for airborne electronic equipment are available in many capacities to handle a broad range of requirements. Units consist of an air pump and motor assembly, pressure switch, check valve, tank valve, and terminal connectors. They meet government specifications and can be modified to your needs.

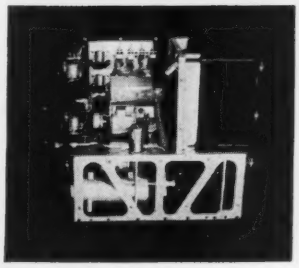


eliminate the "BUGS"

with Eastern aviation products







★ **COOLING UNITS**

Hold temperatures to safe operating limits in liquid cooled electronic tubes or similiar devices. By virtue of long experience and using standard component parts, Eastern can suit your specific needs at a minimum cost for equipment.

★ **REFRIGERATION-TYPE**

Enable specified components to be held to fairly constant temperatures by use of various types of refrigeration units. Because of the variation in methods possible, Eastern units fill every requirement where the use of a refrigeration cycle is called for.

★ *SPECIAL UNITS*

Eastern's continual research and development program keeps pace with the growing aviation industry. As new problems occur with progress in aircraft development, Eastern units are constantly developed to fill their function as planes fly higher, or faster, or with greater load capacity.

Eastern welcomes the chance to help engineers "take out the bugs" with equipment that cools, pressurizes, or pumps. From the extensive line of existing units, new adaptations, or custom-made designs, Eastern is ready to meet every challenge for equipment that handles your needs *the best today . . . better tomorrow.*

Eastern

EASTERN AVIATION PRODUCTS

INDUSTRIES, INC.

100 SKIFF ST.
HAMDEN 14, CONN.

Write for Aviation Products Catalog, Bulletin 330.

ENGINEERS...LOOK TEN YEARS AHEAD!



A Douglas engineer lives here

Will your income and location allow you to live in a home like this...spend your leisure time like this?

They can...if you start your Douglas career now!

Your objectives are probably high professional standing, good income, good security and good living. All four can be achieved at Douglas.

Douglas has the reputation of being an "engineer's outfit," with the three top administrative posts being held by engineers. Maybe that's why it's the biggest, most successful unit in its field. Certainly it offers the engineer unexcelled opportunities in the specialty of *his* choice ...be it related to missiles or commercial or military aircraft.

You've looked around. Now look ahead... and contact Douglas.

For further information about opportunities with Douglas in Santa Monica, El Segundo and Long Beach, California and Tulsa, Oklahoma, write today to:

DOUGLAS AIRCRAFT COMPANY, INC.
C. C. LaVene, 3000 Ocean Park Boulevard, Santa Monica, California

DOUGLAS



First in Aviation

NEW MUSCLES FOR SKY GIANTS



with "Tailor-Made" Propellants

by Olin

The Olin Explosives Division's leadership in both double-base and composite propellant technology offers designers and engineers "tailor-made" solid rocket power plants. Given your requirements for thrust and duration, an optimization of performance characteristics is made possible through selection from a wide spectrum of propellants.

Where requirements dictate the discovery and utilization of new propellants, Olin's complete laboratories and testing facilities give developmental projects every expectancy of early success. So why not call Olin the next time a problem can possibly be solved by up to date technology in the solid propellant propulsion field. A capable group of explosives and propellant specialists is ready to help.

Employment Inquiries Are Invited From Qualified Engineers And Scientists.

OLIN SOLID PROPELLANTS AND EXPLOSIVE PRODUCTS ARE READY FOR USE IN THE FOLLOWING APPLICATIONS

- Missile Propulsion Units, Boosters, Retarding and Attitude Control Rockets, Sustainer and ATO Motors
- High Speed Rocket Sled Engines
- Solid Propellant Turbo Jet Engine Starter Cartridges
- Gas Generation and Auxiliary Power Units
- Power Packages for External Stores, Canopies and Pilot Seat Forced Ejection Systems
- High Explosives, Ignitors, Fuses, Detonators, Flares, Pyrotechnics
- Explosive Formation of Metal Parts

Olin
TRADEMARK
EXPLOSIVES DIVISION
OLIN MATHIESON CHEMICAL
CORPORATION
EAST ALTON, ILLINOIS



Left to right: Dr. Howard Baller (radar systems and counter-measures, computers); Dr. Cledo Brunetti, Director of Engineering and R & D (electronic design, automation); Donald F. Melton (nuclear handling, automation equipment); Dr. John E. Barkley, Associate Director for R & D (solid state, infrared)

These leaders are pioneering scientific frontiers at General Mills

Can men like these and missiles

Yes, particularly if your creative engineering problems involve aircraft and allied systems such as:

- **Guidance and Navigational Controls**
- **Radar and Infrared Detection**
- **Aircraft and Ground Fire Controls**
- **Underwater and Mechanical Equipment Designs**

Outstanding scientists like these have been closely involved in precision ordnance instrument projects at General Mills since 1940. Together with their staffs they have all had both practical and theoretical experience in their fields of specialization. Now, you can utilize their recognized abilities in the development of your aeronautical and industrial control systems.

To carry their development work into actual instruments and automatic equipment, General Mills' Mechanical Division has complete, high-level facilities for production engineering and precision manufacturing. All types of operations in the manufacturing proces

CREATIVE RESEARCH AND DEVELOPMENT

PRECISION ENGINEERING AND PRODUCTION

MECHANICAL DIVISION OF



Zeke Soucek (seated), General Manager of Mechanical Division; Dr. Carl F. Kober, Associate Director for Systems Engineering (radar, infrared and inertial systems); Harold E. Froehlich (balloons and meteorological systems); Dr. Otmar M. Stuetzer (microwave optics, semiconductor physics); Dr. Gottfried K. Wehner (behavior of metals in space flight)

help develop aircraft systems for you?

From raw materials to finished systems can be carried out by the Mechanical Division.

Close tolerance work (as in the assembly of such units as the Y-4 Bombsight, the General Mills Flight Recorder, and the fabulous Autofab Machine for automatic assembly of electronic circuits) has developed master technicians and unusually high standards for production, inspection, performance testing and on-time delivery.

WRITE FOR THIS FREE BOOKLET! Thirty-two illustrated pages give you a complete description of this fast-growing operation, its accomplishments and facilities. See how General Mills can serve you—save you money and manpower too! Write to Dept. JP6, Mechanical Division of General Mills, 1620 Central Ave. N.E., Minneapolis 13, Minn.



Creative Engineers: *Ask about the opportunity to work with these and other outstanding scientists. Urgent projects of military and industrial significance are underway at General Mills.*

OF General Mills, Inc.

These Du Pont Lino-Writ Products can help you get perfect, high-contrast oscillographic recordings

YOUR CHOICE OF PAPER SPEED



Why take a chance with critical . . . and often expensive . . . oscillographic recording data? Du Pont makes a special paper for your specific needs:

- Lino-Writ 1 is best suited for average instrument use where machines record comparatively low frequencies and amplitude vibrations.
- Lino-Writ 2 – a new Du Pont paper – is especially designed for critical recording at intermediate frequencies where high paper travel speed is required. Supplied in splice-free rolls up to 400 feet, there's no danger of losing part of a test record on a splice.
- Lino-Writ 3 is ideal for recording high-frequency traces at high paper travel speeds without loss of important detail.

Du Pont Lino-Writ oscillograph recording papers are supplied in sizes for every recording purpose, in standard-weight Type B, and tough, extra-thin Type W.



CHEMICALS FOR FAST, EASY PROCESSING

Handy Du Pont prepared chemicals – 57-D Developer or fast-working Lino-Writ Developer and 10-F Fixer – assure you of clean, high-contrast recordings. You'll be able to scan stain-free records in just 15 to 20 seconds!

FOR RAPID STABILIZATION MACHINES



Your best bet for rapid-stabilization processing equipment is Du Pont's Lino-Writ Rapid Processing Chemicals Kit. It contains a complete machine charge – developer, stop bath and stabilizer – packaged in convenient, puncture-opening tins.

SEND FOR FREE BOOKLET about Du Pont oscillographic recording papers and chemicals. This fact-filled booklet also contains helpful information about processing and choice of paper surface.

DU PONT
OSCILLOGRAPHIC PRODUCTS

DU PONT
REG. U. S. PAT. OFF.

BETTER THINGS FOR BETTER LIVING . . . *THROUGH CHEMISTRY*

E. I. du Pont de Nemours & Co. (Inc.)
Photo Products Department
2420-17 Nemours Building, Wilmington 98, Delaware

Please send me information about Du Pont Lino-Writ and Lino-Writ processing chemicals.

*Name*_____

*Firm*_____

*Street*_____

*City*_____ *State*_____

326

SMALL, LIGHT, POWERFUL

AIR MOTORS FOR MISSILES



Instantaneous Acceleration — Accurate Regulation — Minimum Consumption

Bendix-Pacific has developed a line of high performance Air Motors which have been completely qualified for generating hydraulic and electric power in missiles.

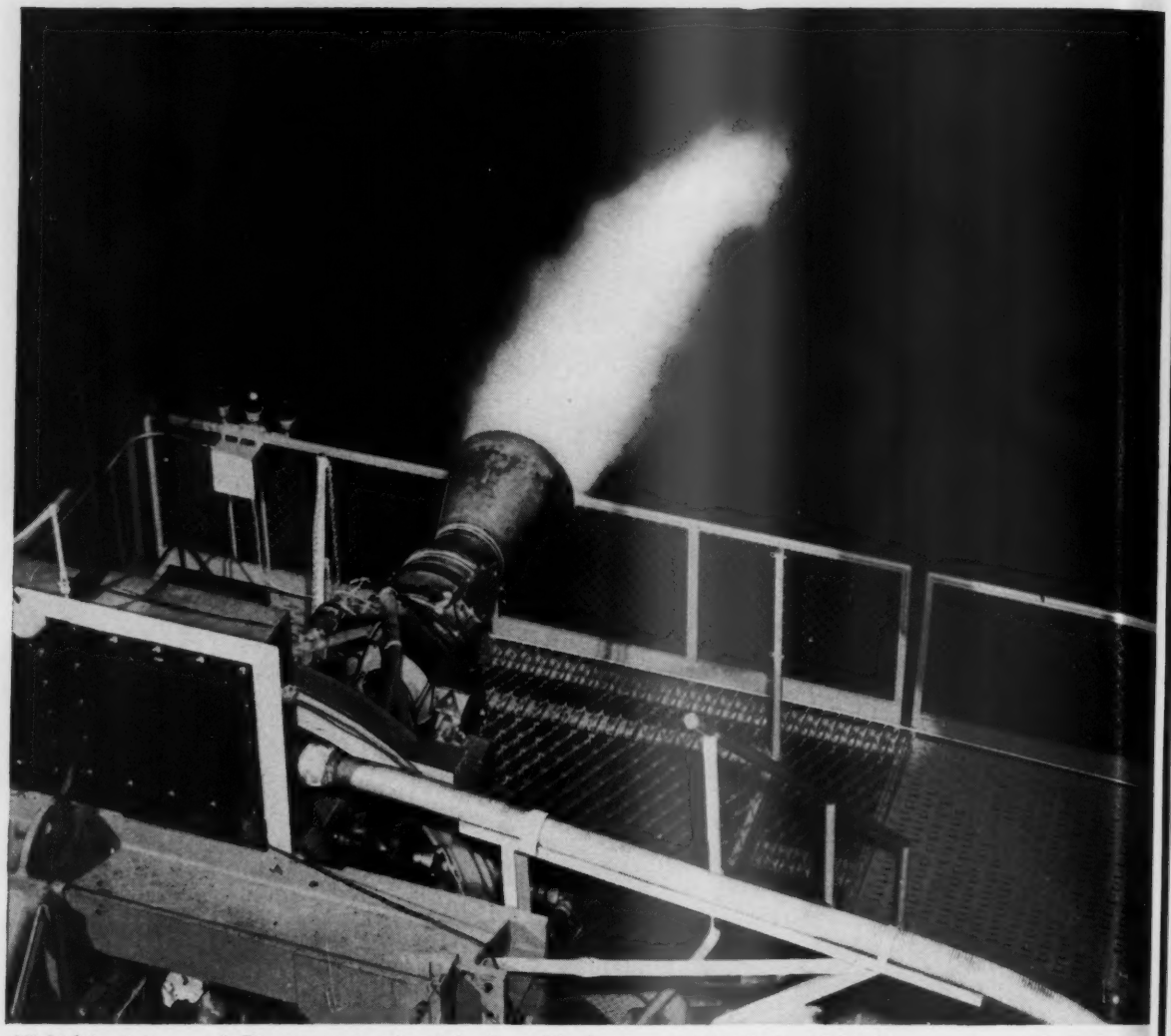
These are constant displacement rotary vane type motors which develop 2¾ H.P. per 100 P.S.I. inlet pressure. The motors can be used with up to 300 P.S.I. Efficiency approaches 70% between 3000 and 6000 R. P. M.

The motors are qualified for applications over an ambient range of 20° to 160°F and accelerations of 60G. They have been operated with inlet gas temperatures over 1000°F. The motors which have a basic weight of 1½ pounds, are available with or without governors.

Sales engineers are available to discuss
in detail your potential requirements.

Bendix
PACIFIC DIVISION
Bendix Aviation Corporation
NORTH HOLLYWOOD, CALIF.

EAST COAST OFFICE: 475 5th AVE., N.Y. 17 • DAYTON, OHIO—120 AMERICAN BLDG., DAYTON 2, OHIO • WASHINGTON, D.C.—SUITE 653, 1701 "K" ST., N.W.
CANADIAN DISTRIBUTORS: AVIATION ELECTRIC LTD., MONTREAL 9 • EXPORT DIVISION: BENDIX INTERNATIONAL, 205 E. 42nd ST., NEW YORK 17



Night firing tests on early ROCKETDYNE engines helped speed the development of today's models whose power cannot be disclosed.

Today's Rocket Engine can send a missile half-way around the earth

Even as you read this, rocket engines capable of sending a guided warhead half-way around the earth are being developed and produced by ROCKETDYNE, a Division of North American Aviation, Inc. . . . and larger, still more powerful units are on the way.

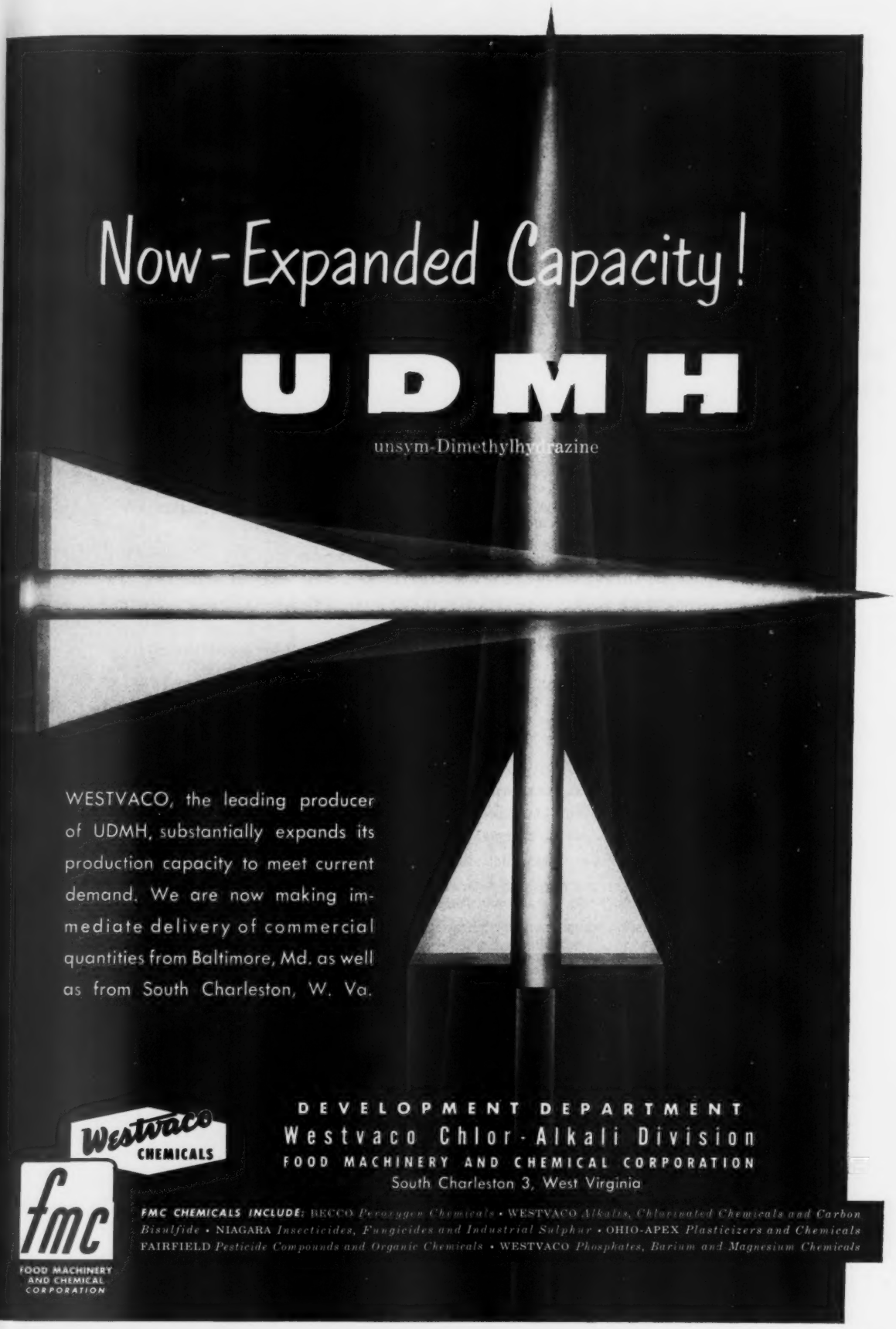
Behind these bare facts is a 10-year story of how the Air Force and ROCKETDYNE faced up to one of the biggest engineering challenges of the last decade. Security restrictions do not permit us to give you the details, but we *can* tell you that ROCKETDYNE has manufactured the largest liquid-propellant rocket engine in the free world. ROCKETDYNE is developing and producing rocket engines for many of the major guided missile projects in this country.

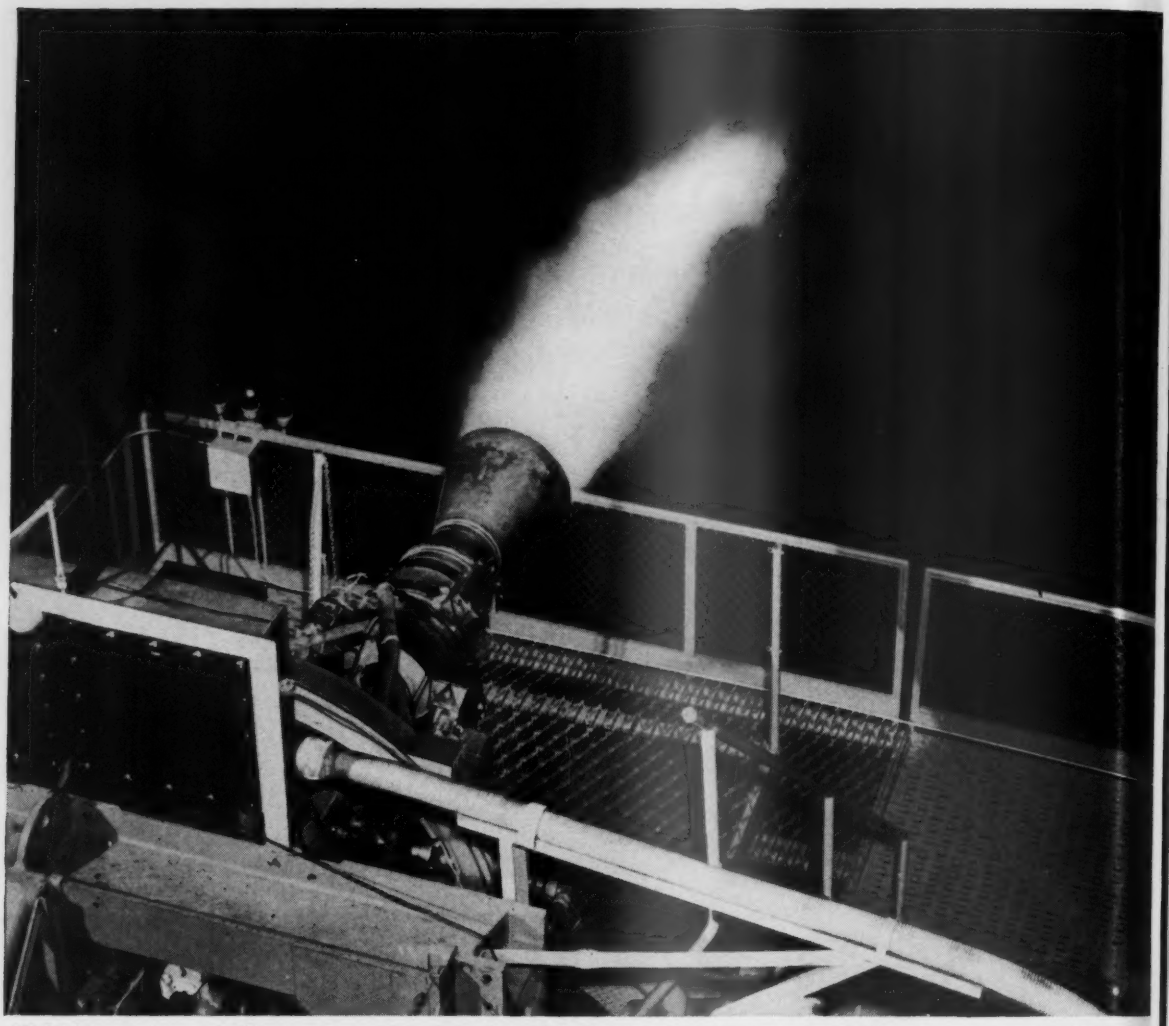
If you are an engineer—and interested in this young and challenging field—write ROCKETDYNE, Personnel Manager, Dept. R-2, 6633 Canoga Ave., Canoga Park, California . . . located near Los Angeles in the West San Fernando Valley.

ROCKETDYNE

A Division of North American Aviation, Inc.

BUILDERS OF POWER FOR OUTER SPACE


Now-Expanded Capacity!
UDMH
unsym-Dimethylhydrazine
WESTVACO, the leading producer of UDMH, substantially expands its production capacity to meet current demand. We are now making immediate delivery of commercial quantities from Baltimore, Md. as well as from South Charleston, W. Va.
Westvaco CHEMICALS
fmc
FOOD MACHINERY AND CHEMICAL CORPORATION
DEVELOPMENT DEPARTMENT
Westvaco Chlor-Alkali Division
FOOD MACHINERY AND CHEMICAL CORPORATION
South Charleston 3, West Virginia
FMC CHEMICALS INCLUDE: BECCO Peroxygen Chemicals • WESTVACO Alkalis, Chlorinated Chemicals and Carbon Bisulfide • NIAGARA Insecticides, Fungicides and Industrial Sulphur • OHIO-APEX Plasticizers and Chemicals FAIRFIELD Pesticide Compounds and Organic Chemicals • WESTVACO Phosphates, Barium and Magnesium Chemicals



Night firing tests on early ROCKETDYNE engines helped speed the development of today's models whose power cannot be disclosed.

Today's Rocket Engine can send a missile half-way around the earth

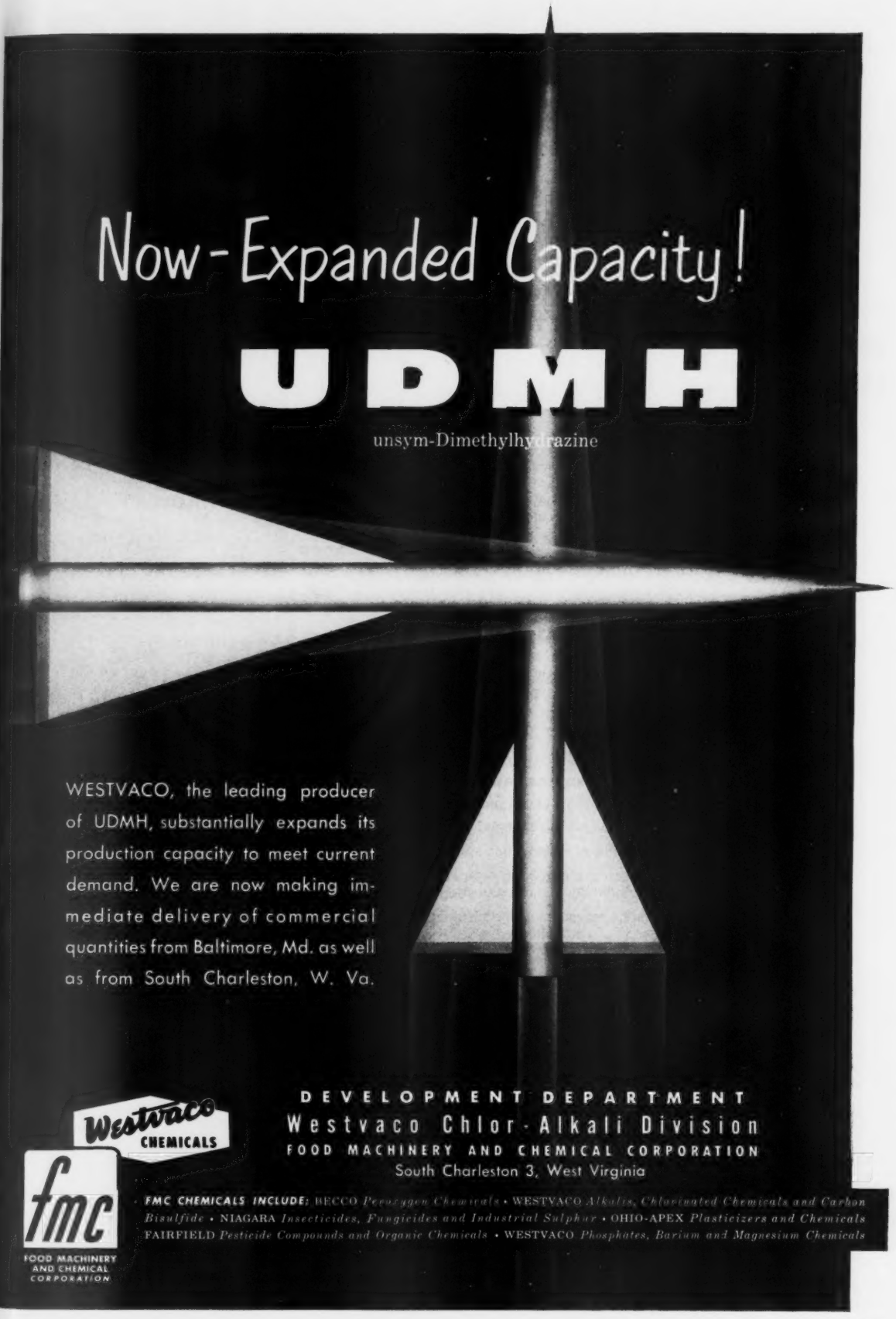
Even as you read this, rocket engines capable of sending a guided warhead half-way around the earth are being developed and produced by ROCKETDYNE, a Division of North American Aviation, Inc. . . . and larger, still more powerful units are on the way.

Behind these bare facts is a 10-year story of how the Air Force and ROCKETDYNE faced up to one of the biggest engineering challenges of the last decade. Security restrictions do not permit us to give you the details, but we *can* tell you that ROCKETDYNE has manufactured the largest liquid-propellant rocket engine in the free world. ROCKETDYNE is developing and producing rocket engines for many of the major guided missile projects in this country.

If you are an engineer—and interested in this young and challenging field—write ROCKETDYNE, Personnel Manager, Dept. R-2, 6633 Canoga Ave., Canoga Park, California . . . located near Los Angeles in the West San Fernando Valley.

ROCKETDYNE *A Division of North American Aviation, Inc.*

BUILDERS OF POWER FOR OUTER SPACE


Now-Expanded Capacity!
UDMH
unsym-Dimethylhydrazine
WESTVACO, the leading producer of UDMH, substantially expands its production capacity to meet current demand. We are now making immediate delivery of commercial quantities from Baltimore, Md. as well as from South Charleston, W. Va.
Westvaco CHEMICALS
fmc
FOOD MACHINERY AND CHEMICAL CORPORATION
DEVELOPMENT DEPARTMENT
Westvaco Chlor-Alkali Division
FOOD MACHINERY AND CHEMICAL CORPORATION
South Charleston 3, West Virginia
FMC CHEMICALS INCLUDE: BECCO Peroxygen Chemicals • WESTVACO Alkalis, Chlorinated Chemicals and Carbon Bisulfide • NIAGARA Insecticides, Fungicides and Industrial Sulphur • OHIO-APEX Plasticizers and Chemicals FAIRFIELD Pesticide Compounds and Organic Chemicals • WESTVACO Phosphates, Barium and Magnesium Chemicals

AERODYNAMICISTS • THERMODYNAMICISTS

expansion

CREATES OPPORTUNITY AT GENERAL ELECTRIC'S AIRCRAFT GAS TURBINE DIVISION

for specialists in applied research

The development of new propulsion systems for aircraft and the initiation of special research and development projects have created new positions for both specialists and supervisors. One of these projects includes a nuclear-powered engine; others involve advanced jet and rocket engines.

MODERN FACILITIES VALUED AT $100,000,000

To aid GE engineers and scientists General Electric has built one of the world's greatest privately owned aircraft propulsion facilities at the Development Center in Evendale, Ohio.

Of special interest to aerodynamicists and thermodynamicists are such installations as a wind tunnel capable of providing Mach 2.5 speeds; test tanks where the efficiency of jet compressors can be determined at 20,000 RPM speeds at 4500 HP; a high temperature flame tunnel; a Thrust Augmentation Test Cell; a new Computations Building, where the most advanced electronic brains (IBM 704) help solve complex development problems... and many others.

EXPLORE THESE AREAS

Aerodynamic design of compressors and turbines

Design and evaluation of engine cooling systems

Design studies of air induction systems and components

Investigation programs with regard to application of new compressor-turbine combination and combustion-augmentation design concepts

Combustion research and systems development with both liquid and solid propellants

Preliminary thermo-mechanical design of components

Basic fluid mechanics studies on inlets, nozzles and diffusers

Thermodynamic calculations of jet and rocket engine cycles

Cycle analysis and performance reports

CAN YOU QUALIFY? Are you a graduate engineer with experience in aerodynamics or thermodynamics?

IF SO, SEND COLLECT WIRE for appointment to discuss the specific opportunities that may exist for you with the Aircraft Gas Turbine Division of General Electric.

Or write to Mr. Mark Peters

GENERAL ELECTRIC

AIRCRAFT GAS TURBINE DIVISION
Technical Recruiting Bldg. 100
Cincinnati 15, Ohio

As Higher and Higher Altitudes Are Attained STRATOPOWER HYDRAULIC PUMPS ARE THERE...

AND—*NOT JUST FOR THE RIDE!*

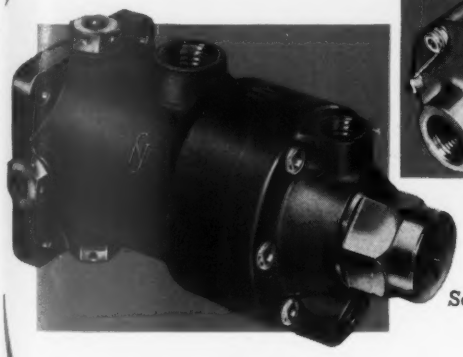
Design for tomorrow's aircraft! That's the keynote of the engineering back of the new STRATOPOWER Hydraulic Pumps. Aircraft, Rockets, Guided Missiles or Satellites . . . the PUMP is vital to the successful performance of the project. Engineers responsible for the design of hydraulic systems for these vehicles provide a sure source of Fluid Power with—

STRATOPOWER®

HYDRAULIC PUMPS

Series 65F Fixed Displacement Pump





Series 65W Variable Delivery Pump

The 65F Series Fixed Displacement Pumps and the 65W Series Variable Delivery Pumps are designed to operate dependably at temperatures in excess of 400°F and at drive speeds of over 10,000 rpm. These Pumps are light in weight and have exceptionally high horsepower/weight ratios. The new STRATOPOWER design can easily be adapted to fit special requirements to save space and weight in aircraft and missiles where every pound saved is truly more than worth its weight in gold.

In the air and on the ground, STRATOPOWER Hydraulic Pumps assure reliable hydraulic Utility Systems and Boost Systems, and add to the high performance requirements of Auxiliary Power Units, Radar Scanners and Stabilized Platforms.



WATERTOWN DIVISION
THE NEW YORK AIR BRAKE COMPANY

STARBUCK AVENUE • WATERTOWN • N. Y.

INTERNATIONAL SALES OFFICE, 90 WEST ST., NEW YORK 6, N. Y.

WATERTOWN DIVISION
The New York Air Brake Company
730 Starbuck Ave., Watertown, N. Y.

I would like more information on STRATOPOWER Series 65 Hydraulic Pumps.

Name_____ Title_____

Company_____

Address_____

City_____ Zone_____ State_____



Official U. S. Navy Photograph

The U. S. S. Boston (CAG-1), the Navy's first guided missile cruiser, with Terrier Missiles and their launchers at the stern.

NAVY BUREAU OF ORDNANCE DEVELOPS WEAPON SYSTEMS FOR USE AGAINST ATTACK BY SEA OR AIR

The recent unveiling of the Navy's first ready-for-combat anti-aircraft guided missile weapon system —TERRIER—is but one result of the research and development work being done by the U. S. Navy's Bureau of Ordnance and a coordinated team of industrial and educational institutions.

From its establishment in 1842, the Bureau of Ordnance has provided the weapons with which the Navy has fought victoriously in six wars. With the evolution of armament, from the first muzzle loading cannons to today's complex weapons systems, it has directed the design, development, and production of the computers, fire control, and other types of equipment comprising the Navy's air, surface, and underwater ordnance.

The Research and Development Division of the Bureau of Ordnance has the responsibility of initiating and coordinating the research and development of the many projects which result in such end products as guided missiles, homing torpedoes, aircraft laid mines, and the launching and control systems for these weapons.

The job of guiding a key element of a modern day weapon system from the idea stage to the ready-for-combat stage involves a wealth of technology—drawing upon the skill, farsightedness, and courage of responsible scientific and technical personnel in the Bureau of Ordnance and its laboratories, and their counterparts in universities and industrial organizations.

This is one of a series of ads on the technical activities of the Department of Defense. 103

FORD INSTRUMENT COMPANY
DIVISION OF SPERRY RAND CORPORATION
31-10 Thomson Avenue, Long Island City 1, New York
Beverly Hills, Cal. • Dayton, Ohio



Ford Instrument Company engineer placing equipment designed for Navy instrument in one of the environmental test chambers.

ENGINEERS
of unusual abilities can find a future at FORD INSTRUMENT COMPANY. Write for information.



REACHING FOR THE *Moon*

. . . taxes your knowledge of the many complexities of rocket fueling — energy, weight, supply, cost, conductivity, ignition qualities.

It will pay you to consider the characteristics of Pennsalt Fluorine and Pennsalt Chlorine Trifluoride. Both are now available in unlimited quantities.

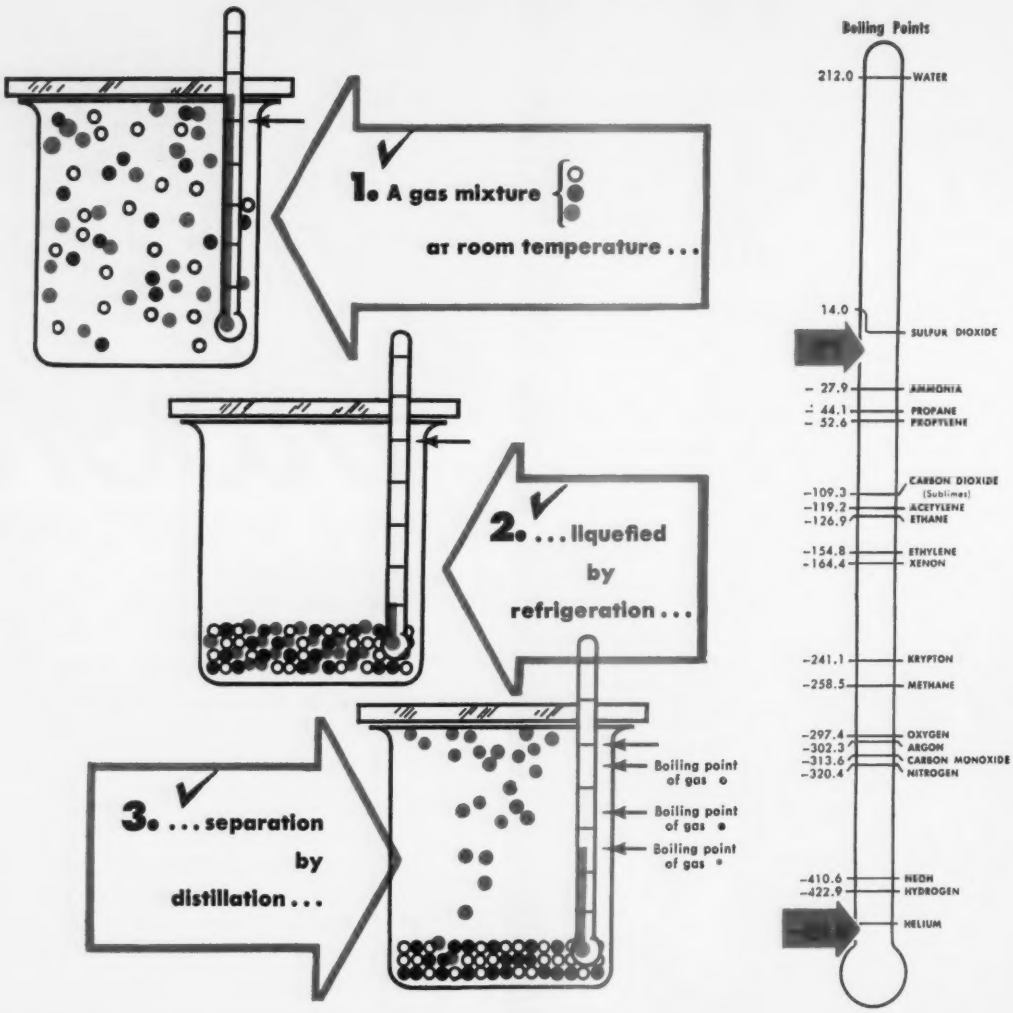
Whether yours is a research or a purchasing job, Pennsalt's wide experience in developing and supplying interhalogen compounds and fluorinated oxidants will be of value to you. Plan now to discuss your liquid rocket-propellant problems with a Pennsalt representative. Call or write Technical Services Department 264, Industrial Chemicals Division, Pennsylvania Salt Manufacturing Company, Three Penn Center Plaza, Philadelphia 2, Pa.

Pennsalt Chemicals

PENNSYLVANIA SALT MANUFACTURING COMPANY

LOW-TEMPERATURE PROCESSING

—a basic method of producing oxygen for propellants



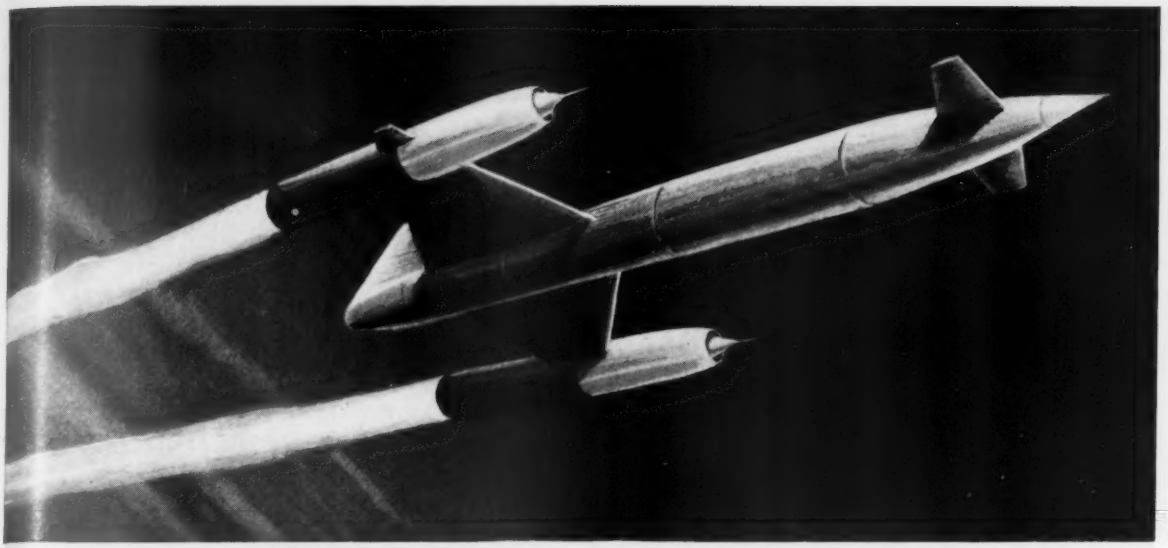
The production of oxygen and nitrogen in unlimited quantities from the free air is accomplished most economically by "low-temperature processing". So, too, is the separation of industrial waste gases and fluid flows into their valuable components.

The method is basic. A gas mixture is liquefied by refrigeration—produced by expansion of the compressed mixture. The temperature of the mixture is then allowed to rise to the boiling points of the constituent gases, one by one.

As the temperature reaches the boiling point of each gas successively, the particular component can be drawn off from the mixture (fractional distillation). Basically, low-temperature gas separation processes depend on changing the state of matter. This is also the genesis of other low-temperature separation processes—removing solids from liquids, and making solids from gases. Dewaxing oil and freezing xylenes out of petroleum products are examples of the first; making dry ice out of waste carbon dioxide, an example of the second.

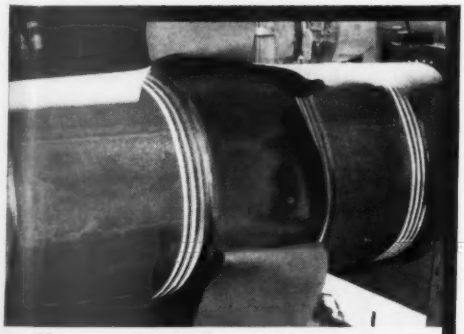
Engineering and production executives interested in this process may obtain more complete information by requesting (on company letter-head, please) a free copy of our booklet "Low-Temperature Processing of Gases, Liquids, Solids".

Air Products
INCORPORATED
Dept. O, Box 538 Allentown, Pa.



New, highly advanced ramjet engines designed and built by Marquardt Aircraft Company of Van Nuys, California, for supersonic missiles use Norton Rokide "A" spray coating. The Rokide coating aids in assuring successful flight by greatly increasing the resistance of the tailpipe to excessive heat and abrasion.

Norton ROKIDE* coating plays vital role in Supersonic missiles



The uncoated high temperature alloy of this ramjet engine tailpipe failed during an especially severe testing in 14.2 seconds. Metal temperature exceeded 2200°F.



Coated with Rokide "A" on the forward portion only, an identical tailpipe was tested for 18.3 seconds without failure. Maximum metal temperature was 1800°F.

ROKIDE "A" aluminum oxide coating is one of three Norton refractory spray coatings — including ROKIDE "ZS" zirconium silicate and ROKIDE "Z" stabilized zirconia — now being widely used in modern high temperature applications.

In reaction motors and in various AEC projects, for example, the high melting point and low thermal conductivity of ROKIDE "A" coating reduces the temperature of the underlying material and permits higher operation temperatures. It is both thermally and electrically insulating, and its hardness, chemical inertness and stability in combustion temperature provide high resistance to excessive heat, abrasion, erosion and corrosion.

ROKIDE "A" Coating vs. Stainless Steel

While less dense than stainless steel, ROKIDE "A" coating is about five times as hard, has a considerably higher melting point and is very much lower in thermal conductivity and thermal expansion.

Process and Licensing Policy

ROKIDE coatings are applied in molten state by a metallizing spray gun. Coatings may be applied to parts of all sizes and shapes accessible to the spray gun equipment. Licenses for the use of the ROKIDE coating process can be obtained from Norton Company. For further facts on ROKIDE coatings — and for aid in problems involving high temperature materials — write, mentioning your requirements, to NORTON COMPANY, Refractories Division, 637 New Bond Street, Worcester 6, Mass.

*Trade-Mark Reg. U. S. Pat. Off. and Foreign Countries

NORTON
REFRACTORIES
Engineered... Rx ...Prescribed

Making better products... to make your products better

NO OBJECTION TO PUBLICATION ON GROUNDS OF MILITARY SECURITY
6 MAR 1956 15
OFFICE OF SECURITY REVIEW
DEPARTMENT OF DEFENSE
AS AMENDED

complete missile facilities

from conception through completion

"delete" "delete"
missile facilities at locations

PARSONS

SITE SELECTION MASTER PLANNING DESIGN CRITERIA
FACILITY DESIGN COMPLETE INSTRUMENTATION CONSTRUCTION

THE RALPH M. PARSONS COMPANY
NEW YORK
PASADENA
WASHINGTON

ENGINEERS • CONSTRUCTORS
LOS ANGELES

ANKARA
BAGHDAD
BEIRUT
JEDDAH
KARACHI
NEW DELHI
PARIS



High Thrust Test Stand Designed by Parsons for Edwards Air Force Base

JUNE 1956
VOLUME 26 NUMBER 6
JET PROPULSION
Journal of the AMERICAN ROCKET SOCIETY
Editor-in-Chief
MARTIN SUMMERFIELD

Generalized Theory of the Optimum Thrust Programming for the Level Flight of a Rocket-Powered Aircraft

PLACIDO CICALA[1] and ANGELO MIELE[2]
Politecnico di Torino, Italy — Purdue University, Lafayette, Ind.

Two theories are presented for the analysis of the optimum burning program for horizontal flight. The first theory is based on Green's theorem which leads to a simple straightforward proof of the necessary and sufficient conditions for the existence of a maximum. A linear relationship between thrust and engine mass flow is assumed. Hibbs' results are generalized by lifting any restriction concerning the shape of the drag polar and by considering a finite maximum burning rate for the engine. Two regions of best range are detected, one subsonic-transonic, the other one supersonic. The influence of the boundary conditions on the optimum technique of flight is discussed. A simple similarity rule for stratospheric solutions is pointed out.

The second theory, based on the variational method of Lagrange multipliers, considers the general case of an arbitrary one-to-one correspondence between thrust and propellant mass flow. Particular attention is devoted to the case of a polygonal thrust characteristic. An example of application is worked out.

The concept of index value presented in a previous note is here emphasized. Such an index value appears to be a very effective device in controlling the composition of the optimum path for discontinuous Eulerian solutions.

Nomenclature

a = speed of sound (ft sec^{-1})
C_{Di} = "induced" drag coefficient
C_L = lift coefficient
C_{LE} = lift coefficient corresponding to the maximum lift-drag ratio
$C_{L_{max}}$ = maximum lift coefficient
D = drag (lb)
D_L = partial derivative of drag with respect to lift, calculated at constant altitude and constant velocity
D_V = partial derivative of drag with respect to velocity, calculated at constant altitude and constant lift (lb ft^{-1} sec)
g = acceleration of gravity (ft sec^{-2})
h = altitude (ft)
K = C_{Di}/C_L^2 = ratio of induced drag coefficient to square of lift coefficient
L = lift (lb)
m = instantaneous mass of the aircraft (lb ft^{-1} sec^2)
m_* = $m \exp [V/V_e]$ = modified mass (lb ft^{-1} sec^2)
M = Mach number
p = atmospheric pressure (lb ft^{-2})
p = index value (ft sec^{-1})
Re = Reynolds number
S = reference surface (ft^2)
t = time (sec)
T = thrust (lb)
V = absolute velocity of the solid part of the aircraft, i.e., velocity referred to a reference frame rigidly connected to the earth (ft sec^{-1})
V_e = equivalent relative exit velocity of the gases, i.e., velocity referred to a reference frame rigidly connected to the solid part of the aircraft (ft sec^{-1})
V_s = stalling velocity (ft sec^{-1})
W = instantaneous weight of the aircraft (lb)
X = horizontal distance (ft)
β = $-\dot{m}$ = instantaneous burning rate of the rocket engine (lb ft^{-1} sec)
γ = ratio of specific heat at constant pressure to specific heat at constant volume = 1.4 for air
λ = Lagrange multiplier (sec)
λ = V/V_e = ratio of flight velocity to equivalent exit velocity of the engine
μ = Lagrange multiplier (lb^{-1} ft^2 sec^{-2})
μ = m/m_r = nondimensional mass
μ_* = m_*/m_r = nondimensional modified mass
ρ = air density (lb ft^{-4} sec^2)

Subscripts

f = final condition
i = either an initial condition or a variable index
r = reference condition

Superscripts

$\cdot$ = denotes derivative with respect to time
$'$ = denotes derivative with respect to mass

Introduction

THE analysis of the optimum burning program for the flight of a rocket-powered vehicle has received considerable attention in recent years. The particular case of a vertical path has been investigated by Hamel (1)[3] and, more recently, by Tsien and Evans (2). The other case of a horizontal path has been studied by Hibbs (3).

The problem which Hibbs (3) attacked may be formulated as follows: "To determine the mass-velocity relationship which maximizes the range of an aircraft in straight level flight for an established consumption of propellant, the end velocities being given." A parabolic polar with constant coefficients

Received July 27, 1955, and presented at the AMERICAN ROCKET SOCIETY Fall Meeting, September 18–21, 1955, Los Angeles, Calif.
[1] Professor.
[2] Associate Professor of Aeronautical Engineering. Mem. ARS.
[3] Numbers in parentheses indicate References at end of paper.

was considered. Moreover, the equivalent jet velocity (V_e) was assumed independent of the mass flow of the engine ($\beta = -\dot{m}$).

According to Hibbs, the above variational problem consists in finding the extremals of an integral having the form

$$\int_{m_i}^{m_f} [A(V,m) + V'B(V,m)]\, dm \quad \ldots\ldots\ldots\ldots [1]$$

where m is the instantaneous mass of the airplane, and V is the translational velocity of the solid part of the aircraft.

The integrand function being linear in V', it follows that the Euler equation associated with the integral [1] has order zero. In other words, the Eulerian solution degenerates into an equation in finite terms

$$\frac{\partial A}{\partial V} - \frac{\partial B}{\partial m} = 0 \quad \ldots\ldots\ldots\ldots\ldots\ldots [2]$$

which, in general, does not satisfy the boundary conditions of the fixed-end points problem (m_i, V_i, m_f, V_f given). Moreover, in the present singular case the classical sufficiency tests of the calculus of variations (for instance, the Legendre test) fail to prove the maximal character of the Eulerian path, even in the simple case of boundary conditions satisfying Equation [2].

Aware of the above situation, Hibbs postulated a cornered, discontinuous solution generally formed by pulse burning patterns ($\dot{m} = -\infty$), coasting flights ($\dot{m} = 0$), and flights according to Equation [2]. This correct intuition was justified (3) on the basis of physical considerations, while the proof was carried out through a series of successive steps rather than through a complete, unitary technique.

On the other hand, a general demonstration is now possible in the light of the methods developed by the senior writer in (7) and by the junior author in (4, 5).

In (7) general equations and procedures for determining optimum flight techniques have been presented.

In (4, 5) a method has been developed and applied (6, 14) to a wide class of variational problems of interest in the mechanics of flight. Such a technique is of convenient use in all the cases where an integral of the form [1] is to be maximized or minimized, subject to a number of inequalities involving the variables appearing under integral sign and their derivatives.

For instance, the exclusion of propellant refueling in flight implies the following inequality [3]

$$-\infty \leq \dot{m} \leq 0 \quad \ldots\ldots\ldots\ldots\ldots\ldots [3]$$

which in turn yields

$$m_f \leq m \leq m_i \quad \ldots\ldots\ldots\ldots\ldots\ldots [4]$$

Scope of the Present Research

In the present paper two theories are presented for a generalized analysis of the optimum burning program for horizontal flight.

The first theory is based on Green's theorem (4, 5) and on the special properties of the function ω (Equation [13]) and leads to a simple, straightforward proof of the necessary and sufficient conditions for the existence of a maximum. A constant value is assumed for the effective exit velocity (V_e) as in Hibbs' paper (3). Several generalizations are introduced, specifically: (a) any restriction concerning the shape of the drag polar is lifted; (b) a finite maximum burning rate is assumed for the engine (β_{max}); (c) a finite maximum value is considered for the lift coefficient ($C_{L_{max}}$).

The generalization (a) is equivalent to assuming a drag function of the form $D = D(V, m)$ as shown in Part I of this paper. The generalization (b) is equivalent to abandoning Equation [3] and to replacing it with the other

$$0 \leq \beta \leq \beta_{max} \quad \ldots\ldots\ldots\ldots\ldots\ldots [5]$$

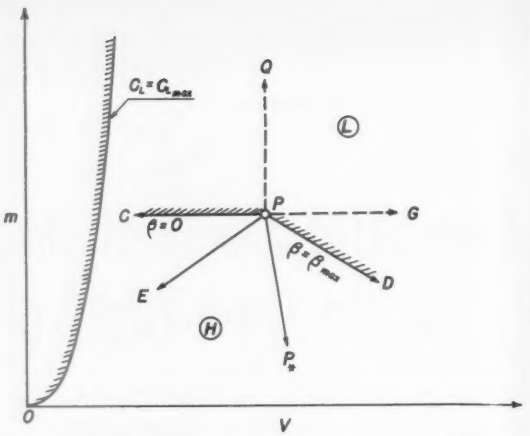


Fig. 1 Displacements of the aircraft in the (V, m)-plane

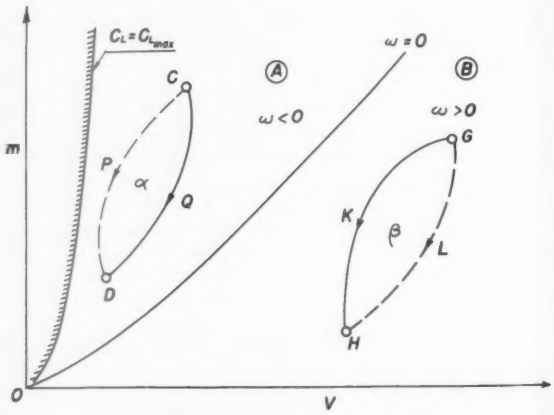


Fig. 2 Regions of the (V, m)-plane

where β_{max} is the assumed finite maximum burning rate for the engine. The generalization (c) is equivalent to excluding (Figs. 1 and 2) all the points of the (V, m)-plane belonging to the forbidden region bound by the m-axis and by the curve of equation $C_L = C_{L_{max}}$.

The second theory is based on the Euler-Lagrange equations (7) for the variational problem formulated as a problem of Mayer type. As a further generalization, an arbitrary one-to-one correspondence between thrust and propellant mass flow is considered. Particular attention is devoted to the case of a polygonal characteristic $T(\beta)$, by which the behavior of the power plant may be approximated with any desired degree of accuracy. For this problem use is made of the concept of index value, introduced in a previous note by the senior writer (7). The use of such a variable—related to the Lagrange multipliers—appears of considerable interest to the effect of controlling the composition of the optimum paths for the case of discontinuous Eulerian solutions.

PART I SOLUTION BY GREEN'S THEOREM FOR THE CASE OF A LINEAR THRUST CHARACTERISTIC

Angelo Miele[4]

IN THIS section of the paper an application of the method outlined in (4, 5) is developed. A straight and level flight is assumed. In addition to the hypotheses previously indicated, the so-called aerodynamic lag is neglected, i.e., lift

[4] This writer is indebted to the National Advisory Committee for Aeronautics, Washington, D. C., for kindly supplying unclassified drag data for wing-body combinations at transonic and supersonic speeds.

(L) and drag (D) forces are calculated as in steady flight. The rocket-powered aircraft is ideally regarded as a particle of variable mass.

I-1 Fundamental Equations

The equations of the straight level motion of a rocket-powered aircraft are the following (15, 16)

$$D + \dot{m}\,(V_e + mV') = 0 \quad \ldots\ldots [6]$$

$$L - mg = 0 \quad \ldots\ldots [7]$$

where g is the acceleration of gravity, $\dot{m} = dm/dt$, $V' = dV/dm$, and V_e is the equivalent exit velocity of the rocket engine, assumed constant in the present treatment.

If the aerodynamic lag is neglected, the drag may be regarded as a function $D(h, V, L)$ of altitude, velocity and lift, even accounting for viscosity and compressibility effects. After considering the constancy of the altitude and eliminating the lift by means of Equation [7], the drag is reduced to a function $D(V, m)$ of velocity and mass only. As a consequence, Equation [6] may be rewritten as follows

$$\frac{V}{\beta} + \Phi V' + \Psi = 0 \quad \ldots\ldots [8]$$

where

$$\Phi = -\frac{mV}{D(m,V)} = \Phi(m, V) \quad \ldots\ldots [9]$$

$$\Psi = -\frac{V_e V}{D(m,V)} = \Psi(m,V) \quad \ldots\ldots [10]$$

The horizontal distance flown by the aircraft is given by

$$X = -\int_{m_i}^{m_f} \frac{V}{\beta}\,dm = \int_{m_i}^{m_f} (\Phi V' + \Psi)dm \quad \ldots\ldots [11]$$

The next step is to determine the special function $V = V(m)$ which maximizes X for *given end conditions* m_i, V_i, m_f, V_f, the class of arcs investigated being submitted to the inequalities [4], [5] and to

$$\frac{m}{V^2} \leq \frac{\rho S}{2g} C_{L_{\max}} \quad \ldots\ldots [12]$$

where $C_{L_{\max}} = f(M, Re)$; i.e., $C_{L_{\max}} = f(V)$ at a given altitude.

I-2 Admissible Displacements

Consider an airplane having the state of flight (V, m) at time instant t and let P be the representative point of the aircraft in the (V, m)-plane. After a time interval $dt = t_* - t$, the new mass of the aircraft is $m_* = m + dm$, the new velocity is $V_* = V + dV$ and the new vector position of the airplane in the (V, m)-plane is $\overrightarrow{OP_*} = \overrightarrow{OP} + \overrightarrow{PP_*}$.

The class of admissible displacements $\overrightarrow{PP_*}$ is determined by the inequality [5] and is bound by two limiting conditions (see Equation [8] and Fig. 1): a displacement $\overrightarrow{PC}$ ($\beta = 0$) corresponding to coasting flight and a displacement $\overrightarrow{PD}$ ($\beta = \beta_{\max}$) corresponding to the maximum burning rate of the engine.

While a displacement like $\overrightarrow{PE}$ is physically possible, a displacement like $\overrightarrow{PQ}$ is physically impossible, because the mass of the aircraft cannot increase. A displacement like $\overrightarrow{PG}$ is also physically impossible, because the constancy of the mass implies zero thrust and therefore a negative acceleration dV/dt. In conclusion, the two lines $\beta = 0$ and $\beta = \beta_{\max}$ split the (V, m)-plane into two regions associated with point P: a region (H) whose points are accessible to the aircraft in horizontal flight and a region (L) which is forbidden to the airplane because of the physics of the motion.

I-3 Properties of the Function $\omega(V, m)$

The following function of the variables V and m is now defined

$$\omega(V, m) = \frac{\partial \Psi}{\partial V} - \frac{\partial \Phi}{\partial m} \quad \ldots\ldots [13]$$

After accounting for Equations [9] and [10], Equation [13] is rewritten as follows

$$\omega = \frac{V}{D^2}\left\{VV_e \frac{\partial}{\partial V}\left(\frac{D}{V}\right) - m^2 \frac{\partial}{\partial m}\left(\frac{D}{m}\right)\right\} \quad \ldots\ldots [14]$$

For the particular case of a parabolic polar with coefficients depending on the Mach (M) and Reynolds (Re) numbers, i.e., for a drag function of the form

$$D = A(V, h)V^2 + B(V, h)\frac{m^2}{V^2} \quad \ldots\ldots [15]$$

Equation [14] yields

$$\omega = \frac{AV_eV^2}{D^2}\left\{1 + \frac{V}{V_e} + \frac{V}{A}\frac{\partial A}{\partial V}\right\} - \frac{BV_em^2}{D^2V^2}\left\{3 + \frac{V}{V_e} - \frac{V}{B}\frac{\partial B}{\partial V}\right\} \quad \ldots\ldots [16]$$

It is of particular interest to determine the locus of the points where $\omega = 0$ (Fig. 2). Such a locus is defined by

$$VV_e \frac{\partial}{\partial V}\left(\frac{D}{V}\right) - m^2 \frac{\partial}{\partial m}\left(\frac{D}{m}\right) = 0 \quad \ldots\ldots [17]$$

in general, and by

$$m = V^2\sqrt{\frac{A(V + V_e) + VV_e(\partial A/\partial V)}{B(V + 3V_e) - VV_e(\partial B/\partial V)}} \quad \ldots\ldots [18]$$

for a polar of the form [15]. In particular, if the coefficients of the parabolic polar are independent of both the Mach and Reynolds number, the following result is obtained (3)

$$m = V^2\sqrt{\frac{A}{B}}\sqrt{\frac{\lambda + 1}{\lambda + 3}} \quad \ldots\ldots [19]$$

In the following discussion it will be assumed that the solution of Equation [17] is unique; that the function ω is negative in the region (A) located at the left of the curve $\omega = 0$; that the function ω is positive in the region (B) placed at the right of the curve $\omega = 0$ (Fig. 2). The above hypotheses are readily verified for the particular case of a parabolic polar with constant coefficients. The results of the present note, however, may be immediately extended to the case where more than one solution $V = V(m)$ exists for the equation $\omega = 0$; see (6).

I-4 Lemma I

"Consider two admissible arcs CPD and CQD which belong to the region A ($\omega < 0$), connect the same end-points C and D, and enclose the area α. The path of higher range is the one (CQD) which leaves the enclosed area α at the right."

The above statement may be proved by showing that the difference of range (Fig. 2)

$$\Delta X = X_{CQD} - X_{CPD} = \int_{CQD} (\Phi V' + \Psi)dm - \int_{CPD} (\Phi V' + \Psi)dm \quad \ldots\ldots [20]$$

is positive.

The above difference may be written as a cyclic integral

$$\Delta X = \oint_{CQDPC} (\Phi\,dV + \Psi dm) \quad \ldots\ldots [21]$$

and transformed into a surface integral associated with the area α by using Green's theorem.[5]

$$\Delta X = -\iint_{\alpha}\left(\frac{\partial \Psi}{\partial V} - \frac{\partial \Phi}{\partial m}\right) dV dm = -\iint_{\alpha} \omega\, dV\, dm \,. \quad [22]$$

The ω-function being negative in the region α, it follows

$$\Delta X > 0 \,. \quad [23]$$

which proves the above lemma.

I-5 Lemma II

"Consider two admissible arcs GKH and GLH which belong to the region B ($\omega > 0$), connect the same end-points G and H, and enclose the area β. The path of higher range is the one (GKH) which leaves the enclosed area β at the left."

Proof of this statement is omitted, since it follows closely the technique outlined in the previous section.

I-6 Boundary Conditions

Four types of boundary conditions (4, 5, 6) exist, depending on the relative position of the points I and F with respect to the curve $\omega = 0$. Four cases of flight must be accordingly analyzed, the terminology being as follows:

Table 1

Case of flight	Region where point I belongs	Region where point F belongs
I	A	B
II	A	A
III	B	A
IV	B	B

I-7 Optimum Paths

As a corollary to lemmas I and II, the following rule about the geometry of the extremal path in the (V, m)-plane is established: "An observer who ideally moves along the optimum path must 'keep left' as much as it is permitted by the boundary conditions of the problem in the region A and must 'keep right' as much as possible in the region B."

It follows that if the terminal points I and F belong to the curve $\omega = 0$, the optimum path is identical to the curve $\omega = 0$.

If, on the contrary, the end-points do not belong to $\omega = 0$, the optimum path has a cornered, discontinuous character, being generally composed of three arcs: an initial arc IM, a central arc MN of equation $\omega = 0$, and a final arc NF (Table 2 and Fig. 3). The initial arc IM is to be flown at the maximum burning rate of the engine if point I belongs to region A or in coasting flight if point I belongs to region B. The final arc NF is to be flown with engine shut-off if point F belongs to region A or at the maximum burning rate of the rocket if point F belongs to region B.

Table 2

Case of flight	Arc IM	Arc MN	Arc NF
I	$\beta = \beta_{max}$	$\omega = 0$	$\beta = \beta_{max}$
II	$\beta = \beta_{max}$	$\omega = 0$	$\beta = 0$
III	$\beta = 0$	$\omega = 0$	$\beta = 0$
IV	$\beta = 0$	$\omega = 0$	$\beta = \beta_{max}$

[5] The negative sign arising from the transformation of the line integral [21] into the surface integral [22] stems from the clockwise character of the circuit CQDPC.

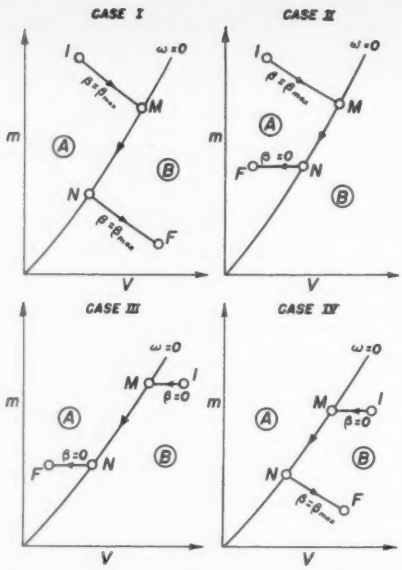


Fig. 3 Optimum paths for various types of boundary conditions

I-8 Proof

An analytical proof is here offered for one of the four types of boundary conditions listed in Table 1, namely for the case of flight designated as case II, i.e., for the horizontal motion of a rocket-powered aircraft between two end-conditions involving relatively low speeds. For cases I, III, and IV the demonstration is analogous, being based on the consideration of Sections I-2, I-3, I-4, I-5 concerning the class of admissible displacements, the properties of the ω-function, and the use of Green's theorem.

For case II the optimum path is composed of an initial arc IM flown at maximum burning rate, followed by a moderate burning ($\omega = 0$) along MN and by a final coasting flight NF.

The above statement can be proved by showing that the range associated with the path IMNF is always greater than the range associated with any other admissible path joining the same end-points I and F (Fig. 4).

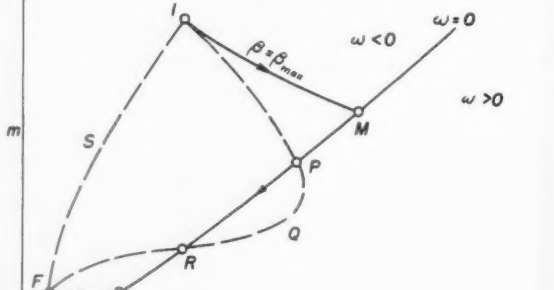


Fig. 4 Comparison between the optimum path and an arbitrary control path (boundary conditions of Type II)

If the control path does not intersect the curve $\omega = 0$ (for instance the pattern ISF) the inequality

$$X_{IMNF} > X_{ISF} \,. \quad [24]$$

is immediately justified on the basis of lemma I.

On the other hand, for a control path intersecting $\omega = 0$

(for instance the pattern IPQRF), the inequality to be proved is

$$X_{IMNF} > X_{IPQRF} \quad [25]$$

which is equivalent to

$$X_{IMP} + X_{PR} + X_{RNF} > X_{IP} + X_{PQR} + X_{RF} \quad [26]$$

The truth of the inequality [26] stems from the circumstance that each term on the left is orderly larger than the corresponding term on the right. As a matter of fact

$X_{IMP} > X_{IP}$, because of lemma I
$X_{PR} > X_{PQR}$, because of lemma II
$X_{RNF} > X_{RF}$, because of lemma I

It must be emphasized that the above mathematical technique has the main advantage of enabling one to account for any number of inequalities imposed upon a variational problem. Moreover, it avoids the difficulties associated with the Legendre, Weierstrass, and Jacobi conditions for the problem under consideration.

The main limitation stems from the circumstance that Green's theorem applies only to linear integrals.[6] Nevertheless, as far as the mechanics of flight is concerned, the above technique is of considerable importance, in so far as linear integrals frequently occur in this type of study. Linear integrals are found, for instance, in the study of the climbing technique for minimum time (4, 5, 6), of the climbing flight for minimum fuel consumption (5, 6), and of the steepest climb (5). Moreover, even the thrust programming for vertical flight (1, 2) may be treated, with a convenient transformation of coordinates, within the general frame of the problems of linear type.

I-9 Considerations on the Range Integral

The expression for the range integral (Equation [11]) may be considerably simplified if the problem is transferred from the (m, V) coordinate system into the (m_*, V) coordinate system, where m_* is a modified mass defined as follows

$$m_* = m \exp [V/V_e] \quad [27]$$

With the introduction of the new variable m_*, Equation [11] reduces to

$$X = V_e \int_{m_{*i}}^{m_{*f}} \frac{\Phi}{m_*} dm_* \quad [28]$$

For the particular case of a coasting flight (m = const), Equations [11] or [28] yield

$$X = \int_{V_i}^{V_f} \Phi \, dV \quad [29]$$

For the other particular case (3) of an ideal pulse burning pattern ($\beta = \infty$), m_* is a constant, because of Equation [8]; therefore Equation [28] yields

$$X = 0 \quad [30]$$

I-10 Remarks on the Composition of the Extremal Path

The extremal paths indicated in Table 2 and Fig. 3 correspond to the most common types of boundary conditions encountered in flight. It is to be noted, however, that for some types of boundary conditions the curve $\omega = 0$ may not participate in the composition of the extremal path.

Consider, for instance, the case of flight designated by II, i.e., the case where the initial point I and the final point F both belong to the low speed region A (Fig. 5). For *given* values of m_i, V_i, V_f the composition of the extremal path is a function of the final mass m_f.

[6] Green's theorem does not apply to the nonlinear case considered in Part II.

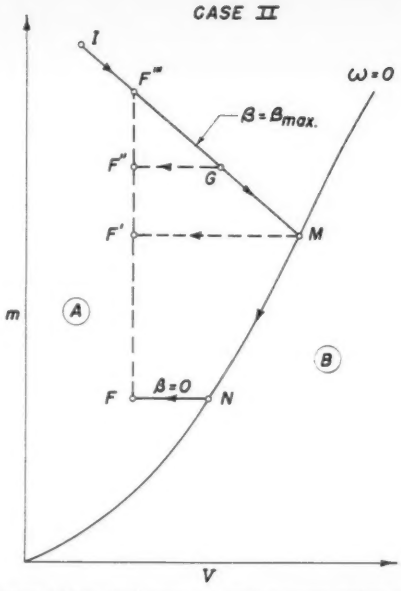


Fig. 5 Effect of the final mass m_f on the composition of the extremal path for boundary conditions of Type II

For $m_f < m_M$, the curve $\omega = 0$ is a part of the extremal trajectory. On the contrary, for $m_f > m_M$ (for instance, $F \equiv F''$) the optimum path is only composed of a flight IG with maximum engine output followed by a coasting pattern GF″.

For the limiting case where F belongs to the curve $\beta = \beta_{max}$ starting at I ($F \equiv F'''$), the coasting flight disappears and the optimum path reduces to the single pattern IF‴ flown with maximum engine output.

Analogous considerations may be developed for the case of flight designated by IV.

I-11 Free and Unfree Variations

An interesting interpretation of the results derived with Green's theorem may be achieved with the method of *free* and *unfree* variations, described in Bolza (13).

Consider, for instance, boundary conditions of type I (Fig. 6). The extremal path is the line IMNF composed of two flights IM and NF with maximum engine output and of a moderate burning MN along $\omega = 0$. The closed line IHKNFGMI bounds the region R where all the admissible arcs belong (Section I-2).

It is to be noted that the portion MN of the optimum path

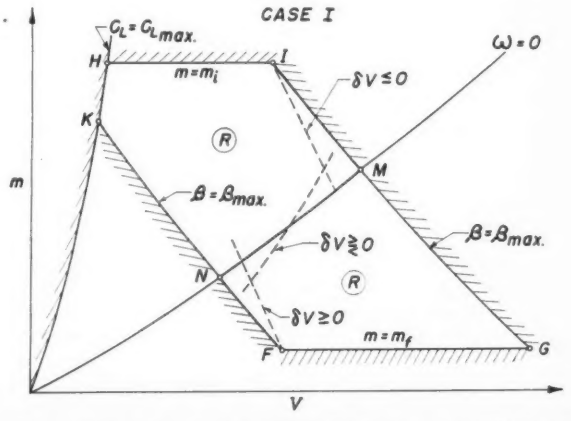


Fig. 6 Free and unfree variations for boundary conditions of Type I

lies in the *interior* of R. On the other hand, the two remaining arcs IM and NF belong to the *boundary curve* IHKNFGMI of the region R.

As a consequence, for a given value of m, variations of the type $\delta V \gtrless 0$ must be considered for the path MN. On the contrary, one-sided variations $\delta V \leq 0$ must be considered along IM and one-sided variations $\delta V \geq 0$ along NF.

According to (13), the above considerations lead to the following conditions to be satisfied for maximum range and for boundary conditions of type I

$$\left.\begin{aligned} \frac{\partial F}{\partial V} - \frac{d}{dm}\left[\frac{\partial F}{\partial V'}\right] &\leq 0, \text{ along IM} \\ \frac{\partial F}{\partial V} - \frac{d}{dm}\left[\frac{\partial F}{\partial V'}\right] &= 0, \text{ along MN} \\ \frac{\partial F}{\partial V} - \frac{d}{dm}\left[\frac{\partial F}{\partial V'}\right] &\geq 0, \text{ along NF} \end{aligned}\right\} \quad \ldots\ldots\ldots [31]$$

where $F = \Phi V' + \Psi$.

The development of [31] leads to

$$\left.\begin{aligned} \omega &\leq 0, \text{ along IM} \\ \omega &= 0, \text{ along MN} \\ \omega &\geq 0, \text{ along NF} \end{aligned}\right\} \quad \ldots\ldots\ldots [32]$$

the function ω being defined by Equation [13].

The method of free and unfree variations, therefore, leads to the conditions to be satisfied by $\omega(V, m)$ in order to achieve maximum range. It is to be noted that the above results are consistent with the hypotheses of Section I-3, i.e., with the properties of which the function ω is physically endowed.

I-12 Problems with Variable End-Points

Green's theorem may also be successfully applied to variational problems with variable end-points as the following example shows.

Suppose that the initial point (m_i, V_i) is fixed and belongs, for instance, to the region A. Suppose also that the final mass m_f is given (Fig. 7), while the final velocity V_f is free of choice.

In such a case the path maximizing the range is composed of a flight IM with maximum engine output, followed by a flight MN with moderate burning along $\omega = 0$ and by a final coasting flight NF having a terminal velocity V_f equal to the stalling velocity V_s corresponding to $m = m_f$.

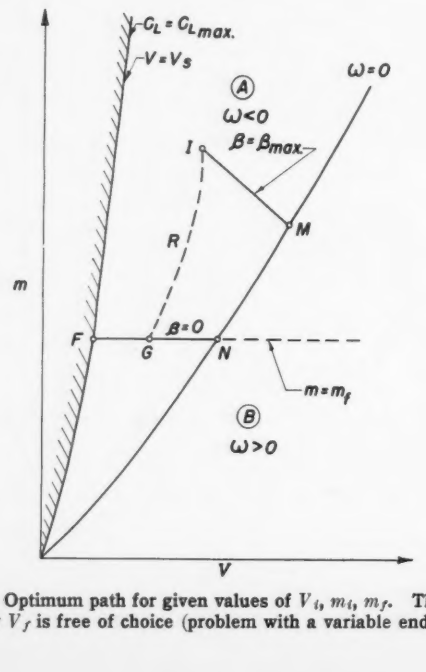


Fig. 7 Optimum path for given values of V_i, m_i, m_f. The final velocity V_f is free of choice (problem with a variable end-point)

To prove the maximal character of the path IMNF, the arbitrary control path IRG starting at I and ending on the generic point G of the line $m = m_f$ is considered for comparison.

The difference of range

$$\Delta X = X_{IMNF} - X_{IRG} \quad \ldots\ldots\ldots [33]$$

is rewritten as

$$\Delta X = (X_{IMNG} - X_{IRG}) + X_{GF} \quad \ldots\ldots\ldots [34]$$

The quantity $X_{IMNG} - X_{IRG}$ is positive, because of lemma I (Section I-4). Moreover, X_{GF} is also positive; it represents the range flown in coasting flight from the condition G to the condition F. It is therefore inferred that $\Delta X > 0$.

I-13 Method of Solution for the Equation $\omega(V,m) = 0$

As it appears from Table 2 and from Fig. 3, the curve $\omega = 0$ plays an important role in the solution of the minimal problem. As a matter of fact, with the only exception of the special case outlined in Section I-10, the curve $\omega = 0$ always enters into the composition of the extremal path. The important property of the curve $\omega = 0$ is that its equation only depends on the characteristics of the aircraft and of the engine. Once the aircraft is known and the engine is known, $\omega = 0$ can be calculated independently of the boundary conditions of the problem.

It is to be noted that for the case where compressibility effects are accounted for the solution of the equation

$$\omega(V,m) = \left[\frac{\partial \Psi}{\partial V}\right]_m - \left[\frac{\partial \Phi}{\partial m}\right]_V = 0 \quad \ldots\ldots\ldots [35]$$

is difficult. Substantial simplifications, however, may be achieved if the problem is transferred from the (m, V)-plane into the (m_*, V)-plane, where m_* is defined by Equation [27]. The transformation of coordinates yields

$$\left[\frac{\partial \Phi}{\partial V}\right]_{m_*} = 0 \quad \ldots\ldots\ldots [36]$$

the function $\Phi(m_*, V)$ being defined by Equation [9].

As a consequence, the problem of finding the solution of $\omega = 0$ is analytically equivalent to determining the minimum of Φ as a function of V for constant values of m_*.

Further improvements may be achieved for special forms of the drag polar. For instance, for a parabolic polar with coefficients depending on the Mach number only, i.e., for

$$C_D = C_{D0}(M) + K(M)\, C_L^2 \quad \ldots\ldots\ldots [37]$$

Equation [36] may be shown equivalent to

$$\left[\frac{\partial \eta}{\partial M}\right]_\alpha = 0 \quad \ldots\ldots\ldots [38]$$

following a transformation from the (V, m_*, Φ) coordinate system into the (M, α, η) coordinate system where

$$\eta(M,\alpha) = \frac{D\alpha}{WM} = \alpha^2 F_0(M) + F_i(M) \quad \ldots\ldots\ldots [39]$$

$$F_0(M) = M\, C_{D0}(M) \exp\,[Ma/V_*] \quad \ldots\ldots\ldots [40]$$

$$F_i(M) = \frac{K(M)}{M^3 \exp\,(Ma/V_*)} \quad \ldots\ldots\ldots [41]$$

$$\alpha = \frac{\gamma p S}{2\, W_r \mu_*} \quad \ldots\ldots\ldots [42]$$

$$\mu_* = \mu \exp\,[Ma/V_*] \quad \ldots\ldots\ldots [43]$$

$$\mu = m/m_r \quad \ldots\ldots\ldots [44]$$

In conclusion, for a drag polar satisfying Equation [37]

finding the solution of $\omega = 0$ is equivalent to locating the minimum of η as a function of M for constant values of α.

Another method of solution consists in using Equation [18]. If the effects associated with the Reynolds number are neglected, Equation [18] yields a straightforward solution for the function μ (M). Such an advantage, however, is counterbalanced by the necessity of estimating the values of the tangents to the diagrams $C_{D0}(M)$, and $K(M)$.

I-14 Similarity Rule for Stratospheric Solutions

The following problem has a special practical importance: "Given the function $\mu_1(M_1)$ which is the solution of $\omega = 0$ at $h = h_1$ to determine the new function μ_2 (M_2) solution of $\omega = 0$ at $h = h_2$."

For stratospheric flight $(da/dh = 0)$, Equations [38] to [44] show that a constant value of α $(\alpha_1 = \alpha_2)$ at two different altitudes $h_1 \neq h_2$ determines the *same* solution $M_1 = M_2$. From Equation [42] it follows

$$\frac{\mu_2}{\mu_1} = \frac{\rho_2}{\rho_1} \quad \ldots\ldots\ldots\ldots\ldots\ldots\ldots\ldots [45]$$

Knowing the solution of $\omega = 0$ at $h = h_1$, the new solution at $h = h_2$ is therefore obtained by amplifying the ordinates of the μ (M) diagram according to the *scale factor* ρ_2/ρ_1 (Fig. 8).

It is to be noted (Equation [19]) that the above simple similarity rule is also true for tropospheric flight $(da/dh \neq 0)$ as long as the polar is parabolic and has constant coefficients.

I-15 Thrust Required along the Curve $\omega = 0$

It is of interest to determine the amount of thrust required to maintain the aircraft along the optimum path.

From Equation [6] and from the definition of thrust $(T = \beta V_s)$ the following expression is derived

$$D/T = 1 + m\, V'/V_s \quad \ldots\ldots\ldots\ldots\ldots\ldots [46]$$

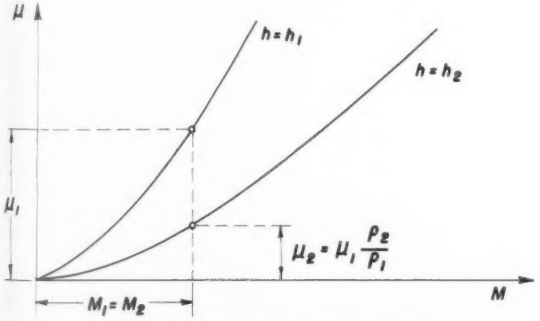


Fig. 8 Similarity rule for stratospheric solutions

Since V' is positive along $\omega = 0$, one deduces that the controls of the rocket engine must be adjusted in such a way as to generate, at all points of $\omega = 0$, a thrust less than the drag of the aircraft.

For the special case of a parabolic polar with constant coefficients C_{D0} and K, Equations [19] and [46] yield

$$\frac{T}{D} = \frac{\lambda + 2(\lambda + 1)(\lambda + 3)}{\lambda + (\lambda + 1)(\lambda + 2)(\lambda + 3)} \quad \ldots\ldots\ldots [47]$$

where $\lambda = V/V_s$.

The above equation is rigorously valid for the incompressible flow case. Nonetheless, it gives a good qualitative idea of the thrust required for the compressible flow case, as long as dC_{D0}/dM, dK/dM are reasonably small as it occurs in the all-supersonic region. In this connection it is to be noted that the thrust required at supersonic Mach numbers along $\omega = 0$ may be considerably less than the drag of the aircraft.

For the transonic region, however, Equation [47] is no longer valid. It underestimates the thrust-drag ratio required, which (for this flow region) is a number close to unity.

I-16 Numerical Example[7]

To evaluate the engineering importance of the previous results, a numerical example is carried out for a hypothetical aircraft identical in shape to the AGARD model No. 2. Such a model is described in (17). It combines a fuselage of fineness ratio 8.5 with a delta-wing having a circular arc section 4 per cent thick and embodies small vertical fins necessary for lateral stabilization in flight.

A polar of the form [37] is assumed. The function $C_{D0}(M)$ is known from flight test data (17). The function $K(M)$, which determines the so-called induced drag, is estimated on the basis of available theoretical and experimental information.

The following data are considered for the aircraft:

$$W_r = 13{,}191 \text{ lb}$$
$$S = 269 \text{ sq ft}$$
$$V_s = 6600 \text{ fps}$$

The atmospheric air is assumed a diatomic gas with $\gamma = 1.4$. In addition, the speed of sound is assumed $a = 971$ fps (stratospheric flight).

Fig. 9 indicates the function $M(\alpha)$ which solves $\omega = 0$ for stratospheric flight, according to Equations [38] to [44].

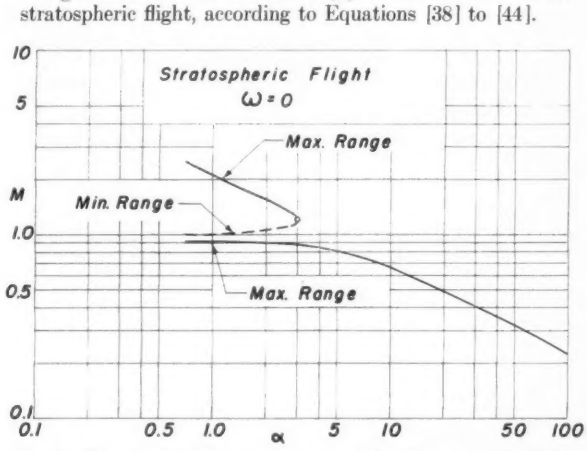


Fig. 9 Solution of the equation $\omega = 0$ for stratospheric flight

For high values of α the solution of Equation [38] is unique; on the other hand, for low values of α several Mach numbers, corresponding to stationary values of η, exist. Careful analysis (Fig. 9) points out the existence of three solutions for $\alpha < 3$: a subsonic-transonic solution of *maximum range* (lower curve); a transonic solution of *minimum range* (dotted line, intermediate curve) having no interest for flight operations; and a supersonic solution of *maximum range* (higher curve).

It is to be noted that only one region of best range was detected by Hibbs (3) due to the fact that he considered a parabolic polar with coefficients independent of the Mach number. The present theory, on the contrary, accounts for compressibility effects and leads to the existence of two regions of best range, one subsonic-transonic, the other one supersonic.

This result is interesting, but hardly surprising. As a matter of fact, in a mathematically analogous problem (6), i.e., the optimum climbing technique for a rocket-powered aircraft, the writer had already detected the existence of two regions of best climb, one subsonic-transonic, the other one supersonic.

[7] This author is indebted to S. A. Ellis, W. B. Fouts, and J. D. Mulholland, undergraduate students at Purdue University, for their fine cooperation in the numerical analyses and in the preparation of the drawings of Part I of the present report.

Fig. 10 translates the data of Fig. 9 from the (M, α) language into the more understandable (M, μ) language for the particular altitude h = 70,000 ft. The solution at any other stratospheric altitude may be readily obtained by using the similarity rule indicated in Section I-14.

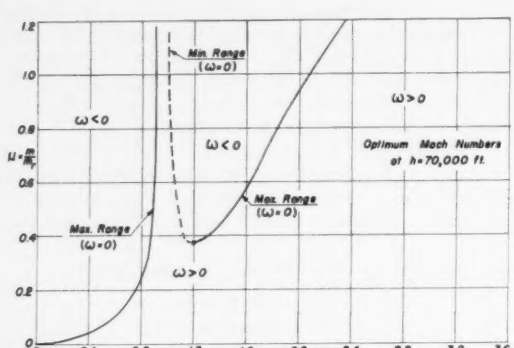


Fig. 10 Solution of the equation $\omega = 0$ at h = 70,000 ft

I-17 Occurrence of an Infinite Number of Extremals

The optimum paths indicated in Fig. 3 and the proof of Section I-8 are based on the assumption that *only one* solution exists for the equation $\omega = 0$. The above hypothesis is fully verified for the case where the airstream is incompressible, as Equation [19] shows.

On the other hand, for the delta-wing-fuselage combination of [17], compressibility effects determine the existence of two solutions of $\omega = 0$ having flight interest.

For such a case, a further investigation is in order. Consider, for instance, the case of an initial supersonic condition I and of a final subsonic condition F (Fig. 11).

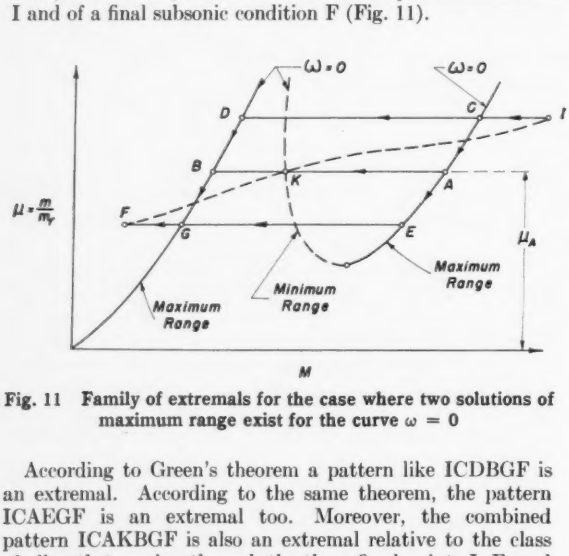


Fig. 11 Family of extremals for the case where two solutions of maximum range exist for the curve $\omega = 0$

According to Green's theorem a pattern like ICDBGF is an extremal. According to the same theorem, the pattern ICAEGF is an extremal too. Moreover, the combined pattern ICAKBGF is also an extremal relative to the class of all paths[8] passing through the three fixed points I, F, and K; the third one being the point where the curve $m = m_A = m_B$ intersects the solution of $\omega = 0$ corresponding to *minimum range* (Fig. 11).

The variational problem has, therefore, a special mathematical structure, in so far as the occurrence of two curves $\omega = 0$ implies the existence of an infinite number of extremals, all satisfying the same boundary conditions.

The next step is to establish which of these infinite extremals is to be preferred from the point of view of maximizing the range. This problem evidently does not belong any more to the domain of the calculus of variations. It rather belongs to the ordinary theory of maxima and minima.

As a matter of fact, for the family of extremals now defined, the range from the condition I to the condition F *only* depends on the mass ratio μ_A at which the gliding from the supersonic solution to the subsonic solution is performed. In this connection some typical computations are illustrated in Fig. 12.

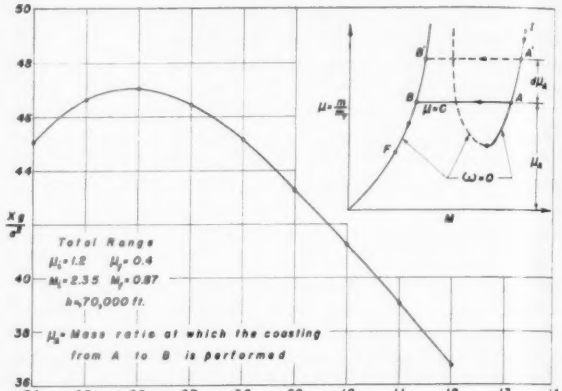


Fig. 12 Range associated with the family of extremals IABF

Fig. 12 refers to the following boundary conditions. The initial point I ($\mu_i = 1.2$; $M_i = 2.35$) is located on the high-speed solution of $\omega = 0$; the final point F($\mu_f = 0.4$; $M_f = 0.87$) is located on the low-speed solution of $\omega = 0$. The curve IABF is a member of the family of extremals for the problem under consideration, each element of the family being characterized by a different value of μ_A. The propellant mass is $^2/_3$ of the initial mass of the aircraft and the altitude of flight is h = 70,000 ft.

The range X associated with the above family of extremals is plotted (Fig. 12) as a function of μ_A. Results show that—for the boundary conditions here considered—the range has a maximum when the gliding is performed at $\mu_A = 0.6$. In other words, the achievement of the best technique of flight demands: (a) to use the supersonic solution up to the moment when the mass of the aircraft is about 50 per cent of the initial mass; (b) to glide to the subsonic region; (c) finally to use the subsonic solution.

Results, however, strongly depend on the boundary conditions of the problem, as is shown by Fig. 13. The new set of boundary conditions is as follows. The initial point I ($\mu_i = 1.2$; $M_i = 0.91$) is located on the low-speed solution of $\omega = 0$; the final point F($\mu_f = 0.4$; $M_f = 1.31$) is located on the high-speed solution of $\omega = 0$. The curve IABF is a member of the family of extremals for the problem under considera-

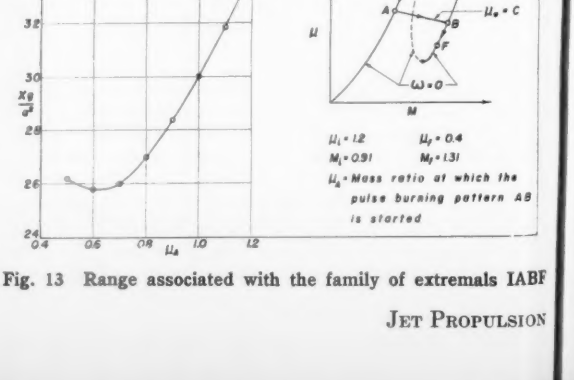


Fig. 13 Range associated with the family of extremals IABF

[8] The extremal nature of the generic pattern ICAKBGF may be proved both with Green's theorem and with the method of partial variations (13).

tion, each element of the family being characterized by a different value of μ_A, the mass ratio at which the aircraft leaves the subsonic solution of $\omega = 0$ to accelerate to the supersonic region. The pattern AB is a curve $\beta = \beta_{max}$. Due to the qualitative character of the example and in order to simplify the computations, such a trajectory is replaced with a pulse burning pattern $\mu_* = \text{const.}$

In Fig. 13 the range X associated with the above family of extremals is plotted as a function of μ_A. Results show that—for the boundary conditions considered here—it is convenient to fly as much as possible along the supersonic solution, avoiding completely the use of the subsonic branch of $\omega = 0$.

I-18 Criterion for the Choice of the Best Extremal

Green's theorem may lead to an interesting qualitative criterion for the choice of the best extremal for the case where two solutions exist for the equation $\omega = 0$.

Consider, for instance, the condition of flight analyzed in Fig. 12 and focus the attention on the family of extremals IABF, for which $X = f(m_A)$. The *optimum* extremal has to satisfy the obvious condition

$$\frac{dX}{dm_A} = 0 \qquad [48]$$

By applying Green's theorem, the infinitesimal variation of range between the path IABF and the neighboring path IA'B'F may be calculated

$$dX = X_{IA'B'F} - X_{IABF} = dm_A \int_{V_B}^{V_A} \left(\frac{\partial \Psi}{\partial V} - \frac{\partial \Phi}{\partial m} \right) dV \qquad [49]$$

the above integral being evaluated along the line $m = m_A = m_B$. From Equations [48] and [49] one obtains the following final expression

$$\int_{V_A}^{V_B} \frac{\partial \Phi}{\partial m} dV = \Psi_B - \Psi_A \qquad [50]$$

the integral on the left-hand side of Equation [50] being evaluated along the line $m = m_A = m_B$. Equation [50] defines $(m_A)_{opt}$ and, therefore, identifies the *best* possible extremal.

Analogous criteria may be developed for other types of boundary conditions.

I-19 Limitation Concerning the Lift Coefficient

To verify the limitation (12) concerning the lift coefficient, the value of C_L is calculated for the points of the curve $\omega = 0$. For the particular case of a parabolic polar with constant coefficients, the following result is obtained

$$C_L/C_{LE} = \sqrt{(\lambda + 1)/(\lambda + 3)} \qquad [51]$$

where $\lambda = V/V_*$ and $C_{LE} = \sqrt{C_{D0}/K}$. From Equation [51] the inequality $C_L \leq C_{LE}$ follows, C_{LE} being the lift coefficient corresponding to the maximum lift-drag ratio. It may be therefore inferred that the inequality $C_L \leq C_{Lmax}$ is satisfied at all points of the curve $\omega = 0$.

The above conclusions, however, may be subject to modifications for the case where a drag polar of the form [37] is used, as for instance, in the numerical example of Section I-16 (Fig. 10). As a matter of fact, for high mass ratios $\mu = m/m_r$, the curve $C_L = C_{Lmax}$ may intersect the low-speed solution of $\omega = 0$.

Should this possibility develop, the solution of the variational problem would change. Let the coordinates of the hypothetical intersection point of $\omega = 0$ with $C_L = C_{Lmax}$ be designated as $\bar{V}$, $\bar{M}$. Once more with the help of Green's theorem one may show that for $m > \bar{m}$ the extremal $\omega = 0$ is to be replaced by an arc $C_L = C_{Lmax}$. The obvious proof is omitted.

I-20 Conclusions

Green's theorem is applied to the solution of the variational problem associated with the optimum burning program for horizontal flight. A straightforward method for determining extremal paths under different types of boundary conditions is devised.

The technique of maximum range is constituted by the combination of coasting maneuvers, patterns with maximum engine output and flights with moderate burning according to Equation [17].

From a mathematical point of view, the main result of the paper consists in supplying a complete proof of the necessary and sufficient conditions for maximum range and in pointing out the possible existence of an infinite number of extremals satisfying the same differential equations and the same boundary conditions.

From an engineering point of view, the main result consists in extending previous studies to the case where compressibility effects are accounted for and in determining the existence of two regions of best range: one subsonic-transonic, the other one supersonic.

PART II SOLUTION BY MULTIPLIERS METHOD FOR THE CASE OF A GENERIC THRUST CHARACTERISTIC

Placido Cicala

IN A previous note (7) general equations for determining optimum techniques of flight have been presented. An application of these results to the solution of Part I is developed here under more general hypotheses concerning the behavior of the power plant, namely, an arbitrary one-to-one correspondence between thrust T and fuel expenditure β. All the remaining assumptions are identical to those of Part I. Thus the fundamental equations are

$$m\dot{V} + D - T = 0 \qquad [52]$$

$$T = T(\beta) \qquad [53]$$

$$\beta = -\dot{m} \qquad [54]$$

$$D = D(V,L) \qquad [55]$$

$$L = mg \qquad [56]$$

$$\dot{X} = V \qquad [57]$$

II-1 Necessary Conditions for the Optimum

For the problem under consideration the Euler-Lagrange equations (Ref. 8, p. 203) reduce to[9]

$$\dot{\lambda} - \lambda D_v/m + 1 = 0 \qquad [58]$$

$$\dot{\mu} + \lambda[D - T - LD_L]/m^2 = 0 \qquad [59]$$

$$p = dT/d\beta \qquad [60]$$

where $\lambda = \lambda(t)$, $\mu = \mu(t)$ are Lagrange multipliers and $p = \mu m/\lambda$.

Since the time does not explicitly appear in the problem, the following first integral holds[10]

$$V + \lambda\dot{V} = \mu\beta \qquad [61]$$

When this equation is used, Equation [59] may be discarded. Equations [52] to [56], [58], [60], and [61] form a

[9] See (7), Eqs. [13], [14], and [17]. In (7) the quantities μ and λ are respectively indicated as λ_5/λ_1, and λ_3/λ_1. Furthermore, the drag D is considered a function of velocity, height, and angle of attack. The meaning of the partial derivative D_v in (7) is therefore different from the one used here.

[10] See (7), Eq. [15]. The natural condition $c = 0$ is employed here.

third order differential system;[11] initial values for V, m, and t and final values for V and m may be prescribed. The range is subsequently calculated by integrating Equation [57].

In practice, it is not generally feasible to attack the problem in its boundary value form. The differential system must be solved by stepwise integration so that all data must be known at one end-point. As a consequence, if the conditions are prescribed at both end-points, the use of a trial-and-error procedure is in order.

The elimination of the Lagrange multipliers from Equations [58], [60], and [61] leads to an equation which completes the system of Equations [52] to [57], conferring the extremal character to the solution. This technique, however, does not generally bring any simplifications into the computational procedure. For this reason and also because of both the physical meaning of the multipliers and of their use as controlling indexes for the composition of the optimum path, it is not convenient to eliminate λ and μ. The importance of the multipliers and of the quantity p, designated here as *index value*, is stressed by the following application which refers to the comparison of neighboring solutions. Suppose that an extremal path has been found, leading from an initial condition m_i, V_i, for which $\lambda = \lambda_i$, $\mu = \mu_i$ to a final condition m_f, V_f for which $\lambda = \lambda_f$, $\mu = \mu_f$. If an infinitesimal variation of the boundary conditions is considered, the multipliers enable one to determine the corresponding variation in range along the extremal path. If the range X of the Eulerian trajectory is considered as a function of the boundary conditions, i.e., $X = X(V_i, V_f, m_i, m_f)$, one finds[12]

$$\lambda_i = \frac{\partial X}{\partial V_i} \qquad \lambda_f = -\frac{\partial X}{\partial V_f} \qquad [62]$$

$$\mu_i = \frac{\partial X}{\partial m_i} \qquad \mu_f = -\frac{\partial X}{\partial m_f} \qquad [63]$$

This means, for instance, that if the initial velocity is increased by δV_i (the other boundary conditions remaining the same), the range for the extremal path[13] increases by $\lambda_i \delta V_i$. Equations [62] and [63] supply therefore an immediate answer to many questions concerning the relationships between aircraft performance and project parameters.

II-2 The Legendre, Weierstrass, and Jacobi Conditions

According to (7) the conditions of Weierstrass and of Legendre-Clebsch are satisfied in their strengthened form if the thrust characteristic[14] is convex; that is, if $d^2T/d\beta^2 < 0$ everywhere. In (7) it has been shown that if the above inequality does not hold at all points of the thrust curve, the optimum technique of flight will follow a somewhat modified characteristic, represented by the configuration of a tight wire stretched over the original diagram as if it were a solid contour. Fig. 14 shows a hypothetical characteristic (shadowed contour). For maximum range, part of the curve is replaced by the straight dotted segments which bridge the concavities.[15]

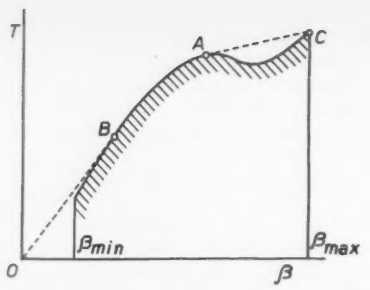


Fig. 14 Hypothetical thrust-burning rate relationship

The investigation of the Jacobi-Mayer condition is much more difficult. Its form depends on the boundary conditions of the problem, i.e., on their fixed or variable end-point nature. From a practical point of view, it is convenient to examine the above condition in a geometrical way, by constructing a field containing the solution to be checked:[16] this field must be *simply* covered with extremals in the neighborhood of the solution under consideration. In this way a set of sufficient conditions for the optimum is completed.

II-3 Polygonal Characteristic

It is now assumed that the characteristic of the power plant is formed by a broken line with straight sides. Let $A_1, A_2, \ldots A_n$ be the corner points (Fig. 15), β_i and T_i the coordinates of A_i ($i = 1, 2, \ldots, n$). Let A_0 (a vertex of the characteristic) be the origin of the coordinate system ($\beta_0 = 0 = T_0$).

The equation of the side $A_{i-1}A_i$ is written in the form

$$T = a_i + b_i\beta \qquad [64]$$

where

$$a_i = (T_{i-1}\beta_i - T_i\beta_{i-1})/(\beta_i - \beta_{i-1})$$
$$b_i = (T_i - T_{i-1})/(\beta_i - \beta_{i-1})$$

From a heuristic standpoint the general conclusions of (7) concerning the nature of the extremal paths[17] for the case of a broken thrust curve, may be readily interpreted if the polygonal diagram is considered as the limiting case of a line having a continuous variation of slope. In this connection one may state that the Weierstrass condition requires that the polygon be convex, i.e., that the whole diagram be located below the straight line containing any of its sides. Furthermore, after focusing the attention on the index value p and on Equation [60], one may deduce that:

(a) If the representative point of the instantaneous condition of flight in the (β, T) diagram occupies a position along the side $A_{i-1}A_i$, then the index p has the value $p = b_i$.

(b) If the value of p ranges between the slopes b_i, b_{i+1} of two adjacent sides of the thrust diagram, then the representa-

[11] Should the mass be chosen as an independent variable and the time eliminated by means of $dt = -(dm/\beta)$, the differential system would reduce to second order, but the coasting flight ($\beta = 0$) would be ruled out.

[12] These properties of the Eulerian solution may be deduced from the equations of virtual displacements for the end-points I, F of the extremal path. With the notation of (7), these equations are written as $\delta^*(I) = \delta^*(F)$. In a somewhat different form this principle is embodied in theorem 2:1 of (9).

[13] Obviously λ cannot be negative. Should the flight technique of an Eulerian solution be modified by introducing a short initial coasting that lowers the initial velocity by δV_i, the range would be increased by $(mV/D - \lambda)_i \delta V_i$. The possibility that the above quantity be positive must be ruled out, not only for the two end-points but also for any other point of the extremal, since every elementary piece of extremal is locally a solution of maximum range when compared with any other neighboring path. It is consequently inferred that $\lambda \geq mV/D$ everywhere.

[14] The general Eq. [24] of (7) contains a multiplier which must be positive for a solution of maximum range, according to the previous footnote.

[15] The power plant may theoretically operate at any point of the dotted segment AC by means of high-frequency alternations between the conditions A and C. For instance, the midpoint of AC may be attained by operating the jet during equal time intervals at points A and C. Such an ideal possibility implies evidently the hypothesis that the jet control system has zero inertia.

[16] To carry on this construction the time t may be eliminated. In accordance to the suggestions of Bliss and Hestenes, the field should be constructed in the three-dimensional space (V, m, X). When possible, it is convenient to use a two-dimensional projection (e.g., on a V, m-plane) according to (10).

[17] According to authoritative sources (8), the discontinuous solutions of a variational problem should not be called *extremals*. The denomination of *extremaloids* is also to be excluded here in view of the singular character of the present problem. As a consequence, the actual solutions will be designated as *extremal paths*.

tive point of the aircraft occupies the corner position A_i. Analogously, if $p < b_n$, the mass flow is $\beta = \beta_n$, whereas a coasting flight ($\beta = 0$) corresponds to an index value $p > b_1$.

It is therefore inferred that the extremal path may be composed of:

(a) arcs along which $p = b_i$ ($i = 1, 2, \ldots . n$) designated here as b_i arcs.

(b) arcs along which $\beta = \beta_i (i = 1, 2, \ldots . n)$ designated here as β_i arcs. In particular, the coasting flight is referred to as a β_0 arc.

The configuration of the above arcs is now first analyzed in the (V, m)-plane with the object of determining the behavior of the multipliers. For the b_i lines ($p = b_i$, $\mu = \lambda b_i/m$), Equation [61] yields

$$\lambda = \frac{mV}{D - a_i} \ldots\ldots\ldots\ldots\ldots\ldots [65]$$

From Equations [58] and [65] the following result is obtained:

$$(D - a_i)(b_i - V) + mg\, VD_L - b_i VD_v = 0 \ldots . [66]$$

Equation [66] is a relationship in finite terms between V and m which is represented by a single curve[18] for each pair of values a_i, b_i. From Equation [66] the value of dV/dm may be calculated. The burning rate is hence determined by means of the expression

$$\beta \left[b_i + m \frac{dV}{dm} \right] = D - a_i \ldots\ldots\ldots\ldots [67]$$

which is derived from Equation [52]. The significant arc of the curve represented by Equation [66] is bounded by the points where the burning rate β calculated from Equation [67] attains the values β_{i-1} and β_i. For the example of Section II-4, the arcs corresponding to the sides A_0A_1, A_1A_2, A_2A_3 of the thrust diagram (Fig. 15) are respectively represented by the arcs B_1C_1, B_2C_2, B_3C_3 of Fig. 16.

The determination of the β_i lines (or lines of constant thrust $T = T_i$) requires the integration of Equation [52]. A one-parameter family of curves corresponds to each value of T_i, all these curves ending at that point of the V-axis where the zero-lift drag equals T_i. One sample curve is represented by the line (c) of Fig. 16 and refers to $\beta = \beta_1$ (point A_1 of Fig. 15). Some of these curves, like the one represented, show decreasing velocities in the upper part and increasing velocities in the lower part. The point where the tangent is parallel to the m-axis corresponds to the condition $D = T_i$. The dotted line (l) of Fig. 16 represents the locus of such points

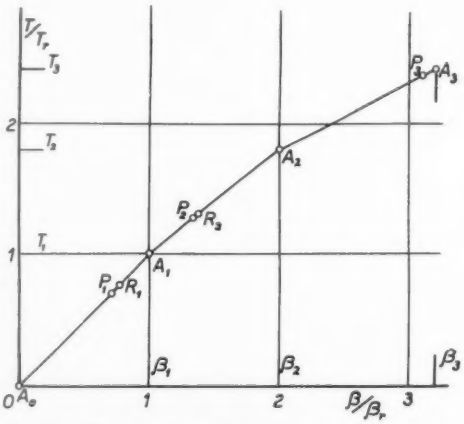


Fig. 15 Polygonal thrust-burning rate relationship

[18] It is here assumed that Eq. [66] establishes a one-to-one correspondence between V and m. This is the case when a parabolic polar with constant coefficients (Eq. [71]) holds.

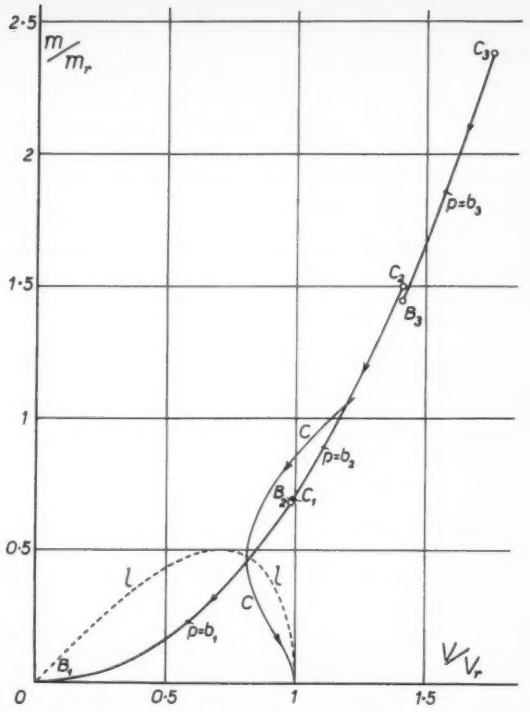


Fig. 16 Basic curves in the (V, m)-plane for the case of a polygonal thrust characteristic

for $T = T_1$. The β_i lines that do not penetrate within the contour $D = T_i$ show decreasing velocities everywhere.

The solution of Equation [58] is expressed by

$$\lambda(t) = \varphi(t) \left[\lambda(t_0) - \int_{t_0}^{t} \frac{dt}{\varphi} \right] \ldots\ldots\ldots\ldots [68]$$

where

$$\varphi(t) = \exp \left[\int_{t_0}^{t} \frac{D_v}{m}\, dt \right] \ldots\ldots\ldots\ldots [69]$$

From Equation [68] the value of λ may be calculated along a β_i curve once its value at one particular point $t = t_0$ is known. The index value is consequently calculated from Equation [61] which may be rewritten as

$$p = \frac{mV}{\beta\lambda} + \frac{T - D}{\beta} \ldots\ldots\ldots\ldots [70]$$

The relationship $\lambda = mV/D$ holds[19] for the β_0 line (coasting flight). The multiplier μ can be obtained[20] by integration of Equation [59].

The next question is to establish how these particular solutions are to be joined together to form an extremal path. For this purpose the Weierstrass-Erdman corner conditions (8, p. 203) are used; these conditions require (7) that the values of the multipliers, and consequently of p, be continuous at the junction points. This is the main concept for the analysis of two possible cases:

(a) junction of a curve $\beta = \beta_i$ with a curve $\beta = \beta_{i-1}$ or $\beta = \beta_{i+1}$.

(b) junction of a curve $p = b_i$ with a curve $\beta = \beta_{i-1}$ or $\beta = \beta_i$.

[19] This value of λ is deduced from Eqs. [52], [61] and agrees with Eq. [58].

[20] As a matter of fact, Eq. [59] cannot be stated for the lines m = const without a further analysis, since it is derived by varying m. Eq. [59], however, may be proved to hold, by direct comparison of varied extremals and by means of Eq. [63].

For the first case the transition occurs when the index p along the β_i curve reaches the limiting values b_i or b_{i+1}, respectively.

Transitions of the second type may occur at any point of a b_i line. The location of the corner and the type of adjoining curve (a β_i arc or a β_{i+1} line) depend on the position of both terminals of the extremal path.[21] If the value of λ given by Equation [65] is replaced in Equation [70], one obtains $p = (T - a_i)/\beta$. This equation is satisfied by $p = b_i$, $T = T_i$, $\beta = \beta_i$, as well as by $p = b_i$, $T = T_{i-1}$, $\beta = \beta_{i-1}$. Both these transitions, therefore, may occur without any discontinuity in the multipliers.

II-4 Numerical Example

The above concepts are now used to construct a V, m diagram[22] of extremal paths having their common terminal at a fixed point 0. It is assumed that the thrust curve is formed by three straight sides (Fig. 15).

A parabolic drag polar

$$D = AV^2 + B\frac{m^2}{V^2} \qquad [71]$$

with constant coefficients A, B is considered. The reference magnitudes for Figs. 15, 16, 17 and the data for the thrust curve are

$$V_r = b_1 \quad m_r = b_1^2\sqrt{A/B} \quad T_r = Ab_1^2 \quad \beta_r = Ab_1$$

$$\beta_1 = \beta_r \quad \beta_2 = 2\,\beta_r \quad \beta_3 = 3.2\,\beta_r$$

$$T_1 = T_r \quad T_2 = 1.8\,T_r \quad T_3 = 2.4\,T_r$$

The lines $p = b_1$, $p = b_2$, and $p = b_3$ are, respectively, represented by the curves B_1C_1, B_2C_2, and B_3C_3 of Fig. 16 and by the arcs 1–2–3, 6–7–8, and 11–12 of Fig. 17. The end-points 3, 8, 12 of Fig. 17 correspond respectively to the end-points C_1, C_2, C_3, of Fig. 16.

The extremal paths are now determined starting from the point of arrival. The integration procedure is therefore performed backward.

The process starts with the extremal paths for which the index value is $p = b_1$, at points of the line 0–1 (a β_0 line) where $\lambda = mV/D$ (Fig. 17). The junction $(\beta_1 \rightarrow \beta_0)$ occurs[23] on the line 0–1. The subsequent integration along the line $\beta = \beta_1$ leads to a point where the index p attains the value b_2. At such a point the junction $(\beta_2 \rightarrow \beta_1)$ takes place.[24] The dotted line 5–5* is a *corner line* (11), i.e., the locus[25] of the transition points between lines $\beta = \beta_1$ and $\beta = \beta_2$.

Another class of paths contains part of the curve $p = b_1$ (arc 1–3). Any point of this arc may be reached either through a line $\beta = \beta_0$ or through an arc $\beta = \beta_1$. The first case corresponds to initial points located at the right of the arc 1–3 between the lines $m = m_1$, and $m = m_3$. For the second case, the arc 2–6, of equation $\beta = \beta_1$, has a particular importance. Along this arc the index value starts from $p = b_1$ at point 2 and reaches the value $p = b_2$ at point 6, i.e., just at the intersection with the b_2 line. For the arcs $\beta = \beta_1$ starting at points of the line 1–2 ($p = b_1$) the index p reaches the value b_2 at points of the corner line 5–6. Such a corner line is the locus of the junctions $(\beta_2 \rightarrow \beta_1)$.

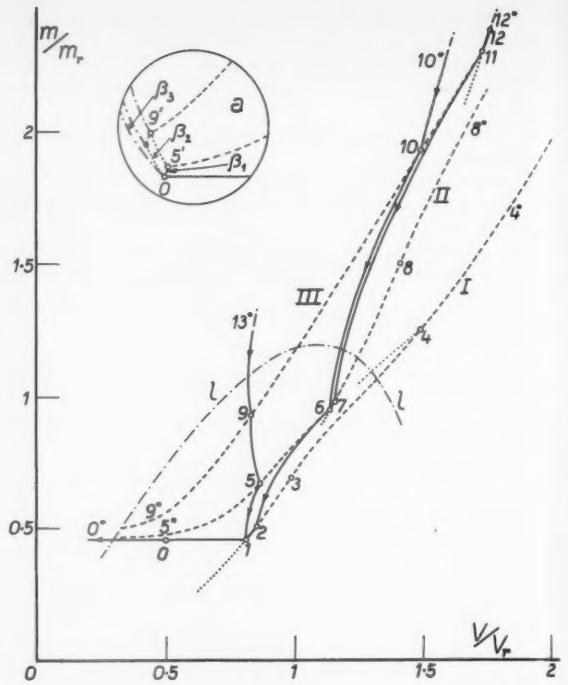


Fig. 17 Extremal paths for the case of a polygonal thrust characteristic

For the arcs $\beta = \beta_1$, ending at points of the line 2–3, the index p never attains the value b_2. As a matter of fact—along these arcs—p initially decreases, but soon increases again attaining the value $p = b_1$ at points located on the arc 3–4. The arc 3–4, therefore, belongs to that corner line along which the junction $(\beta_1 \rightarrow \beta_0)$ occurs. The arc 2–6 ($\beta = \beta_1$) is here called a *bridge*, because all paths coming from the b_2 line pass through it to the b_1 arc.

The process is now continued according to the concepts previously outlined. Starting from the corner line 5–6 the lines $\beta = \beta_2$ are integrated. The new corner line 9–10 is the locus of the junction $(\beta_3 \rightarrow \beta_2)$. Other possible paths have a part in common with the arc 6–8 ($p = b_2$). The integrations are now performed starting from points of the arc 6–8 and moving along lines $\beta = \beta_1$ or $\beta = \beta_2$. Concerning the lines $\beta = \beta_1$ the index p reaches the value $p = b_1$, at points of the line 4–4* where the junction $(\beta_0 \rightarrow \beta_1)$ occurs. For the arcs $\beta = \beta_2$ there are two possibilities: (a) the index p attains the value b_3 along $\beta = \beta_2$, (b) the index value never attains the value b_3. For the subcase (a) one may determine the arc 10–11 of the corner line where the junction $(\beta_3 \rightarrow \beta_2)$ occurs. Such an arc ends at point 11 on the line $p = b_3$. Concerning the subcase (b), one may proceed to the construction of the arc 8–8* where the junction $(\beta_1 \rightarrow \beta_2)$ occurs. The arc 11–7 ($\beta = \beta_2$) is the *bridge* between the arc 11–12 ($p = b_3$) and the arc 6–7 ($p = b_2$).

It is evident that this procedure may be repeated along the same lines for the case where the polygonal characteristic has a greater number of sides.

The zone of the diagram near the end-point 0 is represented (enlarged scale) in the circle of Fig. 17. The β_1 line 5′–0 breaks the corner line 5–5* and forms a locus for corners $(\beta_2 \rightarrow \beta_1)$. Similarly, the β_2 arcs ending at points

[21] See, e.g., the case of a straight characteristic (Part I). The position of the transition points to and from the curve $\omega = 0$ (that is, the line $p = b$) is defined by the location of the two end-points of the extremal path. In such a case the initial-value problem is undetermined, while the boundary-value problem is determined.

[22] In connection with the singular character of the problem, the graph fails to comply with some of the conditions of a Mayer field; for instance, infinite solutions pass through the points of a line $p = b_i$. Nonetheless, it can be used to carry on a sufficiency proof of the solution.

[23] The transition from a β_i line to a β_{i-1} line is indicated with the symbol $(\beta_i \rightarrow \beta_{i-1})$. The transition from a β_i line to a b_i line is designated as $(\beta_i \rightarrow b_i)$.

[24] Thereafter, the index value b_2 is reached once again. The branch of corner line consequently obtained must be discarded because it does not satisfy the condition requiring that the two positive directions of the tangents at the corner point lie on the same side of the corner line (11, Section 10-c).

[25] A numeral with an asterisk denotes generic point. Thus, for instance, 13* is the generic point of the line $\beta = \beta_3$ passing through 9 (Fig. 17).

of the arc 0–5′ determine the last part of the broken corner line 9*–9′–0 for junctions ($\beta_3 \rightarrow \beta_2$). From this representation it is evident that some paths end at 0 without a final coasting, some even without a β_1 arc. The line $\beta = \beta_3$ and the line $m = m_0$ passing through 0– constitute the *border* lines for that zone of the (m, V)-plane from which an extremal path can lead to 0. This area is called here a *covered zone.*

The composition of the extremal paths for the above covered zone is clearly pointed out by the corner lines I, II, III, i.e., by the lines 0–1–2–3–4–4*, 0–5′–5–6–7–8–8* and 0–9′–9–10–11–12–12*. The above lines divide this area into four regions

(a) the β_3 region, above line III.
(b) the β_2 region between lines III and II.
(c) the β_1 region between lines II and I.
(d) the β_0 region between line I and the lower border line.

In every β_i region the Eulerian paths are composed of β_i arcs. When the extremal path intersects a corner line, it crosses it, enters into an adjacent region, and experiences, in general, a change in slope. An exception, however, is represented by the case where the intersection occurs on the part of a corner line which belongs to a b_i curve. In such a case the extremal path follows the successive b_i arcs and the transition lines designated as bridges.[26]

It appears, therefore, that, once the corner lines corresponding to a given end-point 0 are traced, the extremal path starting from any point (m, V) of the covered zone may be immediately found. The resulting solution is unique in any case.[27] Let A, B be any pair of points located on one of these extremal paths, the point B being closer to 0 than point A; let $X(A, B)$ be the range along the extremal path AB; let $X'(AB)$ be the range associated with any other nonextremal path joining the same end-points A, B. One may show that $X(A, B) > X'(A, B)$ in any case.[28]

The configuration of the corner lines is modified, of course, if the position of the end-point 0 is changed. It is to be noted, however, that the modification only affects a part of the (m, V) graph. For example, a decrease in the velocity of point 0 modifies only the part at the left of the line 9′–5′–0; a decrease in the final mass influences only the part at the left of the line 13*–9–5–1; an increase in final mass[29] leaves unchanged the part of the diagram at the right of the line 10*–10–6–2, provided $m_0 < m_2$.

[26] For example, if the initial point belongs to a line $\beta = \beta_3$ intersecting the arc 11–12, the following extremal path (Fig. 17) is the line 11–7–6–2–1–0. The corresponding points of the thrust characteristic (Fig. 15), which represents the operation of the jet are as follows: P_3 (point 11), A_2 (arc 11–7), R_2 (point 7), P_2 (point 6), A_1 (arc 6–2), R_1 (point 2), P_1 (point 1), A_0 (arc 0–1).

[27] Though each point of a b_i line may be reached along extremal paths arriving from three different directions, nevertheless the solution *starting* from any such point is unique. The multipliers λ, μ are single-valued functions of the coordinates of the points of the covered zone, with only the exception of μ along the segment 0–1. This restriction does not invalidate Hilbert's integral $\int(\lambda dV + \mu dm)$, which results to be independent of the integration path, as it occurs in a Mayer field.

[28] The sufficiency proof for the optimum requires a particular attention in so far as the actual problem is singular, whereas the literature refers (11, 12) to nonsingular cases. Nonetheless, in view of the properties of the previous footnote, a theorem analog to Theorem 10:1 of (11) can be stated. More directly, Hilbert's integral may be employed to show that the difference $X - X'$ equals the time integral of the quantity

$$E = \frac{\lambda}{m}(T - T') + \mu(\beta' - \beta)$$

where λ, μ, T, β are functions of the coordinates calculated for the extremal path, β' and $T'(\beta')$ are the governing quantities for the alternate path. E is the so-called excess function having the following properties: $E = 0$ for $\beta = \beta'$ and at the border of the regions β_{i-1} and β_i if $\beta_{i-1} \leq \beta' \leq \beta_{i+1}$; $E > 0$ everywhere else, for any value of β'. The conclusion $X > X'$ is therefore reached.

[29] The position of the *bridges* is independent of the particular end conditions.

It is obvious that, should the angle between adjacent sides of the thrust curve vanish, the corner lines would approach each other, tending to shrink into a single curve, namely, the curve $\omega = 0$ of Part I.

II-5 Conclusions

The method presented here, based on the concept of index value, allows the solution of a rather complex variational problem without substantial difficulties. Such an index constitutes a direct guide for the composition of discontinuous extremals, clearly indicating the points where the component curves must be joined.

The corner lines on which the index p attains the critical value for the transition from one regime of jet operation to another are extremely helpful in solving the boundary value problem for which both end-points of the extremal path are given. Evidently it is not necessary for practical applications to explore the whole (m, V) field as has been done in this paper in order to give a complete picture of the problem. When the simple and clear results of Part I are kept in mind, a few extremal paths are sufficient to trace the arcs of corner lines involved in a particular problem; thereafter, the solution is straightforward.

In the example of Section II-4 the case of a low final velocity has received detailed consideration in view of its practical importance as it corresponds to the maximum range attainable for a given propellant weight. The same equations, however, may be used for other types of boundary conditions.

One of the specific results of the example developed here is that the curvature of the thrust curve of the engine appears to have a considerable influence on the optimum burning program. Its effect is to reduce the period during which full power is used,[30] increasing—as a consequence—the periods of utilization of that part of the characteristic where the ratio T/β attains higher values.

[30] Consider an initial condition of flight such that the drag of the aircraft is less than the maximum thrust of the engine. For the case considered in Fig. 17, this means that the initial point of the extremal path lies below the dotted line (l) corresponding to $D = T_3$. Consequently, it is seen that a large part of the extremal path must be flown at reduced power, provided the thrust characteristic has such a camber as supposed here.

References

1 Hamel, G., "Über eine mit dem Problem der Rakete Zusammenhängende Aufgabe der Variationsrechnung," *ZAMM*, vol. 7, 1927, pp. 451–452.

2 Tsien, H. S., and Evans, R. C., "Optimum Thrust Programming for a Sounding Rocket," *Journal of the American Rocket Society*, vol. 21, September 1951, pp. 99–107.

3 Hibbs, A. R., "Optimum Burning Program for Horizontal Flight," *Journal of the American Rocket Society*, vol. 22, July-August 1952, pp. 206–212.

4 Miele, A., "Problemi di Minimo Tempo nel Volo Non-Stazionario degli Aeroplani," *Atti della Accademia delle Scienze di Torino, Classe di Scienze Matematiche, Fisiche e Naturali*, vol. 85, 1950–1951, pp. 41–52.

5 Miele, A., "Soluzioni Generali di Problemi di Ottimo in Volo Non-Stazionario," *L'Aerotecnica*, vol. 32, 1952, pp. 135–142 (translated as *NACA TM* 1388, October 1955).

6 Miele, A., "Optimum Climbing Technique for a Rocket-Powered Aircraft," JET PROPULSION, vol. 25, August 1955, pp. 385–391.

7 Cicala, P., "Le Evoluzioni Ottime di un Aereo," *Atti della Accademia delle Scienze di Torino, Classe di Scienze Matematiche, Fisiche e Naturali*, vol. 89, 1954–1955.

8 Bliss, G. A., Lectures on the Calculus of Variations, University of Chicago Press, 1945.

9 Bliss, G. A., and Hestenes, M. R., "Sufficient Conditions for a Problem of Mayer in the Calculus of Variations," *Trans. American Math. Soc.*, vol. 35, 1933, pp. 305–326.

(*Continued on page 473*)

A Mechanism for High-Frequency Oscillation in Ramjet Combustors and Afterburners

DON E. ROGERS[1] and FRANK E. MARBLE[2]

Daniel and Florence Guggenheim Jet Propulsion Center, California Institute of Technology, Pasadena, Calif.

An experimental investigation was made of the behavior of a small two-dimensional combustion chamber, burning a uniform mixture of air and fuel vapor under conditions of high-frequency oscillation or screech. Measurements were made of the limits of stable screech, the amplitude and frequency of pressure oscillations over a wide range of mixture ratio, inlet air temperature, and combustor flow rate. Spark schlieren photographs and high-speed motion pictures taken of the combustion process showed, in agreement with other investigations, that the high-frequency oscillation is accompanied by vortices shed periodically from the flameholder lip with the same frequency as the oscillation. The following mechanism of exciting the oscillations is suggested. A mode of transverse oscillation is excited as the result of periodic transport of combustible material, associated with the vortices, into the hot wake of the flameholder. The vortices, in turn, are generated at the flameholder lips by the fluctuating transverse velocity. When the ignition time delay lies in the proper range, the phase relationship between oscillations in transverse velocity and combustion intensity is such that the oscillation is amplified.

Introduction

THE phenomenon of screeching combustion instability in ramjets and afterburners is characterized by its relatively high and extremely regular frequency and by the fact that the sustaining mechanism is not associated with periodic fluctuations in fuel injection or air flow rates. In addition to an intense high-frequency acoustic disturbance, screeching combustion is accompanied by marked shortening of the flame zone, severe increase in heat transfer rates, and, frequently, failure of the combustion chamber. A complete understanding and control of these high-frequency combustion instabilities constitute one of the central problems in development of high performance afterburners and ramjet burners.

Although most early discussion of the problem was confined to private communications, it is relatively clear that this unique phenomenon and some features of its mechanism were first recognized by workers in the Research Division of the United Aircraft Corporation. More recently the problem of resonant oscillations in air-breathing combustion systems has been discussed by R. Newton and J. Truman (1)[3] showing that, for several burners of different sizes, the observed frequencies of screech instability correspond to some simple mode of transverse oscillation in the burner. Although the role of transverse oscillations is certainly an important one, a comparison of frequencies does not constitute a very sensitive criterion of the mechanism since the frequencies of high order modes are rather closely spaced. Furthermore an unstable oscillation, that is, one which is amplified by some feeding mechanism, need not correspond exactly to a normal mode. Oscillatory frequencies of cylindric burner configurations were computed by F. K. Moore and S. H. Maslin (2) assuming that pressure sensitivity of the combustion process accounts for the excitation. The most detailed measurements that have appeared are those of W. E. Kaskan and A. E. Noreen (3) in which schlieren photographs provide considerable detail of the process. There is a similarity between the photographic studies presented by these authors and some of those discussed here. Kaskan and Noreen suggest that the exciting disturbance arises from the distortion or stretching of the flame front near the flameholder, caused by the acoustic disturbance. The influence of flame distortion was also discussed previously in this regard by P. L. Blackshear (4).

The present paper covers a set of experiments performed in a small burner during 1953, for the purpose of elucidating the high-frequency instability; they were first reported in (5). Measurements were made of screech limits, amplitude, and frequency of the oscillation; photographic studies were obtained of the combustion details. Although the experimental results are incomplete in many ways, they add considerable interesting detail to existing published work. As a result of these studies, furthermore, the authors suggest a mechanism that is essentially different from those previously set forth.

The authors are most grateful to members of the staff of the Jet Propulsion Laboratory, California Institute of Technology, for assistance in carrying out the experimental work described herein and for the use of their excellent facilities. The two schlieren photographs which appear as Figs. 13 and 14 were obtained by Calvin L. R. Barker of the Jet Propulsion Laboratory during the current extension of the experimental work.

Experimental Exploration of Screeching Phenomenon

The exploratory investigation of screeching combustion was carried out in a small combustion chamber of rectangular cross section in order that the observed phenomena would be of nearly two-dimensional character. Mixtures of air and vaporized fuel entered a large plenum chamber to a converging nozzle having a contraction ratio of 28/1, to the combustion chamber, and then were discharged at atmospheric pressure. A photograph of the nozzle and working section is shown in Fig. 1. Air was supplied at a sufficiently high pressure that the flow rate could be accurately controlled by means of an adjustable sonic throat. Mixture temperature in the working section was controlled to within ±5 F by passing the air through a conventional shell-and-tube heat exchanger located far upstream of the settling chamber. A gasoline type fuel was injected into the airstream about 40 feet ahead of the plenum chamber so that a completely uniform mixture of fuel vapor and air was obtained at the working section under all conditions.

Received Sept. 15, 1955.

[1] Graduate Student; at present, Assistant Senior Engineer, Aerojet-General Corp. Mem. ARS.

[2] Associate Professor.

[3] Numbers in parentheses indicate References at end of paper.

The plenum chamber contained six screens, of 150 mesh each, located so as to reduce large-scale disturbances and to provide general control of the turbulence level. The resulting flow entering the combustion chamber had a uniform velocity profile, except within boundary layer regions of normal thickness, and a turbulence of low but undetermined level.

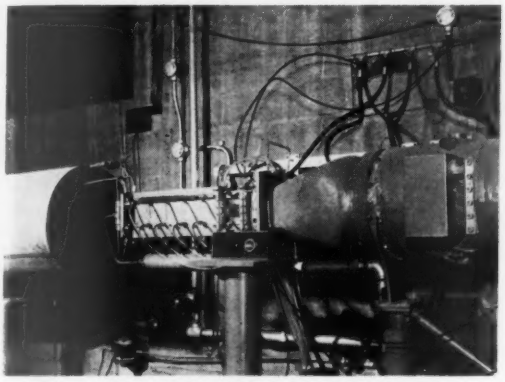


Fig. 1 View of the plenum chamber and nozzle

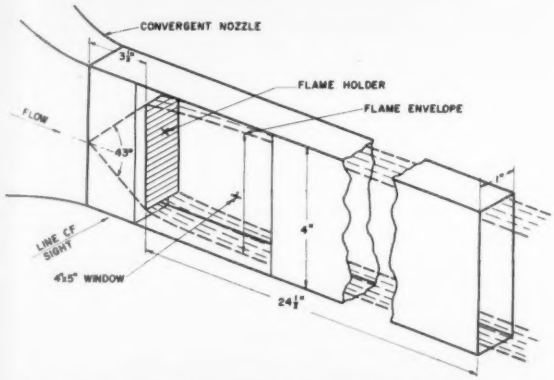


Fig. 2 Schematic diagram of the experimental combustion chamber

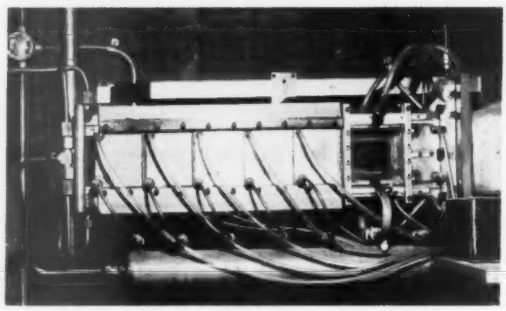


Fig. 3 Side view of the combustion chamber

A schematic diagram of the combustion chamber and flameholder is shown in Fig. 2. The combustor was of 1 in. by 4 in. rectangular cross section and extended $24^1/_2$ in. in length beyond the end of the wedge-shaped flameholder. The apex of the flameholder was located $1^1/_2$ in. downstream of the chamber inlet. Vycor glass windows permitted a field of view consisting of the region 4 in. by 5 in. immediately downstream of the flameholder. The chamber was fabricated of stainless steel to alleviate the corrosion problem arising from cooling water in the walls. The side walls of the burner were constructed of plate segments, Fig. 3, each of which was separately cooled and sealed. Since the plates were each 4 in. long in the axial direction, the design permitted variation of burner length in increments of 4 in.

The flameholder used throughout the investigation was a solid wedge with apex angle of 43 deg and an axial length of $3^1/_2$ in. It was constructed of stainless steel and was equipped with an independent water-cooling circuit. Ignition was accomplished by inserting an electrode into the combustion chamber and allowing a spark to jump to the downstream side of the flameholder. This probe could be retracted after ignition to allow smooth unobstructed gas flow. A complete description of equipment details and experimental procedures is given in (5).

Frequency and Amplitude Measurements

It was observed during the present experiments, as well as in the work of previous investigators, that the simplest and least destructive technique for entering the regions of screeching combustion was to increase the fuel-air ratio of the mixture ratio while holding the airflow rate and other free-stream conditions constant. The most direct indication of screech is the total pressure loss across the combustion chamber. Roughly speaking, the total pressure loss is a measure of the heat release that takes place within the combustion chamber; as this heat release increases, the momentum pressure loss across the combustor increases. Since, during screeching operation, the flame zone is observed to contract substantially, a greater portion of the burning process takes place within the chamber so that the onset of screech is accompanied by an increase in pressure loss.

A typical diagram illustrating the transition into an out of screeching operation is shown in Fig. 4 where the dimensionless pressure loss across the combustion chamber is given for a wide range of fuel-air mixture ratios. The total pressure loss is reduced to a dimensionless form through division by the absolute stagnation pressure at the combustion chamber inlet; the mixture strength is presented as the equivalence ratio, that is, the quotient of actual fuel-air ratio to the fuel-air ratio at stoichiometric. For the free stream speed or air mass flow shown, the lean blowoff limit of the flameholder occurred at an equivalence ratio of about 0.72. As the equivalence ratio was increased to about 0.85, the combustor entered screeching operation as indicated by the substantial increase in pressure drop. Screeching operation continued at greater values of mixture ratio until the rich instability limit was reached. Here the combustion process may be described as rough, that is, exhibiting a series of random pulsations or explosions of considerable violence. As the equivalence ratio was reduced, the pressure loss retraced its previous trend until it reached the region of transition between screeching and normal operation. Here it remained in screech until the mixture ratio was considerably lower than that required for the transition into screech. Although such a hysteresis effect may be associated with a pulsation involving finite amplitudes, the effect shown here is probably associated with heat transfer. When the burner is operating in the screeching condition, portions of the

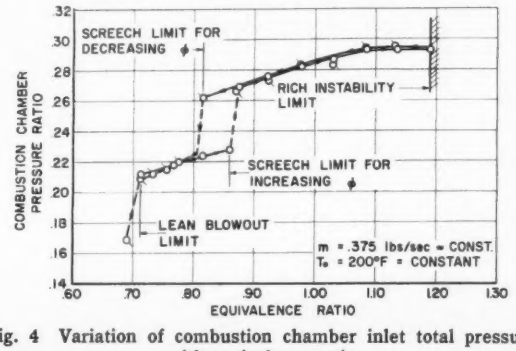


Fig. 4 Variation of combustion chamber inlet total pressure with equivalence ratio

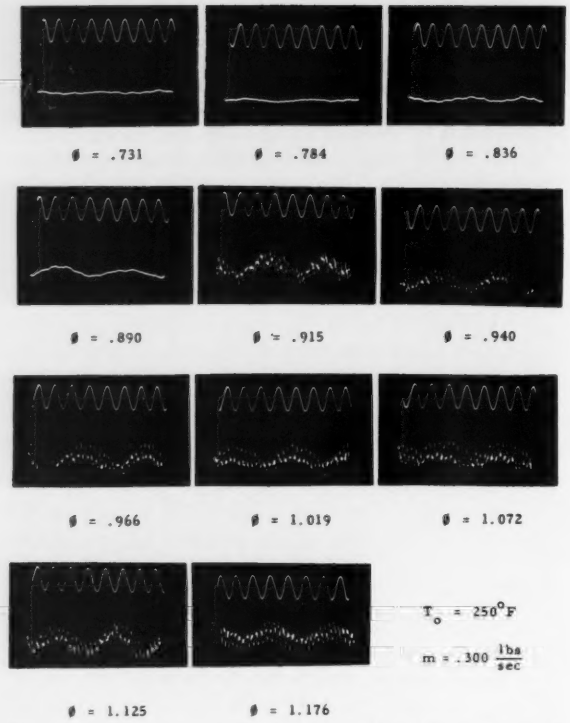


Fig. 5 Typical pressure fluctuation records for a range of equivalence ratios

chamber heat up appreciably above the temperatures encountered during steady operation. Inasmuch as it will appear that the screech limit occurs at leaner mixture ratios when the gas temperature is higher, it is reasonable to suppose that heating of the chamber itself would affect it in a similar manner. This accounts for the hysteresis appearing in Fig. 4.

Frequency and amplitude of the oscillations are of particular significance and these were measured with Photocon capacitance-type gages of 100 psi range and a natural frequency of 75,000 cps. The output of each gage was observed on a Dumont dual beam oscilloscope and recorded photographically. The gages were water cooled, mounted flush with the inside surface of the wall, and could be installed at a variety of positions on the duct. A typical set of response patterns for various mixture ratios is shown in Fig. 5 where the gage is located on the center line of the duct, 11 in. downstream from the flameholder face. In each diagram the lower curve represents the trace of the pressure oscillation while the upper curve is the timing frequency of 1000 cps. The onset of screeching operation is clearly delineated by the increase in amplitude of the pressure oscillation. The pulsations clearly consist of two distinct frequencies, a low-frequency oscillation of about 285 cps and the high-frequency oscillation, characteristically associated with screech, of about 3800 cps. The low-frequency oscillation corresponds roughly to the longitudinal mode of the chamber resonating as if it were closed at the flameholder, while the high-frequency oscillation corresponds roughly to the fundamental (antisymmetric) transverse mode across the 4-in. dimension of the duct. The high-frequency component is of principal interest. Because the gage was located on the center line of the duct for the photographs of Fig. 5, the relative magnitude of the high-frequency component is shown considerably too small. The significance of pressure measurement location has since been discussed in (6).

The frequency of the screeching oscillation is quite insensitive to changes in mixture ratio and, as indicated in Fig. 6, decreases only in a minor way as the airflow rate through the combustion chamber is increased. The Mach number employed as the ordinate in Fig. 6 is an average one based on the total mass flow, unblocked cross-sectional area for flow at the flameholder lip, and the free stream conditions. This is used as a convenient indication of the Mach number near the flameholder lip, which is the significant value in the present problem. Fig. 6 also shows that the frequency of longitudinal oscillation is completely unaffected by the changes in flow rate.

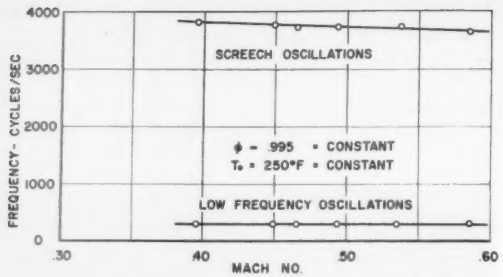


Fig. 6 Variation of frequency with the average Mach number at the flameholder lip

Measurements of fluctuating pressures permitted a rough determination of amplitude of the pressure oscillations and the manner in which it varied with mixture ratio and average Mach number. The amplitudes of high- and low-frequency components of oscillation are shown in Fig. 7 where the ratio of peak-to-peak pressure difference to the stagnation pressure at the combustion chamber inlet is used as the ordinate. For these measurements the pressure pickup was located on the top wall of the combustion chamber $^1/_4$ in. downstream of the flameholder lip. The pressure amplitudes shown are therefore approximately those of importance in screech excitation. The onset of screech at an equivalence ratio of about 0.90 is indicated by a large increase in amplitude of pressure oscillation.[4] Below this value the amplitude of high-frequency oscillation is barely perceptible but, after its initial jump, increases rather slowly with mixture ratio. The low-frequency longitudinal component is present, as indicated in Fig. 5, even below the screech limit, although its amplitude also doubles when screech is encountered. It appears likely that the longitudinal oscillation is excited to moderate amplitude by any disturbance in the chamber such as random pulses associated with rough burning. The abrupt increase at screech indicates some coupling with the high-frequency component or with the generating mechanism, but it appears that, at least in the present case, the exciting mechanism is associated with the high-frequency component. Changes in length of the combustion chamber changed the frequency and amplitude of the low-frequency component but had negligible effect upon the screech component. Thus it seems clear that the excitation took place in the high-frequency component and the screech phenomenon is relatively independent of the longitudinal oscillation.

Although the limited results available are not conclusive on this point, it was observed that the screech amplitude tended to decrease as the average lip Mach number increased and that high values of the Mach number inhibited screech. At average Mach number values of the order of 0.90 the combustor screeched only intermittently. As the Mach number was further increased it was not possible to initiate screech, and the combustor operated smoothly over the entire range of mixture ratios.

[4] These measurements were made in a chamber with cooling properties different from the chamber employed during other measurements. This feature accounts for the difference in lean screech limit.

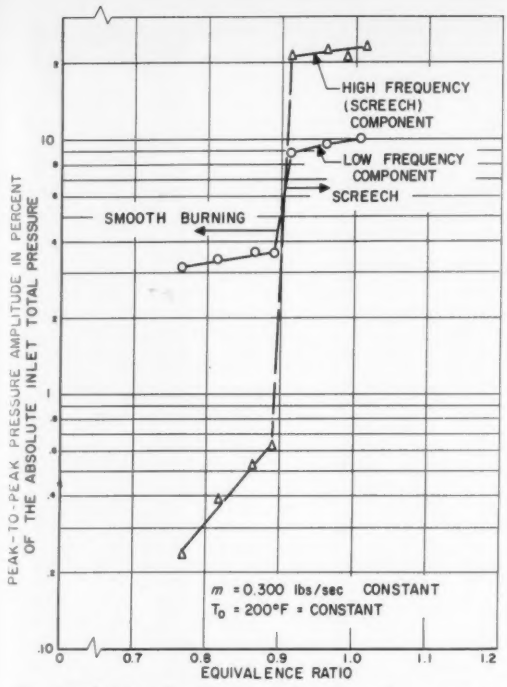


Fig. 7 Amplitude of pressure fluctuations for a range of equivalence ratios

Limits of Stable Operation

As indicated previously, there are mixture ratio limits within which the combustor must operate in order that stable screech be observed. Of particular interest is the lean screech limit because this limit appears to be associated directly with the exciting mechanism while the rich limit is not. This lean limit is rather insensitive, Fig. 8, to variations in lip Mach number; except for a substantial change at very low flow rates, the lean limit remains at an equivalence ratio of about 0.85. The amplitude of oscillation decreased as the Mach number increased but, below an average Mach number of 0.9, this has no influence upon the lean limit.

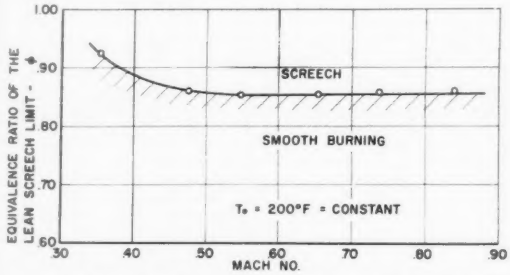


Fig. 8 Variation of the lean screech limit with average Mach number

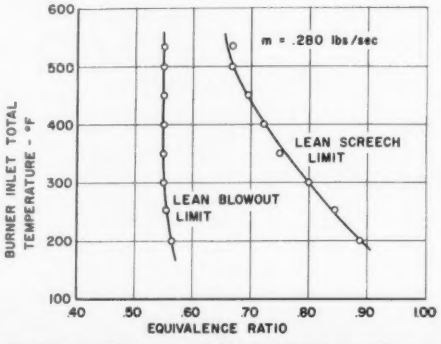


Fig. 9 Variation of lean screech limit with inlet total temperature

Since combustion processes are notoriously sensitive to initial temperature of the mixture, it is to be expected that the lean screech limit will be significantly influenced by changes in temperature of the mixture entering the combustion chamber. This conjecture is confirmed by the observed strong decrease in screech limit, Fig. 9, as the burner inlet temperature is increased. The lean blowoff limit of the flameholder is also shown and clearly as the inlet temperature increases above 500 F, the screech limit very nearly reaches the lean blowoff limit, indicating that, for this inlet temperature, the burner will screech over its entire range of useful operation.

Optical Study of the Screech Mechanism

The most direct manner of obtaining detailed information concerning the mechanism of screeching combustion is through photographic investigation. Photographs of the region near the flameholder show that the combustion zone in the mixing region downstream of each lip is normal, Fig. 10, during smooth operation but takes on a scalloped appearance, Fig. 11, during screeching operation. Spark schlieren photographs of the process reveal considerably more detail of the flow. These optical studies were conducted using a single-pass, double-mirror schlieren system of conventional arrangement. The spark schlieren pictures were obtained using a high-intensity spark source of 2 to 3 microsec duration. The high-speed motion pictures were obtained with a Western Electric Fastax camera using a General Electric mercury vapor lamp for illumination.

A spark schlieren picture of smooth combustion is shown in Fig. 12. As described in detail in (7), the boundary layer from the bluff body separates, spreads through turbulent mixing into the hot zone of recirculating combustion products, and ignites before the end of the recirculating zone is reached, thereby producing a propagating flame. A comparable photograph of screeching combustion, Fig. 13, shows the profound modification of the flow field that accompanies the

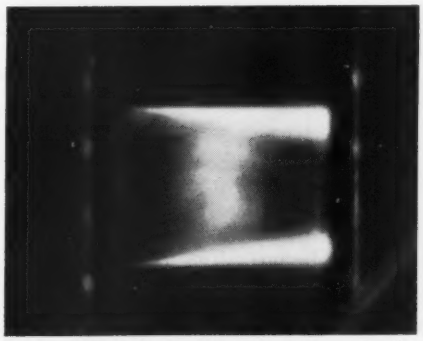


Fig. 10 Direct photograph of smooth combustion

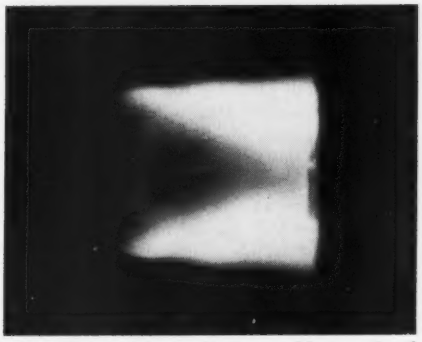


Fig. 11 Direct photograph of screeching combustion

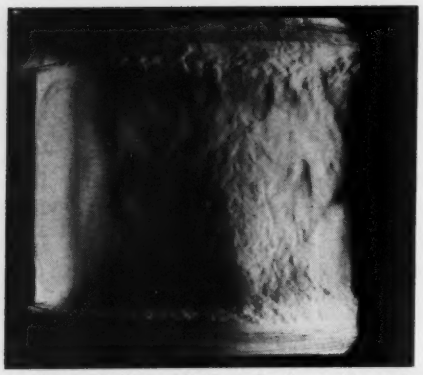


Fig. 12 Spark-schlieren photograph of smooth combustion

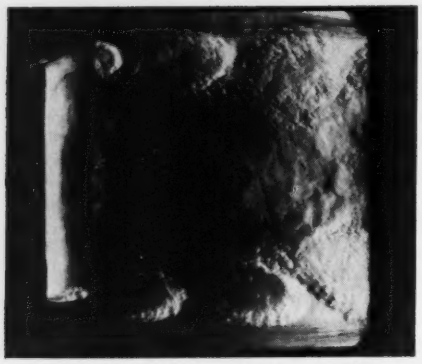


Fig. 13 Spark-schlieren photograph of screeching combustion

pressure fluctuations. The transverse fluctuations across the combustion chamber are associated with the formation of vortices which are, in turn, shed alternately from the lips of the flameholder. In this photograph one vortex is in the process of formation on the lower lip while a fully developed vortex has drifted downstream from the upper lip; the transverse (upward) velocity, existing at the time of the photograph, has moved both of them off center toward the upper part of the photograph. Vortices from previous cycles, burned and partially decayed, appear downstream in the wake.

Now if these vortices are associated with the high-frequency transverse oscillation, they must be shed with the same frequency. To obtain this information in particular and a more complete picture of the shedding process in general, high-speed schlieren motion pictures were taken of the screeching combustion. The maximum camera speed of about 7000 frames per sec was insufficient to obtain detailed history of one vortex. However, by photographing the process while the camera frame frequency was accelerating through the frequency of vortex shedding, successive positions of successive vortices could be traced, thereby giving the effect of slowing down the process. This also provided, through the timing marks on the film, an accurate means for obtaining the frequency of vortex shedding. Two sequences of pictures are shown in Fig. 14. Figs. 15 and 16 compare the vortex shedding frequencies thus obtained with the screech frequencies from pressure measurement for a range of lip Mach numbers and equivalence ratios. The agreement, well within accuracy of the measurement, leaves little doubt that the two phenomena are associated and that the vortex wake is in no way connected with the Kármán vortex street formed in the wakes of bluff bodies in a certain Reynolds number range. It seems apparent, in fact, that the vortices are formed as a result of the transverse velocity associated with the sloshing oscillation. Referring for convenience to Fig. 13, the upward velocity associated with a particular phase of



Fig. 14 Typical high-speed schlieren motion pictures of screeching combustion

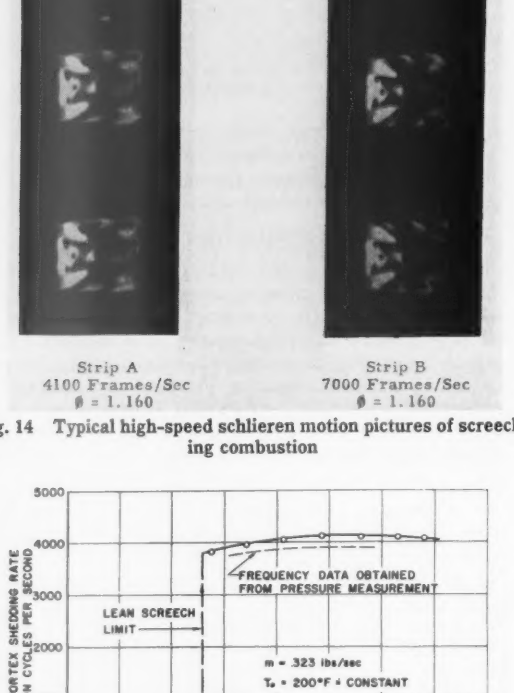


Fig. 15 Variations of vortex shedding rate with equivalence ratio

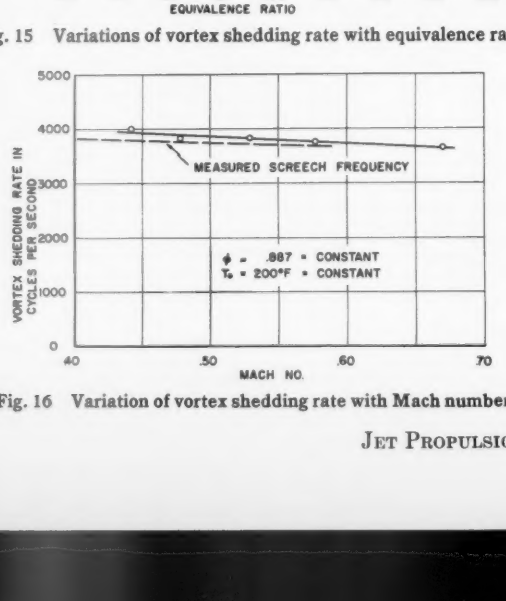


Fig. 16 Variation of vortex shedding rate with Mach number

the pressure oscillation induces a flow about the lower lip conducive to the formation of a vortex. In a later phase of the motion the transverse velocity is reversed and a similar vortex is formed at the upper lip. Thus the frequency of vortex formation at each lip will be equal to the frequency of the screeching oscillation. This corresponds to the observation.

Mechanism of Screeching Combustion

At least two proposals have been made concerning mechanisms by which the high-frequency oscillations may be excited. In their analytic study of the predominant modes of combustion chamber pulsation, Moore and Maslen (2) postulate a pressure dependent burning rate similar to that encountered in liquid propellant rocket motors. Although hydrocarbon mass combustion rates are dependent upon the pressure they are equally or more sensitive to changes in the temperature. The experiments reported here as well as those discussed in (3) do not indicate pressure fluctuation of sufficient magnitude to raise the local temperature by a large factor. Since the gas immediately downstream of the lip may be subjected to violent temperature fluctuations associated with the mixing process, it seems likely that periodic temperature fluctuations would overshadow pressure disturbances in exciting variations of burning rate. In (3) Kaskan and Noreen consider a mechanism involving the flame front distortion and employ the original suggestion of Blackshear (4) that the fluctuations in burning rate may result from fluid dynamic stretching of the flame front. In the former work it is reasoned that the vortex formation extends the existing flame front and thus produces, periodically, a higher burning rate and a resulting pressure pulse. When the phase relation between vortex formation and combustion is proper, the oscillation will be amplified or sustained. Now there is little doubt that, under proper conditions, such changes in flame area may excite pressure fluctuations, but under the circumstances of combustion in a region of high shear and intense turbulence, such as exists in the separated boundary layer, the concept is somewhat vague. The rate of combustion increases linearly with the flame front area but much more rapidly due to increase in ambient temperature. Since the phenomenon is so intense it seems that a more vigorous means of excitation dominates the picture associated with mixing between combustible gas and hot products of combustion in the wake. On the basis of existing experiments on high-frequency oscillations in combustion chambers and the present knowledge of processes involved in flame stabilization on bluff bodies, it is suggested that the following mechanism excites and sustains the oscillations.

Under conditions of normal smooth operation the combustible gas passes about the bluff body, separates from the surface, and mixes with the hot recirculating wake in a thin turbulent shear zone. As shown in (7), if the wake is sufficiently long and the recirculating zone sufficiently hot, the fresh gas will be ignited and a propagating flame established. During high-frequency oscillation, fluctuating pressure, temperature, and velocity fields are superimposed upon this steady field; in particular an oscillating transverse (or sloshing) velocity field is added to the existing field for steady combustion. As the flow angle with respect to a flameholder lip is increased by this transverse velocity, a vortex forms, Fig. 17, similar to the starting vortex formed when an airfoil enters a cross velocity field or gust. The transverse velocity which formed the vortex helps transport it into the hot recirculating wake zone of the flameholder. Since the vortex consists principally of unburned gas from the boundary layer of the bluff body, this transport process carries a large amount of combustible material into the hot zone. The shear layer which formed the vortex is strongly turbulent so that this combustible material mixes with the hot wake gas and, after an appropriate length of time, ignites and burns.

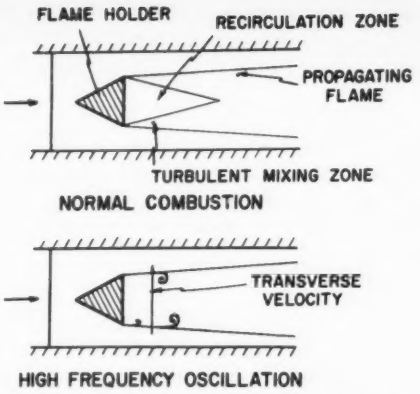


Fig. 17 Vortex formation associated with transverse velocity field

The combustion of this large amount of material generates a pressure wave which in the present circumstances, since the vortex is off center in the duct, excites the antisymmetric modes of the duct. To support an oscillation of large amplitude, this exciting process must (a) occur in the proper phase of the cycle to provide amplification, and (b) be of sufficient magnitude to overcome the various damping influences present.

The Ignition Time Delay

The combustion oscillation lags the oscillations in transverse velocity because of the time required to form the vortex as well as the time required for mixing and ignition of the fresh gas associated with the vortex. The fluctuations in transverse velocity and combustion rate must bear a certain phase relation in order that energy may be fed into the oscillating motion. The classical criterion for reinforcement of oscillations by heat release is that the heat be released when the pressure at the point of heat release is near its maximum value. Thus to excite the fundamental transverse mode of oscillation in the present configuration the heat should be released as the gas mass starts toward the center of the duct from the side where the combustion pulse took place. This condition is fulfilled either when both vortex formation and burning occur early in the return cycle of gas motion, or when combustion takes place an integral number of periods after vortex formation where the transverse gas motion is again the same. Some information on the ignition time delay of such systems is available from flame blowoff experiments with bluff bodies. The flame stabilization process on bluff bodies involves also an ignition delay accompanied by a mixing process; if the time required for the combustible mixture to flow past the hot recirculation zone is less than that required to mix and ignite the combustible, then the flame will not propagate into the combustible stream and is said to blow off from the bluff body. Observations of blowoff velocity during normal combustion permit rather straightforward estimates of this time delay (8), as about 0.00028 sec at stoichiometric mixture, inlet gas temperature of 610 R, and atmospheric pressure. Now the period of the oscillation observed in the present burner is about 0.00026 sec. Therefore it is clear that the combustion pulse does not occur directly after the vortex is formed but with a delay of about one complete period as indicated in Fig. 18. From flame stabilization experiments of (7) and (8) it appears that the ignition time delay is characterized by the fuel, increases strongly as the mixture varies from that giving maximum flame temperature, and decreases strongly as the temperature of the combustible mixture is increased. From this viewpoint, the screeching oscillation does not occur at sufficiently lean mixtures because the ignition delay increases so markedly as the mixture drops below stoichiometric that the phase of

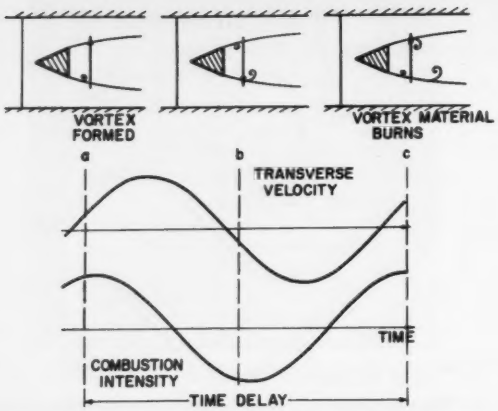


Fig. 18 Time delay required to excite transverse oscillations

excitation is improper for amplifying the oscillation. Furthermore, raising the mixture temperature tends to decrease the ignition time lag at a given mixture ratio and hence, as shown in Fig. 9, permits stable screech at leaner mixtures.

It must be emphasized that ignition after a delay of about one period need not be common to all combustion chambers. For a large chamber where the period of the fundamental transverse period is long compared with the ignition time delay of 0.00028 sec, the ignition may take place during the same cycle that manufactured the vortex. This probably occurs when transverse or radial oscillations of the order of 1000 cps are excited in large burners. It might also be inquired whether screech should be possible when the time delay is of several periods' duration. There seems to be no observation indicating such behavior, but neither has any systematic investigation of that point been pursued. With the mechanism proposed, however, excitation after several periods' time delay seems rather improbable for two reasons. First, if the delay between vortex formation and combustion is very long, both the vortex and the mixing region between stream and wake become quite diffuse in comparison with the amplitude of transverse gas motion. The original vortex material would then have associated with comparable amounts of fresh gas and combustion products so that local high-intensity combustion should be suppressed. Second, a delay of several periods situates the vortex a considerable distance downstream of the flameholder when combustion takes place. This configuration is less advantageous for exciting transverse oscillation than that of combustion taking place quite near the flameholder face.

Damping Influences

Although viscous damping, surface absorption, etc., certainly play roles in the screeching phenomenon, the principal damping effect of the present experiments is the transport of fresh undisturbed gas into the burner region. This damping force arises physically from the fact that the energy associated with the transverse oscillation is continually being transported out of the chamber while fresh gas is entering in which the oscillation must be generated. The damping force is proportional to the mass flow rate through the combustor and its phase is always such as to decrease the amplitude of oscillation. A high free stream velocity may be expected to have a further tendency to damp the motion because it transports the vortex farther downstream within one cycle than does a low stream velocity. Consequently, since the hot recirculating zone is of fixed length, the vortex may eventually be transported out of the main portion of the wake before mixing and combustion may be effected. Finally the influence of the local Mach number at the flameholder lip may be considered. As the Mach number approaches and locally exceeds unity, the pressure pulse originating at the burning vortex can influence the flow pattern only within the Mach wedge and hence is incapable of generating another vortex. Consequently, in agreement with observation, screeching combustion cannot be supported as the lip Mach number exceeds unity.

Concluding Remarks

The experiments performed and the mechanism suggested pertain, in detail, only to a very simple combustion chamber with essentially two-dimensional flow. Although the mechanism probably does not account for all combustion chamber oscillations of high frequency, the ideas may be extended fruitfully to a wide variety of geometric conditions. In the first place, only the fundamental transverse mode of oscillation was observed. It is clear that, for a given fluid dynamic and ignition delay in burning the vortex, that mode will be observed for which this phase lag produces the greatest divergence. For example, increasing the chamber size would result in selection of higher modes such that the frequencies are of the same general order as that observed in the small chamber. However, when the burner size becomes so large that the period of some mode is long enough to permit combustion during the same cycle that produced the vortex, distinctly lower frequencies should be observed. In a burner of axially symmetric geometry, two patterns of screech appear possible. The vortices may be shed either periodically as discrete rings or continuously as a helical vortex line.

Simple methods for alleviating screech also suggest themselves; the general aim would be to arrange the burner so that an induced mode of oscillation would not manufacture vortices in the critical region. One obvious technique is to prevent reflection at the burner shell or to scatter the reflected wave so that the induced velocities near the flameholder are small. Another technique would be to disperse the flameholding element (axially and radially) in such a fashion that pressure waves are not reflected with great strength in the neighborhood of any flameholder. Such preventative means would be of particular importance in afterburners where the burner inlet temperature is so high that the unstable region would cover the entire range of useful mixture ratios.

References

1 Newton, R. T., and Truman, J. C., "An Approach to the Problem of Screech in Ducted Burners," *Transactions, The American Society of Mechanical Engineers* (to be published).

2 Moore, Franklin K., and Maslen, Stephen K., "Transverse Oscillations in a Cylindrical Combustion Chamber," NACA Technical Note no. 3152, Oct. 1954.

3 Kaskan, W. E., and Noreen, A. E., "High Frequency Oscillations of a Flame Held by a Bluff Body," presented at Annual Meeting of the ASME, New York, N. Y., Nov. 28, 1954.

4 Blackshear, P. L., "Driving Standing Waves by Heat Addition," NACA Technical Note no. 2772, 1952.

5 Rogers, Don E., "An Experimental Investigation of High Frequency Combustion Instability in a Fuel Air Combustor," Thesis for the degree of Aeronautical Engineer, California Institute of Technology, May 1954.

6 Blackshear, P. L., Rayle, W. D., and Tower, L. K., "Study of Screeching Combustion in a 6-inch Simulated Afterburner," NACA Technical Note no. 3567, Oct. 1955.

7 Zukoski, E. E., and Marble, Frank E., "The Role of Wake Transition in the Process of Flame Stabilization on Bluff Bodies," *Combustion Researches and Reviews, 1955*, The Advisory Group for Aeronautical Research and Development, NATO, Butterworths Scientific Publications, London, 1955.

8 Zukoski, E. E., and Marble, Frank E., "Experiments Concerning the Mechanism of Flame Stabilization in the Wakes of Bluff Bodies," Proceedings of the Symposium on Gas Dynamics, Northwestern University, August 22–24, 1955.

On the Motion of a Missile Under Water

WALTER P. REID[1]

U. S. Naval Ordnance Test Station, China Lake, Calif.

Differential equations of motion of a missile are derived on the basis of certain simplifying assumptions initiated originally by others with the underwater motion of a missile in mind. Comments are made on the significance of these assumptions, and the analytical solution to the equations is developed.

Nomenclature

A	=	constant defined by Equation [6]
C	=	$2(B + \mu A)/MW$
D	=	drag, assumed to be given by Equation [4]
E	=	$2B\mu/MW$
f	=	$B/(Bv^2 + AT)$
h	=	maximum diameter of missile
K_D	=	drag coefficient defined by Equation [4], assumed to be constant
K_L	=	lift coefficient defined by Equation [5], assumed to be constant
K_Q	=	cross-spin coefficient defined by Equation [3], assumed to be constant
L	=	lift, assumed to be given by Equation [5]
M	=	effective mass of missile, assumed to be constant
Q	=	cross-spin or pitching force, assumed to be given by Equation [3]
R	=	radius of curvature of the trajectory at a particular point (R lies in the plane of the paper in Figs. 1 and 2)
s	=	$2B/M$
T	=	thrust due to propelling force, assumed constant
t	=	time
u	=	parameter used as a variable of integration
V	=	value that v approaches as $t \to \infty$
v	=	speed of missile
W	=	weight of missile (weight in vacuum minus buoyant force)
x, z	=	horizontal, vertical coordinates
α	=	angle of attack of missile (angle that the axis of the missile makes with the direction of motion)
θ	=	angle that the direction of motion of the missile makes with the x-axis
μ	=	$K_D\rho h^2$
ρ	=	fluid density
ω	=	$(d/dt)(\theta - \alpha)$
$f_0, x_0, z_0, \vartheta_0$	=	values of f, x, z, θ at initial time t_0

Introduction

NUMERICAL methods have been used recently by G. A. Spassky, H. M. Berger, F. G. White, and others in some classified reports to solve certain differential equations of motion of a stable, symmetrical nonspinning missile. The equations have been derived in those reports on the basis of certain assumptions which were found to be applicable to the motion of a missile under water. Very good agreement was found between the calculated trajectories and those obtained experimentally. In this paper an analytical solution is given for these equations. The derivation given below of the differential equations of motion was inspired by the treatment in the aforementioned reports, but is quite different. Moreover, the equations obtained here (Equations [11] and [12]) are not the ones used by the above workers, but can be shown to be linear combinations of their equations.

Received Aug. 30, 1955.

[1] Head, Applied Mathematics Branch; now Staff Member, Theoretical Division of the Los Alamos Scientific Laboratory (University of California), Los Alamos, N. Mex.

Derivation of the Differential Equations

In the following derivation it has not seemed feasible to try to mention all of the simplifying assumptions made. Effects due to rotation of the earth, lack of perfect symmetry in construction of the missile, variation of coefficients such as K_L and K_Q with α, as well as other items of this sort are ignored without comment.

Fig. 1 shows the physical situation to be treated, with vectors indicating the forces. The motion of the missile is taken as being in the plane of the paper. The angular momentum and angular acceleration of the missile are considered to be small. Effects of the discharging gases other than thrust are not taken into account. Only the forces shown and a small torque are assumed to be acting on the body.

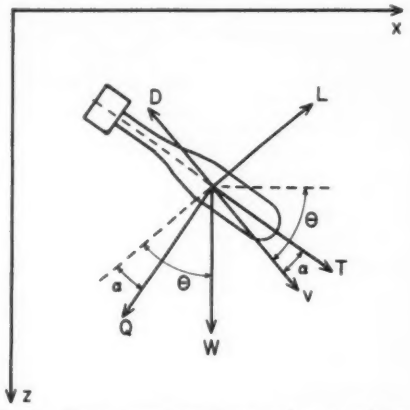


Fig. 1 Forces assumed to be acting on missile

The application of Newton's second law of linear motion in directions tangent and normal to the trajectory, respectively, gives

$$M\,dv/dt = T\cos\alpha + W\sin\theta + Q\sin\alpha - D \quad [1]$$

$$Mv\,d\theta/dt = W\cos\theta - T\sin\alpha + Q\cos\alpha - L \quad [2]$$

The cross-spin force, the drag, and the lift are designated by Q, D, and L, respectively, and may be written (see Ref. (1),[2] page 24)

$$Q = K_Q\rho h^3 v\omega \quad [3]$$

$$D = K_D\rho h^2 v^2 \equiv \mu v^2 \quad [4]$$

$$L = K_L\rho h^2 v^2 \sin\alpha \quad [5]$$

In addition to Equations [1] and [2], a statement concerning the rotation of the body is needed. Usually this consists of equating the sum of the torques to the rate of change of angular momentum of the missile and discharging gases. In this paper, however, it will be assumed that α is approximately equal to the "yaw of repose" (see Ref. (1), page 58), or that

$$\sin\alpha \approx A/R = (A/v)\,d\theta/dt \quad [6]$$

where

$$A = K_H h/K_M \quad [7]$$

[2] Reference at end of paper.

For a missile that continues to point approximately in the direction it is going, α and ω are small. Because of this, one may write

$$\cos \alpha \approx 1 \quad [8]$$

$$Q \sin \alpha \approx 0 \quad [9]$$

$$\omega \approx d\theta/dt \quad [10]$$

From Equations [1], [4], [8], and [9] one obtains

$$M dv/dt = T + W \sin \theta - \mu v^2 \quad [11]$$

When Equations [2], [3], [5], [6], [8], and [10] are combined, the result is

$$W \cos \theta = (Bv + AT/v)\, d\theta/dt \quad [12]$$

where

$$B = M - K_Q h^3 \rho + K_L \rho h^2 A \quad [13]$$

This completes the derivation of the differential equations. The next thing to do is to solve them. In doing so, no further assumptions will be made; hence it is appropriate to stop at this point to consider the significance of the assumptions that have been made.

Comments on the Differential Equations

It should be mentioned first that equations equivalent to Equations [11] and [12] (linear combinations of them with different notation) have been solved by numerical methods and found to give results in agreement with experiment for cases of missiles traveling in water. At least for these cases, then, the assumptions seem to be justified.

The assumptions made in deriving Equations [11] and [12] have the same effect as if the forces L and Q on the missile were removed and the missile were then treated as a particle, with α specified, but as a particle whose transverse and longitudinal masses are not the same. To see this, consider Fig. 2 in which there is a particle moving in the direction shown by v and subject to forces W, T, and D. From Newton's second law as applied in the direction of motion and perpendicular to it (in the plane of the paper), one gets Equations [11] and [12], respectively, provided that α is given by Equation [6], and that the mass is taken as M for the first case, and B for the second.

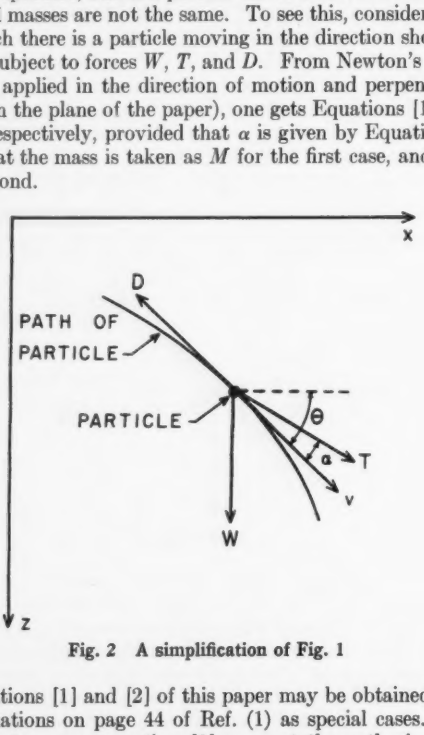


Fig. 2 A simplification of Fig. 1

Equations [1] and [2] of this paper may be obtained from the equations on page 44 of Ref. (1) as special cases. The decision to use assumption [6] was not the author's. The assumption was obtained from a classified report by G. A. Spassky, W. E. Hicks, and J. M. Rowe. It is introduced there by taking the sum of the aerodynamic torques to be zero, and then using Equation [10] above. Also, the assumption that the sum of the torques is equal to zero was the underlying motivation for a report by H. M. Berger. The purpose was to show that the assumption is good in the large number of special cases where the conditions set forth in that report are satisfied.

Solution to the Differential Equations

General Solution

Upon dividing Equation [11] by Equation [12], one obtains

$$v\, dv/d\theta = (T + W \sin \theta - \mu v^2)(Bv^2 + AT)/(MW \cos \theta) \quad [14]$$

let

$$v^2 = 1/f - AT/B \quad [15]$$

then Equation [14] becomes

$$df/d\theta + (s \tan \theta + CT \sec \theta) f = E \sec \theta \quad [16]$$

where s, C, and E are as defined in the notation. The last equation is first-order linear. It has as its integrating factor

$$(\sec \theta + \tan \theta)^{CT} \cos^{-s} \theta \quad [17]$$

Upon multiplying through by this and integrating, one gets

$$f = \frac{f_0 \cos^s \theta\, (\sec \theta_0 + \tan \theta_0)^{CT}}{\cos^s \theta_0\, (\sec \theta + \tan \theta)^{CT}} + \frac{E \cos^s \theta}{(\sec \theta + \tan \theta)^{CT}} \times \int_{\theta_0}^{\theta} \frac{(\sec u + \tan u)^{CT}}{\cos^{s+1} u}\, du \quad [18]$$

This gives f and hence v, as a function of θ. To get the x coordinate of the position of the missile, note that

$$x = x_0 + \int_{t_0}^{t} v \cos \theta\, dt \quad [19]$$

By means of Equations [12] and [15] this may be written

$$x = x_0 + (B/W) \int_{\theta_0}^{\theta} (1/f)\, d\theta \quad [20]$$

Similarly

$$z = z_0 + \frac{B}{W} \int_{\theta_0}^{\theta} \frac{\tan \theta}{f}\, d\theta \quad [21]$$

And then finally, from Equation [12] one may get t for any θ by means of the relation

$$t = t_0 + (B/W) \int_{\theta_0}^{\theta} (v f \cos \theta)^{-1}\, d\theta \quad [22]$$

Application to the Steady State

Consider next the limiting, or steady-state, solution to this problem for the case when $T = 0$.

In the steady state there is, by definition, no variation with time, so from Equation [12] it follows that

$$\cos \theta = 0$$

or

$$\theta = \pi/2 \quad [23]$$

This result serves as a partial check on the reasonableness of the equations, since $\pi/2$ is clearly the value that θ should have in the steady state.

From Equation [11] one gets the steady-state speed, V, for the case of zero thrust as

$$V = \sqrt{W/\mu} \quad [24]$$

which again is the result that should be obtained.

Since v, and hence $1/f$, never become infinite, one sees from Equation [20] that the path followed by the missile approaches asymptotically a vertical line as $t \to \infty$.

Reference

1 Rosser, J. B., Newton, R. R., and Gross, G. L., "Mathematical Theory of Rocket Flight," McGraw-Hill Book Co., Inc., New York, 1947.

Optimalizing Control in the Presence of Noise Interference[1]

SEDAT SERDENGECTI[2]

Daniel and Florence Guggenheim Jet Propulsion Center, California Institute of Technology, Pasadena, Calif.

The performance of a modified peak-holding optimalizing control system depends in part on the ability of the controller to detect the input signal frequency component in the output of the controlled system. This paper describes several techniques that may be used for detecting this component and analyzes one of them in great detail. The subject of the detailed analysis is the method of filtering through cross-correlation. A statistical analysis is also carried out in order to demonstrate the efficiency of this method.

Introduction

IN THE peak-holding type of optimalizing controller, which was introduced by C. S. Draper and Y. T. Li (1),[3] the two basic functions of an optimalizing control system are combined. One is the detection of the input setting that yields the maximum output. The second is the adjustment of the input to make it agree with the optimum setting, thereby actually maximizing the output. For example, the peak-holding optimalizing controller may include an output sensing instrument whose function is to follow the output when the output is increasing but to hold the maximum value of the output when the output is decreasing. The input drive unit of the control system reverses its direction whenever a fixed critical difference exists between the reading of the output sensing instrument and the output itself. In this manner the input is forced to hunt about the optimum input setting. The resultant hunting frequency of the input is a function of the variations in the input-output relationship of the controlled system. The input hunting frequency will only be constant when this relationship is constant, and in such a case the optimalizing control is unnecessary because the system can be easily calibrated once and for all. The dynamic analysis of the peak-holding type of system for a constant input-output relationship was considered by H. S. Tsien and the author in a previous paper (2).

In the presence of noise interference, the above method of detecting the maximum of the input-output relationship is not useful. Because of superimposed noise on the "actual" output, the output sensing instrument would never indicate the true optimum state of the controlled system. Furthermore, the input reversal instants would occur earlier or later, in a random manner, depending on whether the magnitude of the output with superimposed noise was greater or less than the magnitude of the "actual" output. It is clear that the noise interference effects would result in a random fluctuation in the input hunting frequency of the system. Thus the true optimum state of the controlled system might never be reached, and the system would fail to accomplish the original purpose of the optimalizing control: to constrain the system near the optimum state.

Since the purpose is to operate near the optimum state in spite of the "drift" of the system and of the noise interference, one may modify the peak-holding type of system by fixing the input hunting frequency and by specifying the input drive speed. Thus the input drive unit of the modified controller functions completely independent of the input-output relationship of the controlled system and of the noise interference. We now have two distinct problems to solve. First, a procedure must be devised for detecting whether the system is in the optimum state (correct mode of operation) or not. Second, on the basis of the amount of incorrect mode of operation, the system must be driven to the optimum state by the proper input adjustments and kept there with a prescribed minimum error in the presence of noise. Since the input adjustment depends on the outcome of the detection process it is obvious that the longer the latter takes, the slower the former will be. However, there is a limit to how slow the input adjustment can be and still permit the controller to keep up with the constantly shifting input-output relationship of the controlled system. In practice this means that the input hunting frequency in the case of the modified peak-holding controller will nearly always be higher than the nominal hunting frequency of a peak-holding controller when both are to be used for the same application.

The detection of the mode of operation of the modified peak-holding type of controller may be based on the following facts. We observe from Fig. 1 (A) that the correct or optimal mode of operation of this controller is achieved when the output hunts symmetrically about the point of maximum output. In this case the time variation of output is independent of whether the input is increasing or decreasing. Consequently, the output will fluctuate with twice the frequency of the input. The correct mode of operation may be characterized therefore by the fact that the output has no Fourier component of frequency equal to that of the input. The other diagrams of Fig.

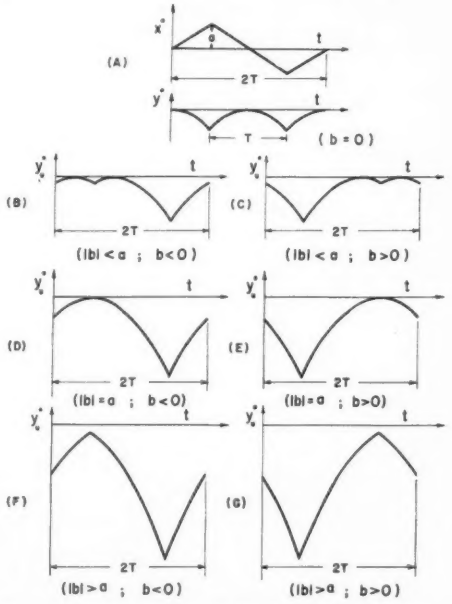


Fig. 1 Performance of an ideal peak-holding optimalizing control system for various amounts of incorrect input

Received July 24, 1955.

[1] This paper is based on part of a thesis submitted by the author for partial fulfillment of the requirements of Ph.D. in Mechanical Engineering, California Institute of Technology.

[2] Research Fellow in Jet Propulsion.

[3] Numbers in parentheses indicate References at end of paper.

1 show the output variation when the system is operating in various incorrect modes; it will be noted that the output contains some component of the input frequency for each of these incorrect modes. However, the foregoing facts are based on the existence of a parabolic relationship between the input and the output in the neighborhood of the optimum output. Although it may still be possible to apply the optimalizing principle when a small amount of asymmetry is contained in the input-output characteristic relationship, the hunting of the output will not be symmetrical about the optimum point.

We shall begin our analysis by indicating a few procedures for detecting the presence of the fundamental frequency or input hunting frequency component in the output of the system.

The author is grateful for his opportunity to prepare this work with the guidance of H. S. Tsien, whose continued interest and very kind criticisms were essential for the success of this investigation.

Detection Procedures

The difference between correct and incorrect modes of operation, as indicated in the introduction, is the occurrence of the first harmonic component in the output signal in the former case and the occurrence of both the fundamental and the first harmonic components in the output signal in the latter case. To illustrate the detection procedures, then, one could assume the noise-free output signal in the incorrect mode of operation to be

$$y = A + B \sin w_i t + C \cos w_i t + D \sin 2w_i t + E \cos 2w_i t$$

where w_i is the circular input hunting frequency. In the following sections, it will be seen that the form of the output y given by this equation is exactly that of the output from a sinusoidal input optimalizing controller in the incorrect mode of operation. The coefficients D and E of the first harmonic component are only functions of the dynamic characteristics of the controlled system. The coefficients B and C of the fundamental component are proportional to the amount of incorrect input b and are also functions of the dynamic characteristics of the controlled system. The d-c component A is a function of both the incorrect input and the dynamic characteristics of the controlled system.

Since the detection process must be accomplished under conditions of noise interference, the detection scheme must reduce the noise interference effects as much as possible. Such detection procedures fall in one or the other of two distinct types.

(A) *Direct Sampling and Averaging Technique*

From observations on Fig. 1, for an ideal optimalizing control with input parameters a and b, one can summarize the following facts:

1 When $b < a$, and when $b = 0$ (correct operation), two minimum points of the "potential" output occur during each input hunting cycle, and are located at the input reversal instants. In these cases, the maximum points of the "potential" output are located symmetrically with respect to the minimum points.

2 When $b \geq a$, there is always one minimum and one maximum point of the "potential" output per input cycle, and these are located at the input reversal instants.

When the input and output linear group characteristic time constants, τ_i and τ_0, respectively, of the controlled system are small compared to the output hunting period T of the system in the correct mode of operation, the conclusions mentioned above remain unchanged, with the exception of the locations of the maximum and minimum points. However, one must give special care to the first case. For instance, when $b < a$, there occurs only one minimum and one maximum point per input cycle when the characteristic time constants τ_i and τ_0 are of the same order of magnitude as T, or larger. Thus for small values of τ_i and τ_0, one can conclude that the locations of the minimum points of the output are independent of the amount of incorrect input b, and depend only on the dynamic characteristics of the controlled system. On the other hand, the locations of the maximum points are dependent on the amount of incorrect input b when $b < a$, and are independent of the amount of incorrect input b when $b \geq a$. Therefore the method in this case would be to locate a minimum point of the output signal and to investigate whether or not a maximum point of the output occurs after $T/2$ sec. When the maximum point of the output occurs $T/2$ sec after the occurrence of the minimum point, the control system is in the correct mode of operation. Otherwise the input level must be changed to produce the desired condition.

To locate either a minimum or a maximum of the output signal under noise interference, consider two sets of N samples. One set is taken at the time instants

$$t = 0, 2T, 4T, \ldots, 2(N-1)T$$

and the other set is taken at the instants

$$t = \tau, \tau + 2T, \tau + 4T, \ldots, \tau + 2(N-1)T$$

where $\tau \leq T/2$. One can choose N such that when average values of these samples are considered, the noise interference effects are made sufficiently small. Denoting the average of the first set of samples by $\bar{y}_1$ and that of the second by $\bar{y}_2$, one can distinguish the following three cases:

(a) When $\bar{y}_1 < \bar{y}_2$, the maximum point is behind and the minimum point is ahead of the sampling instants.

(b) When $\bar{y}_1 > \bar{y}_2$, the maximum point is ahead and the minimum point is behind the sampling instants.

(c) When $\bar{y}_1 = \bar{y}_2$, there occurs either a maximum or a minimum point of the output which is located approximately half way between two sampling instants.

By displacing the sampling instants, one can always obtain case (c). The choice of τ must be such that two sets of samples are distinguishable when samples are taken as in the cases (a) and (b), and such that when case (c) occurs the maximum or the minimum point is located very nearly half way between two sampling instants.

(B) *Explicit Detection of the Fundamental Component*

The following three methods may be considered as representative examples of this class:

1 *Narrow Band-Pass Filters.* Any convenient filter in this category can be utilized. The detection criterion in this case is to tune the filter circuit on the fundamental component frequency and to minimize the measured amplitude of the fundamental component by varying the input level.

2 *Direct Integration Technique.* Starting at any time origin $t = 0$, the output signal is integrated with respect to time for a complete cycle of the first harmonic component. The next integration is performed ΔT sec after the previous integration has been terminated, and so on. Thus the integrations are performed starting at time instants

$$t = 0, T + \Delta T, 2(T + \Delta T), \ldots, (N-1)(T + \Delta T)$$

and complete data have been obtained when $N\Delta T = 2T$.

When the starting instants of the integration procedure are displaced, the resulting integrals have approximately the following form

$$I_N = C \sin [w_i N(\Delta T) + \Phi] \qquad [N = 0, 1, 2, \ldots, (2T/\Delta T) - 1]$$

where C and Φ are constants. The noise interference effects are somewhat suppressed by the integration process and there is no contribution to the integrals from higher harmonics. When N equivalent integrators are used for this process, a complete set of data is available in $2T$ sec, since each integration process can start ΔT sec after the preceding one ends.

The criterion in this case is that the amplitude C of I_N should be a minimum which is reached by varying the input

level. In this condition the system is as close to the correct mode of operation as possible.

3 *Filtering by Correlation Method.* This method uses the principle of correlating the output signal with a sinusoidal signal of fundamental frequency w_i. The details of this procedure will be given in the following sections.

The preceding discussions indicate only a few procedures of many possible ways of detecting and eliminating the incorrect modes of operation of the modified optimalizing control system. The primary objective in the following sections is to demonstrate a statistical analysis designed to assess the merit of the proposed method of filtering by correlation. The ultimate choice of the design has to be based upon such an analysis for each of the various possible methods and upon other engineering factors.

Mathematical Analysis of the Incorrect Mode of Operation

To determine the dynamic effects of the controlled system on the performance of the modified optimalizing control system, neglecting noise interference effects, a modified optimalizing controller with an incorrect input will be analyzed.

In a similar manner as in the previous paper by Tsien and the author (2), the "potential" input x_u^*, specified as a sawtooth curve with period $2T$, amplitude a, and an amount of incorrect input b can be expanded into a Fourier series as

$$x_u^* = b + \frac{8a}{\pi^2}\sum_{n=0}^{\infty}\frac{(-1)^n}{(2n+1)^2}\frac{1}{2i}\left[e^{\frac{2n+1}{2}iw_0t} - e^{-\frac{2n+1}{2}iw_0t}\right] \quad \ldots [1]$$

where w_0 is the circular output hunting frequency in the correct mode of operation and is defined as

$$w_0 = 2\pi/T = 2w_i$$

In operator form, the actual input x_u and the actual output y_u are obtained as

$$x_u = b + \frac{8a}{\pi^2}\sum_{n=0}^{\infty}\frac{(-1)^n}{(2n+1)^2}\frac{1}{2i}\left[F_i\left(\frac{2n+1}{2}iw_0\right)e^{\frac{2n+1}{2}iw_0t} - F_i\left(-\frac{2n+1}{2}iw_0\right)e^{-\frac{2n+1}{2}iw_0t}\right] \quad \ldots [2]$$

and

$$y_u = -kb^2 + \frac{8abk}{\pi^2}i\sum_{n=0}^{\infty}\frac{(-1)^n}{(2n+1)^2}\left[F_0\left(\frac{2n+1}{2}iw_0\right)\times F_i\left(\frac{2n+1}{2}iw_0\right)e^{\frac{2n+1}{2}iw_0t} - F_0\left(-\frac{2n+1}{2}iw_0\right)\times F_i\left(-\frac{2n+1}{2}iw_0\right)e^{-\frac{2n+1}{2}iw_0t}\right] + \frac{16}{\pi^4}a^2k\sum_{n=0}^{\infty}\sum_{m=0}^{\infty}\times \frac{(-1)^{n+m}}{(2n+1)^2(2m+1)^2}\left[F_0\{(n+m+1)iw_0\}F_i\left(\frac{2n+1}{2}iw_0\right)\times F_i\left(\frac{2m+1}{2}iw_0\right)e^{(n+m+1)iw_0t} - F_0\{(n-m)iw_0\}\times F_i\left(\frac{2n+1}{2}iw_0\right)F_i\left(-\frac{2m+1}{2}iw_0\right)e^{(n-m)iw_0t} - F_0\{-(n-m)iw_0\}F_i\left(-\frac{2n+1}{2}iw_0\right)F_i\left(\frac{2m+1}{2}iw_0\right)\times e^{-(n-m)iw_0t} + F_0\{-(n+m+1)iw_0\}F_i\left(-\frac{2n+1}{2}iw_0\right)\times F_i\left(-\frac{2m+1}{2}iw_0\right)e^{-(m+n+1)iw_0t}\right] \quad \ldots [3]$$

Comparison of Equations [2] and [3] indicates that the output y_u has the same hunting period as the input x_u. The hunting loss D_u of this incorrectly operating control system is the time average of the output y_u; i.e.

$$D_u = kb^2 + \frac{32a^2k}{\pi^4}\sum_{n=0}^{\infty}\frac{1}{(2n+1)^4}F_i\left(\frac{2n+1}{2}iw_0\right)\times F_i\left(-\frac{2n+1}{2}iw_0\right) \quad \ldots [4]$$

It is clear from Equation [4] that the hunting loss D_u depends on the magnitude of the incorrect input b.

With the assumption that the transfer functions of the input and output linear groups can be represented closely by those for first order systems, i.e.

$$F_i(iw) = 1/(1 + iw\tau_i) \quad \ldots [5]$$

and

$$F_0(iw) = 1/(1 + iw\tau_0) \quad \ldots [6]$$

and with the introduction of a dimensionless parameter l for incorrect operation defined as

$$l = b/a \quad \ldots [7]$$

the actual output y_u and the hunting loss D_u, given by Equations [3] and [4], respectively, become

$$y_u = N^2T^2k\left\{-(l^2/4) - (-1)^j l\left[\left(\frac{l}{T} - j\right) - \left(\frac{\tau_0}{T} + \frac{\tau_i}{T}\right) + \frac{(\tau_0/T)^2e^{-\left(\frac{l}{T}-j\right)/(\tau_0/T)}}{\left(\frac{\tau_0}{T} - \frac{\tau_i}{T}\right)\cosh(T/2\tau_0)} - \frac{(\tau_i/T)^2e^{-\left(\frac{l}{T}-j\right)/(\tau_i/T)}}{\left(\frac{\tau_0}{T} - \frac{\tau_i}{T}\right)\cosh(T/2\tau_i)}\right]\right\} + 2N^2T^2k\left\{-\left[\frac{1}{2}\left(\frac{l}{T} - j\right)^2 - \left(\frac{\tau_0}{T} + \frac{\tau_i}{T}\right)\left(\frac{l}{T} - j\right) + \frac{1}{2}\left(\frac{\tau_i}{T}\right)^2 + \frac{\tau_i\tau_0}{T^2} + \left(\frac{\tau_0}{T}\right)^2\right] - \frac{1}{2}\frac{(\tau_0/T)^2}{\left(\frac{\tau_0}{T} - \frac{\tau_i}{T}\right)}\left[\frac{2(\tau_i/T)^3\tanh(T/2\tau_i)}{\left(\frac{\tau_0}{T} - \frac{\tau_i}{T}\right)\left(2\frac{\tau_0}{T} - \frac{\tau_i}{T}\right)} - 1\right]\times \frac{e^{-\left(\frac{l}{T}-j\right)/(\tau_0/T)}}{\sinh(T/2\tau_0)} + \left[\left(\frac{l}{T} - j\right) + \frac{(\tau_i/T)^2}{\left(\frac{\tau_0}{T} - \frac{\tau_i}{T}\right)}\right]\times \frac{(\tau_i/T)^2e^{-\left(\frac{l}{T}-j\right)/(\tau_i/T)}}{\left(\frac{\tau_0}{T} - \frac{\tau_i}{T}\right)\cosh(T/2\tau_i)} + \frac{1}{2}\frac{(\tau_i/T)^3}{\left(2\frac{\tau_0}{T} - \frac{\tau_i}{T}\right)}\times \frac{e^{-2\left(\frac{l}{T}-j\right)/(\tau_i/T)}}{\cosh^2(T/2\tau_i)}\right\} \quad \ldots [8]$$

when

$$-1/2 \le [(l/T) - j] \le 1/2$$

where

$$j = 0, 1, 2, \ldots$$

and

$$D_u = N^2T^2k[\tfrac{1}{4}(l^2 + \tfrac{1}{3}) - (\tau_i/T)^2 + 2(\tau_i/T)^3\times \tanh(T/2\tau_i)] \quad \ldots [9]$$

where $N = 2a/T$ is again the input drive speed.

Figs. 2 and 3 show the dimensionless plots of the actual output for several particular values of l, for the cases when $(\tau_0/T) = 0.15$ and $(\tau_i/T) = 0.10$. The plots in these figures have

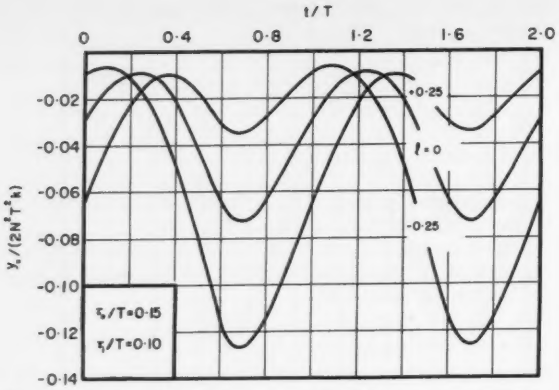


Fig. 2 Actual output for $\tau_i/T = 0.10$ and $\tau_0/T = 0.15$ with parameter

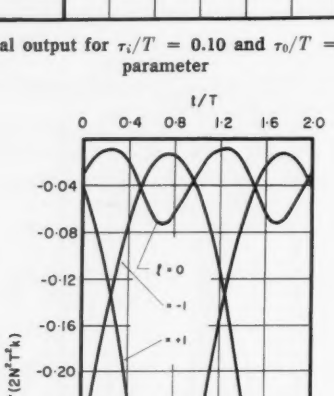


Fig. 3 Actual output for $\tau_i/T = 0.10$ and $\tau_0/T = 0.15$ with l parameter

essentially the same shape as those for the corresponding cases illustrated in Fig. 1. The differences are again the rounding of the sharp corners and the time lag due to dynamic effects.

Detection and Elimination of the Incorrect Mode of Operation Without Noise Interference

The parameter l, defined by Equation [7], is introduced in such a manner that it is not only possible to detect the incorrect mode of operation, but it is also possible to determine the magnitude and the sign of the incorrect input $b = (NT/2)l$. Therefore the problem is to devise a scheme to determine the parameter l. As was explained in a previous section, one of the possible schemes is as follows: the actual output y_u is cross-correlated with a sinusoid which has an amplitude A, frequency w_i, and a time displacement τ with respect to the actual output signal y_u.

In general, the cross-correlation of a function $f(t)$ with $g(t)$ is defined as

$$\chi(\tau) = \lim_{\theta \to \infty} \frac{1}{2\theta} \int_{-\theta}^{\theta} f(t + \tau)\overline{g(t)}dt \quad \ldots\ldots\ldots [10]$$

where $\overline{g(t)}$ is the complex conjugate of $g(t)$. For periodic real functions $f(t)$ and $g(t)$, the cross-correlation function given by Equation [10] reduces to

$$\chi(\tau) = \frac{1}{2\theta} \int_{-\theta}^{\theta} f(t + \tau)g(t)dt \quad \ldots\ldots\ldots [11]$$

where 2θ is the smallest common period of the two functions $f(t)$ and $g(t)$.

Choose

$$f(t + \tau) = A \sin w_i(t + \tau)$$

and

$$g(t) = y_u(t)$$

then the cross-correlation function $\chi(\tau)$ given by Equation [11] becomes

$$\chi(\tau) = \frac{A}{2} \cos w_i\tau \int_0^2 y_u(t') \sin \pi t'dt' + \frac{A}{2} \sin w_i\tau \int_0^2 y_u(t') \cos \pi t'dt' \quad \ldots\ldots\ldots [12]$$

where the integration variable has been changed to $t' = t/T$.

By substitution of Equation [8] into Equation [12] and by performing the integrations, $\chi(\tau)$ is obtained as

$$\chi(\tau) = \frac{2AN^2kl}{w_i^2[1 + (w_i\tau_0)^2][1 + (w_i\tau_i)^2]} \times \{(w_i^2\tau_0\tau_i - 1) \cos w_i\tau + w_i(\tau_0 + \tau_i) \sin w_i\tau\} \quad \ldots [13]$$

Thus, with a specified set of characteristics of the controlled and control systems, the amplitude A of the sinusoid, and the value of the cross-correlation function $\chi(\tau)$ for a given value of τ, the parameter l can be computed by using Equation [13]. Fig. 4 shows dimensionless plots of the cross-correlation function for $l = +1$ for various values of τ_i/T and τ_0/T.

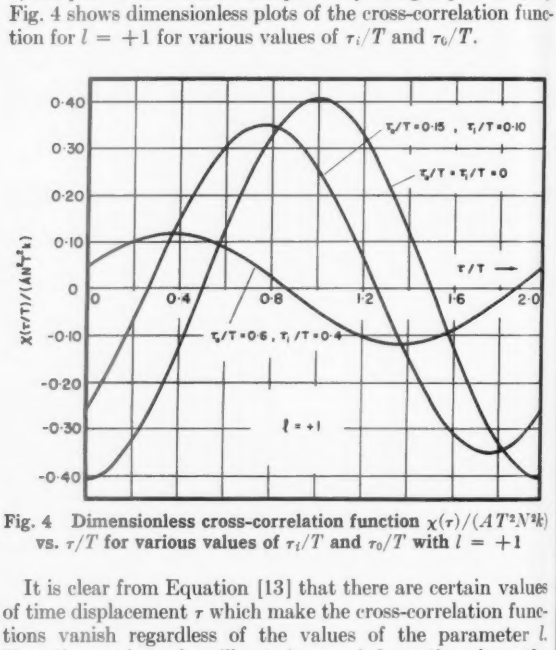


Fig. 4 Dimensionless cross-correlation function $\chi(\tau)/(AT^2N^2k)$ vs. τ/T for various values of τ_i/T and τ_0/T with $l = +1$

It is clear from Equation [13] that there are certain values of time displacement τ which make the cross-correlation functions vanish regardless of the values of the parameter l. Since these values of τ will not give any information about the incorrect mode of operation, they cannot be utilized. The forbidden values of τ are found by setting Equation [13] equal to zero, thus

$$(w_i\tau \mp n\pi) = \text{arc tan} \frac{(1 - w_i^2\tau_0\tau_i)}{w_i(\tau_0 + \tau_i)} \qquad (n = 0, 1, 2, \ldots) \ldots [14]$$

When it is necessary to use a computer for the determination of the parameter l, one must choose τ such that the absolute value of the cross-correlation function is the largest. By differentiating $\chi(\tau)$ with respect to τ and setting it equal to zero, one obtains the desired values of τ as

$$(w_i\tau \mp n\pi) = \text{arc tan} \frac{w_i(\tau_0 + \tau_i)}{(w_i^2\tau_0\tau_i - 1)} \qquad (n = 0, 1, 2, \ldots) \ldots [15]$$

When the only information available is the input hunting

frequency w_i, Equation [13] can be written as

$$\chi(\tau) = \alpha \cos w_i\tau + \beta \sin w_i\tau \quad [16]$$

where α and β are defined as

$$\alpha = \frac{2AN^2kl}{w_i^2} \frac{(w_i^2\tau_0\tau_i - 1)}{[1 + (w_i\tau_0)^2][1 + (w_i\tau_i)^2]} \quad [17]$$

$$\beta = \frac{2AN^2kl}{w_i^3} \frac{w_i(\tau_0 + \tau_i)}{[1 + (w_i\tau_0)^2][1 + (w_i\tau_i)^2]} \quad [18]$$

From Equations [17] and [18] it is seen that the coefficient β will always have the same sign as the parameter l, and the coefficient α will have the same sign as l when $w_i^2\tau_0\tau_i > 1$, but the opposite sign to l when $w_i^2\tau_0\tau_i < 1$. When only two distinct values of the cross-correlation function $\chi(\tau)$ are known for two given values of time displacement, except when $\tau_1 - \tau_2 = n\pi/w_i$, it is possible to determine coefficients α and β from Equation [16]. Although there is not enough information to determine the value of the parameter l with either Equation [17] or Equation [18], one knows that the sign of l is the same as that of the coefficient β. Since the characteristic time constants τ_i and τ_0 of the controlled system are not available, the information obtained through the coefficient α is unreliable. Thus knowing only w_i, the input hunting frequency, and evaluating two distinct values of the cross-correlation function for two distinct values of time displacement, it is still possible to detect the incorrect mode of operation and the direction in which it occurs. To eliminate the incorrect mode of operation in this case, the input level can be varied by increments in accordance with the sign of the coefficient β. After each stepwise variation of input, two new cross-correlation processes must be carried out. This elimination of the incorrect mode of operation through a trial-and-error technique is continued until both cross-correlations obtained vanish; that is, $l = 0$ or $\alpha = \beta = 0$. This mode of operation is then the correct mode of operation.

Detection and Elimination of an Incorrect Mode of Operation with Noise Interference

In the previous section, the detection and elimination criterion of the incorrect mode of operation was formulated for a modified optimalizing control system, free from noise interference effects. Needless to say, noise from both external and internal sources is present and affects the performance of the control system. However, when the noise interference effects are considered, the fundamental concept of the detection and elimination criterion introduced in the previous section is still valid. The method is again to determine a parameter l' which is an indication of the amount of the incorrect mode of operation.

For simplicity of analysis, the noise function $n(t)$ is assumed to be superimposed on the actual output $y_u(t)$; thus the signal $F(t)$ indicated by an output measuring instrument is of the form

$$F(t) = y_u(t) + n(t) \quad [19]$$

Then the cross-correlation function $R(\tau)$ of $F(t)$ with a sinusoid of the form $A \sin w_i(t + \tau)$ is

$$R(\tau) = \lim_{\theta \to \infty} \frac{A}{2\theta} \int_{-\theta}^{\theta} F(t) \sin w_i(t + \tau)dt$$

By using Equations [12] and [19], an approximate cross-correlation $R_m(\tau)$ depending on a parameter m, the number of input cycles over which the correlation process is carried out, can be defined as

$$R_m(\tau) = \chi(\tau) + \frac{A}{2mT} \int_0^{2mT} n(t) \sin w_i(t + \tau)dt \quad [20]$$

When a value of the cross-correlation function $R_m(\tau)$ and complete control and controlled systems characteristics are available, the parameter l', an indication of the incorrect operation mode, can be computed approximately by replacing $\chi(\tau)$ with $R_m(\tau)$ in Equation [13]. Thus

$$l' = \frac{w_i^2R_m(\tau)[1 + (w_i\tau_0)^2][1 + (w_i\tau_i)^2]}{2AN^2k\{(w_i^2\tau_0\tau_i - 1) \cos w_i\tau + w_i(\tau_0 + \tau_i) \sin w_i\tau\}} \quad [21]$$

The amount of incorrect input which must be eliminated is then $b' = (NT/2)l'$. Since the cross-correlation process is carried out for a finite value of m, the noise inteference effects are not completely eliminated, and b' is not necessarily the actual amount of incorrect input. For example, $l' = 0$ may not mean that the system is operating in the correct mode. Thus, there is a certain probability of error associated with the value of the parameter l'.

When the cross-correlation process is carried out for two distinct values of time displacement and only the input hunting frequency w_i is known, it is still possible to detect and to eliminate the incorrect operation mode with a certain probability of error due to noise interference effects. In this case the cross-correlation function $R_m(\tau)$ can be written as

$$R_m(\tau) = \alpha' \cos w_i\tau + \beta' \sin w_i\tau \quad [22]$$

With two distinct values of $R_m(\tau)$, one can determine the coefficients α' and β' from Equation [22]. Again, with a certain probability of error, one can say that the sign of the parameter l is the same as that of the coefficient β', and one can vary the input level in increments in order to eliminate the incorrect mode of operation. In this case the information obtained by using the coefficient α' is again unreliable.

To refine the process of elimination of the incorrect mode of operation the cross-correlation function $R_m(\tau)$, given by Equation [20], must be as free as possible from noise interference effects. One way to reduce noise interference effects is to choose m to be large; that is, to carry out the cross-correlation process for a large number of cycles, and thus reduce the noise interference effects to a minimum by an averaging process. However, the larger the value of m which is chosen, the longer it will take to obtain the desired information.

Another possible way to reduce the noise interference effects is to choose a reasonably small value of m and to carry out the cross-correlation process for several values of time displacement. With these several values of cross-correlation functions, it is possible to produce a cross-correlation function of the form

$$R_m^*(\tau) = \alpha^* \cos w_i\tau + \beta^* \sin w_i\tau \quad [23]$$

such that it is the best estimation of Equation [16]. When only one cross-correlator is used, this process is time-consuming, but when it is feasible to use a number of equivalent cross-correlators, this process takes a rather short time.

One of perhaps several ways of producing Equation [23] through a cross-correlation process for several values of time displacement can be outlined as follows:

Consider a set of values of cross-correlation functions

$$R_{m_0}, R_{m_1}, R_{m_2}, \ldots, R_{m_j}, \ldots, R_{m_k}$$

which correspond to time displacements

$$0 = \tau_0, \tau_1, \tau_2, \ldots, \tau_j, \ldots, \tau_k = 2\pi/w_i$$

where each of these time displacements differs by an equal increment $\Delta\tau$ from the preceding one. For the value of time displacement τ_j, the corresponding error of estimation in cross-correlation function is given by

$$R_{m_j} - R_m^*(\tau_j)$$

Since the problem is to fit a simple curve to given data, the method of least squares is considered to be satisfactory. The method of least squares requires that the sum of squares of

the errors be a minimum. The sum of the squares of the errors G is given by

$$G = \sum_{j=1}^{k} [R_{m_j} - (\alpha^* \cos w_i\tau_j + \beta^* \sin w_i\tau_j)]^2 \quad \ldots\ldots [24]$$

Inspection of Equation [24] shows that the sum of the squares of the errors G is a function of α^* and β^*; thus the coefficients α^* and β^* must be determined such that G is a minimum. The requirement for the minimum will be satisfied when the partial derivatives of G with respect to both α^* and β^* vanish, thus the particular values of these coefficients are found to be

$$\left.\begin{aligned} \alpha^* &= \frac{2}{k}\sum_{j=1}^{k} R_{m_j} \cos\frac{2\pi}{k} j \\ \beta^* &= \frac{2}{k}\sum_{j=1}^{k} R_{m_j} \sin\frac{2\pi}{k} j \end{aligned}\right\} \quad \ldots\ldots [25]$$

As was done for the case shown by Equation [21], a parameter l^* may be computed to be

$$l^* = \frac{w_i^2 R_m^*(\tau)[1 + (w_i\tau_0)^2][1 + (w_i\tau_i)^2]}{2AN^2k\{(w_i^2\tau_0\tau_i - 1)\cos w_i\tau + w_i(\tau_0 + \tau_i)\sin w_i\tau\}} \quad \ldots [26]$$

Fig. 5 shows a complete block diagram of a modified optimalizing control system using a cross-correlator, a variable time displacement sine wave generator, and a computer to filter out the noise interference effects. This control system can be operated to produce either the parameter l' by using only one value of time displacement or the parameter l^* by using several values of time displacement.

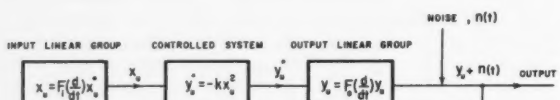


Fig. 5 Block diagram of a modified optimalizing control system with filtering by means of cross-correlation

Probable Error in Detection and Elimination of the Incorrect Mode of Operation in the Presence of Noise Interference

In the previous section it was shown that with noise interference effects, the criterion for detection and elimination of the incorrect mode of operation can be based either on the parameter l' (or l^*) or on the coefficient β' (or β^*)[4] depending on how much information is available about the system. Since the parameter l' or the coefficient β' is computed in a finite length of time, the noise interference effects are not completely eliminated, and it is conceivable that the parameter l' or the coefficient β' will contain the following two types of error:

Type I: Error in the magnitude of the parameter l' or β'. For example, l' and l have the same algebraic signs but their magnitudes differ.

Type II: Error in both algebraic sign and magnitude of the parameter l' or β'. For example, to obtain l' as a negative quantity while l really is a positive quantity, or vice versa.

Type I error is not a serious type of error since the input level is corrected in the right direction. When l' is large in magnitude, Type I error is expected to occur more frequently than Type II error. When the magnitude of l' is reduced in order to reach the correct mode of operation, both Type I and Type II errors are expected to occur frequently. Type II error is more serious than Type I error, since the occurrence of Type II error is a false alarm, and the input level is changed in the wrong direction. Therefore confining the system as closely as possible to the correct mode of operation results in the frequent occurrence of Type II error. Thus the control system designer must decide upon a certain probability of occurrence of Type II error as being satisfactory, and compute a limiting value of the parameter l' or β' which leads to the best mode of operation. For example, denoting this limiting value of l' by l'^*, the computer then should be equipped with a device such that whenever $|l'| \leq |l'^*|$, the input level is left unchanged; otherwise alteration of input level is carried on.

In the following analysis, the principal objective is to determine the probability of occurrence of Type II error in the detection and elimination criterion introduced in the previous section. Then a theoretical illustration will be presented so as to demonstrate how the limiting parameters l'^* and β'^* can be computed.

The probability of occurrence of Type II error is equivalent to the probability of having $ll' < 0$ or $\beta\beta' < 0$. From Equations [13] and [21] it is clear that the probability of having $ll' < 0$ is equivalent to the probability of having $\chi(\tau)R_m(\tau) < 0$. To compute the probability that $\beta\beta' < 0$ or $\chi(\tau)R_m(\tau) < 0$, consider the following relations

$$\zeta = \beta\beta' = \beta'^2 - (\beta' - \beta)\beta' \quad \ldots\ldots [27]$$

$$\xi = \chi(\tau)R_m(\tau) = [R_m(\tau)]^2 - [R_m(\tau) - \chi(\tau)]R_m(\tau) \quad \ldots [28]$$

from Equations [16], [20], and [22] one can show that

$$\left.\begin{aligned} \beta' &= \frac{1}{T}\int_0^{2T} R_m(\tau)\sin w_i\tau\, d\tau \\ (\beta' - \beta) &= \frac{A}{2Tm}\int_0^{2Tm} n(t)\cos w_i t\, dt \end{aligned}\right\} \quad \ldots\ldots [29]$$

By substitution of the expressions given by Equations [20] and [29] into Equations [27] and [28], the relations for the variables ζ and ξ are found to be

$$\zeta = \left[\frac{1}{T}\int_0^{2T} R_m(\tau)\sin w_i\tau\, d\tau\right]^2 - \left[\frac{1}{T}\int_0^{2T} R_m(\tau)\sin w_i\tau\, d\tau\right] \times \left[\frac{A}{2Tm}\int_0^{2Tm} n(t)\cos w_i t\, dt\right]$$

$$\xi = [R_m(\tau)]^2 - R_m(\tau)\left[\frac{A}{2Tm}\int_0^{2Tm} n(t)\sin w_i(t+\tau)dt\right]$$

With the assumption that the noise considered in this analysis is a stationary random function and its time average $\overline{n(t)}$ vanishes, the mean values and mean deviations of the statistical variables ζ and ξ are, respectively

$$\bar{\zeta} = \beta'^2 = \left[\frac{1}{T}\int_0^{2T} R_m(\tau)\sin w_i\tau\, d\tau\right]^2 \quad \ldots\ldots [30]$$

$$\bar{\xi} = [R_m(\tau)]^2 \quad \ldots\ldots [31]$$

and

$$\sigma_\zeta = \left[\frac{1}{T}\int_0^{2T} R_m(\tau)\sin w_i\tau\, d\tau\right] \times \left\{\frac{A^2}{(2Tm)^2}\int_0^{2Tm} dt'' \int_0^{2Tm} dt'\, \overline{n(t')n(t'')}\cos w_i t' \cos w_i t''\right\}^{1/2} \quad \ldots [32]$$

[4] In this section the analysis will be carried out for primed quantities. However, the results can be used equivalently for starred quantities.

$$\sigma_\xi = R_m(\tau)\left\{\frac{A^2}{(2Tm)^2}\int_0^{2Tm} dt'' \int_0^{2Tm} dt' \overline{n(t')n(t'')} \times \sin w_i(t' + \tau) \sin w_i(t'' + \tau)\right\}^{1/2} \quad \ldots\ldots [33]$$

For a control system designer, the power spectrum of the noise, rather than its correlation function, is more readily available. The correlation function of noise, $\overline{n(t')n(t'')}$, is related to the power spectrum of the noise, $\Phi_{nn}(w)$, by

$$\overline{n(t')n(t'')} = \int_0^\infty \Phi_{nn}(w) \cos w(t' - t'')dw \quad \ldots\ldots [34]$$

By substitution of Equation [34] into Equations [32] and [33], and carrying out the integrations with respect to t' and t'' the mean deviations σ_ζ and σ_ξ now become

$$\sigma_\zeta = \left[\frac{1}{T}\int_0^{2T} R_m(\tau) \sin w_i\tau \, d\tau\right] \times \left\{\frac{A^2}{\pi^2 m^2}\int_0^\infty \Phi_{nn}(w) \frac{(w/w_i)^2 \sin^2(\pi m w/w_i)}{[(w/w_i)^2 - 1]^2} dw\right\}^{1/2} \quad \ldots\ldots [35]$$

and

$$\sigma_\xi = R_m(\tau)\left\{\frac{A^2}{\pi^2 m^2}\int_0^\infty \Phi_{nn}(w) \frac{\sin^2(\pi m w/w_i)}{[(w/w_i)^2 - 1]^2} dw + \frac{A^2}{\pi^2 m^2} \sin^2 w_i\tau \int_0^\infty \Phi_{nn}(w) \frac{\sin^2(\pi m w/w_i)}{(w/w_i)^2 - 1} dw\right\}^{1/2} \quad \ldots\ldots [36]$$

When the first probability distributions of the statistical variables ζ and ξ are not known, it is possible to make a broad approximation of the errors ϵ_ζ and ϵ_ξ, the probability of finding $\beta\beta' < 0$, and the probability of finding $ll' < 0$, respectively. First, for this purpose the probability of large deviation from the mean will be estimated.

Assume, for example, that the ζ's distribute themselves around the mean $\bar{\zeta}$ symmetrically and that $\bar{\zeta}$ is positive and sufficiently large. Then the probability of the occurrence of large deviations from the mean is given by Bienaymé-Chebyshev's inequality (Ref. 3)

$$P[|\zeta - \bar{\zeta}| \geq K\sigma_\zeta] \leq (1/K^2) \quad \ldots\ldots [37]$$

The error ϵ_ζ is one half of the probability given by Equation [37] when $K\sigma_\zeta$ is replaced by $\bar{\zeta}$. Thus

$$\epsilon_\zeta = \tfrac{1}{2}P[|\zeta - \bar{\zeta}| \geq \bar{\zeta}] \leq \tfrac{1}{2}(\sigma_\zeta/\bar{\zeta})^2 \quad \ldots\ldots [38]$$

Similarly, the error ϵ_ξ, the probability of finding $ll' < 0$, can be approximated as

$$\epsilon_\xi \leq \tfrac{1}{2}(\sigma_\xi/\bar{\xi})^2 \quad \ldots\ldots [39]$$

A sharper approximation of the errors ϵ_ζ and ϵ_ξ will be obtained when the probability distribution is assumed to be unimodal. Then the Gauss inequality (3) can be used in place of the Bienaymé-Chebyshev inequality. In this case, the errors ϵ_ζ and ϵ_ξ are found to be

$$\epsilon_\zeta \leq \frac{2}{9}(\sigma_\zeta/\bar{\zeta})^2 \quad \ldots\ldots [40]$$

and

$$\epsilon_\xi \leq \frac{2}{9}(\sigma_\xi/\bar{\xi})^2 \quad \ldots\ldots [41]$$

When the first probability distributions of ζ and ξ are known, it is possible to compute ϵ_ζ and ϵ_ξ exactly. For example, since ζ is a stationary random variable, its first probability distribution W_1 is a function of ζ only. Then the probability that $\zeta < 0$ is simply the error ϵ_ζ; thus

$$\epsilon_\zeta = \int_{-\infty}^0 W_1(\zeta)d\zeta$$

By the assumption of the first probability distribution of ζ as Gaussian, the error ϵ_ζ is found to be

$$\epsilon_\zeta = {}^1/_2\left[1 - \text{erf}\left(\frac{1}{\sqrt{2}}\frac{\bar{\zeta}}{\sigma_\zeta}\right)\right] \quad \ldots\ldots [42]$$

Similarly, the error ϵ_ξ is obtained as

$$\epsilon_\xi = {}^1/_2\left[1 - \text{erf}\left(\frac{1}{\sqrt{2}}\frac{\bar{\xi}}{\sigma_\xi}\right)\right] \quad \ldots\ldots [43]$$

It is to be noted that whether the probability of the occurrence of Type II error is approximated, for example, by one of Equations [39] or [41], or is computed by assuming a first probability distribution, Equation [43], ϵ_ξ depends only on the quotient $\bar{\xi}/\sigma_\xi$. Fig. 6 shows the probability of the occurrence of Type II error as a function of the quotient $\bar{\xi}/\sigma_\xi$ or $\bar{\zeta}/\sigma_\zeta$.

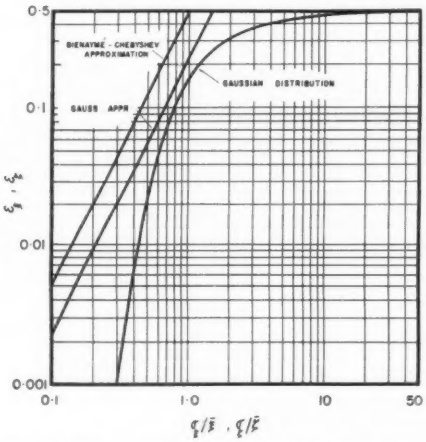


Fig. 6 Probability of occurrence of Type II error vs. the quotient $\sigma_\xi/\bar{\xi}$ or $\sigma_\zeta/\bar{\zeta}$

In order to demonstrate a possible way of choosing the limiting parameter l'^* or β'^* when the probability of Type II error is assigned and the statistical properties of the noise interference are given, one can form the following quotients

$$\beta'\frac{\sigma_\zeta}{\bar{\zeta}} = \sqrt{\overline{n^2(t)}}\, A\left\{\frac{1}{\pi^2 m^2}\frac{1}{\overline{n^2(t)}}\int_0^\infty \Phi_{nn}(w) \times \frac{(w/w_i)^2 \sin^2(\pi m w/w_i)}{[(w/w_i)^2 - 1]^2} dw\right\}^{1/2} \quad \ldots\ldots [44]$$

$$l'\frac{\sigma_\xi}{\bar{\xi}} = \frac{\sqrt{\overline{n^2(t)}}}{D}\frac{\pi^2}{2}\frac{1}{\overline{n^2(t)}}\left\{\frac{1}{\pi^2 m^2}\int_0^\infty \frac{\Phi_{aa}(w)\sin^2(\pi m w/w_i)}{[(w/w_i)^2 - 1]^2} dw + \frac{\sin^2 w_i\tau}{\pi^2 m^2}\int_0^\infty \frac{\Phi_{nn}(w)\sin^2(\pi m w/w_i)}{(w/w_i)^2 - 1} dw\right\}^{1/2} \times \frac{\left[\frac{1}{12} - (\tau_i/T)^2 + 2(\tau_i/T)^3 \tanh(T/2\tau_i)\right][1 + (w_i\tau_0)^2][1 + (w_i\tau_i)^2]}{\{(w_i^2\tau_0\tau_i - 1)\cos w_i\tau + w_i(\tau_0 + \tau_i)\sin w_i\tau\}} \quad \ldots\ldots [45]$$

where Equation [44] is obtained from Equations [30] and [35], and Equation [45] is obtained from Equations [21], [31], and [36]. The parameter D is the hunting loss of the control system in the correct mode of operation.

When all system characteristics are available and when the power spectrum of the noise can be estimated, then l'^* is obtained from Equation [45] by using the quotient $\sigma_\xi/\bar{\xi}$, which is obtained from Fig. 6 with the assigned value of ϵ_ξ. To illustrate a typical procedure, choose $\tau = 0$; then Equation [45]

becomes

$$l'^* = \frac{\sqrt{\overline{n^2(t)}}}{D} \cdot \frac{\bar{\xi}}{\sigma_\xi} \cdot g \cdot f \quad \ldots\ldots\ldots\ldots\ldots [46]$$

where

$$g = \left\{ \frac{1}{\pi^2 m^2} \frac{1}{\overline{n^2(t)}} \int_0^\infty \Phi_{nn}(w) \frac{\sin^2(\pi m w/w_i)}{[(w/w_i)^2 - 1]^2} \, dw \right\}^{1/2}$$

and

$$f = \frac{\pi^2}{2} \times \frac{\left[\frac{1}{12} - (\tau_i/T)^2 + 2(\tau_i/T)^3 \tanh(T/2\tau_i)\right][1 + (w_i\tau_i)^2][1 + (w_i\tau_0)^2]}{(w_i^2\tau_0\tau_i - 1)}$$

Fig. 7 shows the characteristic noise function g as a function of the ratio w_n/w_i with m as parameter for typical noise power spectrum $\Phi_{nn}(w) = \gamma^2/(w_n^2 + w^2)$; where γ is a constant and w_n is a characteristic noise frequency. From this figure it is observed that for $w_n/w_i \lesssim 1$, the function g decreases in magnitude very rapidly for the first few values of the parameter m and for the values of the quotient w_n/w_i away from unity, the effect of the parameter m on the function g is unimportant. Fig. 8 shows the controlled system dynamic characteristics function f as a function of τ_0/τ_i with $(\tau_0 + \tau_i)/T$ as parameter. Figs. 9 and 10 show the limiting value l'^* as a function of the dimensionless noise level $\sqrt{\overline{n^2(t)}}/D$ with m as a parameter. On each of these figures, two values of l'^* are presented which correspond to five and ten per cent probability of the occurrence of Type II error due to noise interference effects, which are characterized by a power spectrum of the form $\Phi_{nn}(w) = \gamma^2/(w^2 + w_n^2)$ and characteristic frequency $w_n = w_i$. Thus Figs. 6 through 10 are typical illustrations of the analysis which must be carried out to determine the parameter l'^*.

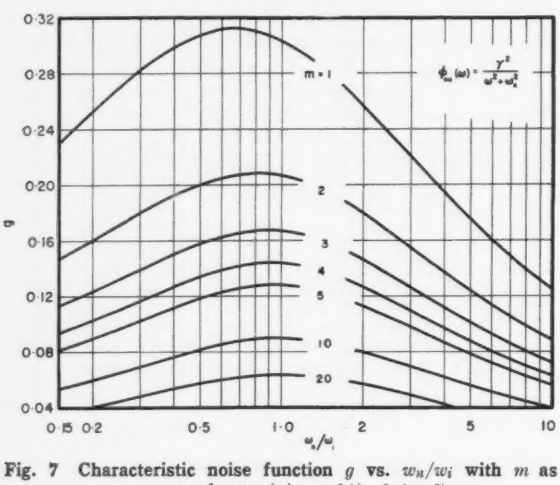


Fig. 7 Characteristic noise function g vs. w_n/w_i with m as parameter for $\Phi_{nn}(w) = \gamma^2/(w_n^2 + w^2)$

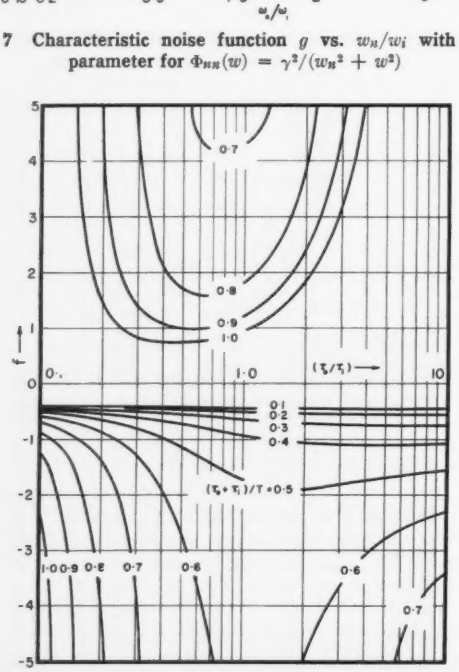


Fig. 8 Controlled system dynamic characteristics function f vs. τ_0/τ_i with $(\tau_0 + \tau_i)/T$ as parameter

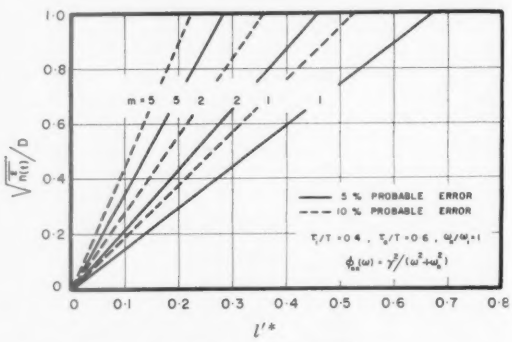


Fig. 9 Dimensionless noise level $\sqrt{\overline{n^2(t)}}/D$ vs. l'^* with m as parameter for $\tau_i/T = 0.40$, $\tau_0/T = 0.60$, $w_n/w_i = 1$, and $\Phi_{nn}(w) = \gamma^2/(w_n^2 + w^2)$

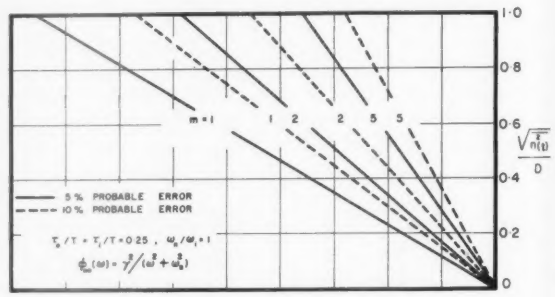


Fig. 10 Dimensionless noise level $\sqrt{\overline{n^2(t)}}/D$ vs. l'^* with m as parameter for $\tau_i/T = \tau_0/T = 0.25$, $w_n/w_i = 1$, and $\Phi_{nn}(w) = \gamma^2/(w_n^2 + w^2)$

Concluding Remarks

In (2) it was indicated that the sawtooth form of input is the simplest type that is suitable for a peak-holding optimalizing control. However, in this work, the optimalizing control scheme is changed in such a manner that any periodic signal can be used as the input and the resulting control system will again hunt around the optimum state. As an illustration, one can consider a simple sinusoidal form of "potential" input with an amount of incorrect input b, i.e.

$$x_s^* = b + a' \sin w_i t \quad \ldots\ldots\ldots\ldots\ldots [47]$$

If it is assumed that the input and output linear groups can be closely approximated by first order systems, then the actual input x_s, the actual output y_s, and the hunting loss D_s in the incorrect mode of operation are found to be

$$x_s = b + \frac{a'}{1 + (w_i\tau_i)^2} \{\sin w_i t - (w_i\tau_i) \cos w_i t\} \quad \ldots [48]$$

$$y_s = -kb^2 - 2a'bk\frac{[1 - w_i^2\tau_0\tau_i]\sin w_i t - w_i(\tau_0 + \tau_i)\cos w_i t}{[1 + (w_i\tau_0)^2][1 + (w_i\tau_i)^2]} +$$

$$\frac{a'^2k}{2}\left\{\frac{2[w_i\tau_0(1 - w_i^2\tau_i^2) + w_i\tau_i]\sin 2w_i t}{[1 + (2w_i\tau_0)^2][1 + (w_i\tau_i)^2]^2} - \frac{1}{1 + (w_i\tau_i)^2} + \right.$$

$$\left.\frac{[1 - (w_i\tau_i)^2 - 4w_i^2\tau_i\tau_0]\cos 2w_i t}{[1 + (2w_i\tau_0)^2][1 + (w_i\tau_i)^2]^2}\right\} \ldots [49]$$

and

$$D_s = kb^2 + \frac{a'^2k}{2}\frac{1}{1 + (w_i\tau_i)^2} \ldots\ldots\ldots\ldots [50]$$

Similarly, the noise-interference-free cross-correlation function is obtained as

$$\chi_s(\tau) = \frac{Aa'bk}{[1 + (w_i\tau_0)^2][1 + (w_i\tau_i)^2]} \times$$
$$\{(w_i^2\tau_0\tau_i - 1)\cos w_i\tau + w_i(\tau_0 + \tau_i)\sin w_i\tau\} \ldots\ldots [51]$$

It is observed that the form of Equation [51] is exactly the same as that of Equation [13]. The only difference is a multiplicative constant. Therefore it is unnecessary to carry out the remainder of the analysis for this type of control system. The fundamental concepts introduced in previous sections are perfectly valid in the present analysis.

The analyses which have been carried out so far have considered, for the sake of simplicity, a single output due to a single input. For some controlled systems to which the optimalizing control scheme can be applied, it may be necessary to consider several simultaneous inputs. In this case one has to consider a negative definite input-output characteristics surface in $n + 1$ dimensions. For example, referred to the optimum point an operation surface of this sort may be defined as

$$y^* = -\sum_{k=1}^{n} A_k x_k^{*2} + \sum_{\substack{k=1 \\ (k\neq j)}}^{n}\sum_{j=1}^{n} C_{kj}x_k^* y_j^* \ldots\ldots [52]$$

where A_k and C_{kj} ($C_{kj} \neq C_{jk}$) are characteristic constants of the controlled system, and n is the number of inputs such that for all real values of x^*, $y^* \leq 0$. Therefore $x^* = 0$ corresponds to the optimum point. For the purpose of illustration of the detection and elimination of incorrect mode of operation in this case, consider a sinusoidal input optimalizing control without dynamic effects. Thus, in the incorrect mode of operation each input x_k^* has the form

$$x_k^* = b_k + a_k \sin w_k t \ldots\ldots\ldots\ldots [53]$$

where b_k is the amount of incorrect input of the kth input, and each input hunting frequency w_k is distinct. By substitution of Equation [53] into Equation [52], the output y_u^* due to incorrect mode of operation is obtained as

$$y_u^* =$$

$$-\sum_{k=1}^{n} A_k\{(b_k^2 + {}^1/_2\, a_k^2) + 2b_k a_k \sin w_k t - {}^1/_2 a_k^2 \cos 2w_k t\}$$

$$+\sum_{\substack{k=1 \\ (k\neq j)}}^{n}\sum_{j=1}^{n} C_{kj}\{b_k b_j + b_j a_k \sin w_k t +$$

$$b_k a_j \sin w_j t + {}^1/_2 a_k a_j\,[\cos(w_k - w_j)t - \cos(w_k + w_j)t]\} \ldots [54]$$

In the correct mode of operation, all the b_k are zero; thus the output in the correct mode of operation is

$$y^* = -\sum_{k=1}^{n} A_k\left\{{}^1/_2 a_k^2 - {}^1/_2 a_k^2 \cos 2w_k t\right\} +$$

$$\sum_{\substack{k=1 \\ (k\neq j)}}^{n}\sum_{j=1}^{n} {}^1/_2 C_{kj} a_k a_j\,[\cos(w_k - w_j)t - \cos(w_k + w_j)t] \ldots [55]$$

It is observed from Equations [54] and [55] that the output contains components with frequency w_k only in the incorrect mode of operation. Thus the detection criterion of the incorrect mode may be based on the existence of the components with frequencies w_k, when these frequencies are properly selected.

Since the controlled system may not respond properly to high-frequency variation of the inputs, the range of input hunting frequencies must not be very large. In particular, one should assign low frequencies to the inputs where their corresponding input linear groups have large characteristic time constants. When n is not large, it may be sufficient to choose the ratio of the highest to the lowest input hunting frequencies to be equal to 2, thus one may choose ω_k as

$$w_k/w_1 = [(n - 1) + k]/n \qquad (k = 1, 2, \ldots, n)$$

Then, these assorted frequencies will never be equal to the combination frequencies, for example, $2w_k$, $w_k - w_j$, and $\omega_k + \omega_j$, which can exist in both correct and incorrect modes of operation.

The incorrect inputs, the b_k, can be determined by either the correlation technique or by measuring the amplitudes of the components with frequencies w_k. In general there are obtained k linear equations in the b_k's from which the b_k may be determined. For the case of the correlation technique, the output should be cross-correlated simultaneously with signals of the form $\alpha_k \sin w_k(t + \tau_k)$. By taking the period of the cross-correlation process as $(2n\pi)/w_k$, the contribution to the cross-correlation function will come from the particular component with frequency w_k. It is clear that the largest period of the cross-correlation is inversely proportional to the lowest input hunting frequency and this period increases as the number of inputs is increased.

References

1 Draper, C. S., and Li, Y. T., "Principles of Optimalizing Control Systems and an Application to the Internal Combustion Engine," The American Society of Mechanical Engineers Publication, Sept. 1955.

2 Tsien, H. S., and Serdengecti, S., "Analysis of Peak-Holding Optimalizing Control," *Journal of the Aeronautical Sciences*, vol. 22, August 1955, pp. 561–570.

3 Cramér, H., "Mathematical Methods of Statistics," Princeton University Press, 1951, p. 183.

Generalized Theory of the Optimum Thrust Programming for the Level Flight at a Rocket-Powered Aircraft

(*Continued from page 455*)

10 Larew, G. A., "The Hilbert Integral and Mayer Fields for the Problem of Mayer in the Calculus of Variations," *Trans. American Math. Soc.*, vol. 26, 1924, pp. 61–67.

11 Reid, W. T., "Discontinuous Solutions in the Non-Parametric Problem of Mayer," *American Journal of Mathematics*, vol. 57, 1935, pp. 69–93.

12 Follinger, O., "Diskontinuierliche Lösungen von Variationsproblemen mit Gefällebeschränkung," *Mathem. Annalen*, vol. 126, 1933, pp. 466–480.

13 Bolza, O., "Lectures on the Calculus of Variations," G. E. Stechert Company, New York, 1946.

14 Miele, A., "Traiettorie Ottime di Volo degli Aeroplani Azionati da Turboreattori," *L'Aerotecnica*, no. 4, 1952, pp. 206–219 (translated as NACA T.M. 1389, September 1955).

15 Gantmacher, F. R., and Levin, L. M., "Equations of Motion of a Rocket," NACA T.M. 1255, 1950.

16 Barkley, J. R., Newton, R. R., and Gross, G. L., "Mathematical Theory of the Rocket Flight," McGraw-Hill Book Co., Inc., New York, 1947.

17 Piland, R. O., "The Zero-Lift Drag of a 60° Delta-Wing-Body Combination (AGARD Model 2) Obtained from Free-Flight Tests Between Mach Numbers 0.8 and 1.7," NACA T.N. 3081, April 1954.

Ground Handling and Launching Procedures for an Alcohol-Oxygen Rocket Missile

T. M. PETTEY, JR.[1]

General Electric Company, Schenectady, N. Y.

The problem of handling and launching a large liquid-fueled missile is indeed complex. Some of the complexities of the problem are illustrated in this paper which treats the equipment and procedures used by the General Electric Co. in test programs involving several types of missiles using turbo-pumped feed systems. In the program described, missiles were shipped in reusable steel shipping containers with the missile suspended inside by an arrangement of rubber shear mounts. Assembly equipment included a lifting beam and several adjustable dollies. For field transportation and erection, a modified German Meillerwagon was used. The launching stand was a tubular steel framework on which a turntable for azimuth adjustment was mounted. The missile was supported on the turntable by four support arms which retracted at take-off. Electrical connections and gas, water, and liquid oxygen disconnects to the missile were supported from a ring on the turntable. Servicing equipment included a movable access platform, an alcohol supply truck, remotely controlled oxygen supply and gas pressurizing supply systems, and a hydrogen peroxide supply system. The use of this equipment is described in a typical cycle which follows a missile from the factory through the field test, assembly, erection, preparation, and launching.

Introduction

THE problem of handling and launching a large liquid-fueled guided missile is indeed complex. Here we will treat several phases of the problem as it applies to a missile in the development stage.

In the General Electric Company, we have been active in several guided missile projects with missiles varying in size from the V-2 to the Hermes A-1 missiles. Our experience has included both pressurized and pumped propellant feed systems, as well as solid propellants. Because the pumped feed system missiles present a greater variety of interesting problems, we shall limit this discussion to them.

Launching and handling include many operations; among these are: 1 packing and shipping; 2 preparation and testing; 3 field transportation; 4 erecting and aligning; 5 propellant and pressurizing gas supply; 6 launching.

These operations are logically divided into two categories: handling—which includes shipping, transportation, and erecting; and launching—which includes loading propellants, pressurizing with gas, and the actual firing operation. In the following discussion we will treat some of the problems encountered in each of these categories and solutions that were used in an actual missile program.

The missiles involved were approximately thirty feet long and three feet in diameter; their weights varied from four to six tons. Propellants were ethyl alcohol and liquid oxygen. Ninety per cent hydrogen peroxide was used to drive the turbo-pump. Dry nitrogen gas provided suppression pressure in the propellant tanks, pressure for the H_2O_2 tank, and for the various pneumatic valves of the propulsion system.

Presented at the ARS 25th Anniversary Annual Meeting, Chicago, Ill., Nov. 14–18, 1955.

[1] Manager, Handling Equipment Engineering, Special Defense Projects Dept.

Equipment

A Handling

1 Shipping

The principal problem in shipping is one of protection—protecting the missile from transportation shock and vibration, from dirt and moisture, from sudden pressure changes, and from damaging blows by bumping or striking other objects. Although a complete discussion of this problem is far beyond the scope of this paper, a short description of the shipping equipment is apropos.

In this development program, missiles were shipped in reusable steel containers approximately 32 feet long and 6 to 8 feet in diameter. (See Figs. 1 and 14.) The containers were cylindrical and split along the horizontal centerline. The top was bolted to the bottom section and an O-ring gasket was used as a seal. Access ports were placed at each end of the container, as were internal desiccant boxes. A small window permitted visual inspection of the interior and of a humidity indicator. After loading and closing, the container was pressurized to an internal pressure of 3 to 5 psig with clean, dry air.

The missile was mounted inside the container in a cradle which was in turn fastened to the container shell through four shock mount assemblies. These shock mounts consisted of clusters of sandwich-type rubber shear mounts. Telescoping hydraulic dampers, similar to automobile shock absorbers, were used to control the amplitude and velocity of the missile travel inside the container. The cradle consisted of two built-up box section beams connected by three channel cross members. The missiles were mounted in this cradle by trough rings

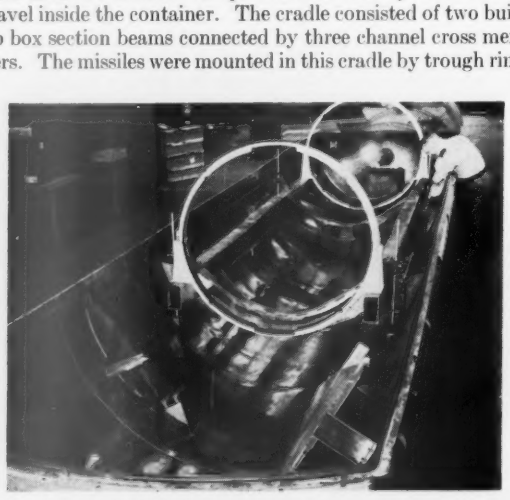


Fig. 1 Interior of shipping container

which clamped onto handling rings on the missile. Road tests showed that with this mounting, shocks of up to 33 g on the container produced no more than 8 g on the missile.

2 Preparation and Testing

Since the operations in this program were part of a development program, equipment was provided for assembly, disassembly, testing, and checkout in a hangar near the launching site. Equipment for checkout and testing was not elaborate. It included gages, a source of gas pressure, various electrical and electronic test instruments, and an electric power supply.

A lifting beam was used for removing missiles from the container and for other handling by means of a traveling overhead crane. For test work the missiles were supported on simple dollies which provided adjustment in height and angle to permit easy assembly and disassembly. (See Fig. 2.) Handling dollies were provided for the tail section, midsection, warhead section, and instrument section of the missile. The midsection dolly was also used to support the completely assembled missile.

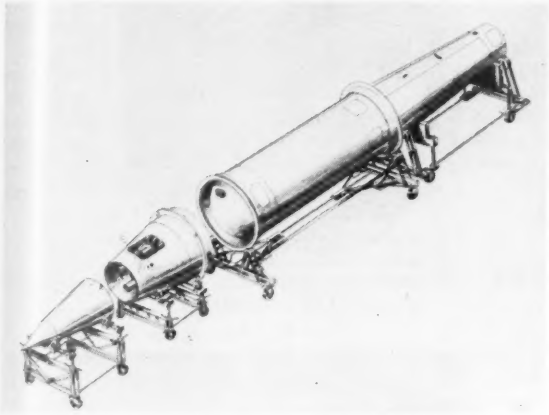


Fig. 2 Missile assembly using handling dollies

3 Transportation and Erecting

Missiles were transported from the assembly and test hangar to the launching site on a modified Meillerwagon, the German vehicle used for transport and erection of V-2 missiles. This vehicle was also used to erect the missiles and place them on the launching stands. (See Figs. 3 and 4.)

In this modification, cradle supports were installed at the proper location on the Meillerwagon boom such that they mated with the handling rings on the missile and also placed the missile tail ring, when the boom was vertical, at the correct height above the ground to clear the launching stand. A bracket was added on the forward end of the boom to support a chain hoist which lowered the missile by means of a sling attached to the forward handling ring. The cradle supports held the missile during transportation and in the erecting process. When the boom was in a vertical position the missile was released from the cradle and became suspended from the chain hoist. It could then be lowered onto the launching stand.



Fig. 3 Field transport of V-2 missile on Meillerwagon; transport of missiles described was quite similar



Fig. 4 Erecting missile using modified Meillerwagon. Missile outline is classified and has been deleted

B Launching

1 Launching Stand

The missile design dictated launching vertically from a system of four struts engaged in sockets cast as an integral part of the rocket motor thrust supports. With this as a basis, the principal requirements of the launching stand were established as follows:

1 A platform on which the support struts may be fixed.
2 A means of retracting the support struts at take-off.
3 A means of orienting the missile in azimuth.
4 A provision for accurate leveling of the platform.
5 A method of turning the jet exhaust to prevent excessive ground erosion and at the same time to prevent burning of the missile.
6 Provision for connecting electrical, pneumatic, and liquid services to the missile and for breaking these connections at take-off.
7 Adequate footing to permit the use of launching stand on soft ground.

In addition to these functional requirements, the launching stand had to be suitable for transportation by standard military vehicles; it could not exceed 96 inches in width and it could not be excessively heavy. Further, the launching stand had to provide a base for the missile sufficiently firm to prevent overturning in a wind of fifty miles per hour.

Since the missile was not a rigid structure, there was a problem in making connections between the launching stand and the missile tail. The launching stand was reasonably rigid but the missile tail ring was subject to both vertical and horizontal movements caused by such factors as expansion or contraction due to heating by the sun and cooling by filling with liquid oxygen. Wind loads produce a small rocking displacement and the weight of the propellants produces a settling as the missile is filled. Horizontal motion of the tail ring could be limited by guide pins but the vertical movement had to be accommodated by the missile-to-launching stand connectors. Manufacturing tolerances had to be consid-

ered. Generally, a fair degree of flexibility was required for the disconnects. The simultaneous engagement of four supports, two guide pins, and six to twenty service connectors presents a difficult problem to the missile erecting crew. This problem was greatly reduced by provision for moving the launching stand parts of the connections out of the way when the missile was placed on the launching stand and making the connections one by one in a later operation.

All of the requirements mentioned above were met in the design of the launching stand.

To provide orientation in azimuth, the missile support struts were mounted on a turntable which in turn was mounted on the launching stand base. Since such an arrangement required a large hole in the center for the jet exhaust, the selection of a suitable bearing was difficult. Large diameter roller bearings are quite expensive. An integral roller bearing is difficult to fabricate and many plain bearings have high friction. The bearing selected consisted of cloth base G.E. Textolite segments placed in a groove on the base, bearing against a smooth steel ring on the turntable. Lubrication was by an oil base dispersion of molybdenum disulfide. Lateral displacement of the turntable was prevented by bronze blocks or small ball bearings attached to the base. C-clamps built onto the turntable prevented vertical separation of the two parts during transport and handling.

The solution to the problem of flexibility in the service connections was often difficult. Each disconnect or cluster of disconnects was adjustable to two positions vertically for easy mating of the missile to the launching stand. The mating portions of the disconnects were made long enough to accommodate relative movements of $\pm 1/4$ inch vertically. Mounting for the disconnects on the launching stand provided $1/8$ inch horizontal movement in any direction and up to two degrees of angular movement.

In order to allow the opening of access doors on the missile tail section, the support struts are placed asymmetrically with two struts between one pair of fins and the other two between the opposite pair. This arrangement provided less stability in one plane but proper placement of the struts on the launching stand provided adequate stability to meet the requirements.

Fig. 5 shows one of the launching stands. The jet deflector is ribbed to form a solid frame and rests on four (4) jacks at the corners. Eight heavy wall tubes act as legs topped by a box section ring. An L-section ring rests on top and rotates for azimuth lineup. This top ring is extended into a rectangular surface and the support strut assemblies rise from each corner. From the center extends the pull-off support ring carrying all the disconnects and the alignment pins.

The alignment pins were of extreme importance. To get two pins to bear firmly on the tail ring, a taper was found necessary. This taper was fairly blunt and bore on the edge of a hole in the tail ring. To keep the pin seated, a strong spring pushed the pin against the tail ring. The pin was made of hardened stainless steel and had several inches of travel using a pneumatic damper to slow its travel. The spring kept the pin tight in the missile tail ring, giving precise guidance until the pin travel limit was reached; as the missile continued, the end of the pin still restrained it for another inch and a half. Thus, the tail is not allowed to move sideways until the missile is clear of the disconnects.

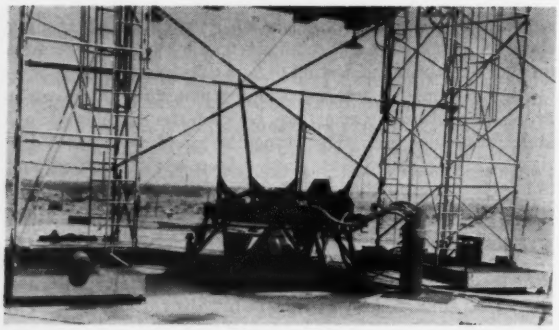


Fig. 5 Launching stand

Mounted on the basic launching stand structure are the service connections to the missile. These components had to be reliable and heat resistant and at the same time compact enough to connect to the missile thru the relatively small tail ring. Typical examples are shown in Figs. 6 and 7.

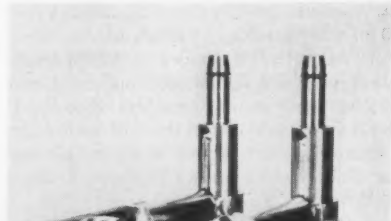


Fig. 6 High pressure gas disconnect. Note heavy construction for flame resistance



Fig. 7 Launching stand showing liquid oxygen and high pressure gas disconnects and guide pins

All the disconnects have a bulky appearance. This results from the need to build with heavy metal masses. For flame resistance there is less difference between materials than between thin and heavy sections. Thin sections or parts isolated by gaskets are frequently destroyed. This makes protection by covers impractical, since in the limited space available it is difficult to get a massive cover and an actuator strong enough to position it quickly.

For electrical connectors a bulkhead AN connector was mounted on the top of the pull-off support ring well outside of the missile diameter. From this fixed connector a short cable arched up to the missile. This cable was flexible and fairly flame resistant. Damage resulting from a slow take-off could be corrected by replacing only the short cable.

For all the fluid connections to the missile that did not require a check valve operator, a very simple sliding tube disconnect was used. It easily accommodated the $1/2$-inch vertical slide required, sealed tightly at 4500 psi, had a low pres-

sure drop, and was fairly easy to build. Being unbalanced, this connector required a strong bracket to resist pressure separation.

The connectors for small fluid flows were modified from Wiggins quick disconnects. The clamping devices were removed and the mating halves held together by a preloading spring. Schreader valves which are a part of each Wiggins coupling open when mated and close when parted. The preloading spring in the disconnect was required to activate the end seals of the couplings and to follow the vertical motion of the missile. This special disconnect was used in preference to commercial breakaway couplings because of its smaller size; four lines could be placed in the space required for one regular breakaway.

The disconnect for oxidizer filling was designed with due emphasis on the extremely low temperatures involved. Metals in the cold zone were stainless steel and bronze, the plastics were Kel-F and Teflon. The missile connector was female with a lip seal of Teflon and a light, blow-open check valve. The ground piece was a close fit in the lip seal and was supported on a spherical segment washer giving the required angular and transverse freedom. To drain a filled missile, a small pneumatic cylinder pushed a prod to open the missile check valve.

A take-off switch was installed on the stand to signal take-off to the ground control circuits. This switch was designed to permit testing with the missile on the stand. Supplementing the take-off switch, to provide the ultimate in simplicity and reliability but somewhat less accurate, was a breakwire, a simple loop of wire tied from the stand to the missile and broken by take-off.

The most difficult and complex of the disconnects was the hydrogen peroxide vent and relief valve. This valve meets a formidable list of requirements in addition to the standard ones of flexibility and operation expected of all the disconnects. The valve was not reactive with 90 per cent H_2O_2 operated up to 1000 psi internal pressure and was fail-safe. Loss of control pressure or seal failure safely vented the missile storage tanks even if pressurized. The missile part included a check valve; the ground part provided a push rod to open the check valve when required. A strong spring supplied the force for sealing the valve and opening the check; reverse operation was supplied by a pneumatic cylinder. Silicone rubber O-rings were used in contact with H_2O_2. The H_2O_2 vent line included a special hose capable of carrying 90 per cent H_2O_2 at 1000 psi.

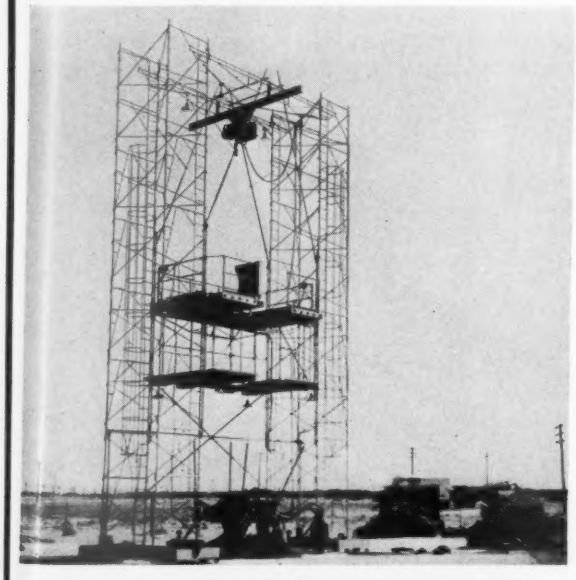


Fig. 8 Access platform in place over launching stand

2 Access Platform

To provide a safe working platform for use after the missiles were erected, a lightweight movable structure similar to a gantry crane was used (Fig. 8). Two adjustable platforms with cutouts for the missile were placed at suitable heights to permit work through all the missile access doors. A small electric hoist was attached to the top of the structure to raise and lower tools, spare parts, etc., to the work platforms. This structure could be braced by guy wires to support the missile in high winds.

3 Propellant Supply and Loading

(*a*) *Alchohol Supply.* (See Fig. 9.) A standard U. S. Army tank truck—a 750-gallon tank on a $2^1/_2$-ton truck—was used. To this truck was added an electrically driven pump with valving to control the flow or to reverse it. A 50-foot length of two-inch hose with a suitable connector for the missile was carried on a hand-driven reel.

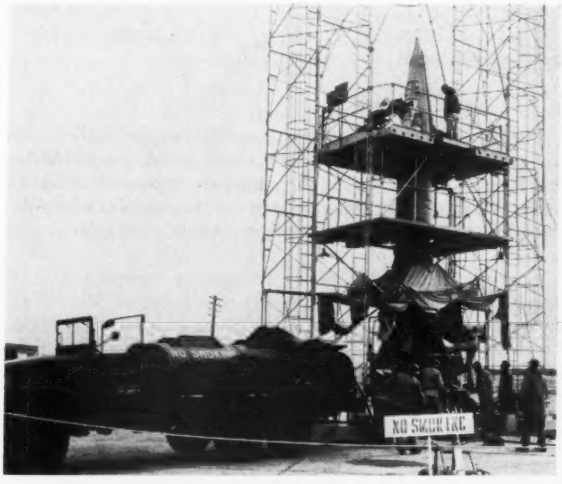


Fig. 9 Filling missile tanks with alcohol. Note canvas cover on missile for weather protection

(*b*) *Hydrogen Peroxide Supply.* Ninety per cent of H_2O_2 was loaded by gravity flow into the missiles. The H_2O_2 filling tank was a standard 30-gallon Becco shipping drum to which a drain line was added. From the drum, a flexible plastic hose (Koroseal Grade 117 or polyethylene) approximately 12 feet long, led to a pneumatic-operated shutoff valve which in turn was attached to the H_2O_2 external fill and drain connection. This fill and drain connection screwed into the missile H_2O_2 fill and drain valve. When the connection was tight in the fill and drain valve, a hand-operated plunger in the connection was turned to open the fill and drain valve. From the external connection, a second pneumatic-operated shutoff valve and plastic hose led to a water-filled dump tank. The two pneumatic-operated valves could be operated from a remote station. The quantity of H_2O_2 loaded into the missiles was controlled by weighing a predetermined quantity into the filling tank prior to the filling operation.

(*c*) *Liquid Oxygen Supply.* The lox supply systems used in flight testing the missiles were gas-pressurized, remote-controlled, mobile supply tanks (Fig. 10). These systems were selected as the most readily available and lowest cost equipment to fulfill the requirements for lox supply at the proving ground.

To fill the missile (with the missile fill and drain valve and lox tank vent valve open), the lox supply tank was pressurized with N_2 gas, through the pressurizing valve to approximately 50 psig. The missile filling valve was opened permitting lox flow from the buggy through the filling hose to

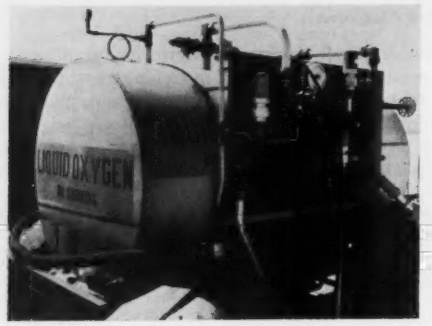


Fig. 10 Liquid oxygen supply tank

the missile. Visual observation of vapor and/or liquid at the missile lox vent valve outlet indicated when the missile tank was filled. Since the lox is filled through a pull-off connection on the launching stand, remote filling, topping, or draining may be accomplished at any time prior to the start of the actual launching sequence. The lox buggy was filled directly from a commercial supply truck.

4 Gas Supply System

The principal function of the ground gas supply system was to furnish high pressure gas to the missile for prelaunch checks and for operation in flight. An additional function was added in that those parts of the missile gas control system which do not function after take-off were removed to the ground gas control system.

In the gas supply system dry nitrogen gas was pumped into two alloy steel spheres (Fig. 11), to a pressure of 3000 to 3500 psig. These spheres were manifolded so that they could be used singly or in combination. This arrangement permitted maximum use of gas from the spheres before refilling.

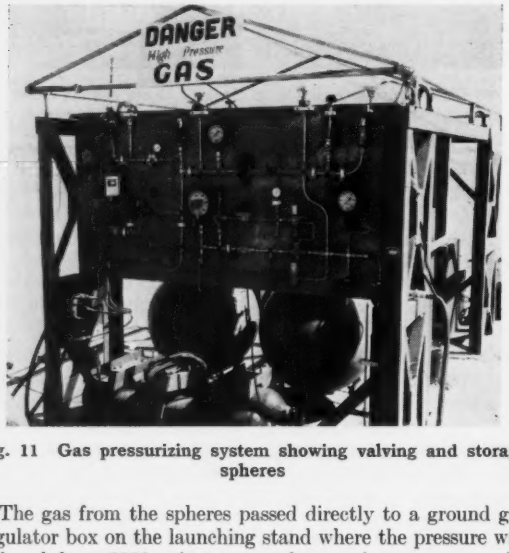


Fig. 11 Gas pressurizing system showing valving and storage spheres

The gas from the spheres passed directly to a ground gas regulator box on the launching stand where the pressure was reduced from 3500 psig to several operating pressures. In addition to pressure reduction, several valving and measuring functions were performed by a ground gas control box which, like the ground gas regulator box, was mounted on the launching stand. (See Fig. 12).

The functions performed by the regulator and control boxes are basically the supply of gas to the propulsion system and the operation of the engine controls; among these functions are:

(*a*) Supply of high pressure gas to the missile storage tanks. (*b*) Supply purging gas prior to take-off (a safety precaution). (*c*) Provide pressurizing gas to the propellant tanks prior to take-off. (*d*) Provide operating pressure for pneumatic valves in the missile prior to take-off. (*e*) Provide tank-venting functions. (*f*) Measure and relay missile tank pressure information on the ground to the operator.

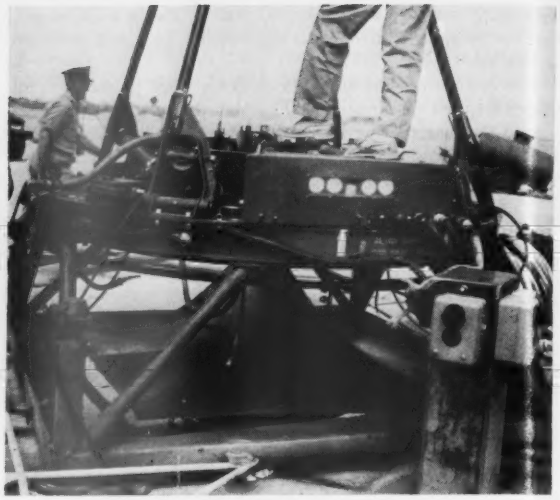


Fig. 12 Launching stand. Ground gas control box is in foreground

5 Launching Controls

All operations at the launching site were controlled from a concrete blockhouse. Remote operation of the starting controls was provided from a Launching Control Unit (Fig. 13). This unit contained the switches and interlocks necessary to launch the missile and instruments to indicate the condition or readiness of various missile components. An operator had manual control of all missile functions. Although several functions were interlocked so that the proper sequence of operations must take place, the operator could override the interlocks when he deemed it advisable. Among the functions controlled from the launching control unit were lox tank filling missile pressurization, engine starting, and guidance equipment alignment.

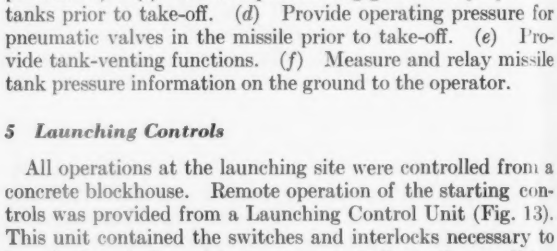


Fig. 13 Control operator at launching control console

Launching and Handling Operations

The launching and handling operations are probably most easily understood by following a typical missile from the factory to its launching.

A Shipping

At the factory in Schenectady the missile is loaded into the shipping container by an overhead crane. It is then fastened to the cradle and the container cover bolted in place. Desiccant boxes are filled with fresh desiccant and the container is pressurized to five psig. The missile in its container is now ready for shipment by truck to the proving ground (Fig. 14).

Upon arrival at White Sands Proving Ground, the container is taken to the hangar where it may be put in temporary storage or opened immediately. To remove the missile, the container is depressurized, the cover unbolted and removed, the missile is detached from the cradle and lifted from the container to the midsection dolly by means of an overhead crane and a lifting beam. The missile is now ready for checkout.

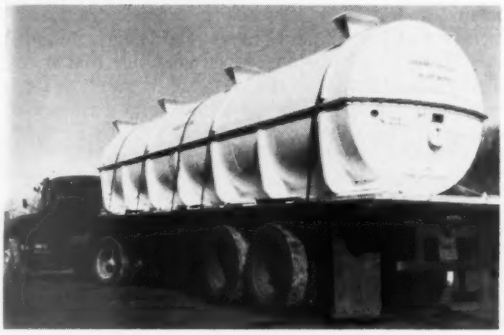


Fig. 14 Shipping container loaded for shipment

B Checkout and Preparation

In the hangar a functional test is applied to the missile electrical and guidance systems. The valves of the propulsion system are checked for operation and the entire propulsion system is checked for leaks at one-half normal operating pressure. Any defective or questionable components are replaced or adjusted and the inevitable last-minute design changes are incorporated.

After the checkout is completed the missile is loaded onto the Meillerwagon, again using the lifting beam and overhead crane. The handling rings of the missile are secured and the sling attached. At this point the missile is transported to the launching site.

C Erecting

When the missile, on the Meillerwagon, arrives at the launching site, the Meillerwagon is backed into position for erecting. The boom and the missile are erected to the vertical position and the missile handling rings are disconnected from the cradle allowing the missile to swing clear of the boom and hang from the chain hoist. With the launching stand leveled, the missile is lowered so that the two guide pins on the launching stand are engaged. The four support arms are now moved into place and the missile is lowered further so that the support arms engage the sockets on the missile. During these operations, the several disconnects on the launching stand have been in the retracted position so that they do not interfere with the mating of the missile and the stand.

After a quick check of the missile level on the launching stand, the sling is disconnected from the missile and the Meillerwagon is moved away after the boom is lowered. The access platform is moved into place over the missile and secured. The disconnects on the launching stand are moved up to mate with their missile counterparts. If the missile is to remain on the stand more than a few hours, the protective canvas cover (Fig. 9) is strapped in place. The missile is now ready for alignment on the target and the final launching preparations.

D Launching

In the actual launching procedure, missile batteries are installed and a final electrical adjustment is made. The alcohol tank truck is brought up, the hose connected to the missile, and with the missile alcohol tank vent open, alcohol is pumped into the tank to the proper level. A meter on the pump indicates the quantity of alcohol delivered. The hose s disconnected and the alcohol truck is moved away and the canvas cover is removed.

At this point, the liquid oxygen supply tank is filled from a commercial lox trailer and the connection is made from the lox supply system to the launching stand.

A predetermined quantity of hydrogen peroxide is loaded into the missile from the H_2O_2 supply system.

With the foregoing operations complete, the access platform is removed and rolled out of the immediate area of the missile. Oxygen is loaded from the supply tank to the missile after the launching area has been cleared of personnel. When the lox is loaded (as observed from the vented vapor) a final check on missile guidance alignment is made.

Now the missile gas storage tanks are pressurized through the ground gas control and regulator boxes. After a brief final check of missile readiness, the missile is launched (Fig. 15).



Fig. 15 Missile just after take-off

In addition to the operations mentioned, there are several others such as telemetry preparations, range safety, and tracking by optical means and radar which are taking place simultaneously with the missile launching preparations. Although these additional operations are of great importance, and they add considerably to the complexity of the launching procedure, they are outside the scope of this paper and will not be discussed here.

Conclusion

As we have seen, there are many operations in handling and launching large liquid-fueled guided missiles, especially in a development program. One of the cardinal principles for the designer of launching and handling equipment, and for the sequence of launching operations he develops, is that no matter how good a missile system may be in all other respects, if it cannot be launched and handled simply and easily, it can never be useful.

To sum up the problem, launching and handling of missiles are complex, but with proper cooperation of designers and with simplicity as a byword, simple and efficient equipment may be designed with a minimum of trouble.

Combustion in Turbulent Flow

A Summary of Remarks at a Special Panel Meeting, April 14—15, 1955, held at The Johns Hopkins University, Applied Physics Laboratory

Table of Contents

BERL, W. G.—Introduction
Applied Physics Laboratory (The Johns Hopkins University), Silver Spring, Md.
WESTENBERG, A. A.—Flame Turbulence Measurements by the Method of Helium Diffusion
Applied Physics Laboratory (The Johns Hopkins University), Silver Spring, Md.
GRUMER, J.—Schlieren and Direct Photographic Studies of the Turbulent Flame Structure
U. S. Bureau of Mines, Pittsburgh, Pa.
BERLAD, A. L.—Radiation from Turbulent Flames
National Advisory Committee for Aeronautics, Cleveland, Ohio
WOHL, K.—Combustion in Turbulent Flow
University of Delaware, Newark, Del.
OLSEN, H. L., and GAYHART, E. L.—Incipient Flame Propagation in a Turbulent Stream
Applied Physics Laboratory (The Johns Hopkins University)
BOLZ, R. E., and BURLAGE, H., JR.—The Influence of Turbulence on Flame Propagation Rates
Case Institute of Technology, Cleveland, Ohio
KOVASZNAY, L. S. G.—A Comment on Turbulent Combustion
The Johns Hopkins University, Baltimore, Md.
PAI, S. I.—On the Flow Patterns of Flame
University of Maryland, College Park, Md.
SUMMERFIELD, M.—Turbulent Flames in Gases
——Comments on A. L. Berlad, K. Wohl, H. L. Olsen and E. L. Gayhart, B. Karlovitz, and R. Friedman
Princeton University, Princeton, N. J.
KARLOVITZ, B.—Remarks on Turbulent Flames
Combustion and Explosion Research, Inc., Pittsburgh, Pa.
BERL, W. G., RICE, J. L., and ROSEN, P.—Flames in Turbulent Streams
Applied Physics Laboratory (The Johns Hopkins University)
WEISS, M. A.—Flame Spreading from Baffles
Esso Research and Engineering Co., Linden, N. J.
ZELINSKI, J. J., BAKER, W. T., MATTHEWS, L. J., III, and BAGNALL, E. C.—An Investigation of the Burning Rates of Confined Turbulent Flame Jets
Applied Physics Laboratory (The Johns Hopkins University), Silver Spring, Md.
MARKSTEIN, G. H.—Interactions of Flames and Flow Disturbances
Cornell Aeronautical Laboratory, Inc., Buffalo, N. Y.
CHU, B. T.—A Model for the Flame Front in a Viscous Heat Conductive Gas Mixture for Hydrodynamic Investigations
——Comments on Landau Instability
The Johns Hopkins University, Baltimore, Md.
FRIEDMAN, R.—One-Dimensional Laminar Flame Front Structure
Westinghouse Research Laboratory, East Pittsburgh, Pa.
FRISTROM, R. M.—The Applicability of One-Dimensional Models to Three-Dimensional Laminar Bunsen Flame Front
Applied Physics Laboratory (The Johns Hopkins University), Silver Spring, Md.
BERL, W. G.—Summary

EDITOR'S NOTE: Although the publication of this summary has been delayed approximately one year, it is felt by the participants that the subject is even more alive now than it was then, and that publication at this time can serve a useful purpose. The printing and the distribution of this manuscript in JET PROPULSION have been financed by the Applied Physics Laboratory of The Johns Hopkins University. It is included in this issue as a service both to APL and to the membership of the ARS. The meeting was supported under Contract NOrd 7386 with the Bureau of Ordnance, U. S. Navy.

Introduction

W. G. BERL

I AM very happy to greet all of you in the new laboratory of JHU/APL. We have called you together for a two-day round table discussion in the difficult field of combustion, with particular emphasis on the turbulence aspects. There is no lack of combustion meetings nowadays. Compared to the modest interest in the field before the war, there has now arisen a veritable floodtide of effort and interest. International Combustion Symposia, AGARD meetings, the annual meetings of the Rocket and Mechanical Engineering Societies, and others act as forums where new information can be presented and it is, on the whole, a good sign that large audiences and large collections of reports have found each other. It occurred to some of us, however, that a certain difficulty has arisen, that the very size of numbers tends to dampen the free and spontaneous flow and exchange of information between the people who are actually on the front lines of research. If the audiences are large and the schedules crowded and inflexible, spontaneity departs and little time remains to look carefully and critically at the work, to discuss frankly and at length the new ideas and the new experiments that are springing up, to report frankly the weaknesses and difficulties of one's own work, and to speculate about new approaches that should be taken in the future.

At our meetings today and tomorrow we have invited and have had a surprising response from the majority of the men who have made and are still making the major contributions to the field. You see here today chemists, engineers, physicists, and mathematicians, pointing up the inescapable conclusion that no one specialty of science is adequate by itself to solve the outstanding problems. We are forced into a closer union to lay a common understanding and to learn to pick up the nuggets of information from a variety of fields. You will note that the general subject falls quite naturally into four fields—experimental tools and observations on turbulent flames, conceptual ideas and flame models, engineering applications, and a return to flames in laminar flow and their aerodynamic interplays.

Now, let me take a few minutes to review very sketchily what are some of the questions we would like to have answered and the problems we would like to see solved. First of all, let us look backward for a moment to inspect the past. The first significant quantitative measurements on a system of current interest is the work of the remarkable French team of LeChatelier and Mallard. They published an extensive memoir in the French *Annales de Mines* in 1883 about the propagation of a combustion wave through a tube using ionization probes, continuous pressure measurements, and photography to obtain a continuous record of the wave propagation. They rediscovered the quenching effect of walls, made into such a remarkably utilitarian tool years before by Sir Humphry Davy in his wire-mesh safety lamp, and they also experienced the transformation of deflagration into a detonation, reported only the year before by Berthelot and Vieille. LeChatelier and Mallard with their quantitative measurements made the significant discovery that the initially uniform flame movement became increasingly more oscillatory with distance and that the average transformation velocity increased considerably. This is the first observation of an accelerating effect on flame propagation.

After this extensive French effort a hiatus of over fifty

years descended. Only occasional and incidental reports of internal engine combustion researchers refer to a possible interaction between flame and flow to account for the complex phenomena during the passage of a flame across the combustible mixture in an engine cylinder. During this long and silent period, however, a very intensive development along chemical kinetic and fluid dynamic lines had occurred, quite unrelated and unbeknown one from the other. In addition, engineers probed into new engines and power plant equipment requiring answers to questions well beyond the reach of LeChatelier.

The latest period of development, in the very midst of which we find ourselves today, began formally with a long article by Damkohler in the 1939 *Jahrbuch* of the German Academy for Air Research. It is here, for the first time, that the modern fluid dynamic concepts are applied to flames. He speaks of the two models where the scale of the fluctuations are either much larger or much smaller than the width of the chemical reaction zone. He predicts a Reynolds number effect on the shape of the Bunsen cone and defines a "turbulent" flame speed which with minor alterations is still popular today. After Damkohler the development passed into the hands of the people present in this room and the current status of the art is largely due to them.

Now what are the problems against which we must take an active stand? It has been said that the state of turbulent flow and the mathematical tools available to describe it are inadequate, that the problem of the structure of a one-dimensional flame has not been solved with rigor, and that it is foolhardy to mate the two and expect to obtain satisfying answers. Though this may be true, we all realize that progress in understanding is being made even now and that considerable advances have indeed been achieved by applying known techniques, proposing simple models, and by setting down engineering correlations which are of great use even though they are too complex to satisfy the curiosity of the scientist.

We are, however, badly in need of new tools and new concepts. We are also in need of a spirit of caution, foregoing the desire for broad generalizations before the chinks that make up the details of the problem have been filled in. It is necessary to propose new hypotheses in place of old and test them and reject them cheerfully if the evidence turns against them.

We shall hear several reports on the application of new tools. It is probably no exaggeration to state that progress in the field depends on more and better tools, simple enough to give adequate and trustworthy quantitative information. How can we confirm the alluring and vexing hypothesis of "flame induced" turbulence unless we can measure something quantitative in the hot gas flow beyond the reaction zone? How will we settle the suggestion of "preferential diffusion" in cellular flames unless we possess analytical tools that will discriminate and correlate the fluctuations, keeping in mind that we are dealing not only with velocity fluctuations but with composition and temperature fluctuations as well? How do we deal with the effect of velocity gradients and nonhomogeneous flow unless we learn to describe them more quantitatively? How do we determine reaction rates and heat release in a nonuniform and fluctuating stream?

Apart from reliable tools we need simple answers to simple questions: What are the diffusion coefficients at high temperature? How do we eliminate the effect of boundary layers on stabilized flames? How do flow disturbances propagate along a reaction zone; when do they amplify or attenuate? Do curved tip flames really burn faster? Where do the chemical kinetics enter into the turbulent flame model? When does a flame front cease to be fluctuating and become dispersed? Why do high-speed pictures of flames show cellular structures of large size compared to the scale of the turbulence? How clear is the meaning of "turbulent" flame speed?

To these and other questions we seek answers. They will be forthcoming in due time. It will be surprising if they will not also give rise to basic new concepts which the field of combustion has so often contributed to scientific thought in the past.

Flame Turbulence Measurements by the Method of Helium Diffusion[1]

ARTHUR A. WESTENBERG

ABSTRACT

A TECHNIQUE is described for measuring transverse turbulence intensity in flames which makes use of the diffusion of helium. The latter is detected by a thermal conductivity method. The effects of various experimental parameters and the reliability of the technique are discussed. Results obtained in highly turbulent flames stabilized on various baffles in a 5-cm × 20-cm duct are given and compared with results obtained under comparable cold flow conditions. It appears that, under the conditions of these experiments, the amount of "flame-generated" turbulence detectable at a fixed point in the duct by this technique is probably small.

CONCLUSIONS

Results of this work may be summarized briefly:

1 It has been shown that transverse turbulence intensity of fairly large magnitude (roughly 4 per cent or more) may be successfully measured in a baffle-stabilized flame and in cold flow by the helium diffusion method, using thermal conductivity detection.

2 The measured helium distributions are Gaussian within experimental error, and up to the maximum distance x used (~2 cm) exhibit the behavior expected of diffusion times small compared to the Lagrangian time scale of turbulence.

3 The technique is quite sensitive to small changes in intensity of turbulence, but gives absolute magnitudes for this quantity which are probably too high (especially at the lower intensities) due to the flow disturbance of the source.

4 In cold flow, the intensity $(\langle v^2 \rangle_{avg})^{1/2}/U$ at a fixed point in the flow is essentially independent of U over the range examined.

5 In cold flow, the intensity downstream of a baffle increases with the characteristic dimension of the baffle but is independent of its geometry.

6 With a flame stabilized on the baffle, the above effect of baffle dimension is drastically reduced.

7 At a fixed distance downstream of the baffle, the absolute turbulence intensity $(\langle v^2 \rangle_{avg})^{1/2}$ is not very different whether a flame is present or not—under the conditions of these experiments.

[1] From *The Journal of Chemical Physics*, vol. 22, no. 5, May 1954, pp. 814–823.

Schlieren and Direct Photographic Studies of the Turbulent Flame Structure[1]

JOSEPH GRUMER

THE concept that the turbulent flame brush is composed of a fluctuating, wrinkled, essentially continuous, laminar combustion wave is essentially supported in the literature by very short duration schlieren, shadow, and smoke photographs of the brush. This wrinkled laminar wave concept has been the basis of theories of turbulent burning velocity, flame-generated turbulence, and stability of turbulent flames. Tests of these theories have been inconclusive. Examination of the evidence presented to support the underlying concept,

[1] This research is a part of the work being carried out by the Bureau of Mines under Contract CS 630-55-29, supported by the Office of Scientific Research, Air Research and Development Command.

namely, the aforementioned instantaneous schlieren, shadow, and smoke photographs of the turbulent flame brush, therefore seems desirable.

New experiments, bearing on schlieren photography, reveal the technique to be ambiguous at best in revealing the structure of the turbulent brush. Density patterns were observed to move faster than the turbulence intensity, laminar burning velocity, and cold approach flow; to shift orientation with turning of the schlieren knife edge; to differ for turbulent flames piloted by a laminar hydrogen-air flame and those piloted by heating the port electrically; and to be present in the absence of turbulent flame when a pilot and a turbulent air stream were provided. In addition, a slowly fluctuating, very rich, mildly turbulent flame was photographed and observed directly by its emitted luminosity and indirectly by schlieren. The flame surfaces could not be discerned in the involved schlieren pattern. The flame shape was obvious to the eye and to the direct-view camera. Smoke photography, though not as extensively studied as schlieren, is also questioned as technique for elucidating the structure of the turbulent flame brush because of conceivable uncertainties arising from the interaction of incident light and the amount and particle sizing of the smoke, temperature and delay time for vanishing the smoke, pickup of radiant heat, and possible chemical reaction between smoke and flame. These observations point to the conclusion that schlieren photography (and very likely shadow and smoke photography) as previously employed does not prove the existence of a wrinkled laminar wave in the brush.

On the other hand, new experiments, wherein a 10,000 Reynolds number turbulent brush was photographed directly at speeds of 1 and 2 millisec with f:1 and f:2 lenses, indicate that the brush is made up of discontinuous flamelets of varying intensity, most of which are inclined nearly parallel to the flow. New experiments, with high Reynolds number flames employing the electronic probe to analyze the continuity of flame in the brush, also indicate discontinuity. Grids were inserted in pipe flow burners to increase the level of turbulence intensity. Then the electronic probe, completely passed through the turbulent brush, records the absence of high ionization for significant percentages of time.

These studies are being continued, and publication of the results obtained may be expected in a reasonably short time.

Radiation from Turbulent Flames

A. L. BERLAD

THERE have been several papers which have dealt with the radiation characteristics of turbulent flames. Gaydon and Wolfhard (1)[1] investigated the effect of turbulence on the spectra of premixed ethylene-air flames. They concluded that the low levels of turbulence employed did not significantly affect the over-all flame radiation characteristics. Clark and Bittker (2) measured filtered total flame radiation for both laminar and turbulent propane-air flames using an apparatus shown schematically in Fig. 1. Their results (typified by the data of Fig. 2) indicated that there was no appreciable difference between the radiation characteristics of the laminar and turbulent flames investigated. Summerfield et al. (3) photographed turbulent methane-air flames in various regions of the spectrum. These authors noted a large separation on their photographic plates between CH and H_2O. This was taken as an indication that the turbulent flame was a zone of thickened reaction.

These three studies represent important first steps in the use of a relatively new (and potentially powerful) technique in the study of turbulent flames. However, none of the present

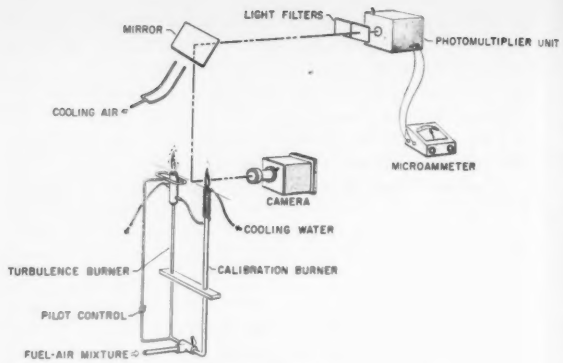


Fig. 1 Flame radiation measurements

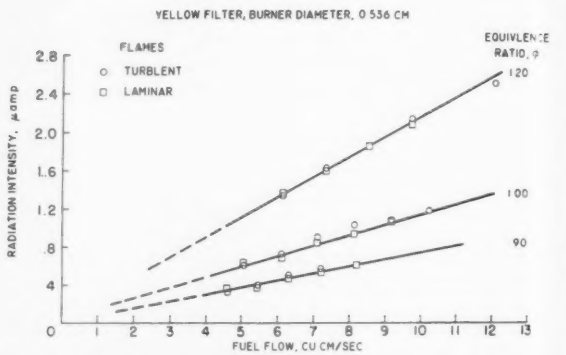


Fig. 2 Variation of laminar and turbulent flame intensities with fuel flow

data represent "proof positive" for any given structure for a turbulent flame. The results of Clark and Bittker are consistent with the idea that the turbulent flames investigated are "wrinkled" combustion waves. In fact, these results are also consistent with several other turbulent flame "structures." It should be noted, however, that it seems very improbable that the spectral radiation patterns and intensities observed for structured laminar flames could be preserved if a given laminar combustion wave were suddenly transformed into a zone of homogeneous reaction.

If future radiation studies are to be truly indicative of turbulent flame structure and chemistry, the experimental techniques so far employed will have to be refined. Thus, devices capable of giving reliable time and space average monochromatic intensities should be used. A photographic plate cannot satisfy this criterion. If relative concentrations of reaction zone emitters are to be used as indications of flame structure, emitters normally present *only* in high heat release regions are to be preferred.

In essence, then, studies of the radiation from turbulent flames may prove to be of very great value in the interpretations of flame structure. Before this can be realized, however, more refined experimental techniques will have to be employed.

REFERENCES

1 Gaydon, A. G., and Wolfhard, H. G., "Comparison of the Spectra of Turbulent and Laminar Flames," *Fuel*, vol. 33, July 1954, pp. 286–290.

2 Clark, T. P., and Bittker, D. A., "A Study of the Radiation from Laminar and Turbulent Open Propane-Air Flames as a Function of Flame Area, Equivalence Ratio, and Fuel Flow Rate," NACA RM-E54F29, August 1954.

3 Summerfield, M., et al., "The Physical Structure of Turbulent Flames," JET PROPULSION, vol. 24, July-August 1954, pp. 254–255.

[1] Numbers in parentheses indicate References at end of papers throughout.

Combustion in Turbulent Flow

K. WOHL

I SHOULD like to report on some of our experiments on premixed turbulent hydrocarbon-air flames burning either from tubes in an open atmosphere or in ducts. The open flames were held at the rim of a 1-in. tube by a pilot flame. The velocity did not exceed 50 ft/sec. The turbulence of the approach stream was varied by screens. The average turbulent burning velocity $\overline{S}_t$ was measured from the area at which 50 per cent of the reactable oxygen was consumed.

The observed values of $\overline{S}_t/S_0$ of methane (S_0 = normal burning velocity) are such as may be expected from theories based on the model of a wrinkled flame front if flame-generated turbulence is not taken into consideration. This characterizes a "passive" flame. Fuel rich butane flames display higher flame turbulence (larger $\overline{S}_t$ values, more strongly distorted flame fronts) at equal conditions, while flame front distortions are suppressed in lean butane flames. This is due to different stabilities of the laminar flame fronts which on their part are connected with the difference between the diffusivities of fuel and oxygen (Markstein (2) and others). The increase of $\overline{S}_t/S_0$ toward the rich side is larger than can be accounted for by the increase of flame front area. It is assumed that enriched gas escapes through open tips or ridges in the flame front and that the gas burning in the flame front has an average composition closer to the stoichiometric so that the laminar burning velocity is increased. The fluctuations of lean butane-air flames are suppressed only at low intensities u' of approach turbulence (up to about 5 per cent); at higher values of u' this deficiency is made up by an abnormally steep rise of $\overline{S}_t$. At conditions of strong disturbances, therefore, factors other than preferential diffusion seem to determine flame front stability (2). The excessively high flame turbulence on the rich side was also obtained with butane-air flames burning in an atmosphere of nitrogen (3) and with propane-air flames burning in a duct (4).

The scale of approach stream turbulence has no noticeable effect on burning velocity as long as the scale is small. The scale of flame front structure decreases with increasing approach intensity even if the approach scale increases. If one proceeds from rich to very rich butane-air flames, the flame front scale does not continue to decrease while $\overline{S}_t/S_0$ does, due to the disproportioning mechanism mentioned above (1).

The mean reaction rate calculated from flame thickness and burning velocity (1 and 3) should, according to the wrinkled flame front model, decrease with increasing intensity and scale of turbulence. Actually it increases with increasing approach turbulence and butane concentration (i.e., intensity of flame turbulence). This seems partly due to a decrease of flame front scale l and partly to a break-through of the flame front. For the latter case the reaction rate can be assumed to be proportional to u'/l, (5).

For flames burning in ducts the impact pressure was measured beside composition so that local values of turbulent burning velocity as well as values of flame thickness or reaction rate along flow lines could be determined. With stoichiometric butane-air flames burning in a 3-in. tube from a central pilot flame at 0.2 atm (velocities up to 68 ft/sec, turbulence intensities up to 7 per cent), the burning velocity (6) and the maximum reaction rate (7) increased with increasing downstream distance from the flameholder; while with propane-air flames burning in ducts of 1.5 × 2 in. cross section from plates of $^1/_4$ × 1.5 in. cross section at 60 ft/sec and 0.2 per cent approach turbulence, the burning velocity passed through a maximum (4) and the reaction rate (8) decreased in downstream direction. The findings at the higher pressure are probably due to a relatively high importance of turbulence created by the flameholder, and to an increase in the size of the flame front "cells" with increasing distance from the flameholder. The maximum reaction rate found anywhere in the flame is 8 per cent of that in the laminar flame zone at atmospheric pressure, and 12 per cent at 0.2 atm. The difference is in the expected direction but surprisingly small.

Combustion in the axis of the burners is less complete at 0.2 atm than at 1 atm (6, 7, and 8). At 0.2 atm and low and medium approach turbulence, roughly 90 per cent of the reactable oxygen remains unburned independent of the fuel concentration of the butane-air mixture burned. The O_2-deficiency is mostly accounted for by the presence of CO and to a lesser degree by that of H_2 and unburned fuel. The composition of the flame gases in the axis does not perceptibly change over the length of the burner (6). This seems to require an influx of unburned material into the axial region which compensates for the progress of the chemical process. It is thus concluded that the flame front is frequently interrupted at places (though probably not completely disrupted). At high velocities and intensities of turbulence, combustion in the axis becomes more incomplete, especially for lean flames, and increases with distance. Due to the promotion of flame spreading by turbulence, however, the total percentage burned in the duct increases with turbulence.

Summerfield et al. (9) have recently advanced the opinion that the distributed reaction zone model of a turbulent flame would require a separation between the area of maximum reaction rate and maximum luminosity. It seems to us that this is not necessarily expected and that the separation mentioned would require a special explanation in any case. This might possibly be furnished by the model of a continuous flame front containing short-living gaps (see below). Speaking of the facts, we have measured composition and luminosity of a number of turbulent flames. In the case of butane-air flames burning above tubes (50 ft/sec lean to rich, approach turbulence 1–10 per cent) the points of maximum luminosity (measured densitometrically) in the flame axis were located on the average 8 mm upstream of the points of 50 per cent O_2-consumption. In two cross sections of different height perpendicular to the axis, the points of maximum luminosity (corrected for cylindrical flame shape) were found to lie on the average 0.7 mm closer to the axis than the points of 50 per cent O_2-consumption (3). With propane-air flames burning in a rectangular duct (1.5 × 2 in.) at 1 atm, 60 ft/sec and 0.2 per cent approach turbulence, the following results were observed as an average over the 10-in. length of the burner.

Propane, %	Maximum luminosity, %, at points of
3.38	30–40 }
4.03 (stoich.)	20 } O_2-consumption
6.54	10 }

In butane-air flames burning in a 3-in. tube from a pilot flame at 0.2 atm (30–115 ft/sec, 2.7–4.2 per cent fuel), the situation depended largely on approach turbulence. If the latter were low (0.9 per cent), maximum luminosity occurred upstream of 50 per cent O_2-consumption, and 20 per cent of the maximum luminosity was observed upstream of the points where 10 per cent O_2 was consumed. At higher turbulence (7 per cent) and stoichiometric composition, the points of maximum luminosity and 50 per cent O_2-consumption, as well as the points of 20 per cent luminosity and 10 per cent O_2-consumption, coincided with each other. Lean and rich flames at 7 per cent turbulence and low velocity showed maximum luminosity downstream of 50 per cent O_2-consumption and 20 per cent luminosity downstream of 10 per cent O_2-consumption. At higher velocities the behavior of the latter flames was not uniform.

It appears that luminosity occurs in the majority of cases explored prematurely (exceptions being met especially at high turbulence (!)). This seems to require some degree of mixing of burned and unburned material as indicated above.

Some of the combustible gas in a turbulent flame might have a chance to be alternately heated and quenched prior to final burning. There would result an average preheating period during which luminosity might appear though combustion had only progressed little.

REFERENCES

1 Wohl, K., and Shore, L., *Industrial and Engineering Chemistry*, vol. 47, 1955, p. 828.

2 Markstein, G. H., "Selected Combustion Problems," Butterworths Scientific Publications, London, 1954, p. 263.

3 Semi-Annual Progress Report, Project SQUID, April 1, 1954; master thesis, R. Zielinski, University of Delaware, 1954, p. 76.

4 Semi-Annual Progress Report, Project SQUID, April 1, 1954; master thesis, R. Schilly, University of Delaware, 1953, p. 69.

5 Wohl, K., Shore, L., von Rosenberg, H., and Weil, C. W., Fourth Symposium on Combustion, Williams and Wilkins, Baltimore, 1953, p. 620.

6 Report UD-112 for United Aircraft Corporation, University of Delaware, Sept. 1953; also doctor dissertation of D. H. Archer, University of Delaware, Sept. 1953.

7 Semi-Annual Progress Report, Project SQUID, Oct. 1, 1954; also master thesis, R. P. Barbor and J. D. Larkin, University of Delaware, June 1955.

8 Semi-Annual Progress Report, Project SQUID, Oct. 1, 1954; also doctor dissertation, H. von Rosenberg, University of Delaware, June 1955.

9 Summerfield, M., Reiter, S. H., Kebely, V., and Mascolo, R. W., "The Structure and Propagation Mechanism of Turbulent Flames in High Speed Flow," JET PROPULSION, vol. 25, Aug. 1955, pp. 377–384.

Incipient Flame Propagation in a Turbulent Stream[1]

H. L. OLSEN and E. L. GAYHART

ABSTRACT

IN ORDER to extend present knowledge about turbulent flames, and eventually to adapt that knowledge to the design of ramjet engines and high-output propulsive systems dependent on combustion, a series of experiments on turbulent flame propagation has been conducted at the Applied Physics Laboratory. The experiments provide a study of flame kernels propagating outward from a spark source of ignition in a free jet of combustible gas mixture; grids induce a turbulent flow in the free jet. The growth of the flame and the degree to which it is influenced by the turbulent flow field are measured by means of high-speed flash schlieren photography. Inasmuch as the flame kernel is carried along at the average velocity of the gas stream, the flame front must respond only to the turbulent velocity fluctuations. This constitutes an effective and simple experimental situation in which the interaction of flames and turbulent flow fields may be observed. Some of the major conclusions based upon this experimental work indicate that isotropic turbulent flow fields attainable with present equipment do not enhance the rate of flame propagation appreciably within the times observable, while nonisotropic turbulent flow fields immediately downstream from grids of sufficient size increase the rate considerably. The flow property, thought to be responsible for producing the increased flame-propagation rate, is the magnitude of the velocity gradients encountered by the flame, these being greatest in the nonisotropic flow fields mentioned. Quenching of the flame kernels by excessive turbulence has been demonstrated.

[1] From JET PROPULSION, vol. 25, no. 6, June 1955, pp. 276–283.

CONCLUSIONS

The following summarizing statements or conclusions, based upon the preliminary work reported herein, can be made.

1 Isotropic turbulent flow fields, of the kind produced in this work, do not enhance the rate of flame propagation appreciably within the time of observation of this experiment.

2 Nonisotropic turbulent flow fields do alter the apparent rate of flame propagation. The magnitude of the change in rate depends upon the grid size (spacing and wire diameter), and upon stream velocity. (See under "Discussion" in the original paper for a qualification of the words "isotropic" and "nonisotropic.")

3 The apparent rate of flame propagation may be either increased or decreased by the interaction with turbulence. This indicates the existence of an optimum turbulent condition which will result in a maximum combustion rate.

4 Turbulent diffusion is partially responsible for the apparent increase in flame propagation rate. Measurement of the temperature distribution within the flame kernel would be of assistance in assessing this effect.

5 The effect of the turbulence on flame propagation depends upon the equivalence ratio of the combustible gas.

6 It is probable that if flame kernels produced in such isotropic fields as used in Fig. 3 could be observed at considerably later times, an increase in flame propagation rate might be found. Experiments are in progress to test these possibilities.

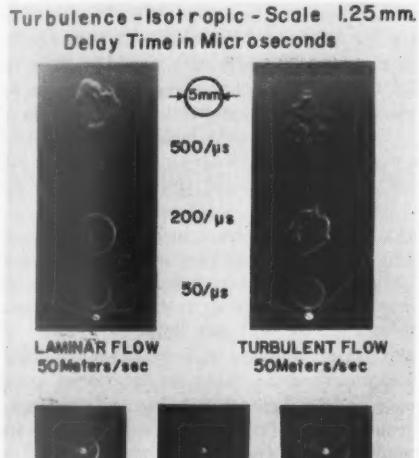


Fig. 3 Effect of turbulent flow on spark kernels in air

The Influence of Turbulence on Flame Propagation Rates[1]

RAY E. BOLZ and HENRY BURLAGE, JR.

ABSTRACT

A TECHNIQUE for the experimental study of laminar and turbulent flame propagation is presented. The method consists of igniting, by a single spark discharge, a small zone in a free jet of fuel-air mixture. This approximately spherically shaped burning zone, called a flame "globule," was shadowgraphed, using a high-speed motion picture camera,

[1] From JET PROPULSION, vol. 25, no. 6, June 1955, pp. 265–275.

as it passed downstream with the mixture. Measurements taken from the photographs resulted in the flame speed data.

CONCLUSIONS

1 The experimental technique appears to have considerable value for the study of the propagation of laminar and turbulent flames. The data appear to be quite consistent and reproducible, and particularly adaptable to the study of the transient phase of the turbulence effect.

2 The measured laminar flame speeds are in good agreement with those obtained by other investigators.

3 An encouraging quantitative correlation between an empirical equation and the experimental data is shown, but the relation to the scale of the turbulence was satisfactory for only one of the two screens used. The correlation was unsuccessful for very lean and rich mixtures. This was due to the fact that the rate of turbulent flame growth, for these cases, was lower than the laminar values.

A Comment on Turbulent Combustion

LESLIE S. G. KOVASZNAY

FROM the different presentations it appears that the two competing pictures of turbulent combustion may both occur under different conditions; furthermore, even a continuous "spectrum" of intermediate phenomena seems to be quite possible.

One picture is the "wrinkled" laminar flame front, where the process is essentially the same as in a steady laminar flame except that the turbulent motion extends the total area of the flame surface. The presence of holes or even of detached portions does not alter this picture. The other picture is a completely disintegrated flame front where the chemical reactions take place in a wide zone (even if it is viewed instantaneously) of turbulent agitation.

If we assume that locally only the rate of deformation controls the break-up of the front we can form a nondimensional parameter proportional to the velocity gradient (vorticity) present in the cold turbulent flow. I propose the following parameter

$$\Gamma = \frac{u'}{\lambda}\frac{\delta}{c} = \frac{\text{typical velocity gradient in approaching cold flow}}{\text{typical velocity gradient in laminar flame}}$$

where

u' = rms turbulent velocity fluctuation
λ = microscale of turbulence in the flow

immediately preceding the combustion region. The properties of the combustion mixture are

c = laminar flame speed
δ = thickness of laminar flame

The parameter can be further modified by introducing

U = characteristic velocity
L = characteristic length of the mean flow

I believe that the high values of Γ will give continuous combustion zones, and low values a "wrinkled" laminar flame. The cross-over should occur somewhere where Γ is of the order of unity.

I would also propose to investigate available experimental information by simply plotting

$$\frac{\text{apparent turbulent flame speed}}{\text{laminar flame speed}} = f(\Gamma)$$

to see whether one obtains a good correlation. The values of u' and λ should be obtained by turbulence measurements; however, for a first trial they could be roughly estimated by using only existing data on turbulent flows.

My main point is that turbulence level alone is not sufficient to characterize turbulent agitation but the microscale is equally important. The turbulence created by the presence of combustion may be significant only if it affects the flow upstream of the combustion zone.

The appearance of distinctly cellular flames can be expected probably only up to a certain value of Γ and they may be completely overshadowed by turbulent mixing at higher value of Γ.

On the Flow Patterns of Flame

S. I. PAI

THERE are three different types of flame, (a) laminar flame, (b) turbulent flame in transition region, and (c) fully developed turbulent flame. We have a fairly good knowledge about the method of analysis of laminar flame which will not be discussed here.

The turbulent flow in transition region is the most difficult problem to analyze. We do not know exactly how to solve such problems even in ordinary fluid dynamics (without heat release or combustion). But we do know that free stream turbulence has some influence on the transition. Various models in turbulent flame deal with essentially such turbulent flow in transition region. Since this is a very complicated phenomenon, it is expected that no single model will explain all the phenomena in this region. Furthermore, there are other factors, such as pressure gradient, etc., to affect the transition. This is why many discussions have been made about this type of flow and no definite conclusion can be drawn.

At high-speed flow or large Reynolds number case, the flow may become fully developed turbulent flow in which the degree of turbulence in the free stream has very little effect in the flow of flame which may be considered as a certain kind of boundary layer flow. In ordinary fluid dynamics, the mean velocity and temperature distributions in fully developed turbulent flow have been successfully analyzed by the phenomenological theories such as Prandtl's mixing length theory, etc. Such theories give fairly good results for jet mixing problems. (See Pai, "Fluid Dynamics of Jets.") It seems to the author that little has been done for the fully developed turbulent flow of flame for which the ordinary phenomenological theory may be extended without much difficulty, particularly for turbulent flame in jet. From some preliminary analysis of the author, he found that the fundamental equations for turbulent flame jet may be transformed into the same form as those of laminar flame jet. Similar methods of solution may be used for both cases. Of course, in the turbulent case, some empirical constants must be determined from experiments.

Such an analysis may also be applied to other turbulent flame problems provided that the Reynolds number of the flow is much higher than the critical value for transition.

Turbulent Flames in Gases

MARTIN SUMMERFIELD

NOMENCLATURE

u' = turbulent velocity component in direction normal to flame zone
λ = microscale of turbulence in approach flow
S_L = normal laminar burning velocity
δ = laminar flame thickness

1 INTRODUCTION

ON THE basis of the experimental information presently available, it appears that turbulent flames can occur in either of two ways, depending on the turbulence level. Under

conditions of *mild* turbulence, the flame brush seems to consist of a laminar flame in irregular motion, either as a continuous wrinkled flame sheet or as discontinuous segments of flame (1). Under conditions of *strong* turbulence, on the other hand, it appears that the reaction zone is considerably disturbed, that as a consequence the chemical reaction is distributed in depth, and that ordinary laminar flames can no longer be recognized (2). Between these two well-defined models, there are probably transition types of turbulent flames. It was Damkohler's idea that a criterion for the occurrence of the distributed reaction zone model is that the turbulence scale L should be much less than the laminar flame thickness δ, (3). An alternate criterion has been proposed by Kovasznay, namely, that the ratio

$$\frac{u'\delta}{\lambda S_L}$$

should be large (4). The underlying thought is that a high value of this ratio would indicate the presence of stronger velocity gradients arising from turbulence than the gradient present in the laminar flame itself and that, consequently, the flame zone would be severely disrupted. No systematic experiments have been performed to test the relative validity of these two criteria. It appears that the flames examined in the work described in the next paragraph can be characterized as reaction zones in depth, and, therefore, that any practical flame in a jet engine combustor is likely to be a reaction zone in depth. The wrinkled flame theories (5, 6) which have been so prominent in the literature of the past five years are probably not applicable at all to practical problems.

2 EXPERIMENTS

In our laboratory, the observations were made on a two-dimensional flame created by a premixed jet of methane and air issuing from a rectangular nozzle, $2 \times {}^1/_2$ in. The flame was anchored by small hydrogen diffusion flames running along the 2-in. sides of the nozzle. Jet velocities ranged up to 100 ft/sec. Turbulence was created by square mesh grids, and from published turbulence decay correlations the turbulence intensity in the approach flow to the flame was of the order of 10 per cent. Observations were made mainly of flames on the fuel lean side of the stoichiometric ratio. In order to find out as much as possible about the physical structure of the flame, the following experiments were performed (2).

(a) Spectrographic traverses of the flame zone were made to determine the relative spatial distributions of CH (4300 AU) and H_2O (9300 AU) emissions.

(b) Simultaneous filtered photographs of the flame were taken through interference filters centered at 4300 AU and at 9300 AU, respectively, to check the results of (a).

(c) Thermocouple temperature traverses through the flame zone were compared with simultaneous photographs taken through the 4300 AU filter.

(d) Flame conductivity was recorded as a function of time at various parts of the flame utilizing a bare wire probe inserted in the flame.

(e) Spark shadowgraphs were taken of the flame.

3 RESULTS

The spectral traverses (a) and (b) showed a marked spatial separation between the *onset* of emission by CH and by H_2O. The actual distance varied with different parts of the flame, from a few millimeters to a couple of centimeters. These results are incompatible with the wrinkled laminar flame model. For the wrinkled flame, the spatial separation should be no more than 0.2 mm. Expressed in time units, the observed spatial separation corresponded to approximately 1 millisec. Recent measurements of Wohl (7) on laminar flames of butane and air indicate a similar time separation. Equality of separation on a time basis would support the treatment of the turbulent flame as a chemical reaction in depth.

It was found in experiment (c) that CH emission was centered at the high side of the temperature traverse, a familiar characteristic of laminar flames on a much smaller scale. This result again indicates a reaction zone in depth and not a wrinkled flame. For a wrinkled flame, the CH emission contour should be centered near the position of 50 per cent temperature rise.

The conductivity fluctuations (d) gave no indication of laminar flame sheets moving on and off the wire probe, as previously reported by Karlovitz (8). In fact, the observed random statistical distribution of conductivity as a function of time casts doubt on the results of Karlovitz pertaining to the fluctuations in position of the supposed laminar flame. The only explanation for the conductivity variations is a model with turbulent fluctuation of reaction rate in a deep zone of chemical reaction.

The spark shadowgraphs (e) of the turbulent flame showed many discontinuities within the zone of observation, the average size of the granular pockets being of the order of 2 mm. Although it is impossible to determine whether the observed discontinuities are flame fronts or merely sharp gradients of temperature and composition, it seems unlikely that so many laminar flames could occur in a limited volume and yet produce an augmentation of burning rate of no more than about 5. In this connection, the remarks made by Grumer at the Conference are significant; namely, that successive, high-speed shadowgraphs of a turbulent flame show that the discontinuities previously identified as flame fronts have apparent velocities that are much too high to be explained either by laminar flame propagation or by turbulence, and that, therefore, it is unlikely that these discontinuities are related in any way to laminar flame fronts.

4 CONCLUSIONS

Although the experiments described above point quite definitely toward a distributed reaction zone model, several experimental checks need still to be made to arrive at a final conclusion. The spectral traverses should be repeated with a spectrophotometer with linear response to improve upon the intensity data obtained from the photographic plates. The extent of self-absorption at 4300 AU and at 9300 AU should be analyzed to determine whether the observed intensity distributions are distorted. The conductivity probe results should be re-examined with a signal discriminator of the type employed by Karlovitz to decide whether there is any basis for identifying the sharp changes in conductivity with the movement of laminar flame sheets on and off the wire probe. There is a serious question as to whether the use of a voltage discriminator in Karlovitz's amplifier circuit did not produce misleading results. The criterion for the break-up of the disturbed laminar flame into a distributed reaction zone, as proposed by Kovasznay, should be tested experimentally.

Inasmuch as the present evidence indicates that strongly turbulent flames do not consist of wrinkled laminar flames, there is need for a new approach to the theory of propagation of turbulent flames. An approach tried by the present author was to treat the turbulent flame by the familiar theoretical methods that have been employed for laminar flames, but with modified diffusivity and reaction rate terms. The comparison of experimental and theoretical flame speed was good but not really conclusive (2). Better measurements need to be made. In particular, it is necessary to measure not only turbulence intensity in the flame zone, but also turbulent diffusivity or turbulent scale.

On the question of flame generated turbulence, more has to be known about the process by which turbulence is generated (if at all!) in the reaction zone. On the experimental side, the findings of Wohl concerning the effect of mixture

ratio on apparent flame turbulence, and the findings of Westenberg on the absence of any increase in turbulence intensity in going through the turbulent flame, cannot be reconciled with the theory of flame generated turbulence recently published by Karlovitz (5). Moreover, this theory cannot be justified on fluid mechanical grounds in particular, with respect to handling of the equation of continuity. In any case, a new set of concepts employing the distributed reaction zone model is needed.

REFERENCES

1 Lewis and von Elbe, "Combustion, Flames, and Explosions," Academic Press, New York, 1951, p. 480.

2 Summerfield, M., Reiter, S. H., Kebely, V., Mascolo, R., "The Structure and Propagation Mechanism of Turbulent Flames in High Speed Flow," JET PROPULSION, vol. 25, 1955, pp. 377–384.

3 Damkohler, NACA T.M. 1112, 1947.

4 Kovasznay, L. S. G., "A Comment on Turbulent Combustion," remarks at the conference on Combustion in Turbulent Flow; JET PROPULSION (this issue) p. 485.

5 Karlovitz, B., "Selected Combustion Problems," AGARD, Butterworths, 1954, p. 248.

6 Scurlock, "Selected Combustion Problems," AGARD, p. 215.

7 Wohl, K., Semi-Annual Reports, Project SQUID, Oct. 1951 and Oct. 1952, University of Delaware.

8 Karlovitz, B., "Fourth Symposium on Combustion," Williams & Wilkins, Baltimore, 1953, p. 617.

COMMENTS ON THE REMARKS OF OTHER SPEAKERS

M. SUMMERFIELD

A. L. Berlad

It would be of great interest to reduce the data on intensity of emission from hydrocarbon flames to absolute units such as ergs/mole of fuel, or photons/molecule of fuel.

K. Wohl

He reports that in turbulent flames the contour at which 50 per cent of the temperature rise has taken place lies distinctly up-stream of the contour at which 50 per cent of the oxygen is consumed. The fact that these two contours do not coincide is further evidence, I believe, that a strongly turbulent flame is not simply a wrinkled laminar flame. On the other hand, for a distributed reaction zone model, the two contours would coincide only if the turbulent Lewis number (mass diffusivity/heat diffusivity) were exactly unity, and this is probably not so. It would be of interest to know where the contours of maximum CH and C_2 light emission lie with respect to the 50 per cent temperature and 50 per cent oxygen contours. This would have a bearing on the physical structure of the flame zone.

H. L. Olsen and E. L. Gayhart

They find that an incipient flame kernel can be quenched by strong turbulence. It is interesting that this quenching always occurs in a time less than 1 millisec. This time interval is significant. It is of the same order as the time of reaction at atmospheric pressure as measured by the traverse time through a laminar flame. Can it be that turbulent mixing of the incipient flame gas with the cold unburned gas around it can result in extinction of the flame only in the early stage (less than 1 millisec) before hot products are formed? Have cases of extinction by turbulence been observed, say, 5 millisec after the gas is ignited? The question is, can strong turbulence extinguish a flame that is fully established? The answer to this question may have an important bearing on the broader controversy of whether turbulence merely wrinkles a laminar flame or thickens the reaction zone.

B. Karlovitz

In view of the questions raised concerning the validity of Karlovitz's interpretation of the conductivity probe signal traces, it would be of considerable interest if he would publish some typical oscilloscope traces at various levels of discriminator cut-off voltage, from zero to the highest value tried. In our experiments, we found no logical cut-off value. The maxima and minima were distributed quite at random in time and in magnitude, so that the on-and-off statistics would mean nothing as to the movements of a so-called flame sheet.

R. Friedman

It would be of great value for the development of the theory of laminar flames if the same superb experimental techniques developed by Friedman were used to obtain temperature distributions in flames of reactions that are at least partly understood kinetically. How about the hydrazine decomposition flame, the dilute ozone flame, the hydrogen-bromine flame? Would Friedman be willing to undertake these researches?

Remarks on Turbulent Flames

BÉLA KARLOVITZ

STRUCTURE OF TURBULENT FLAMES

I BELIEVE that the question is not whether turbulent flames consist of wrinkled laminar combustion waves, but rather, what are the limits of validity of the wrinkled combustion wave theory. At low and medium turbulence intensity, good agreement is found between measurement of the turbulent burning velocity and predictions of the wrinkled combustion wave theory. At the highest turbulence level at which burning velocity measurements were carried out on a $R_e = 100{,}000$ flame, the measured turbulent burning velocity was found considerably higher than it would be calculated by assuming the normal burning velocity for the laminar combustion wave (1). Apparently at high turbulence intensity (u'/S_u in the order of 10 or more) the propagation velocity of the combustion wave is strongly affected by fine scale turbulence. Also, at such high turbulence intensity the combustion wave is so strongly wrinkled that portions of the combustion wave which face each other supply heat in the same volume of unburned gas, whereby the propagation velocity of the combustion wave is greatly increased. Furthermore, high turbulence intensity can produce such steep intermittent velocity gradients which can affect or even interrupt the combustion wave. The resulting effect of these phenomena is that the propagation velocity of the instantaneous combustion wave is not equal any more to the propagation velocity of a normal plain combustion wave, defined as the normal burning velocity S_u, but is significantly higher. Obviously, already a two- or threefold increase in the combustion wave propagation velocity can have a very large effect on the flame. The thickness of the combustion wave is also affected, together with its propagation velocity. Still, at such conditions, the structure of the flame will not be homogeneous, and the concept of the wrinkled combustion wave will be useful in describing such highly turbulent flames. To augment the present simple theory of turbulent flames, it will be necessary to find a way to describe the effect of very strong turbulence on the propagation velocity of the instantaneous combustion wave.

For further progress, measurements are needed on highly turbulent flames. For this purpose new methods of measurement will have to be developed. As one possible approach, the measurement of the volume required by an open turbulent flame brush at very high turbulence intensity is suggested.

At extremely high turbulence intensity, homogeneous volume reaction finally is approached. Such flames were realized experimentally at reduced pressures by Longwell (2). The heat release rate of such flames is very high, 400×10^6 Btu/ft^3 atm^2 hr, and it varies with the square of the pressure.

The heat release rate of a turbulent flame brush consisting of wrinkled combustion waves varies only linearly with pressure, therefore, at atmospheric pressure and above; the homogeneous reaction rate limit is very much higher than heat release rates found in practical combustion systems.

ELECTRONIC PROBE METHOD

With regard to the electronic probe method, it has to be pointed out that clear interpretation of the results is possible only if a discriminator circuit is used. Experimentally it was found that the discriminator voltage has a wide range within which the results of the measurement are not sensitive to the discriminator setting.

FLAME GENERATED TURBULENCE

The continuity of the flow across the turbulent flame brush is satisfied by a pressure drop across the flame brush and not by the velocity introduced into the flow system by the laminar combustion wave.

REFERENCES

1 Karlovitz, B., "Selected Combustion Problems," AGARD, Butterworths, 1954, p. 248.

2 Longwell, J. P., "Selected Combustion Problems," AGARD, Butterworths, 1954, p. 508.

Flames in Turbulent Streams[1]

W. G. BERL, J. L. RICE, and P. ROSEN

ABSTRACT

A DISCUSSION is given of several models indicating how combustion rates can be increased above the laminar flame propagation rate. These models are compared with actual flames stabilized under a variety of flow conditions. The factors influencing combustion in turbulent streams are outlined.

CONCLUSIONS

1 For cases of low turbulence (isotropic, intensity < 10 per cent) and in the absence of velocity gradients the effects on flame propagation are small and are primarily shown in a cellular break-up of the reaction zone. Possible explanations for the spontaneous onset of instability are given by Markstein (Reference (12) in the original paper). Although a rough estimate of total flame surface indicates small changes over the corresponding laminar flame, it cannot be said with certainty, in the absence of detailed knowledge of the direction of streamlines, that these "turbulent" flames are in effect equivalent to folded laminar flames.

2 For cases of higher turbulence intensity (coarse screens, nonisotropic turbulence) more pronounced flow disturbances interact with the flame zone. The photographic evidence becomes less clear as to the structure of the reaction zone, although still giving evidence of cellular structure. The composition profiles appear to indicate that considerable interlacing of hot and cold gas streams is occurring.

3 At higher velocities (200 ft/sec) the photographic evidence becomes even less satisfactory, except to indicate that the continuous reaction zone breaks up into discrete eddies at some distance from the stabilizing elements. There is also evidence that velocity gradients between the combustible jet and the annular igniting jet affect the mixing zone and thus the heat release rate between them. In fact, the structure of the mixing zone is qualitatively similar whether combustion is proceeding in the central jet or not.

Composition profiles indicate that the existence of velocity differences can have a marked effect on the flame length, although, as shown in Fig. 4, the initially high heat release rates are not maintained far beyond the influence of turbulence producing grids or the region where strong velocity gradients exist.

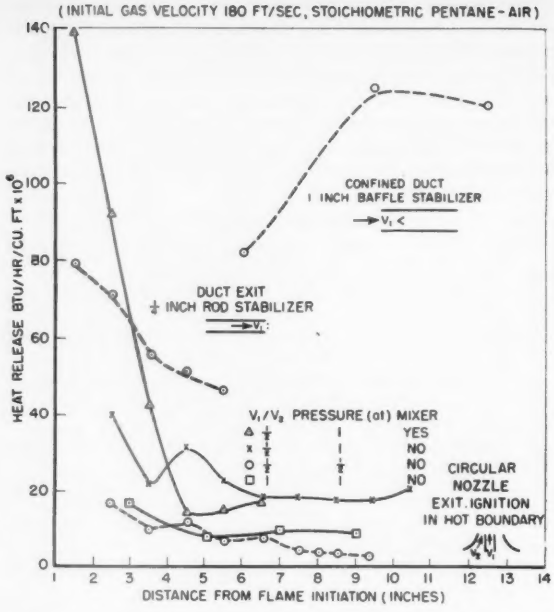


Fig. 4 Heat release rates of a variety of turbulent flames

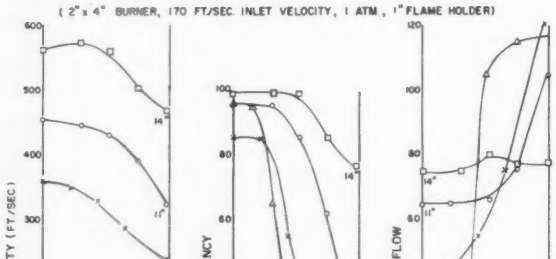


Fig. 5 Velocity, efficiency, and mass flow profiles

4 A significant change in heat release rates occurs if the combustion is proceeding in a constant area combustion chamber. While in the previous cases the acceleration of the hot gases after combustion was comparatively small, in constant area combustion strong velocity gradients are set up not only in the vicinity of flameholding surfaces but again in the downstream sections where the majority of the combustion takes place. Two principal regions of velocity difference can be distinguished. The high-temperature gases in the wake of the flameholder are at first at much lower velocity than the unreacted gas. A typical series of traverse is shown in Fig. 5. The effects of the flameholder are clearly visible in the form of a recirculation zone. A gradual reversal sets in until at some distance downstream the velocity conditions are inverted. Conversion rates increase at the same time,

[1] From JET PROPULSION, vol. 25, no. 7, July 1955, pp. 341–346.

ndicating a dependence between the velocity differences and the chemical transformation rates (Fig. 4). It is not possible, at this time, to specify in detail the interrelation between the numerous parameters, and one can only emphasize the fact that the combustion process, through its effect on the velocity distribution, provides a means leading to better mixing and combustion.

5 In none of the experiments reported here is there unambiguous evidence for homogeneous reaction assumed in the theory of Avery (Reference (5) in the original paper). None of the experimental tools of photography or time average sampling can be used to rule out homogeneity in parts of the reacting mixture. Although strong schlieren gradients are always evidence of steep temperature (or composition) gradients, the absence of such gradients may indicate either homogeneously reacting regions, or equally, regions of gas at equilibrium. The heat release rates are generally low enough to rule out the necessity for postulating homogeneous and near-optimum reaction rates. There are instances, however, such as in strongly mixed reactors (Reference (11) in the original paper) where a considerable fraction of the reaction may proceed under homogeneous conditions.

Flame Spreading from Baffles

M. A. WEISS

A LITERATURE review and an experimental study have been made on flame spreading from baffles in turbulent ducted flow. Two chief objects of this work were to determine the separate effects of geometric and operating variables on flame spreading rates and to attempt to account for the effects in terms of some turbulent flame theory.

Experimental measurements were made in the apparatus shown in Fig. 6. Various baffle configurations were placed (where the single $2^1/_4$-in. V-gutter is shown) in a stream of homogeneous air-fuel mixture. At several distances downstream of the baffle, probe traverses were made to determine local total pressures and oxygen consumption efficiencies. From these data the average over-all efficiency in the plane (normal to flow) could be calculated. Typical time average velocity and efficiency profiles are shown in Figs. 7 and 8.

Flame spreading rates are more easily compared by conversion to equivalent turbulent flame velocity. These were computed by first arbitrarily assuming that the stream consisted of only completely burned and completely unburned gases—the relative amounts of each at any plane corresponding to the average efficiency level observed at that plane. If one then assumes that a zero thickness flame front separates burned and unburned gases, the local turbulent flame velocity is readily defined as the local volumetric rate at which unburned mixture crosses the flame front divided by flame front area. This definition, though arbitrary, is convenient. (It should be emphasized that the assumption that only two efficiency levels exist, 0 and 100 per cent, bears no resemblance to the physical reality illustrated in Fig. 8.)

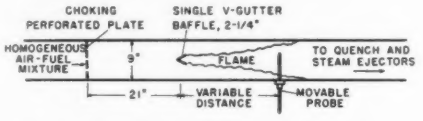


Fig. 6 Sketch of flame spreading apparatus

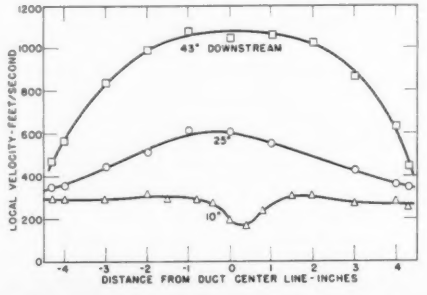


Fig. 7 Velocity profiles downstream of a 2.25-in. V-gutter

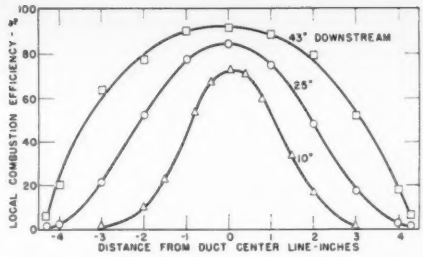


Fig. 8 Efficiency profiles downstream of a 2.25-in. V-gutter

Flame velocities so calculated from the profiles of Figs. 7 and 8 are shown in Fig. 9. Minimum and maximum theoretical velocities, calculated in the same way, are also shown. The minimum rate corresponds to a simple laminar flame. The maximum rate assumes that a core of chiefly burned material is burning in an optimum way. This model is similar to that proposed by Avery and Hart (*Industrial and Engineering Chemistry*, vol. 45, 1953, p. 1634) using the burning rates measured by Longwell and Weiss (ibid., vol. 47, no. 6, 1955). Observed average efficiencies obviously correspond to neither model.

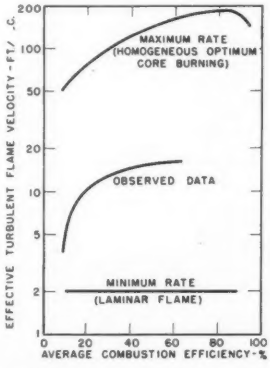


Fig. 9 Effective turbulent flame velocities. Comparison of experimental rates with calculated extremes

One can also assume locally homogeneous burning with each small mass of gas in a profile burning at a rate set by its instantaneous efficiency—again using the data of Longwell and Weiss. (Transfer of mass or heat normal to flow is neglected.) In Fig. 10, such a calculation is shown, starting with a reference profile from Fig. 8. The calculated profiles show no resemblance of general shape to the observed time-average values. Similarly, the effective flame velocities computed from the profiles do not agree with the data.

The specific data of Figs. 7 and 8 have thus not been matched by any of the flames theorized. If all of the data on flame spreading in turbulent ducted flow are considered, one observes generally that (a) the equivalent flame velocities range from about 5 to 50 ft/sec, (b) flame velocity decreases as pressure decreases with an exponent of about 0.1 to 0.7, depending chiefly on geometry, and (c) abrupt gradients in velocity or efficiency are not found. These observations make a wrinkled laminar flame theory an untenable mechanism under almost all the conditions studied here. Similarly,

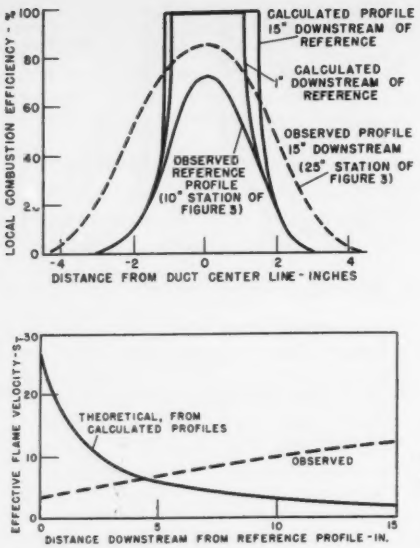


Fig. 10 Data treatment assuming locally homogeneous combustion

homogeneous reaction does not seem a useful approach. It is very likely that flow consists of detached masses of variously burned gases—possibly with a wave motion superimposed. Analyses based on steady flow and composition could then be grossly in error.

Measurement of the effect of pressure on turbulent flames is recommended as a test of current theories. Because there is some knowledge of the effects of pressure on laminar flame speed and turbulence separately, comparison of their theoretically combined effects with observed effects should be instructive.

An Investigation of the Burning Rates of Confined Turbulent Flame Jets[1]

J. J. ZELINSKI, W. T. BAKER, L. J. MATTHEWS III, and E. C. BAGNALL

ABSTRACT

IN this study we have determined the burning rates of confined turbulent flame jets under conditions of operation similar to those found in jet engines. A two-dimensional, inclined, can-type flameholder with three separately ducted stages was placed in a 4-in. × 14.25-in. × 70-in. duct. The flameholder was inclined 17 deg from the horizontal and was placed 8.56 in. from the exit of the test section. Each duct was 4 in. × 2.33 in. and extended 36 in. beyond the upstream end of the flameholder; separate instrumentation and controls were used to insure identical conditions in each stage. A separate pilot burner occupied the upper half of the test section upstream of the flameholder to provide a hot cross-stream into which the jets discharged. Conditions within the combustion zone were determined by twelve wall taps located $^5/_8$ in. above the flameholder surface, eight wall taps in the plane of the exit, and a rake of fourteen water-cooled probes, movable in the exit plane, which were used for gas sampling and measuring stagnation pressure.

This study has been limited to systems of premixed fuel and air and perforations of round holes. The performance of the individual jets has been determined as a function of combustion chamber pressure (P), velocity of the gas through the holes (V), temperature of the fuel-air mixture (T), diameter of the holes (D), equivalence ratio[2] (E), ratio of the total hole area to combustor chamber cross-sectional area (A_h/A_b), and length of the jet (S). Two fuels were used: pentane and kerosene.

For a given set of conditions total pressure, static pressure, and gas composition were measured at 42 points in the exit plane of the combustor. From this information mass flow rate per unit area at each probe position was calculated, and by changing the equivalence ratio between pilot gases and can section gases the distribution of the pilot gases in the exit survey plane was found. By a numerical integration the mass flow from each jet was isolated and an integrated combustion efficiency determined. Since all three jets were burning under essentially identical conditions, this method provided the equivalent of sampling a single jet at three levels along its length. A standard reference condition was chosen: combustion chamber pressure 7.35 psia; jet velocity 500 ft/sec; air-fuel temperature 200 F; equivalence ratio 1.0; hole diameter 3.06 in.; ratio of hole area to combustion chamber area 0.575; and jet lengths 8.5, 16.5, and 24.5 in. In all cases 20 per cent of the total mass flow rate passed through the pilot section. The effect on combustion efficiency was found by varying each variable independently from the standard condition. The values selected were: chamber pressures of 4.90 and 9.80 psia; jet velocities of 300 and 700 ft/sec; air-fuel temperatures of 100 and 340 F; equivalence ratios of 0.7 and 1.3; hole diameters of 1.0 and 1.5 in.; ratios of hole area to chamber area of 0.375 and 0.700.

The results were correlated in an exponential form to give

$$\eta = 1 - e^{-\alpha S}$$

where

α = $0.021\ P^{0.72}V^{-0.76}T^{0.75}D^{-1.2}E^{0.55}(A_h/A_b)^{-1.2}$
η = integrated combustion efficiency
P = combustion chamber pressure, psia
V = jet velocity, ft/sec
T = air-fuel temperature, degree Rankine
D = hole diameter, in.
E = equivalence ratio, dimensionless
A_h/A_b = total hole area/combustion chamber area, dimensionless
S = jet length, in.

Interactions of Flames and Flow Disturbances

G. H. MARKSTEIN

A CONTINUING study of flame-flow interactions of various kinds is being carried out at Cornell Aeronautical Laboratory, Inc., under the sponsorship of Project SQUID. The main results hitherto obtained are:

(a) Small periodic flow disturbances introduced artificially into laminar Bunsen flames were amplified in the region of the flame front (1). An example is shown in Fig. 11. The growth of flame front distortions during their upward travel is evident.

(b) Almost stabilized flames burning in a wide tube under laminar flow conditions may assume a cellular structure indicative of spontaneous flow disturbances created by the flame (2). Typical cellular flames burning in rich mixtures of various hydrocarbons are shown in Fig. 12. The phenomenon occurred also in lean mixtures upon addition of hydrogen, in accordance with the preferential diffusion theory (3). It seems, however, that a valid analysis of cellular flame structure must combine aerodynamic as well as transport and chemical kinetics aspects of the phenomenon. Current analyses (2, 4) are of a very rudimentary nature, since the

[1] To be published in Proceedings of the Gas Dynamics Symposium, Northwestern University, 1955.

[2] Equivalence ratio is defined as the ratio of the actual fuel to air ratio and the stoichiometric fuel to air ratio.

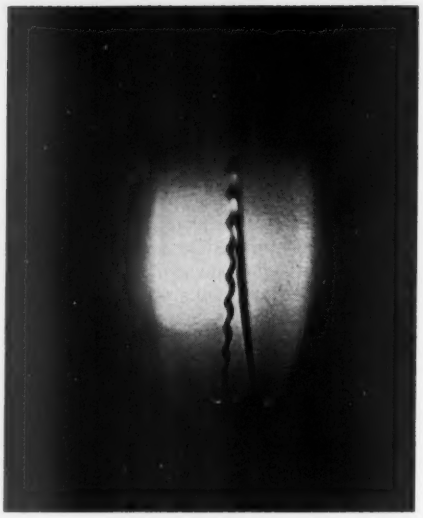


Fig. 11 Spark schlieren photographs of a laminar Bunsen flame distorted by the effect of a wire touching the flame near the base and vibrating in a direction normal to the flame front

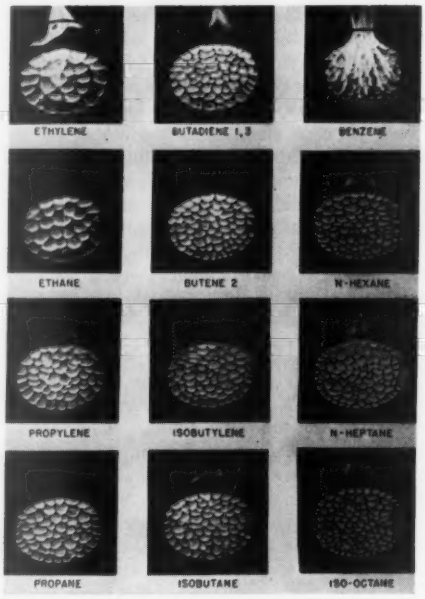


Fig. 12 Cellular flames in hydrocarbon-air-nitrogen mixtures

transport and kinetics effects are lumped into a single phenomenological parameter, and the treatment is linearized. The theory yields a critical wavelength λ_c of the disturbances that separates a stable range $0 < \lambda < \lambda_c$ from an unstable one, $\lambda_c < \lambda < \infty$. Recently, a slot burner method (5) has been developed for the purpose of extending the study of cellular flames to a wider range of mixture compositions. Steady cellular slot burner flames are shown in Fig. 13. The technique has been modified (5a) by using nonsteady slot burner flames with periodically collapsing cells for measuring minimum cell sizes (presumably related to the theoretical λ_c).

(c) Vibratory flame movement in tubes was investigated using high-speed movies and oscillographic pressure records (2, 4, 6). These studies revealed a close connection between vibratory flame movement and cellular flame structure. Regardless of mixture composition, excitation of organ-pipe oscillations by the flame was always accompanied by periodically recurrent cell structure. Combustible mixtures that burned with pronounced cell structure in the absence of oscillations were capable of exciting higher frequencies than "noncellular" mixtures. A generalization of the analysis of flame front stability that included the effect of an alternating acceleration acting normal to the flame (4, 7, 8) gave results in qualitative agreement with these observations.

(d) It appeared desirable to study the interaction of pressure waves and flame fronts under conditions where the pressure waves could be generated and controlled independently from the combustion process. Shock tube equipment has been designed for achieving this aim, and preliminary results have been obtained (9). Fig. 14 shows the effects of passage of shock and expansion waves on flame front structure.

The above results would seem to be significant in various respects for the field of turbulent flame propagation. Common to all the interaction phenomena is the strong coupling between several disturbance fields that occurs in the combustion zone. It has been shown (10) that arbitrary flow perturbations can be decomposed into potential flow, vorticity, and entropy spottiness fields, which in homogeneous flow are coupled only in second order. However, strong first-order coupling between these three modes occurs in nonhomogeneous

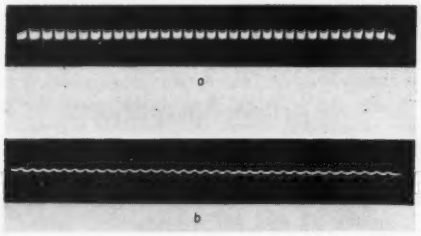


Fig. 13 Cellular slot burner flame. (a) front view; (b) edge-on view

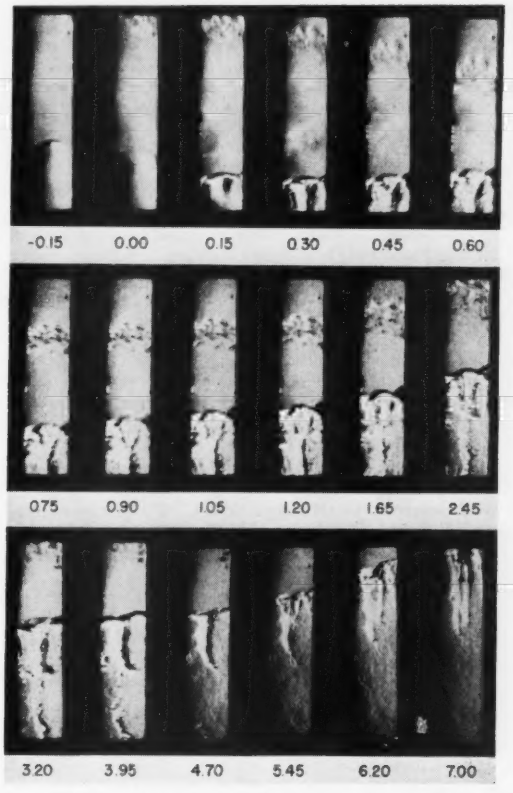


Fig. 14 Schlieren high-speed movie of pressure wave flame front interaction. Numbers below frames denote time in milliseconds from instant when primary shock reaches flame front

regions, particularly in zones of entropy change, such as shock waves or flame fronts. This has been fully recognized for the case of the shock wave (11) but seems not yet to have received sufficient attention with respect to flame propagation. Linearized analysis of the interaction phenomenon has undoubtedly very serious limitations (much more serious in the case of the flame than in that of the shock wave) but nevertheless should yield results of heuristic value. Thus, it has been shown (12) that a resonance phenomenon occurs at the critical wavelength λ_c when a normally incident shear wave interacts with the flame, a result that qualitatively explains certain observations on turbulent flames (13).

In view of the flame instability beyond λ_c a linearized analysis of steady-state response of an infinitely extended flame to incident turbulence would seem, however, of doubtful significance. A recently published analysis of this nature (14), carried out for a "Darrieus-Landau" flame ($\lambda_c = 0$), although not necessarily meaningful in itself, might be of value for extending the analysis to the case of a flame of finite dimensions held on a flameholder. For this case a finite solution would be obtained despite the instability.

The mutual coupling between vorticity and potential flow disturbances seems particularly important because the latter are not convected by the main flow and thus can have a cumulative effect (15), which is probably operative in the phenomena discussed above under (a). The storage of disturbance energy may become even more significant in ducted burners where the potential flow disturbances are partly of the nature of pressure waves that become trapped by resonance modes of the duct. The remarkable increase of flame propagation rates under vibratory conditions, well known since Mallard and Le Chatelier's work, and the observations discussed under (c) and (d) indicate that "noise" may be equally or more important than "turbulence" for determining the burning rate of flames in ducts.

REFERENCES

1 Markstein, G. H., Third Symposium on Combustion, Flame and Explosion Phenomena, Williams & Wilkins, Baltimore, 1949, p. 162.

2 Markstein, G. H., *Journal of the Aeronautical Sciences*, vol. 18, 1951, p. 199.

3 Manton, J., von Elbe, G., and Lewis, B. J., *Journal of Chemical Physics*, vol. 20, 1952, p. 153.

4 Markstein, G. H., Fourth Symposium on Combustion, Flame and Explosion Phenomena, Williams & Wilkins, Baltimore, 1953, p. 44.

5 Markstein, G. H., and Somers, L. M., *Journal of Chemical Physics*, vol. 21, 1953, p. 941.

5a Markstein, G. H., and Schwartz, D., Paper presented at the Gas Dynamics Symposium, Northwestern University, Evanston, Ill., April 22–24, 1955.

6 Markstein, G. H., and Somers, L. M., Fourth Symposium on Combustion, Flame and Explosion Phenomena, Williams & Wilkins, Baltimore, 1953, p. 527.

7 Markstein, G. H., *Journal of the Aeronautical Sciences*, vol. 18, 1951, p. 428.

8 Markstein, G. H., and Squire, W. J., *Journal of the Acoustical Society of America*, vol. 27, 1955, p. 416.

9 Markstein, G. H., and Schwartz, D., JET PROPULSION, vol. 25, 1955, p. 174.

10 Kovasznay, L. S. G., *Journal of the Aeronautical Sciences*, vol. 20, 1953, p. 657.

11 Ribner, H. S., NACA Report 1164, and Technical Note no. 3255, 1954.

12 Markstein, G. H., *Journal of the Aeronautical Sciences*, vol. 20, 1953, p. 581.

13 Wohl, Shore, von Rosenberg, and Weil, Fourth Symposium on Combustion, Flame and Explosion Phenomena, Williams & Wilkins, 1953, p. 620.

14 Tucker, M., NACA Technical Note no. 3407, 1955.

15 Markstein, G. H., Discussion Remarks in Selected Combustion Problems, AGARD Combustion Colloquium, Butterworths Scientific Publications, London, 1954, p. 263.

A Model for the Flame Front in a Viscous Heat Conductive Gas Mixture for Hydrodynamic Investigations

BOA-TEH CHU

THE basic physical mechanism underlying the production of pressure waves as a result of changes in external conditions (such as changes in mixture composition, temperature, pressure, velocity of the flow ahead of the flame) is essentially due to the resulting change of the rate of heat release by the flame. This statement can be shown to be strictly true in the case of a plane flame front if one can ignore the differences in the values of the specific heat ratio r for the burned and unburned gases. It is mainly because of this fact that the flow field predicted on the basis of treating a flame front as a single discontinuity is for many purposes satisfactory.

Nevertheless, of the many phenomena associated with flame propagation and stabilization, there is a large class which depends on the transport properties of the medium. Such phenomena are associated either with material diffusion, as in the case of preferential diffusion, or with momentum and energy diffusion, as in the case of some types of flame stabilization and in problems of the flame-induced instability. The conventional model of the flame front as a simple discontinuity is not adequate to deal with such problems, although these problems are essentially hydrodynamical. There are two difficulties, one conceptual and one practical. Conceptually, it is not clear how one may take into account such diffusion phenomena and yet at the same time treat the flame as a surface of discontinuity. Practically, the difficulty lies in the fact that there are not sufficient boundary conditions to be applied at the flame front when the medium ahead of and behind the flame is considered as viscous, heat conductive, and diffusive. (This is really a consequence of the fact that all the transport phenomena introduce second derivatives in the differential equations, making them of second order instead of the first.)

If the dynamic effects produced by a flame or associated with it have principally a thermal origin, as all evidence seems to indicate, these conceptual and practical difficulties can be circumvented by the following artifice. Consider the flame front as a mathematical "heater" of no thickness which is at the same time a source sheet for the various species of the end product of the combustion and a sink sheet for the reacting species. If one desires to include the intermediate products of combustion, the flame front should also be considered as a doublet sheet. The speed of propagation of the flame, and the rates at which heat is released at the flame front and different components of the mixture are generated or destroyed at the flame front are considered as known functions of the local composition and thermodynamic state of the mixture ahead of the flame. Besides the conservation laws which must be satisfied at the flame front, it is assumed that the rate of diffusion of mass, momentum, and energy across the flame front is respectively proportional to the differences in concentration, velocity, and temperature across the "heater." This model of a flame front is being used to calculate the effect of preferential diffusion on flame stability.

The main differences between such a model of a flame front and the conventional one can perhaps best be seen if we imagine the actual flame (to a crude approximation, to be sure) can be considered as consisting of two zones: the diffusion-conduction zone and the combustion zone. In the conventional model, the two zones are lumped together into a single discontinuity which is called a flame front. In the present model, the combustion zone alone is replaced by a surface of discontinuity, leaving the conduction-diffusion zone as part of the flow field outside the flame front.

Comments on Landau Instability

BOA-TEH CHU

LANDAU showed that a surface of discontinuity separating an incompressible medium of density ρ_1 ahead of it from one of density ρ_2 behind it and propagating into the former with a constant speed, is unstable to small disturbances of all wavelength if $\rho_2/\rho_1 < 1$. It is stable if $\rho_2/\rho_1 > 1$. Since a flame front is essentially such a surface of discontinuity with $\rho_2/\rho_1 < 1$, it is concluded that the flame front as such must be unstable to small disturbances. Landau's results are so simple that one may ask the question: What is the physical cause of this instability and what is the mechanism involved? The following explanation is proposed.

Consider a plane flame front of infinite extent in an open space and choose a coordinate system fixed with respect to the flame front. Before any disturbance is introduced into the flow field, the flows ahead of and behind the flame are both uniform and perpendicular to the flame front (Fig. 15). Now suppose that for one reason or another a part of the flame bulges forward toward the unburned medium. (See Fig. 16.) For simplicity, the bump in the figure may be considered as a two-dimensional one, although the argument applies just as well to a three-dimensional one. Furthermore, the bump size may be finite or infinitesimal. Take two points P_1, P_2 near the edge of the bump. Before the bump is there the flow lines leaving these points are parallel to the undisturbed flow ahead of the flame (Fig. 15). After the bump is there, the flow lines leaving P_1, P_2 must be divergent since the volume of the burned gas produced between the two points is increased in proportion to the increase in the flame area between them. (This statement is still true when the flame is not in an open space but is confined in a device of finite dimension provided that the scale of the disturbance producing the bump is small compared with a relevant characteristic length of the device—but not so small that Markstein's correction to the flame speed must be taken into account.) The velocity of the flow leaving the points P_1, P_2, will then be oriented in directions as those typified by the vectors P_1Q_1, P_2Q_2 in Fig. 16. On the other hand, the normals P_1N_1, P_2N_2 to the flame front at P_1, P_2 converge toward the center of the bump. Consequently, the streamlines of the flow approaching the flame and ending at the points P_1, P_2 must be divergent at the flame front as shown by the vectors R_1P_1, R_2P_2 in Fig. 16. (This follows immediately from the conditions that the velocity component of flow tangent to the flame front must be continuous and the velocity component of flow normal to the flame front increases by a factor ρ_1/ρ_2 when one crosses the flame front from the unburned to the burned side.) Therefore, there is a slowing down of the oncoming flow immediately ahead of the forward bulging bump; and the bump will grow in size in the course of time.

The foregoing argument is valid for both finite and infinitesimal bumps bulging toward the unburned gas. For an infinitesimal bump bulging toward the burned gas, we expect (by reason of linearity) that the disturbance also grows in size. However, for a finite bump bulging toward the burned gas, the same reasoning cannot prove whether the streamlines approaching the bump are divergent or convergent. This is mainly due to the fact that the normal P_1N_1, P_2N_2 to the flame diverge. (See Fig. 17.) The fact that the above reasoning is not conclusive in the examination of a finite bump bulging toward the burned gas may mean either of two things: First, a more detailed analysis of the process involved is necessary before a definite conclusion can be deduced. Or, it may mean that when the bump bulging toward the burned gas has grown to a certain size it ceases to grow further. The last conjecture is very likely to be the truth because experimental evidence seems to show that only bumps bulging toward the unburned gas tend to grow bigger and bigger.

The same reasoning can be applied to examine the less interesting case studied by Landau, i.e., the case $\rho_2/\rho_1 > 1$. It is found that any bump, finite or infinitesimal in size, bulging toward the medium with the density ρ_2 tends to flatten out. So is an infinitesimal bump bulging toward the region with the density ρ_1, while for a finite bump bulging in the same way, no conclusive results can be deduced.

One-Dimensional Laminar Flame Front Structure

RAYMOND FRIEDMAN

FOR some years, we have been engaged in an experimental study of the internal structure of the laminar flame. We have employed flat-flame burners, and have worked at pressures as low as 0.05 atm in order to take advantage of the thickening of the flame with reducing pressure. Results of temperature explorations with thermocouples of 5-micron and 12.5-micron wire have previously been published (Fourth Symposium on Combustion, 1953; and *J. Chem. Phys.*, vol. 22, p. 824, 1954). One of the interesting findings is that, for a lean propane-air flame at low pressure, the temperature continues rising for some distance downstream from the zone of blue luminosity. Recently, we have performed gas-sampling experiments in such a flame. We find a substantial concentration of carbon monoxide just downstream of the luminous zone; this decays exponentially as the gas flow farther downstream. (Cf. Fig. 18.) Apparently, carbon monoxide is a semistable intermediate in hydrocarbon combustion. Some hydrogen was found in the region under discussion, the CO/H_2 ratio being about 5. This ratio would be not 5 but 2 if the water-gas equilibrium were maintained in this flame. Evidently, the water-gas reaction is not fast enough to maintain equilibrium when in competition with the oxidizing reactions.

When the heat-release rate was calculated from the measured rate of disappearance of CO and H_2, and compared with the heat-release rate calculated from the temperature trav-

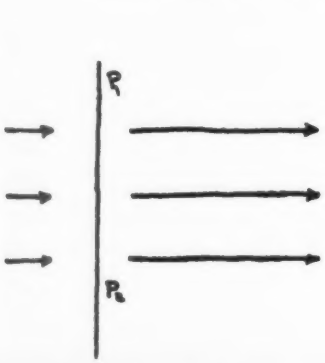


Fig. 15 Schematic Flow Lines

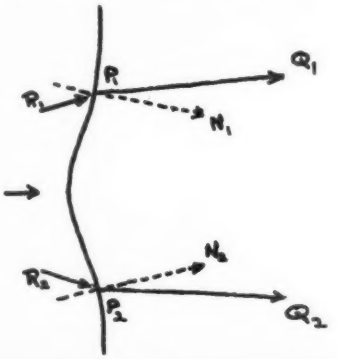


Fig. 16 Schematic Flow Lines

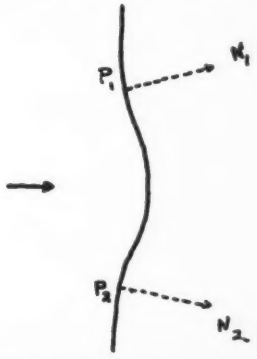


Fig. 17 Schematic Flow Lines

erse, fairly good agreement was obtained. (Cf. Fig. 19.)

A large body of data exists in the literature which shows that the rate of CO oxidation is strongly influenced by water vapor. We have recently studied this effect in these flames by adding up to 13 per cent water vapor to a propane-O_2-N_2 mixture, in such a way as not to affect the flame temperature or the fuel-oxygen ratio. The results (Fig. 20) show that the rate of CO oxidation in the second stage of a hydrocarbon flame is independent of water vapor concentration, over a wide range. (Of course, the range of very low water vapor concentrations could not be studied, as water vapor is a product of combustion.)

Further experiments are now being made in carbon monoxide flat flames, in an effort to clarify this water vapor effect.

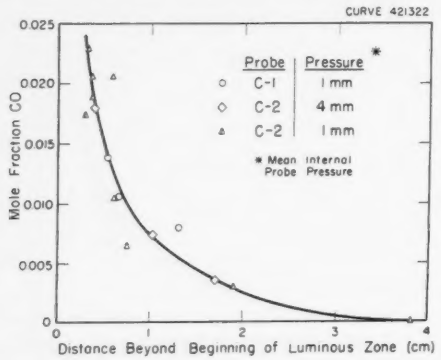


Fig. 18 Linear plot of [CO] vs. x. (Mass air-propane ratio = 30; pressure = 46 mm Hg)

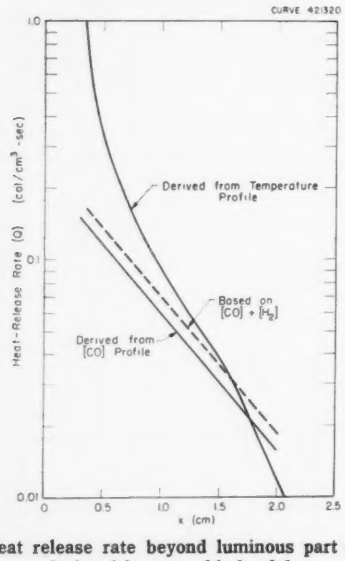


Fig. 19 Heat release rate beyond luminous part of flame as calculated from two kinds of data

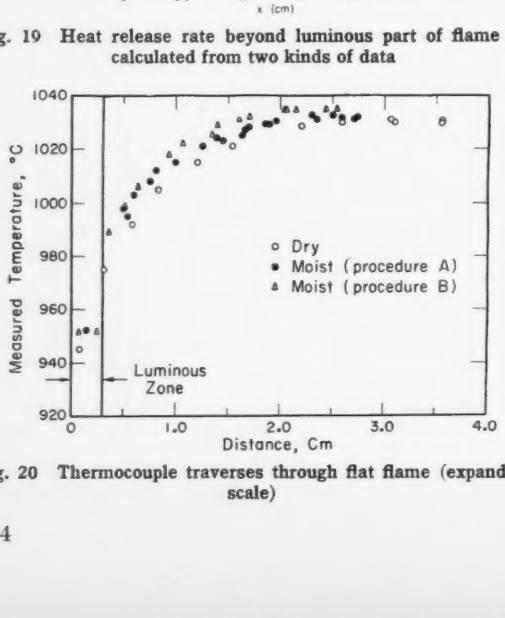


Fig. 20 Thermocouple traverses through flat flame (expanded scale)

The Applicability of One-Dimensional Models to Three-Dimensional Laminar Bunsen Flame Fronts[1]

ROBERT M. FRISTROM

ABSTRACT

THE applicability of one-dimensional models in flame theories has been investigated experimentally in the case of a lean quarter-atmosphere propane air flame. Studies of flow patterns through the flame fronts were made using particle track techniques. From this time-position information, normal gas velocity, stream tube area, and gas density were calculated normal to the flame front. If the density is a single-valued measure of the state of the gas, then one-dimensional models are applicable to Bunsen flames. Unidimensionality was verified for this and several other propane-air flames under a number of conditions. In the reaction region preceding the luminous zone it was also found that the velocity and density profiles were invariant with respect to changes in flame geometry, gas flow, and burner diameter. Therefore, it is a good approximation to speak of single reaction path for this flame, which is a function only of the initial state of the gas.

The measurements indicate that one-dimensional flame theories should be modified to include the effects of area expansion during the course of the reaction. Continuity, diffusion, and heat conduction equations should also be generalized to include the effect of expansion. It was noted that the hydrocarbon flame reaction consists of two regions: a fast propagating reaction associated with the luminus regions and the major portion of the heat release, and a slow secondary reaction associated with the postluminous mantel of the flame. Flow in the primary region is a function only of the initial state of gas and independent of external influences such as gas velocity and flame geometry. Flow in the secondary region could be varied over wide limits with no measurable effect on the propagation of the flame.

Burning velocity was found to be independent of gas velocity, flame geometry, and radius of curvature of flame front, and a function only of the initial state of the gas, providing it was defined as the minimum normal gas velocity ahead of the flame front. A discussion is given of the errors introduced by measuring burning velocity by flow measurements in the throat of the burner.

[1] From the *Journal of Chemical Physics*, vol. 24, no. 4, April 1956, pp. 888–894.

Summary

W. G. BERL

The principal points of interest in "turbulent combustion" are (a) establishment of suitable models for understanding the physical principles, (b) development and evaluation of experimental tools for measuring the significant variables, and (c) accumulating a body of design information that can be applied to engineering problems.

The structure, chemical changes, and flow interaction in laminar flames are at last yielding to experimental analysis. Chemical sampling for stable species in and beyond the reaction zone is now feasible (Fristrom, Friedman) and gives evidence for the step-wise decomposition of hydrocarbons and the surprisingly slow conversion rates of CO. Valuable in-

formation about oxidative reaction mechanisms should be forthcoming which, together with isotopic exchange studies, will assist in unraveling the pathway of the reaction.

The essential similarity of various three-dimensional laminar flame shapes (conical, V, button) has been described by Fristrom, who has measured their velocity and density profiles and has discovered identical time-temperature histories in the main reaction zone. Flame shapes can only be understood by considering the flow field and reaction zone together. The analysis sheds valuable light on some of the problems of how to define flame speed unambiguously.

The status of nonlaminar flames is in a much less satisfying shape in view of the much more numerous and complicated flow possibilities (Pai). A variety of flow-flame interactions are possible (Markstein). The readily analyzable case, where mixing becomes of secondary importance compared to the rate of the chemical reaction, does not appear to apply to stabilized flames in the absence of highly efficient mixing devices (Weiss, Berl, et al.) although it appears to explain the performance trends of the strongly stirred reactor of Longwell and Weiss.

It is generally conceded that the measurement of "turbulent" flame speed by adapting the laminar conventions is unsatisfactory. It averages over the entire length of the flame, even though local rates may be widely different (Berl). A more satisfactory way, laborious and not entirely free from sampling errors, is to determine the point by point state of the gases and deduce therefrom heat release rates (Zelinski et al.). Correlation of flame length and shapes in confined ducts can be obtained in this way and utilized in engine designs.

Although turbulence created by grids and allowed to decay for several mesh lengths produces interesting effects on the details of the flame surface (cell formation) the work of Olsen et al. and of Bolz et al. show that no substantial changes in heat release rates can be achieved in that way. On the other hand, eddies shedding from obstructions may give rise to markedly increased rates. However, an optimum rate of diffusion exists since flame extinction has also been observed through overmixing. The flame-kernel technique should be an extremely valuable tool for the study of flow-combustion interaction provided adequate quantitative methods can be worked out to define the extent of combustion.

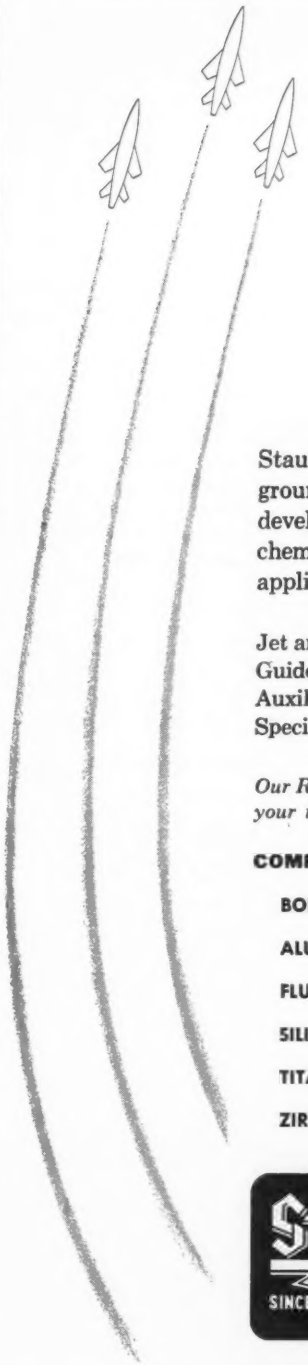
Stabilized flames in turbulent streams present perhaps the most difficult case for analysis. If the flow is confined within ducts, the local flow conditions up to the flame front do not remain constant and the burning behavior is expected to vary all along the reaction zone. To understand such systems, a variety of tools need be used. The helium diffusion method (Westenberg) permits an insight into the diffusion rates before and after combustion. It is handicapped at present by the unavailability of reliable high-temperature molecular diffusion data for the tracer gases. However, the principal conclusion that the absolute turbulance intensity does not differ markedly in front of and behind the reaction zone appears to be established.

The nature of the reaction zone of stabilized flames at Reynolds numbers well above the laminar-turbulent transition region gives rise to interesting arguments. Unfortunately, time-average dependent sampling methods are inadequate to rule out various proposals. Results from optical (Berlad), photographic (Grumer), spectroscopic (Summerfield), sampling (Wohl), and conductivity (Karlovitz) methods do not agree among each other. Consequently, the matter of the structure of these turbulent flames cannot be considered settled at present and further work is required to harmonize the differences of opinion. It would appear desirable to apply the experience of cold-flow turbulent jet mixing to the flame case (Pai, Chu).

(In addition to the authors of communications, the following people contributed to the discussion: R. E. Gibson, W. H. Avery, W. Forstall, Jr., A. Scurlock, S. Corrsin, R. John, R. E. Walker, G. C. Williams.)

Are you interested in...

High energy Propellants?
Metallo-organic Polymers?
Plastic Fabrications?



Stauffer is now "off the ground" in the research and development of new chemicals and materials for application to...

Jet and Ram-jet Engines
Guided Missiles
Auxiliary Power Generators
Special Components

Our Research Staff invites your inquiries concerning...

COMPOUNDS OF

BORON
ALUMINUM
FLUORINE
SILICON
TITANIUM
ZIRCONIUM

Stauffer CHEMICALS SINCE 1885

STAUFFER CHEMICAL COMPANY
Commercial Development Department
380 Madison Avenue, New York 17, N. Y.

erse, fairly good agreement was obtained. (Cf. Fig. 19.)

A large body of data exists in the literature which shows that the rate of CO oxidation is strongly influenced by water vapor. We have recently studied this effect in these flames by adding up to 13 per cent water vapor to a propane-O_2-N_2 mixture, in such a way as not to affect the flame temperature or the fuel-oxygen ratio. The results (Fig. 20) show that the rate of CO oxidation in the second stage of a hydrocarbon flame is independent of water vapor concentration, over a wide range. (Of course, the range of very low water vapor concentrations could not be studied, as water vapor is a product of combustion.)

Further experiments are now being made in carbon monoxide flat flames, in an effort to clarify this water vapor effect.

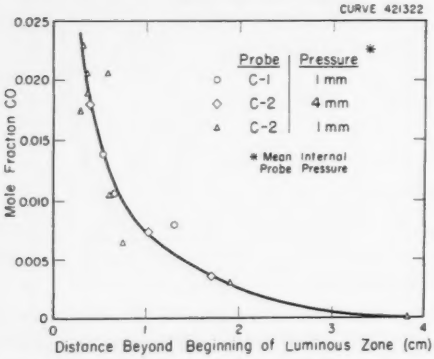


Fig. 18 Linear plot of [CO] vs. x. (Mass air-propane ratio = 30; pressure = 46 mm Hg)

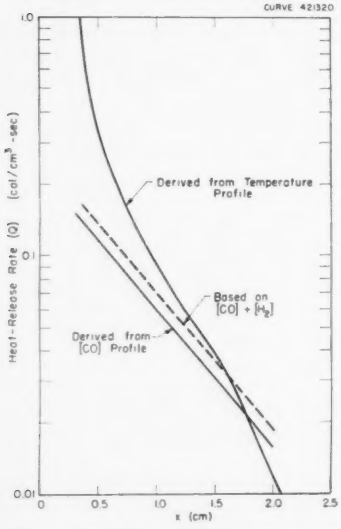


Fig. 19 Heat release rate beyond luminous part of flame as calculated from two kinds of data

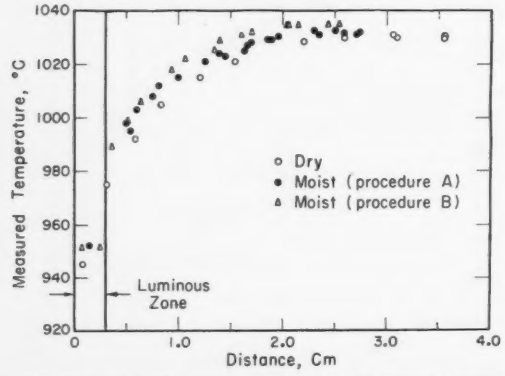


Fig. 20 Thermocouple traverses through flat flame (expanded scale)

The Applicability of One-Dimensional Models to Three-Dimensional Laminar Bunsen Flame Fronts[1]

ROBERT M. FRISTROM

ABSTRACT

THE applicability of one-dimensional models in flame theories has been investigated experimentally in the case of a lean quarter-atmosphere propane air flame. Studies of flow patterns through the flame fronts were made using particle track techniques. From this time-position information, normal gas velocity, stream tube area, and gas density were calculated normal to the flame front. If the density is a single-valued measure of the state of the gas, then one-dimensional models are applicable to Bunsen flames. Unidimensionality was verified for this and several other propane-air flames under a number of conditions. In the reaction region preceding the luminous zone it was also found that the velocity and density profiles were invariant with respect to changes in flame geometry, gas flow, and burner diameter. Therefore, it is a good approximation to speak of single reaction path for this flame, which is a function only of the initial state of the gas.

The measurements indicate that one-dimensional flame theories should be modified to include the effects of area expansion during the course of the reaction. Continuity, diffusion, and heat conduction equations should also be generalized to include the effect of expansion. It was noted that the hydrocarbon flame reaction consists of two regions: a fast propagating reaction associated with the luminus regions and the major portion of the heat release, and a slow secondary reaction associated with the postluminous mantel of the flame. Flow in the primary region is a function only of the initial state of gas and independent of external influences such as gas velocity and flame geometry. Flow in the secondary region could be varied over wide limits with no measurable effect on the propagation of the flame.

Burning velocity was found to be independent of gas velocity, flame geometry, and radius of curvature of flame front, and a function only of the initial state of the gas, providing it was defined as the minimum normal gas velocity ahead of the flame front. A discussion is given of the errors introduced by measuring burning velocity by flow measurements in the throat of the burner.

[1] From the *Journal of Chemical Physics*, vol. 24, no. 4, April 1956, pp. 888–894.

Summary

W. G. BERL

The principal points of interest in "turbulent combustion" are (a) establishment of suitable models for understanding the physical principles, (b) development and evaluation of experimental tools for measuring the significant variables, and (c) accumulating a body of design information that can be applied to engineering problems.

The structure, chemical changes, and flow interaction in laminar flames are at last yielding to experimental analysis. Chemical sampling for stable species in and beyond the reaction zone is now feasible (Fristrom, Friedman) and gives evidence for the step-wise decomposition of hydrocarbons and the surprisingly slow conversion rates of CO. Valuable in-

formation about oxidative reaction mechanisms should be forthcoming which, together with isotopic exchange studies, will assist in unraveling the pathway of the reaction.

The essential similarity of various three-dimensional laminar flame shapes (conical, V, button) has been described by Fristrom, who has measured their velocity and density profiles and has discovered identical time-temperature histories in the main reaction zone. Flame shapes can only be understood by considering the flow field and reaction zone together. The analysis sheds valuable light on some of the problems of how to define flame speed unambiguously.

The status of nonlaminar flames is in a much less satisfying shape in view of the much more numerous and complicated flow possibilities (Pai). A variety of flow-flame interactions are possible (Markstein). The readily analyzable case, where mixing becomes of secondary importance compared to the rate of the chemical reaction, does not appear to apply to stabilized flames in the absence of highly efficient mixing devices (Weiss, Berl, et al.) although it appears to explain the performance trends of the strongly stirred reactor of Longwell and Weiss.

It is generally conceded that the measurement of "turbulent" flame speed by adapting the laminar conventions is unsatisfactory. It averages over the entire length of the flame, even though local rates may be widely different (Berl). A more satisfactory way, laborious and not entirely free from sampling errors, is to determine the point by point state of the gases and deduce therefrom heat release rates (Zelinski et al.). Correlation of flame length and shapes in confined ducts can be obtained in this way and utilized in engine designs.

Although turbulence created by grids and allowed to decay for several mesh lengths produces interesting effects on the details of the flame surface (cell formation) the work of Olsen et al. and of Bolz et al. show that no substantial changes in heat release rates can be achieved in that way. On the other hand, eddies shedding from obstructions may give rise to markedly increased rates. However, an optimum rate of diffusion exists since flame extinction has also been observed through overmixing. The flame-kernel technique should be an extremely valuable tool for the study of flow-combustion interaction provided adequate quantitative methods can be worked out to define the extent of combustion.

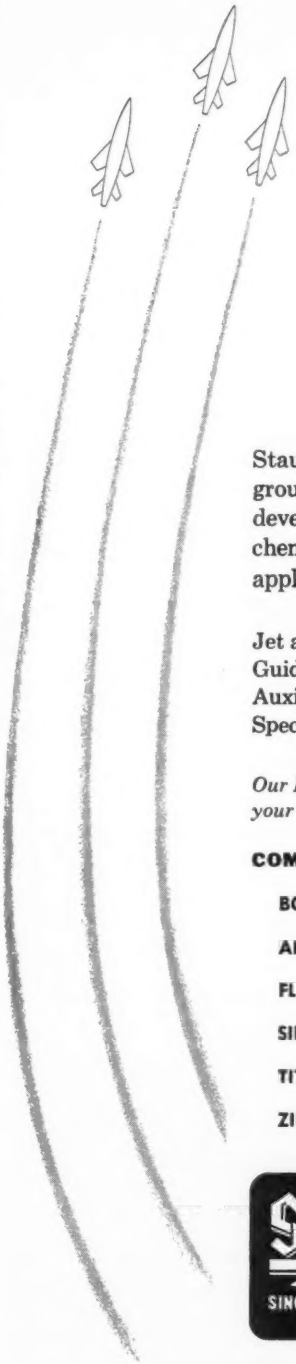
Stabilized flames in turbulent streams present perhaps the most difficult case for analysis. If the flow is confined within ducts, the local flow conditions up to the flame front do not remain constant and the burning behavior is expected to vary all along the reaction zone. To understand such systems, a variety of tools need be used. The helium diffusion method (Westenberg) permits an insight into the diffusion rates before and after combustion. It is handicapped at present by the unavailability of reliable high-temperature molecular diffusion data for the tracer gases. However, the principal conclusion that the absolute turbulance intensity does not differ markedly in front of and behind the reaction zone appears to be established.

The nature of the reaction zone of stabilized flames at Reynolds numbers well above the laminar-turbulent transition region gives rise to interesting arguments. Unfortunately, time-average dependent sampling methods are inadequate to rule out various proposals. Results from optical (Berlad), photographic (Grumer), spectroscopic (Summerfield), sampling (Wohl), and conductivity (Karlovitz) methods do not agree among each other. Consequently, the matter of the structure of these turbulent flames cannot be considered settled at present and further work is required to harmonize the differences of opinion. It would appear desirable to apply the experience of cold-flow turbulent jet mixing to the flame case (Pai, Chu).

(In addition to the authors of communications, the following people contributed to the discussion: R. E. Gibson, W. H. Avery, W. Forstall, Jr., A. Scurlock, S. Corrsin, R. John, R. E. Walker, G. C. Williams.)

Are you interested in . . .

High energy Propellants?
Metallo-organic Polymers?
Plastic Fabrications?



Stauffer is now "off the ground" in the research and development of new chemicals and materials for application to . . .

Jet and Ram-jet Engines
Guided Missiles
Auxiliary Power Generators
Special Components

Our Research Staff invites your inquiries concerning . . .

COMPOUNDS OF

BORON

ALUMINUM

FLUORINE

SILICON

TITANIUM

ZIRCONIUM

Stauffer CHEMICALS SINCE 1885

STAUFFER CHEMICAL COMPANY
Commercial Development Department
380 Madison Avenue, New York 17, N. Y.

Technical Notes

Instrumenting Unmanned Satellites

H. E. LAGOW[1]

Naval Research Laboratory, Washington, D. C.

The purpose of this paper is to discuss some of the problems encountered in instrumenting a satellite. Problems to consider are: orbit, lifetime, orientation, shape, payload, accelerations, temperature, pressurization, residual pressure, forces on satellite, environmental hazards, and data transmission. Many of the problems will depend on the capabilities of the vehicular system used in producing the satellite, but there are a number of considerations that are basic to the technique and will be of general interest for instrumenting satellites. Some of the problems can be discussed and bounded from theory and sounding rocket instrumentation experiences. Others will have to be determined from actual measurements on satellites.

The Orbit

THE plane of the orbit can be predicted in advance of the launching, but eccentricity will critically depend on the burnout velocity of the final stage of powered flight. Here velocity implies both speed and direction. The experimenter should probably be prepared for an elliptical orbit with the satellite's altitude above earth varying from 300 km at perigee to more than 1000 km at apogee. The satellite's altitude and position will have to be measured for most experiments and these measurements will be of prime importance in operating ground stations to receive the telemetering signals.

Lifetime

The satellite's lifetime will depend on the air density at its closest approach to the Earth. Since the air density at these altitudes is known only as to order of magnitude, the lifetime will have to be determined from observations.

Shape and Orientation

The shape of the satellite should be approximately spherical so that drag forces will be independent of the satellite's orientation. Its orientation in space will have to be measured for most experiments since the equipment necessary for measuring the orientation will be lighter and more reliable than equipment for its control. Experiments should be designed so that measurements can be made on a rolling satellite with an arbitrary direction for the spin axis.

Payload

The satellite's limited payload will always be a prime consideration for the instrumenter. It will exclude many experiments and will limit the lifetime of all experiments in the vehicle until a means of recharging batteries is developed. All instrumentation should be transistorized to conserve power and weight. However, the temperature sensitivity of transistors will have to be very carefully considered before they are used.

Accelerations

All instrumentation will have to be designed to withstand high linear and angular accelerations of the order of 100 g's and also be capable of working in the absence of the earth's gravitation field. Rocket experiences would indicate that these problems can be satisfactorily met.

Presented at the ARS 25th Anniversary Annual Meeting, Chicago, Ill., Nov. 14–18, 1955.

[1] Physicist Rocket Sonde Branch. Mem. ARS.

A Satellite's Temperature

A satellite's temperature will be determined almost completely by radiations absorbed and reradiated because heat transfer at the low-air densities, even at the high velocities, will be negligible and because internal power dissipation will have to be negligible due to the payload restrictions. Radiant energy sources are direct sunlight, reflected sunlight and infrared radiations from the earth. By selecting a material with the proper emissivities in the infrared and the visible, it is possible, in theory, to adjust the temperature of the satellite. The nighttime equilibrium temperature would be about −35 C, independent of the emissivity of the satellite. This results from the fact it would be losing energy from twice the area (assume spherical shape) it was receiving energy. The daytime equilibrium temperature will depend rather sharply on the ratio of the emissivity in the infrared to that in the visible. If this ratio is 2, the equilibrium temperature would be 30 C, while if it is 1, the temperature would be 70 C. For most polished metals this ratio is around $^1/_2$ and the equilibrium daytime temperature would be 115 C. However, the heat capacity of the body will prevent the satellite from reaching these extremes. If one assumes that the heat capacity is great enough to make the change from darkness to daylight negligible, the average temperature can be readily computed. An emissivity ratio of 2 gives an average temperature of 10 C. A point that should be considered in connection with the temperature is the possibility that the surface emissivities will change due to the bombardment of ions, molecules, atoms, and micrometeorites. Neither theory nor empirical results are available for estimating this effect; therefore, temperature measurements should be made on the first instrumented satellite.

Pressurization and Residual Pressure Around the Satellite

Some components such as batteries will certainly have to be pressurized if they are to last for weeks or months. Some experiments will require that the residual pressure around the satellite be low compared to the ambient pressure of 10^{-8} to 10^{-11} mm Hg. For these experiments careful consideration of diffusion of gas through the pressurized chambers and vapor pressures of exposed surfaces will be required. Also the effects of meteors piercing the surfaces will have to be measured. It should be pointed out that the satellite offers a considerable advantage over the sounding rocket in regard to residual pressure since gases absorbed in and adsorbed on the surfaces will have time to clean up.

Forces on a Satellite

There are several forces on a satellite which will alter its orbit and eventually destroy it. There will be a retarding force due to collisions with air molecules and perhaps dust particles. The calculation of the drag forces requires density estimates and two assumptions concerning the collision process. Are the molecules specularly or diffusely reflected, and do they leave the surface with a velocity corresponding to the temperature of the surface or more nearly the speed that they struck the surface? Sanger (1)[2] has shown that the drag coefficient for a plate at normal incidence varies by a factor of two under the various assumptions for velocities greater than 6 km/sec. Holt Ashley (2)[1] has shown that the drag coefficient for a sphere is 2 to 2.4. However, for the case of an ogive capped cylinder, $2\theta = 20$ deg, $1/d = 6/1$, he gets a drag coefficient, based on cross-sectional area, of 3.8 for diffuse reflection, and 0.065 for specular reflection. Thus there is a two order of magnitude difference depending

[2] See References at end of paper.

on the reflection process. The drag force at 300 km would be 5×10^{-3} dynes/cm² assuming $\rho = 10^{-8}$ g m/m³ and $V = 7$ km/sec. This force is about 100 times the radiation pressure from direct sunlight (4.6×10^{-5}). At higher altitudes the air drag forces will be less than radiation pressure forces. It is interesting to compute the approximate time loss during one orbit. It is necessary to assign a mass to cross-sectional area ratio for this calculation. Assuming this to be 2 gm/cm², then the satellite will be about 40 millisec late in completing an orbit. There are at least two other forces which will need to be considered in evaluating air density from observed orbit measurements: (a) escaping gas from the vehicle, and (b) energy losses due to eddy currents induced by motion in the earth's magnetic field.

Environmental Hazards

There are a number of hazards to instrumentation in a satellite that are difficult to evaluate. For example, the bombardment of the surfaces with ions, molecules, atoms, and meteors may cause evaporization and sputtering of exposed surfaces that will alter transmission characteristics of windows or even open them. Radiations present other hazards; ultraviolet radiation destroys organic substances in paints and plastics, and cosmic rays might destroy sensitive junctions in transistors.

Data Transmission

The experimenter must radio his measurements to a ground station because the problem of recovery of a record from a satellite is for the distant future. The time during which data can be received at a given station is limited to, at most, a few minutes during each transit. Since this is a small fraction of the orbiting time, the experimenter should consider turning his equipment on for only brief periods when he is within radio range of the ground station.

The above comments represent only a preliminary survey of the problems to be encountered in instrumenting an unmanned satellite.

References

1 Sanger, E., "The Gas Kinetics of Very High Flight Speeds," NACA T.M. 1270.

2 Ashley, H., "Applications of the Theory of Free Molecule Flow to Aeronautics," *Journal of the Aeronautical Sciences*, Feb. 1949.

Methods of Calculating the Equilibrium Laminar Heat Transfer Rate at Hypersonic Flight Speeds[1]

RONALD F. PROBSTEIN[2]

Division of Engineering, Brown University
Providence, R. I.

IN THE April issue of JET PROPULSION, Lees (1)[3] considered the problem of calculating the laminar surface heat transfer rate over blunt-nosed bodies at hypersonic flight speeds for the limiting cases of thermodynamic equilibrium and frozen equilibrium. The purpose of this note is to further clarify how, in the case of thermodynamic equilibrium, where the dissociation and recombination rates are assumed very fast in comparison with the diffusion and convection rates, the conventional laminar heat transfer rate would be altered as a result of the variability of the gas properties due to the large temperature differences existing across the boundary layer. In addition, a simple approximate scheme is presented for computing these heat transfer rates from known constant property solutions, and a sample numerical calculation is carried out to compare with the results of (1) and exact solutions.

Received April 12, 1956.

[1] This work has been supported by the Aeronautical Research Laboratory, Wright Air Development Center, USAF, under Contract AF 33(616)-2798. The author wishes to thank Dr. Frederick R. Riddell of the Research Laboratories, AVCO Manufacturing Corporation, and Professor James A. Fay of the Massachusetts Institute of Technology for their helpful and interesting discussions.

[2] Associate Professor of Engineering.

[3] Numbers in parentheses indicate References at end of paper.

The axially symmetric boundary layer momentum and energy equations for thermodynamic equilibrium can be reduced to a "nearly incompressible" form by utilizing a similarity transformation first introduced by Levy (2), but modified so that the physical properties are evaluated at the surface temperature. One lets

$$s = \int_0^x \rho_w \mu_w u_e r^2 dx \qquad \eta = \frac{\rho_e u_e}{(2s)^{1/2}} \int_0^y r \frac{\rho}{\rho_e} dy \quad \ldots\ldots [1]$$

where ρ is the density, μ the viscosity, and the other symbols are as shown in Fig. 1.[4] Now this transformation is exactly

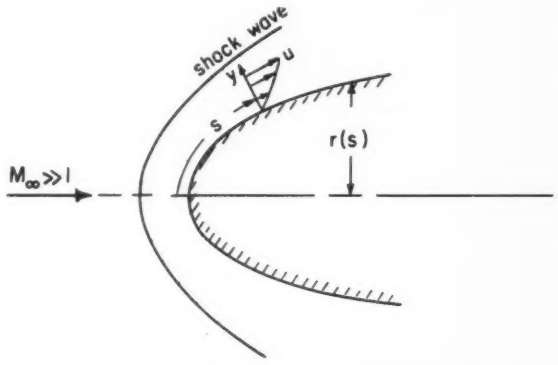


Fig. 1 Coordinate system for body of revolution

the one employed by Lees except that in the definition of η, $\rho_w \mu_w$ is replaced by $\rho_e \mu_e$. Here, w refers to wall conditions, while e denotes quantities evaluated at the edge of the layer. To simplify the discussion the Prandtl number is taken constant and equal to unity, although this is not necessary to the main argument. Actually, Cohen and Reshotko (3) have shown how to correct the surface heat transfer rate calculated for $Pr = 1$, for any Prandtl number different from unity.

The momentum and energy equations and boundary conditions become identical in form with those given by Lees, on utilizing Equation [1], letting the total enthalpy ratio $h_s/h_{se} = g(\eta)$, $\psi(s,\eta) = (2s)^{1/2} f(\eta)$, and $u/u_e = f'(\eta)$, namely

$$(Cf'')' + ff'' = \beta[f'^2 - (\rho_e/\rho)] \quad \ldots\ldots [2]$$

$$(Cg')' + fg' = 0 \quad \ldots\ldots [3]$$

One difference is that here $C(\eta) = \rho\mu/\rho_w\mu_w$, and not $\rho\mu/\rho_e\mu_e$ as in (1). Strictly speaking, of course, in neither case is C a function of η alone since $\rho\mu$ at the wall and layer edge depends on s. However, as noted by Lees, the approximation of similarity is good in the neighborhood of a stagnation point, as well as for the case of slowly varying external flow properties or a highly cooled surface. When the fluid properties and specific heats are assumed constant across the boundary layer, so that $C = 1$ and $\rho_e/\rho = T/T_e$, then Equations [2] and [3] reduce to those of Cohen and Reshotko (4). For this case

$$\frac{\rho_e}{\rho} = \left[1 + \frac{\gamma-1}{2} M_e^2\right] g - \frac{\gamma-1}{2} M_e^2 f'^2 \quad \ldots\ldots [4]$$

[4] Except where specifically noted the symbols used are the same as in (1).

In general, for practical wall temperatures the surface will be below the temperature required to dissociate the gas, so that the heat will be transferred by conduction alone. For such a condition the heat flux at the wall is given by

$$\dot{q}_w = k_w \left(\frac{\partial T}{\partial y}\right)_w = \frac{k_w h_{te}}{c_{pw}} \left(\frac{\partial \eta}{\partial y}\right)_w g_w' \quad \ldots\ldots [5]$$

Therefore, the surface heat transfer rate is directly proportional to g_w'. One particular case of interest is the stagnation point flow where $(\partial\eta/\partial y)_w = [(2/\nu_w)(du_e/ds)]^{1/2}$. Here we may define a Nusselt-Reynolds number combination such that

$$\left(\frac{Nu}{\sqrt{Re}}\right)_{S.P.} = \frac{\dot{q}_w Pr}{(h_{te} - h_w)} \left(\rho_w \mu_w \frac{du_e}{ds}\right)^{-1/2} = \frac{\sqrt{2}\, g_w'}{1 - g_w} \quad \ldots\ldots [6]$$

Thus for a highly cooled wall ($g_w << 1$), the heat transfer parameter is just $\sqrt{2}\, g_w'$. Now, if the parameters C and f were to be regarded as known functions of η, then Equation [3] is linear in Cg' and it is clear that the solution for g_w' is given by

$$g_w' = \frac{1 - g_w}{\int_0^\infty \frac{e}{C}\, e^{-\int_0^\eta (f/C)\, d\eta}\, d\eta} \quad \ldots\ldots [7]$$

One of the principal problems in calculating g_w' arises in the determination of f, which cannot be found independently because of the coupling of the momentum and energy equations due in part to the nonideal nature of the gas being considered. This nonideality enters in two ways: first, in the density enthalpy relation which is part of the pressure gradient term, and second, in the parameter C which modifies the shear term.

Lees has shown when $g_w << 1$ for the case of $C = 1$, the pressure gradient term has little effect on the heat transfer rate, and the value of g_w' does not differ much from the conventional flat plate value. Clearly then we could take $\rho_e/\rho \approx T/T_e$, and the error which would be introduced in the heat transfer rate would be even smaller than that made by dropping the whole term, as has been done in (1).

The second point to be considered concerns the effect of the variation of $\rho\mu$ on the integrated velocity profile. In this regard, it can be seen from Equation [7] that the heat transfer rate is altered by the changed velocity profile, due to the variable $\rho\mu$, only to the extent of the change of the integral of the velocity profile. It is evident, therefore, that the wall heat transfer is not too sensitive to any reasonable variations in the velocity profile. Furthermore, it is to be noted that the function f, unlike C, enters the calculation of g_w' only in the exponential integral term. Since $f \sim (\eta - \text{const}) + O(e^{-\eta^2})$ for large η, and $f \sim \text{const} \cdot \eta^2$ for small η, then it is clear from Equation [7] that for C of order unity the changes in f, due to the realistic gas properties, contribute little to the integral except near the wall. But near the wall two things are true in our definition: first, C is close to one so that the value of f is approximately that given by Cohen and Reshotko (4), and second, for the reason we have already given, any small change in f' close to the wall due to the change in C could not appreciably alter the value of f in the region of the surface. Therefore, one can conclude that the use of the Cohen and Reshotko f in the calculation of g_w' is justified.

Under the preceding approximations the energy and momentum equations are independent, so that the heat transfer can be calculated from Equation [7] once $C(\eta)$ is known. The function C is determined by the static enthalpy, which is in turn given by Equation [4]. In general, therefore, Equation [7] is an integral equation which can be solved only by approximate methods. To simplify the presentation somewhat, a stagnation point example will be chosen in order to make C a function of g alone. However, this is not a necessary condition, although it is probably a good approximation for the cases of interest mentioned previously.

The method utilized in solving the nonlinear integral equation for g_w' is an iteration scheme in which the known value of g for $C = 1 (g^{(0)})$ is utilized to calculate $C(\eta)$ in first approximation ($C^{(1)}$). This then gives a new value for g_w' and the function[5] g ($g_w'^{(1)}$ and $g^{(1)}$) from which a second approximation to $C(C^{(2)})$ could be determined, and with it $g_w'^{(2)}$, etc. This process can be repeated as many times as is necessary until the desired accuracy is obtained.

To complete the solution it is necessary to establish the law of variation for $\rho\mu$. J. A. Fay and F. R. Riddell have suggested the following analytical expression which is found to match the equilibrium data extremely well.

$$C = \frac{a}{\sqrt{\frac{h}{h_{te}}}} + \frac{b}{\frac{h}{h_{te}}} \quad \ldots\ldots [8]$$

Here, the constants a and b are fixed so that C has the correct value and slope at the wall. Fig. 2 is a plot of Equation [8][6] for a flight velocity of about 19,700 ft/sec and a wall temperature of 1000 R. For these conditions[7] $g_w = 0.032$, while $a = 0.238$ and $b = 0.011$.

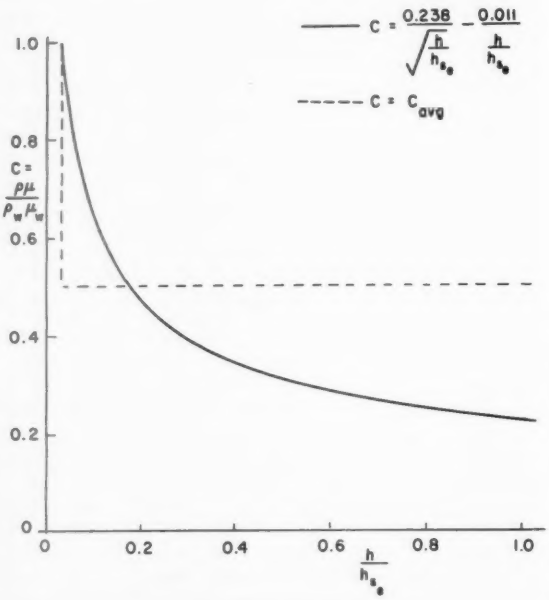


Fig. 2 $C = \frac{\rho\mu}{\rho_w \mu_w}$ as a function of the enthalpy ratio h/h_{te} for a flight speed of 19,700 ft/sec and a surface temperature of 1000 R

Before illustrating the results and method of solution let us determine the value of g_w' in comparison with the value computed by Cohen and Reshotko (4) for $C = 1$. To do this let

$$C = 1 \text{ for } g = g_w$$

$$C = C_{avg} = \text{const} < 1 \text{ for all } g > g_w \quad \ldots\ldots [9]$$

The approximate relation represented by this average function is shown by the dotted curve in Fig. 2. In this case the energy equation can be reduced to the form given by Cehon

[5] $g = g_w' \int_0^\eta \frac{e}{C}\, e^{-\int_0^\eta (f/C)\, d\eta}\, d\eta + g_w.$

[6] Equation [8] is insensitive to altitude, at least in the isothermal region of the stratosphere.

[7] At these velocities h_{te} is approximately dependent only on the flight speed.

Table 1 Equilibrium stagnation point flow

$u_\infty = 19{,}700$ ft/sec, $T_w = 1000$ R
$h_{s_e} = 7050$ Btu/lb, $g_w = 0.032$

"Approximate" solutions

Local heat transfer parameter	Present paper: 1st iteration $Pr = 1$	Present paper: 2nd iteration $Pr = 1$	Present paper: 2nd iteration "corrected" to $Pr = 0.7$	Lees (1) $Pr = 0.7$
g_w'	0.287	0.285	0.247	0.199
$Nu/\sqrt{Re}$	0.420	0.417	0.361	0.282

"Exact" solutions

Local heat transfer parameter	Cohen and Reshotko, ideal gas $\rho\mu = \rho_w\mu_w$: $Pr = 1$ (4)	Cohen and Reshotko, ideal gas $\rho\mu = \rho_w\mu_w$: $Pr = 0.7$ (5)	Mark (6) imperfect gas variable thermal properties: $Pr_{avg} \approx 0.8$	Mark (6) imperfect gas variable thermal properties: "corrected to" $Pr_{avg} = 0.7$
g_w'	0.480	0.417	0.239	0.227
$Nu/\sqrt{Re}$	0.702	0.611	0.349	0.332

and Reshotko by letting $\bar{\eta} = \eta/C$, from which it follows by a direct examination of the differential equation and its solution that

$$(g_w')_{C<1} = C_{avg}(g_w')_{C=1} \quad \ldots\ldots\ldots\ldots\ldots [10]$$

Therefore, the more realistic laminar heat transfer rate must be lower than that calculated by Cohen and Reshotko. Effectively what Lees has done in his paper is to choose this average value of C to be given by $(\rho_e\mu_e/\rho_w\mu_w)^{1/2}$.

By way of pointing out the difference that might be expected, consider the stagnation point boundary layer at a flight velocity of 19,700 ft/sec. For this case $h_s \equiv h$, $C = C(g)$ exactly, and $\beta = 1/2$. Utilizing the $g_w = 0$,[5] $\beta = 1/2$ solution of Cohen and Reshotko (4), the local heat transfer parameters have been calculated by the method outlined. The results which were obtained are presented in Table 1, and it can be seen that the convergence characteristics are excellent with the first iteration giving a value sufficiently accurate for most purposes. Following the technique of (3), the value of g_w' has been corrected for a Prandtl number different from unity in the case of a stagnation point pressure gradient by multiplying the result by $(Pr)^{0.4}$. In the same table are presented the exact calculations of Cohen and Reshotko (4, 5). The most significant conclusion to be drawn from a comparison of these results is that the heat transfer rate for realistic fluid properties is significantly lower than that calculated using the approximation $\rho\mu = \rho_w\mu_w$. This difference will, of course, decrease with decreasing flight speed. Also shown in Table 1, for comparison with the present results, are some exact stagnation point calculations for an imperfect gas with variable thermal properties, carried out by Mark (6) with the aid of a digital computer. In this case the "average" Prandtl number through the layer was about 0.8, so that for comparison purposes this value has also been "corrected" to a $Pr = 0.7$ by means of the previously cited rule. For the flight speed and wall temperature considered, the present approximate calculation is seen to overestimate the heat transfer by about 8.7 per cent when compared with Mark's calculation. Also presented in Table 1 are Lees' approximate results which in terms of the definitions in the present paper would be given, respectively, by $g_w' = C_e^{1/2}(0.47)\,Pr^{1/3}$ and $Nu/\sqrt{Re} = \sqrt{2}\,g_w'$. These results are seen to underestimate the heat transfer by about 15 per cent at most, which is certainly satisfactory for engineering computations.

[5] The distribution profiles are very insensitive to small changes in g_w.

It may be concluded then, that for hypersonic flight conditions the heat transfer rate for a realistic variation of $\rho\mu$ is significantly lower than that calculated using the wall values of $\rho\mu$. And, a very accurate and simple iterative scheme which utilizes the known solutions for constant fluid properties has been presented for calculating this heat transfer.

References

1 Lees, L., "Laminar Heat Transfer over Blunt-Nosed Bodies at Hypersonic Flight Speeds," JET PROPULSION, vol. 26, April 1956, pp. 259–269.

2 Levy, S., "Effect of Large Temperature Changes (Including Viscous Heating) upon Laminar Boundary Layers with Variable Free-Stream Velocity," *Journal of the Aeronautical Sciences*, vol. 21, July 1954, pp. 459–474.

3 Cohen, C. B., and Reshotko, E., "The Compressible Laminar Boundary Layer with Heat Transfer and Arbitrary Pressure Gradient," NACA T.N. 3326, April 1955.

4 Cohen, C. B., and Reshotko, E., "Similar Solutions for the Compressible Laminar Boundary Layer with Heat Transfer and Pressure Gradient," NACA T.N. 3325, Feb. 1955.

5 Reshotko, E., and Cohen, C. B., "Heat Transfer at the Forward Stagnation Point of Blunt Bodies," NACA T.N. 3513, July 1955.

6 Mark, R., "Compressible Laminar Heat Transfer near the Stagnation Point of Blunt Bodies of Revolution," Convair Report no. ZA-7-016, April 11, 1955, San Diego, Calif.

Flame Generated Turbulence

W. PAUL JENSEN[1]

Fuels Research Laboratory, Massachusetts Institute of Technology, Cambridge, Mass.

THE note by Robert A. Gross on Flame Generated Turbulence (1)[2] is interesting especially for its description of using a hot-wire probe directly in a flame. Considering separately the zones occupied by reactants, reacting species, and products, Gross' experimental evidence showed the reaction zone "too complicated to permit any interpretation or conclusion based on these measurements only" and in the product zone some "temperature spottiness." Regarding the reactant zone, he could say more definitely, "...there is no significant increase in the turbulent intensity."

Because the note started with reference to the fact that the possibility of flame generated turbulence was first discussed by Williams, Hottel, and Scurlock (2), it seems appropriate here to call attention to differences in the experiments made by Gross and Scurlock.

Gross' flame (3) was an open one, stabilized on a wire and fed by homogeneously premixed propane and air which flowed through a grid placed over the primary nozzle of a system with a secondary nozzle from which boundary fluid flowed at the rate of the primary gas. Scurlock's flame, similarly fed by premixed, homogeneous gas and air, also flowed through a turbulence-generating grid, but was stabilized on a rod and confined within the walls of a 1 × 3-inch channel, with the tailpipe length variable up to 15 inches. Confinement of the flame produces velocity gradients between burned and unburned gases which can generate turbulence in the flame zone that greatly overshadows grid generated turbulence in the approach stream.

In 1950 John Grover and the writer measured velocity fluctuations with a hot-wire probe in the reactant region $^5/_8$-inch upstream of a 0.057-inch rod stabilizer in a 1 × 3-inch burner duct patterned after Scurlock's. While it is not to be expected that turbulence generated in the flame zone would be transmitted as such upstream to the reactant region, it was evident from the studies made here that shear generated turbulence and the resulting increase in apparent combustion

Received March 3, 1956.

[1] Executive Officer.

[2] Numbers in parentheses indicate References at end of paper.

rate could produce acoustic phenomena which were transmitted upstream. The measured velocity fluctuations were critically dependent on air-fuel ratio and tailpipe length, being smallest near rich blowout and near lean blowout when the tailpipe was short. Peak blowout for this burner-stabilizer combination was at a mean entrance velocity of about 260 fps. With a 10-inch tailpipe downstream of the stabilizer, the velocity fluctuations were ±30 per cent of this mean velocity and their "frequency" roughly 3 to 10 cps. With a 4-inch tailpipe, the fluctuations were reduced to ±5 per cent of the mean velocity and their "frequency" was increased but became so random as to be indefinable as a frequency. With no flame the turbulence intensity was about 1.5 per cent; no measurement of scale was made.

References

1 Gross, R. A., "Flame Generated Turbulence," JET PROPULSION, vol. 25, Dec. 1955, p. 716.

2 Williams, G. C., Hottel, H. C., and Scurlock, A. C., "Flame Stabilization and Propagation in High Velocity Streams," Third Symposium on Combustion Flame and Explosion Phenomena, Baltimore, Williams and Wilkins Co., 1949, p. 21.

3 Gross, R. A., "Boundary Layer Flame Stabilization," JET PROPULSION, vol. 25, June 1955, p. 288.

Hazards Associated With 90 Per Cent Hydrogen Peroxide Aerosols

CHARLES L. PUNTE,[1] LEON Z. SAUNDERS,[1] and EUGENE H. KRACKOW[1]

Chemical Warfare Laboratories, Army Chemical Center, Md.

Studies have been done to determine the toxicological effects produced in mice exposed to 90 per cent hydrogen peroxide (H_2O_2) dispersed as an aerosol. Groups of mice were exposed for 5–15 minutes to airborne concentrations from 4 to 19 mg/l. Significant pulmonary irritation and congestion were found in mice exposed for 5 minutes. Irritating effects to eyes and nose were observed in mice exposed to 10 mg/l of 90 per cent H_2O_2. Survivors of high concentrations (9–19 mg/l) developed corneal damage several weeks after exposure.

SKIN contact with 90 per cent hydrogen peroxide is a significant hazard. Relatively small amounts of liquid in the eye can cause severe corneal damage resulting in visual handicap or permanent blindness (1).[2] Inhalation of saturated 90 per cent H_2O_2 vapors for 8 hours will cause slight pulmonary edema and localized emphysema in rats (2). Under operational conditions involving only vapors, no major respiratory hazard would be offered by a single acute exposure. This conclusion is in general agreement with that cited by other authors (1, 3). This test was undertaken to evaluate the hazard associated with a mist of high concentrations of 90 per cent H_2O_2.

The aerosol was dispersed by passing dry air through three parallel "vaponefrin" glass nebulizers containing 90 per cent H_2O_2. The aerosol thus generated was diluted in a mixing chamber before entering a 20-liter glass exposure chamber.

Two series of H_2O_2 exposures were made, one ranging from 3.6–5.2 mg/l for 5 minutes and the other from 9.4–19.0 mg/l for 5–15 minutes. In each exposure 10 white mice weighing about 20 grams each were used. The disperser was started with the animals in the chamber and sampling of the chamber atmosphere was initiated after the chamber concentration reached equilibrium (4). At the termination of the exposure, the chamber was aerated with fresh air for at least 30 minutes before the animals were removed. The mice were observed during exposure and then daily until sacrificed (2 days to 8 weeks) for pathological studies.

Samples for colorimetric analysis of H_2O_2, (5), were collected by two midget impingers in series, each containing 10 ml of titanium sulfate reagent. Particle size measurements were made before the experiment proper by means of a cascade impactor.

Results of exposing mice for 5 minutes to aerosols of 90 per cent H_2O_2 indicate that concentrations of the order of 3.6 to 5.2 mg/l are sublethal. When the concentration was increased to 9.4 mg/l the lethality range was reached, with death occurring 6 days following exposure. At concentrations ranging from 12 to 19 mg/l for 10 and 15-min exposures, the survival time was reduced in the majority of animals to less than an hour. These results are shown in Table I.

Table 1 Toxicity of 90 per cent hydrogen peroxide aerosol to mice by inhalation

Exposure time, min	Analytical concentration, mg/l	Mortality	Survival time, min
5	3.6	0/10	..
5	4.2	0/10	..
5	5.2	0/10	..
5	5.2	0/10	..
5	9.4	0/10	6 days
10	13.2	5/10	[a]
10	13.4	1/10	6
10	19.0	1/10	11
15	11.8	5/10	5–50
15	16.7	9/10	[b]

[a] 4/10 died between 12 and 120 minutes; a fifth died after 6 days.

[b] 8/10 died between 11 and 48 minutes; a ninth died the next day.

Chamber temperatures varied from 26 to 28 C. The mass-median particle size of the aerosols was approximately 3.5 microns.

The symptoms of the animals during exposure to the low concentrations consisted of a mild nasal irritation, blinking of the eyes, slight gasping, and a loss of muscular coordination. These symptoms generally disappeared within 30 minutes after removal from the aerosol atmosphere. Minor burns were observed on the nose and paws of most animals. The symptoms of the animals during exposure to the higher concentrations were similar to those exhibited at the lower concentrations, except that they were more severe.

Those animals that died as a result of exposure went through a short convulsant period before death. In survivors, the burns of the nose and paws disappeared in less than a week, but the eye inflammation persisted for another week. At the end of the second week the signs of primary irritation had disappeared from the eyes, except for two cases exposed to 19 mg/l for 10 minutes, in which the corneas showed gross opacities, which persisted for the remainder of the observation period (6 weeks).

The mice exposed to the sublethal range of concentrations (3.6 to 5.2 mg/l) showed congestion of the lungs when sacrificed at various intervals over a period of ten days. Four of twenty mice exposed to 5.2 mg/l showed some necrosis of bronchial epithelial cells.

Animals which died during or within about an hour after exposure to 9.4 to 19 mg/l showed pulmonary congestion in most instances. Animals surviving these concentrations for several days or sacrificed after 5 and 8 weeks showed necrosis of bronchial epithelium.

Gross opacities were present in the eyes of four animals exposed to the highest concentration (19 mg/l) and sacrificed after eight weeks. Animals sacrificed five weeks after exposure to this concentration, showed microscopic lesions.

Microscopic lesions were found in the eyes of the animals

Received Feb. 14, 1956.

[1] Aerosol Branch, Directorate of Medical Research.

[2] Numbers in parentheses indicate References at end of paper.

exposed to 9.4 mg/l eight weeks after exposure, while those examined five weeks after exposure to this concentration showed no significant changes.

No cataracts were seen in the mice, and no eye lesions were seen in control mice or in those exposed at the lower levels. These findings indicate that there is an insidious and slowly developing corneal damage subsequent to exposure to high aerosol concentrations of H_2O_2.

References

1 Krackow, E. H., Health Hazards of Military Chemicals, Rep. no. 4, 1950.

2 Comstock, C. C., Hackley, B. B., and Oberst, F. W., *Cml C Med Labs Res Rep.* no. 243, March 1954.

3 Bloom, R., Jr., Davis, N. S., Jr., and Levine, S. D., "Hydrogen Peroxide as a Propellant," *J. of the American Rocket Society*, March 1950.

4 Silver, S. D., "Constant Flow Gassing Chambers," *J. Laboratory and Clinical Medicine*, vol. 31, 1946, p. 1153.

5 Nelson, A., in *Industrial Engineering Chemistry, Anal. Ed.*, vol. 2, 1930, p. 55.

Study of Premixed Flames Using Radioactive Tracers

VADIM KOPYTOFF,[1] CARLOS G. BELL,[2] and ALI BULENT CAMBEL[3]

Northwestern University, Evanston, Ill.

Introduction

DESPITE extensive studies concerning flame stabilizaton phenomena, there are many questions that remain unanswered. For example, the recirculation zone of a flameholder continues to receive considerable attention. Recently, Westenberg, Berl, and Rice (1)[4] used helium to observe the phenomena behind a cone; Zukoski and Marble (2) introduced sodium to determine optically the configuration of the recirculation zone. Again, Marble and Adamson (3) have discussed combustion in a laminar mixing zone analytically while Zukoski and Marble (4) studied related phenomena experimentally. Lately, Schaffer and Cambel (5) have suggested that in opposing jet stabilization a small critical zone is of considerable concern. These and many other studies make it obvious that a simple but thorough exploration of the various regions in an aerothermochemical system is most desirable. This note suggesting the application of radiotracers in the study of flames is submitted for the purpose of stimulating the interchange of speculation on possible techniques with fellow workers.

Among the advantages offered by radiotracers in flame studies the following appear most pertinent: (a) they make possible the introduction and detection of extremely small mole fractions; (b) they allow the homogeneity of the mixture to be maintained; (c) they have little effect chemically on the fuel while allowing the labeling of chosen molecules, both reacting and nonreacting, that enter the flame; (d) they allow specific atoms to be tagged in a way that is entirely unaffected by all physical and chemical reactions suffered both in the flame and during sampling and thus permit more freedom in quantitative studies; (e) they allow handling and measurement techniques that may lessen difficulties in probing and sampling, being based on measurements of physical quantities rather than the more complicated chemical determinations.

Received March 13, 1956.

[1] Teaching Assistant in Mechanical Engineering, Gas Dynamics Laboratory.

[2] Assistant Professor of Civil Engineering, Radionuclear Laboratory.

[3] Associate Professor of Mechanical Engineering, Gas Dynamics Laboratory. Fellow ARS.

[4] Numbers in parentheses indicate References at end of paper.

Basically, the technique consists of injecting a tracer at a desired location in the system, usually before the combustion zone. Samples of the mixture are collected in previously evacuated bottles, and after proper preparation the samples are studied quantitatively, using either a liquid scintillation spectrometer or an internal counter operating in the Geiger-Müller or proportional region.

Properties of Radiohydrogen (H^3) and Radiocarbon (C^{14})

Because hydrocarbon flames are of overwhelming importance, two tracers suggest themselves for their study, namely, radiohydrogen (H^3) and radiocarbon (C^{14}). Radiohydrogen or tritium can be used directly as an additive tracer in the fuel-air mixture. Both tritium and radiocarbon can be used for tagging selected atoms in the hydrocarbon molecule.

Tritium is cheap[5] and, with proper AEC authorization, readily available as a pure gas from the Oak Ridge National Laboratory (6). It is a pure beta-ray emitter (maximum energy 18 kev) with a half-life of 12.5 years that allows storage and convenient handling. On an equal disintegration rate basis, it is one of the least hazardous of all of the radionuclides commonly used. The difficulties previously faced in its counting have been overcome with instruments that are, unfortunately, rather expensive.

Although radiocarbon is much more expensive[6] than tritium, the cost should not be prohibitive if sensitive detection instruments are available. It, too, is a pure beta-ray emitter (maximum energy 155 kev) with a half-life of 5568 years. It is obtainable from Oak Ridge in the form of barium carbonate. Several companies produce radiocarbon-labeled hydrocarbons that are ten or more times as expensive as the

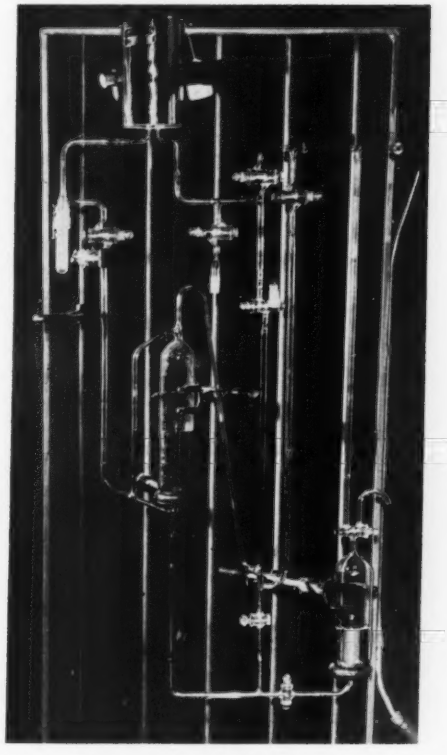


Fig. 1 Vacuum system for handling and oxidizing tritium and hydrogen gases

[5] At this time, $2.00 per curie plus handling charges. A curie is that quantity of radioactive material required to supply 2.2×10^{12} disintegrations per minute. A millicurie is 0.001 of this amount.

[6] About $36.00 per millicurie.

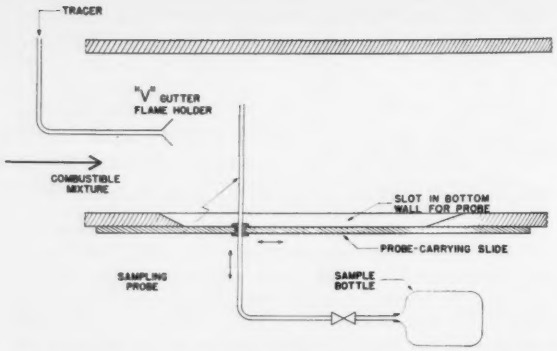


Fig. 2 Schematic of test section, showing tracer admission and sampling probe

carbonate. Radiocarbon is more hazardous than tritium, but also more easily detected.

Experimental Methods

Tracing can be done in two different ways, namely, by direct addition of a tracer and by nuclear tagging of molecules. In the first case, tritium can be diluted to any convenient level with ordinary hydrogen which, being isotopic, is quite similar to tritium. The mixture can then be introduced into the system as desired. Probably most of the tritium collected in the sample will be in the form of radiowater (H^3OH). If it is partially in the form of tritium gas (H_2^3), it can be oxidized rather easily before counting. A preliminary apparatus quite similar to that of Farr and Vier (7) has been built for the purpose of aliquoting and oxidizing pure tritium gas. This apparatus is shown in Fig. 1 and is also suitable for the further oxidation of combustion samples if necessary.

Much more sophisticated experiments are envisaged by the use of tagged fuel. Thus, any specified atom in a hydrocarbon may be replaced by its radioisotope. This will require extreme care in sampling from various regions of the flame, but it could be one of the most important methods of determining the intermediate reactions during combustion. The problem of isotopic chemical effects is appreciated and must be seriously considered when this technique is applied.

The tracer in exceedingly minute quantities is introduced and the samples collected in a two-dimensional combustion chamber shown in Fig. 2. The flameholder is a V-gutter supported by the tracer injector. In the preliminary studies, steady stream insertion of the tracer material is considered. As a second step, discrete injections of tracer can be made in conjunction with time-related sampling. It is believed that this technique will give the residence time, penetration time, mixing rate, and leakage rate in the recirculation zone.

Research in which the fuel molecules (such as propane) are tagged should give valuable information on the concentration-location relationships of various radicals in the flame. These results can then be related on a time scale to give a more detailed picture of the intermediate reactions in the whole process.

The possible sensitivity of radiotracer methods is illustrated by the following preliminary estimates: With a mixture velocity of 80 fps approaching the test section, and 0.1 millicurie of tracer injected over a period of 2 sec (thus providing ample time overlap to take a 0.5-sec sample), the ratio of sample flow to total flow is of the order of 0.002. Yet, even the relatively insensitive scintillation counter will detect a 100-fold variation in tracer content in the sample. If greater sensitivity is found to be necessary, an internal Geiger-Müller counter may be used. This apparatus is screened from cosmic ray noise by anticoincidence tubes and is located within a seven-ton steel shield to further reduce background counts and thus permit extremely low level counting.

As the possibilities of the method seem unlimited, there is little doubt that better qualified workers have initiated similar studies. Their comments are welcomed by the authors.

Acknowledgment

The above investigations are made possible by grants received from the U. S. Atomic Energy Commission and from the Technological Institute of Northwestern University. The study is sponsored jointly by the Gas Dynamics Laboratory of the Mechanical Engineering Department and the Radionuclear Laboratory of the Civil Engineering Dept.

References

1 Westenberg, A. A., Berl, W. G., and Rice, J. L., "Studies of Flow and Mixing in the Recirculation Zone of Baffle-Type Flameholders," NU-ARS-ARDC Gas Dynamics Symposium, Evanston, Ill., August 1955.

2 Zukoski, E., and Marble, F. E., "Experiments Concerning the Mechanism of Flame Blow-Off from Bluff Bodies," NU-ARS-ARDC Gas Dynamics Symposium, Evanston, August 1955.

3 Marble, F. E., and Adamson, T. C., Jr., "Ignition and Combustion in a Laminar Mixing Zone," JET PROPULSION, vol. 24, no. 2, March–April 1954, pp. 85–94.

4 Zukoski, E. E., and Marble, F. E., "The Role of Wake Transition in the Process of Flame Stabilization on Bluff Bodies," *Combustion Researches and Reviews, 1955*, AGARDograph no. 9, Butterworths Scientific Publications, London, 1955, pp. 167–180.

5 Schaffer, A., and Cambel, A. B., "The Effect of an Opposing Jet on Flame Stability," JET PROPULSION, vol. 25, no. 6, June 1955, pp. 284–287.

6 "Radioisotopes, Special Materials and Services," Oak Ridge National Laboratory, Oak Ridge, Tennessee.

7 Farr, J., and Vier, D. T., "The Preparation of a Primary Standard of T Water," Los Alamos Scientific Laboratory, Univ. of Calif., AEC Document LA 1734, August 24, 1955.

*SWAGED MGO FOR OPERATING TEMPERATURES −300 to 2000°F
INSULATED THERMOCOUPLES

SURFACE with STANDARD T/C Head
• Extremely accurate since junction can be welded to surface.

DESIGNING

IMMERSION with LEAD WIRE ADAPTOR
• Fast time response.
• Install in any pipeline without a thermo-well by simply drilling and tapping.
• Pressure and vacuum tight.
• Variable immersion depth—easily replaced.

LEAD WIRE with QUICK DISCONNECT
• Available in long lengths or spliced together to meet your length requirements.

FABRICATING

*SWAGED MgO wire is available from our stock—Diam. .025 to 5/16". Send for Bulletin 4.

Aero Research INSTRUMENT COMPANY, INC.
315 NO. ABERDEEN STREET • CHICAGO 7, ILLINOIS
Sales Representatives throughout the United States and Canada

Notable Achievements at JPL

FIRST TO FLY FM-FM TELEMETERING... From JPL's 3-band FM-FM telemetering System flown in 1944, to its present extremely versatile, compact, transistorized 18-band system, telemetering has been an important factor in the successful development of JPL guided missiles.

Significant firsts in this field are:

In 1948, a 10-band FM-FM System with 15 measurements.

In 1953, an 18-band FM-FM System with 36 measurements.

In 1954, a 14-band FM-FM System with all audio circuits transistorized.



Pioneers in Telemetering Development

JPL JOB OPPORTUNITIES ARE WAITING FOR YOU TODAY!

in these fields

ELECTRONICS
ELECTRONIC RESEARCH
SYSTEMS ANALYSIS
ELECTRO-MECHANICAL
INSTRUMENTATION
INERTIAL GUIDANCE
TELEMETERING
PHYSICS
PACKAGING
MECHANICAL ENGINEERING
AERONAUTICAL ENGINEERING

The success of the Corporal and other JPL guided missile programs is dependent on constantly improved instrumentation techniques. Development, a major portion of the Telemetering Group activity, is directed toward improving system flexibility, accuracy and reliability. This activity is tailored to both immediate and long range instrumentation requirements of the many Laboratory missile programs.

The use of transistors and modern magnetic elements, together with progressive packaging techniques developed from intensive JPL studies, result in greatly improved reliability in missile-borne and ground-recording equipment. In addition, advanced communication studies are being utilized in the design of advanced telemetering equipment to the constant improvement of this art. An example of applied theory, is the use of tracking filter techniques in the communication link—resulting in a significant improvement in telemetering data accuracy.

The size and character of the "Lab" fosters a personal contact and close relationship between data-user and telemetering engineer. This close telemetering support is a basic reason for the development of better ways of measuring drag for the aerodynamicist, motor pressures for the propulsion expert, stresses for the missile designer and of monitoring complex electronic circuits which are the responsibility of the guidance specialist. This close cooperation has become a prime factor in the growth of the laboratory into one of the most successful guided missile development centers in the world.

You are invited to join this progressive group of scientists and engineers. Write us today.

CALTECH jpl JET PROPULSION LABORATORY

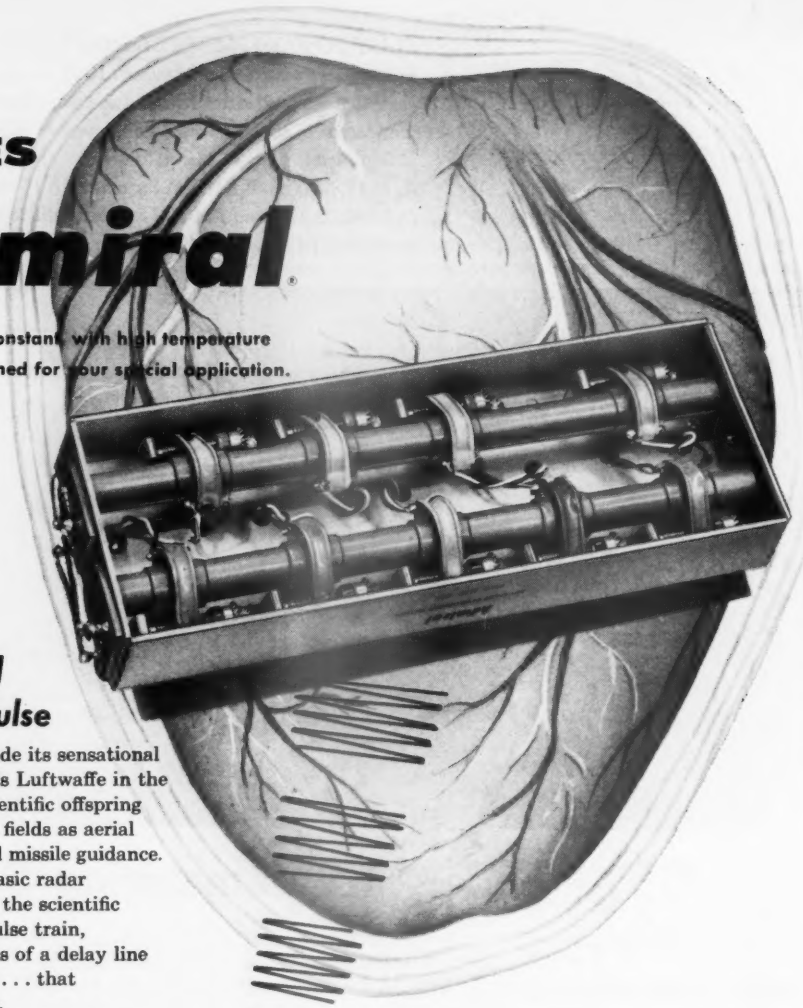
A DIVISION OF CALIFORNIA INSTITUTE OF TECHNOLOGY

PASADENA, CALIFORNIA

DELAY LINES

by Admiral®

. . . fixed and variable, distributed constant with high temperature stability. Designed for your special application.



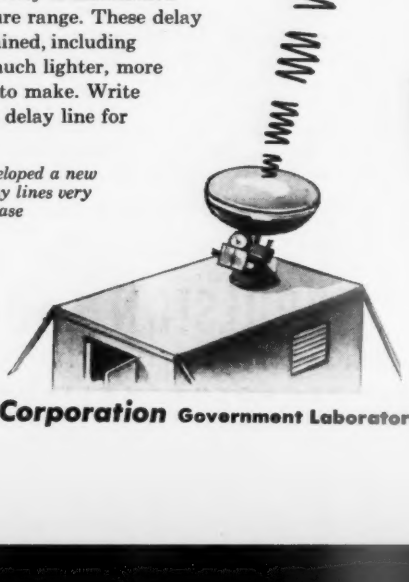
Micro-second Control for an Electronic Pulse

Scarcely fifteen years ago radar made its sensational debut when it helped defeat Hitler's Luftwaffe in the Battle of Britain. Since then its scientific offspring have become commonplace in such fields as aerial navigation, interrogation (IFF) and missile guidance.

All these elaborations of the basic radar principle, and many others now on the scientific horizon, depend on an electronic pulse train, established and controlled by means of a delay line . . . the very *heart* of the apparatus . . . that determines its scope and usefulness.

There was pressing need for a *variable** delay line, self-contained, with utmost accuracy and stability. Now Admiral research has developed such a unit. Where the flexibility of fixed delay lines is limited by the number of taps, the Admiral unit is *infinitely variable* within its overall capacity. It is adjustable with the greatest of ease for any desired interval . . . *without auxiliary circuitry.* Accuracy is limited only by the accuracy of the measuring equipment. Stability is maintained over an extreme temperature range. These delay lines, completely self-contained, including switching apparatus, are much lighter, more compact, and cost far less to make. Write Admiral about designing a delay line for your special application.

**Admiral research has also developed a new procedure for making fixed delay lines very much smaller, with excellent phase characteristics.*



LOOK TO *Admiral* FOR RESEARCH, DEVELOPMENT AND PRODUCTION IN THE FIELDS OF:

COMMUNICATIONS UHF AND VHF • MILITARY TELEVISION • RADAR • RADAR BEACONS AND IFF RADIAC • TELEMETERING • DISTANCE MEASURING MISSILE GUIDANCE • CODERS AND DECODERS CONSTANT DELAY LINES • TEST EQUIPMENT



FACILITIES BROCHURE describing Admiral plants, equipment and experience sent on request.

ENGINEERS: The wide scope of work in progress at Admiral creates challenging opportunities in the field of your choice. Write Director of Engineering and Research, Admiral Corporation, Chicago 47, Illinois.

Admiral Corporation Government Laboratories Division, Chicago 47, Illinois

Jet Propulsion News

Alfred J. Zaehringer, American Rocket Company, *Associate Editor*
Norman L. Baker, Indiana Technical College, *Contributor*

Jet Aircraft, Engines

A NEW version of the B-47 is the RB-47K. The new craft is equipped for both weather reconnaissance and photo work. RB-47K will measure and record wind velocities and directions, moisture, temperatures, and barometric pressures.

● The B-52 is to be equipped with the "BRANE," bombing radar and navigation equipment. The IBM system guides the plane to its target and automatically carries the plane through the bomb run. Meanwhile, the B-52 is beginning to replace B-36 wings. One B-52 wing is now in operation and the complete changeover to the jet bomber will take several years.

● RB-66 tactical reconnaissance aircraft has been accepted for operation with the Air Force. Carrying a crew of three, the swept-wing, twin jet RB-66 is equipped for all-weather day or night operation. It is designed to operate at speeds of 600–700 mph at altitudes of over 40,000 ft. Another Douglas aircraft, the C-133A turboprop cargo plane has had its first rollout. The ship has four P&W T34-P-3 turboprop engines of 6000 hp each. Gross weight of the 148-ft-long plane (span of 179 ft) is 255,000 lb. The 90-ft-long cabin floor can carry 200 troops or heavy ordnance equipment.

● The SE 210 "Caravelle" medium range, twin jet airliner (photo) which made its first flight in May 1955 will be delivered in 1958. The French SNCASE craft is powered by two Rolls Royce Avon turbojets of 10,500-lb thrust each in aft fuselage mounts. Wingspan is 112½ ft; length is 103 ft; height is 28½ ft. Caravelle will transport 70 passengers at a cruising speed of 470 mph and at an altitude of over 35,000 ft. The plane tips the scale at 49,700 lb and maximum takeoff weight is 90,400 lb. Range is 1620 nautical miles.

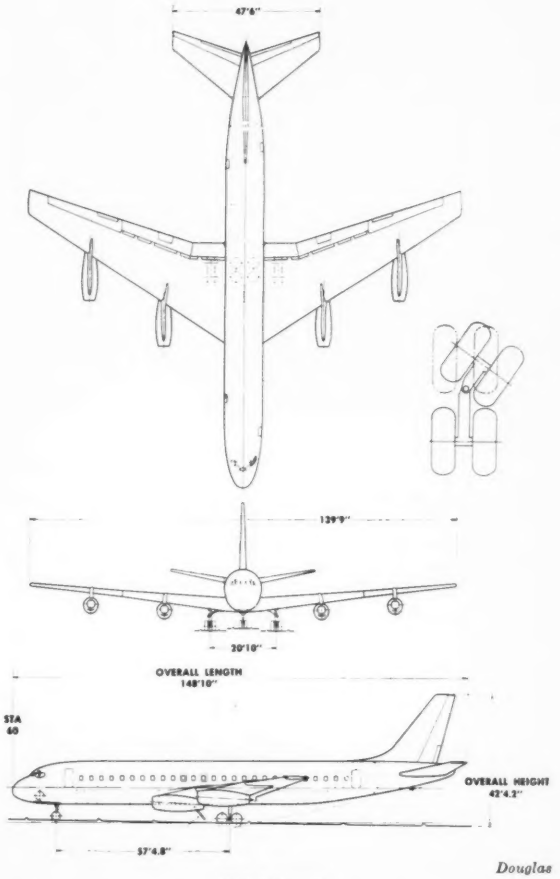


Caravelle in flight

● Specifications of the Vickers-Armstrong V-1000 jet transport are: weight, 247,000 lb; payload, 21,600 lb; range, 4800 nautical miles; speed, 440 knots; capacity, 100 passengers. Cost of the British development of this ship is about $7 million.

● Successor to the J47 turbojet will be the GE J79 in the 12,000-lb thrust class. Of 40-in. diam, it uses a minimum of critical materials and has a thrust-to-weight ratio of about 6:1. The J47 program will be terminated in 1956; entire production amounted to about 35,000 engines.

● The T58 small gas turbine by GE is in an advanced state of development and is rated in the 1000 hp class. The engine, developed for the Navy Bureau of Aeronautics, will be tested for helicopter applications.



Douglas

DC-8 layout

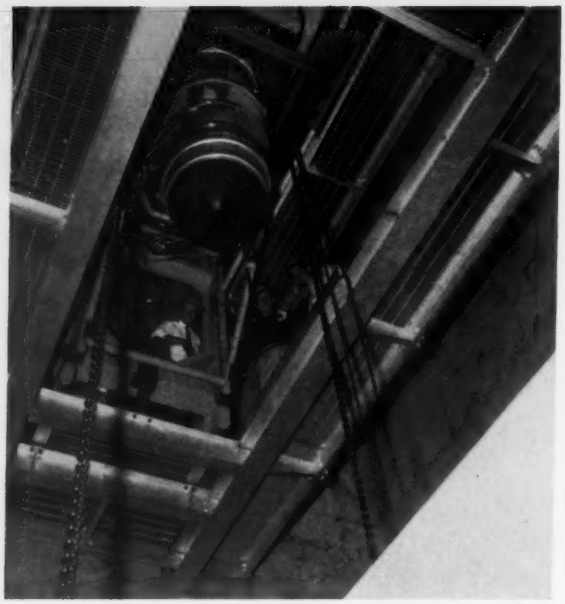
● A refined DC-8 is being offered by Douglas Aircraft (photo). With a span of 139 ft 9 in., length of 148 ft 10 in., and a height of 42 ft 4 in., there are two weight levels: 265,000 lb gross takeoff for general use and 287,500 lb for intercontinental models. The range of the latter model is 6720 statute miles.

● Soviet twin jet transports, TU-104 are being placed into regular commercial service in Russia. The TU-104 flies at a speed of 500 mph at altitudes of over 36,000 ft. Both the TU-104 and converted twin jet bomber Il-28 have been flying trials on the USSR Aeroflot airline system.

● Range of Soviet four-jet bomber may be less than the 10,000 miles of similar U. S. jet bombers.

● A new portable jet engine muffler has been successfully used on the F-84 at Republic Aviation. Full power noise reduction was about 23 decibels according to the company. A series of sound-absorbing chambers is housed in a tank about 10 ft in diam and 20 ft long. Cool air is drawn into the chamber and obviates the need for cooling water. Although 75 per cent sound intensity has been achieved at full power, an organ pipe effect results at idle.

● Model 73 is a two-seat jet trainer by Beech and now flying in test runs. Power comes from a Continental J69-T-9 turbojet of 900-lb thrust. Top speed is 253 knots at 15,000 ft. Weight is 4521 lb.



Ryan

VTO test stand

● Thrusts of jet engines in both horizontal and vertical position can be checked at the new Ryan $0.375 million facility (photo). Capable of handling thrusts up to 35,000 lb, the stands are bolted to thrust tables which are floating on load cells. The load cell includes a solid bar of steel with a strain gage cemented to it. Two load cells are used for each plane of force measurement. As many as seven load cells were used in recent tests.



General Motors

Firebird II jet car

● Firebird II is the latest General Motors experimental gas turbine driven automobile (photo). Increased efficiency results from a heat exchanger which recaptures over 80 per cent of the engine exhaust heat. The body is constructed of titanium. The engine weighs 850 lb and generates over 200 hp at 35,000 rpm gasifier speed. Power turbine speed is 28,000 rpm. Maximum gas temperature is 1650 F.

● The Fairey Delta 2 averaged 1132 mph in a recent speed run in England. One run was made at 1117 mph, another 1147 mph. The British craft is known as the "Droop Snoot."

● S-14 is another two-place jet trainer. The S-14 is built by Fokker and is powered by a Rolls Royce Derwent turbojet of 3470-lb thrust; top speed is 450 mph.

Liquid Propellant Progress

● Jet Propulsion Laboratory, Pasadena, Calif., tested the storage of fuming nitric acids at about 130 F for several months. In aluminum and stainless steel (18–8) alloys, 0.5 per cent hydrofluoric acid in the acid markedly reduced the corrosion. Metal fluoride passivates the surface. Excessive storage pressures are eliminated by concentrations of 12–16 per cent NO_2 and 2–3$^1/_2$ per cent water in the acid.

● U. S. Naval Ordnance Laboratory, White Oak, Md., examined the thermal decomposition of simple nitrite esters. In the case of tert-butyl nitrite, nitric oxide inhibits the decomposition reaction. Other compounds under study are isopropyl nitrite and n-propyl nitrite.

● Wright Air Development Center, Ohio, measured the heat of combustion of ammonia in fluorine. Products were nitrogen and hydrofluoric acid. Heat of reaction was −181.56 kcal.

● Redstone Arsenal, Huntsville, Ala., released data about tetranitromethane (TNM) in rocket use. TNM has a high density (1.64 kg/liter), high oxygen content (69.5) per cent and good performance (I_{sp} of 224 with hydrocarbon fuel). However, TNM has a high freezing temperature of 57 F and is sensitive to detonation. TNM is easier to initiate than TNT but has only about $^1/_4$ the explosive power of TNT.

Solid Propellant Progress

AEROJET-GENERAL Corp., Azusa, Calif., has been investigating propellants composed of synthetic linear polymeric binders and inorganic crystalline oxidizers. In these composites, interaction between the two has been noted. Aerojet has also reported research in nitropolymers and their possible applications in smokeless propellants. Other work is concerned with combustion instability and kinetics of solid phase reactions.

● American Rocket Co., Wyandotte, Mich., reveals that the cost of its ammonium nitrate propellant may be lowered significantly by continuous process techniques now being investigated.

● Atlantic Research Corp., Alexandria, Va., indicates that some of its solid propellant work is concerned with plastisols, polyurethanes, and epoxies.

● Fairchild Engine & Airplane Corp., Guided Missile Div., Long Island, N. Y., has utilized glass-reinforced plastic for the motor construction of the 14DS-1000 (T56) JATO. The T56 uses a double-base propellant.

● Forrestal Research Center, Princeton, N. J., is studying the combustion mechanism of solids. Steady state burning of perchlorates has yielded a theoretical law predicting pressure effect on burning rates from 40 to 1500 psi. Other work is concerned with plateaus, pressure limits, and ignition.

● Grand Central Rocket Co., Redlands, Calif., finds the use of weapons systems engineering useful in designing solid propellant missile powerplants. To avoid insoluble design problems, propellant people, they feel, should be given the widest possible latitudes.

● Jet Propulsion Laboratory, Pasadena, Calif., has said that we are near the limits of new liquid propellants but the limits may be less stringent in solids. It was suggested that great improvements in properties and processing are possible with solids. Also being sought is the control of the rate and direction of burning.

● Naval Powder Factory at Indian Head, Md., is doing work in cast solids, synthetic propellants, and the manufacture of nitroguanidine. Nitroguanidine is interesting from the standpoint that it may offer high performance at low combustion temperatures.

● Phillips Petroleum Co. of Bartlesville, Okla., reports the completion of a solid propellant manufacturing line at Air Force Plant 66 near McGregor, Texas. This is the first plant for large-scale production of T60 RATO using low cost petroleum materials. Propellant uses ammonium nitrate, carbon black, and synthetic rubber.

● Ramo-Wooldridge Corp., Los Angeles, Calif., is interested in solid propellant systems. Morphological studies show at least 6240 possible geometrical grain configurations.

● Standard Oil Co. (Ind.), Whiting, Ind., has established a pilot plant at Seymour, Ind. Work is concerned with low cost propellants based on nonstrategic materials, presumably using petroleum materials. Standard's work started in 1951. The Seymour plant started in 1954 and will work on a prototype scale.

● Surface Combustion Corp. of Toledo, Ohio, supplied chemical dehumidifiers to allow successful processing of propellants at the Phillips Petroleum rocket lab. The installation at Bartlesville processes hygroscopic ammonium nitrate and maintains humidity at 20 per cent RH or lower. Requirements of the system are 30 gpm of 85 F water and 350 lb/hr of 25 psig steam. Electrical power is $^3/_4$-hp pump motor and 1-hp regenerator air fan.

● Thiokol Chemical Corp., Trenton, N. J., points out that while almost any polymer is suitable for a fuel-binder in composites, other factors such as physicals, processing, etc., must be considered. Recent reports indicate that some Thiokol propellants are composed of perchlorates as oxidants and polysulfides as fuel-binders.

● University of Minnesota has reported studies of the infrared spectra of solid propellant flames as a tool in combustion kinetics.

● Utah University worked on the ignition of double-base propellants by detonating gases. Such work might lead to versatile "massless" and nonelectrical igniters for solid propellant rockets.

The Research Scene

NOW in operation at the General Mills Mechanical Division in Minneapolis is a "space chamber." The chamber (photo) can simulate conditions at altitudes of 80–300 miles above the earth. Metals and other materials are bombarded by ionized particles to investigate the "sputtering" or disintegration of metals under prolonged attack by free atoms and molecules. The most important discovery to date in the work is that the sputtering tendency is not caused by the heat generated when the bombarding particle collides with a solid. Momentum of the charged particles and the angle at which they strike determines how many atoms will be dislodged.



General Mills

Space chamber

● Successful forging of titanium turbine blades has been reported by Canadian Steel Improvement, a subsidiary of Avro Canada. The new process is said to overcome titanium's chemical affinity for hydrogen and oxygen which in the past have caused brittleness and scale formation.

● The Polytechnic Institute of Brooklyn will offer a graduate course in rocket propulsion. The new course will begin in Fall 1956, and will cover both liquid and solid propellants. Included will be such basic principles as nonsteady aerothermodynamics, combustion kinetics, flame propagation, and detonation. Flameholding and heat transfer through steady and nonsteady boundary layers will be discussed. Also, the elements, design principles, and programming of liquid and solid engines will be given.

● From Japan to Texas is the span of launching sites in new Skyhook balloon flights. The Navy and Atomic Energy Commission joined hands in the cosmic ray tests in Texas while the Japan tests were carried out by the Navy in transoceanic sounding to gather information about conditions at 30,000 ft and above.

● An international conference on ozone will be sponsored by the Armour Research Foundation in Chicago on November 28–30, 1956. Among topics expected are use of ozone as a rocket fuel, stability problems, and reactions.

Facilities

TWO major building programs are scheduled by Boeing. One is a $21 million development center at Seattle; the other is an $8.5 million facility at Renton. These programs are expected to make more room for the expanding BOMARC project.

● Three new advanced engineering operations in the Special Defense Project Department were announced by General Electric. The department, which is concerned with guided missiles, will now be concerned with airframes, guidance, and nuclear weapons.

● Research in gas turbine engines will be conducted at a new facility in San Diego, Calif. The Solar Aircraft layout will include five test cells for turbojet engines. A 20-ton, 1800-hp diesel engine will provide power in testing compressors and provide compressed air for combustion and turbine research.

● Two G. M. Giannini groups have been announced. The Gyro Division will move to larger quarters in Pasadena. The Controls Division will be located in Hollywood.

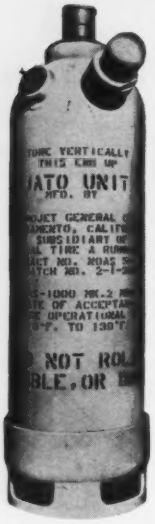
● Components and accessories for jet aircraft will be tested at the Garrett Corporation's new $5 million test facility in Phoenix, Ariz. (photo). The test facility has 90,000 sq ft on a 10-acre plot and has over 75 production test cells and stands. Temperatures of −80 F to 1000 F and altitudes to 75,000 ft can be simulated.



AiResearch

Feed systems and test cells

Solid Propellant Panorama



Aerojet-General

14AS-1000 JATO Rocket Engine, Mark 2 Mod 3

Nominal thrust at 60 F, lb	1025 ± 65
Nominal duration at 60 F, sec	14.3 ± 0.9
Total impulse, lb sec	14,000
Specific impulse, lb sec/lb	186
Operating temp range, F	0–130
Operating pressure @ 130 F, psi	2650
Operating pressure range, psi	1350–2850
Safety diaphragm release range, psi	3300–3700
Design ultimate thrust, lb	3000
Ignition interval at 60 F, sec	0.60 ± 0.3
Diameter, in.	10.25
Over-all length, in.	35.4
Loaded weight, lb	194
Empty weight, lb	115

NOTES: Steel cylinder construction with fore end closed; exhaust nozzle, igniter, and safety diaphragm on aft end. Mounting lugs welded on. Propellant: solid type (ALT-161) is asphalt resin fuel-binder (approx. 25 per cent wt) and potassium perchlorate oxidizer (ca 75 per cent wt) molded into end-burning cartridge secured in chamber. Propellant inert to shock; ignition temp higher than 750 F. Ignition by electrically actuated black powder igniter. Three-point suspension. May be fired in any position. CAA-certified for DC-3, DC-4, DC-6, Convair 240.



Aerojet-General

15KS-1000 JATO Rocket Engine, Mark 6 Mod 1

Rated thrust, lb	1000
Rated duration, sec	15
Total impulse, lb sec	15000
Operating temp range, F	−65 to 140
Specific impulse, lb sec/lb	208

Temperature, F	Ignition delay, sec	Thrust, lb	Duration, sec
−65	0.21	815	18.0
60	0.11	1062	14.0
140	0.09	1320	11.5

Diameter, in.	10.1
Over-all length, in.	33.4
Loaded weight, lb	144
Empty weight, lb	72

NOTES: Steel construction with fore end closed. Igniter on fore end. Exhaust nozzle and safety diaphragm on aft end. Smokeless propellant (ammonium perchlorate oxidant and resin fuel-binder) molded into cartridge secured in chamber. Propellant inert to shock. Glow plug igniter. Two-point suspension.



Thiokol

Solid Propellant Gamut . . . Lineup of motors shows wide variety of sizes ranging from small gas generator auxiliary unit at left to missile motor or RATO unit at right. All of these units are classed as "small"

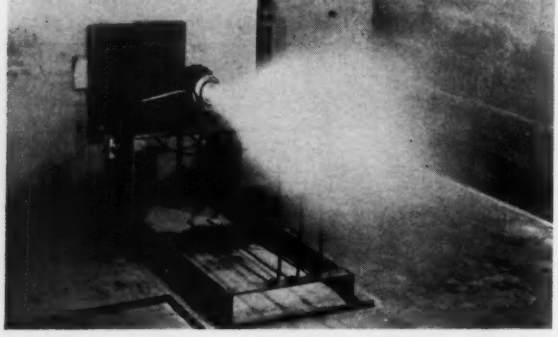


Aerojet-General

5KS-4500 JATO Rocket Engine, Mark 7 Mod 1

Performance:	
Rated thrust, lb	4500
Rated duration, sec	5
Total impulse, lb sec	22,500
Specifications:	
Diameter, in.	9.38
Over-all length, in.	54.6
Loaded weight, lb	236

NOTES: Steel cylinder construction with fore end closed. Exhaust nozzle (canted) and safety diaphragm on aft end. Smokeless propellant, ammonium perchlorate oxidant, resin fuel-binder, molded into cartridge secured in chamber. Propellant inert to shock. Glow plug igniter.



Surface Combustion

Ammonium Nitrate Rocket . . . Motor in static test shows unique exhaust stream—little flash and no smoke appear to be characteristic. Photo illustrates Phillips Petroleum Co., Bartlesville, Okla., work in development of low cost solid propellants for USAF



Thiokol

Beauty and Beast . . . Size of this rocket indicates scale-up possible with modern solid propellants. Vehicle was shown in Huntsville, Ala. Although lacking in details, the beast appears to be about 15–16 ft long, has a diameter of about 15 in. and resembles the GE RV-A-10 rocket. No data were given on the beauty

ARS News

ARS to Cosponsor Symposium on Instrumentation in Satellites with IGY, ISA

Newell to be Chairman

ARS has been invited by the Instrument Society of America to present a technical program on instrumentation in the IGY satellite program on the opening day of the ISA Annual Meeting and Exhibition at New York Coliseum September 17–21.

Coordinating the program for ARS and IGY is Homer E. Newell, Jr., superintendent of the Atmosphere and Astrophysics Division, Naval Research Laboratory. Dr. Newell announces that the tentative program includes papers by Joseph Kaplan, chairman of the IGY U. S. National Committee; W. A. Wildhack, National Bureau of Standards; R. W. Porter, ARS past president and chairman of the technical panel on the earth satellite for IGY; Herbert Friedman and J. T. Mengel of NRL; Fred L. Whipple, Smithsonian Astrophysical Laboratory; and Paul Herget, Cincinnati Observatory.

Subjects covered will include over-all satellite instrumentation, as well as tracking, telemetering, computation, optical observation, and others.

Antelope Valley Section Formed

AN ARS Section centered at Edwards Air Force Base has recently been formed and has been named the Antelope Valley Section.

Richard A. Schmidt, assistant chief of the Rocket Engine Test Lab. at Edwards, is the first president of the organization. Serving with him are: H. S. Stratton, RETL, vice president; A. J. Hoffman, Ramo-Wooldridge Corp., treasurer; and W. Johnson, Rocketdyne, secretary. Directors are D. L. Dynes and R. F. Gompertz, RETL; J. W. Conlon, Reaction Motors, Inc.; and D. R. Bellman, NACA.

The Antelope Valley covers 3500 square miles and embraces Edwards AFB, including RETL and the aircraft test facilities at Palmdale. The aircraft flight test or missile test departments of North American, Convair, Northrop, Lockheed, Chance Vought, Ryan, Douglas, and Aerojet-General are among those at Palmdale.

Robert C. Truax, ARS vice president, spoke at a March 6 meeting of the Section on the early days of rocketry in the U. S.

Levy to Lead New England Section

LAWRENCE LEVY, president of Allied Research Assocs., Boston, has been elected president of the New England Section for the forthcoming year.

Also elected were Charles N. Saffer, Jr., National Northern Tech. Div., National Fireworks Ordnance Corp., vice-president; and A. John Gale, High Voltage Engineering Corp., treasurer. Kathleen Manion of Arthur D. Little, Inc., was re-elected secretary.

Serving as directors for three-year terms are Bruce H. Billings, Baird Assocs., and Richard L. Bolin, ADL.

Section Doings

Alabama. An illustrated talk on the Navy's Viking missile was given by Sears Williams (photo) of the Glenn L. Martin Co., at the March meeting. Following the talk, Mr. Williams summarized the Viking launchings to date, discussed the research data obtained, and presented some of the construction details of the missile. At the April meeting Ernst Stuhlinger addressed the group on interplanetary space travel.

A local educational program for youth is currently being carried out under a standing Committee headed by T. E. McClard. The program includes (a) a local Rocket Club for high school students, (b) a college scholarship fund, (c) a visiting speaker service rendered by engineers and scientists at Redstone Arsenal, and (d) a technical essay contest for high school students.



Sears Williams

Arizona. At a May 1 dinner meeting in Tucson, the installation of officers for 1956–1957 took place. They include C. J. Green, president, who has been re-elected; Sidney Wade, vice-president; George Hacher, secretary; and Frank H. Barris, treasurer. New board members are: E. S. Forman, R. M. Shuman, and Joel Singer.

Cleveland-Akron. Calvin A. Gongwer, manager of Aerojet-General Corporation's Underwater Engine Div., Azusa, Calif., spoke to an audience of some fifty persons at the B. F. Goodrich Research Center in Brecksville on April 26. He revealed that at the optimum operating point the propulsive efficiency of most underwater engines lies between that of the aircraft propeller and the aerial jet engines. Also, it was pointed out that underwater engines have problems analogous to aerial engines. For example, cavitation problems with underwater devices correspond to sonic



Convair

North Texas Section president George Craig (left) discusses ARS activities with Convair-Fort Worth chief engineer and ARS member Frank W. Davis



Charter members of a woman's auxiliary group formed by the National Capital Section. From left to right are Mrs. Mason Comer, Miss Ethna White, Mrs. Erik Bergaust, Mrs. C. Lincoln Jewett, and Mrs. Milton W. Rosen

missile engineers

CONTROL GUIDANCE SERVO COMPUTERS RECORDING OPTICAL RELIABILITY ELECTRO-MECHANICAL TELEMETERING

With 16 years leadership in the vital field of missile research and development, Northrop Aircraft offers unusual opportunities for advancement in the categories listed below. Where better could you be, and grow, than with a pioneer? There's an interesting position for you in one of the following groups:

Guidance and Controls, encompassing research and development of advance automatic guidance and flight control systems for both missiles and piloted aircraft. Specific areas of development include: radio and radar systems, flight control systems, inertial guidance systems, instrument servo systems, digital computer and magnetic tape recording systems, airborne analog computer systems, optical and mechanical systems, and systems test and analyzer equipment. Within these areas activities include: original circuit development, electronic and electro-mechanical design, laboratory and field evaluation of systems under development, and reliability analysis both at a system and component level.

Flight Test Engineering Section, which plans the missile test programs and establishes test data requirements in support of the programs. The data requirements are predicated on the test information required by the Engineering analytical and design groups to develop and demonstrate the final missile design, and are the basis from which the instrumentation requirements are formulated.

The analysis work performed consists of aerodynamic, missile systems, dynamics, flight control, propulsion and guidance evaluation. The Flight Test Engineering Section is also responsible for the field test program of the ground support equipment required for the missile.

Flight Test Instrumentation Section, which includes a Systems Engineering Group responsible for the system design concept; a Development Laboratory where electronic and electro-mechanical systems and components are developed; an Instrumentation Design Group for the detail design of test instrumentation components and systems; a Mechanic Laboratory where the instrumentation hardware is fabricated; and a Calibration and Test Group where the various instrumentation items and systems are calibrated and tested.

There are now a number of openings available for engineers in each of these groups at all experience levels.

If you qualify for any of these challenging opportunities, we invite you to contact Engineering Industrial Relations, Plant 2, Gate 3B, Broadway & Prairie, Northrop Aircraft, Inc., Hawthorne, California; or write Manager of Engineering Industrial Relations, Northrop Aircraft, Inc., 1021 East Broadway, Hawthorne, Calif.



NORTHROP AIRCRAFT, INC.

PIONEERS IN ALL WEATHER AND PILOTLESS FLIGHT

Producers of Scorpion F-89 Long-Range Interceptors and Snark SM-62 Intercontinental Missiles.

5-A-65

velocity problems with aircraft engines. Gongwer described the Minisub, a two-man, water-filled submarine which equals the propulsive efficiency of the porpoise and considerably extends the range of operations of skin-divers who can afford initial outlay of $4800 or do-it-yourself.

Florida. At the April 26 meeting, the following officers were elected for the coming year: Verl O. Smith, chief of the missile test facility, Northrop Aircraft, president; R. L. Yordy, base manager for Cape Canaveral, Pan American World Airways, vice-president; Paul B. Campbell, Boeing Airplane Co., secretary; and Capt. R. H. Reynolds, USAF, AFMTC, treasurer. Directors are: Major General D. N. Yates, AFMTC; A. C. Conrad, RCA Service Co.; R. B. Rypinski, Ramo-Wooldridge Corp.; G. C. Gentry, Patrick AFB; B. G. McNabb, Convair; W. L. Risley, Boeing; and R. S. Mitchell, Pan American, who is the retiring president.

Indiana. On March 26 A. R. Graham of the Purdue University Jet Propulsion Center spoke on satellite vehicles. He discussed the physics involved in establishing a satellite, as well as problems concerning the development of the power plant. The following were elected to office for the coming year: James A. Bottorff, president; R. K. Rose, vice-president; Wayne H. Munyon, secretary; Donald L. Crabtree, treasurer. Directors are P. M. Diamond (retiring president), Graham, D. G. Elliott, Helmut Wolf, B. A. Reese, and M. J. Zucrow (honorary). Faculty advisor is C. F. Warner.

Wayne Stennett of Aerojet-General Corp. spoke at an April 11 meeting and disclosed some of the details of Project Vanguard, such as size and configuration of the three-stage launching vehicle and possible orbits. The talk was illustrated with slides.

Maryland. On April 17, the Section visited Westinghouse Electric Corp., Air Arm Division, at Friendship International Airport, Baltimore. Following dinner there was a guided tour of facilities. Then Col. William O. Davis, deputy commander for operations with the Office of Scientific Research, talked on fundamentals of space flight. He was introduced by Andrew W. McCourt, Section vice-president and manager of the analytical section at Air Arm. Col. Davis pointed out that manned space flight could be anticipated in a much shorter time than would be expected based on the evolution of present-day propulsion. This is because man's creative ingenuity is advancing more and more rapidly.

National Capital. Stanley Smith, Chief, Airplane Projects, of Bell Aircraft, Buffalo, who has lived with the different Bell research planes, gave an interesting talk on the X-2 on April 5. He also speculated on rocket aircraft of the future and urged that the Air Force consider rocket interceptor fighters for defense of such strategic areas as Alaska and our oversea bases.

Krafft A. Ehricke of Convair, San Diego, spoke on the satelloid and showed slides at a meeting on April 20 at the Madison Arms Hotel. At the same meeting, announcement was made of the formation of a woman's auxiliary comprising some 20 wives of Section members (see photo).



As flight systems have become more complex, speeds higher, space and weight-saving more valuable, the increasing rate of technical progress in the aircraft industry has created a serious problem:

Keeping its products up to top level of operational effectiveness—and in the air—has become a major responsibility of the prime contractor.

Martin has been working on that problem for many years; and the result is a new kind of service organization and systems method which now provides for the maintenance of all Martin products—from the company's assembly lines to operational flight lines anywhere in the world—at peak effectiveness and with maximum availability.

It is service on a *systems* basis, and already it's setting a new pace in the industry.

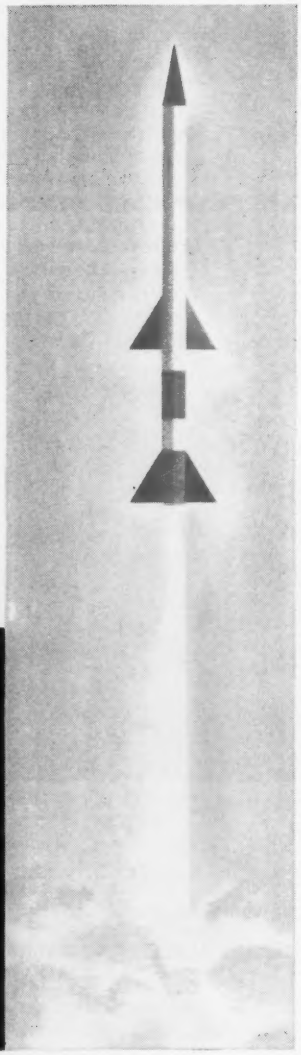
MARTIN

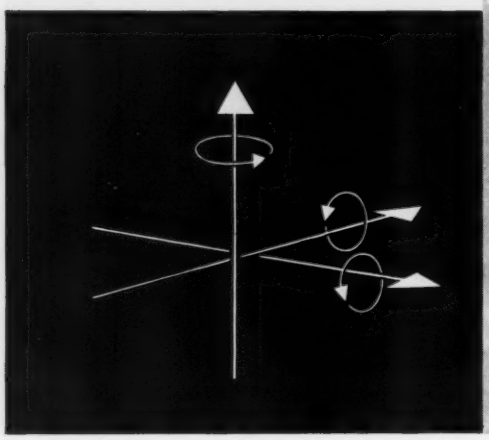
one source responsibility for multi-component rocket thrust testing systems

Now you can get an integrated thrust testing system, including rocket stand structural components, from *one* reliable source.

The Baldwin system measures forces and moments in any plane by SR-4® strain gage type load cells. We furnish the entire facility, including matched instrumentation and structural components, with guaranteed accuracy up to ±0.1%.

For your copy of bulletin 5101, write Dept. 2654, Electronics & Instrumentation Division, BLH Corporation, Waltham, Massachusetts.





BALDWIN BLH LIMA-HAMILTON

ELECTRONICS & INSTRUMENTATION DIVISION
BALDWIN-LIMA-HAMILTON
DIVISIONS: Austin-Western • Eddystone • Hamilton • Lima • Electronics & Instrumentation • Loewy-Hydropress • Madsen • Pelton • Standard Steel Works

New York. Nuclear powered flight was the subject discussed by two speakers from New York University at the April meeting. Lyle B. Borst, chairman of the Physics Dept., covered the requirements and limitations of an aircraft nuclear power plant and the design limitations imposed by the human element. Frederick K. Teichmann, assistant dean of the College of Engineering, discussed problems imposed by a nuclear reactor on weight distribution and airframe design, with some reference to the over-all performance of the vehicle. The meeting was held in the Engineering Societies Building. The following week a joint meeting with the IRE (Westchester Subsection) was held at the Norden Laboratories in White Plains. Arthur S. Westneat of the Applied Science Corporation of Princeton, N. J., discussed some unsolved problems in missile and satellite telemetering.

Princeton Group. Simon Ramo (photo), executive vice-president of Ramo-Wooldridge Corp., Los Angeles, spoke at an April 5 meeting at Princeton University, cosponsored by the Metropolitan Section of the IAS.

His thesis was that missile projects are producing knowledge which promises to have great effect on nonmilitary projects—automatic factories, offices, transportation systems. He discussed the changes required in education necessary to produce the people who can execute these projects.



Simon Ramo

Jerry Grey, assistant professor at Princeton, was elected chairman of the Group at a May 3 meeting, succeeding J. Preston Layton. Vice-chairman is George B. Matthews, research assistant at James Forrestal Research Center, and secretary-treasurer is Marshall Fisher, also of Forrestal.

At the latter meeting Malcolm Jones, a physicist with Project Matterhorn at Princeton, gave a talk and showed slides of 1952–1953 Deacon firings in Greenland.

Sacramento (proposed). At an April 13 dinner meeting Clair Beighley discussed plans for forthcoming programs. Frank Coss, president, spoke on rocket-powered research aircraft, and told of his personal experiences with the Bell X-1 and Douglas D-558 programs. Slides, photos, and a color movie on the X-1A were also shown.

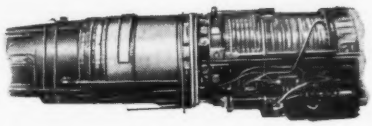
Columbus. Fourth meeting of the proposed Section was held in February with sixty two attending. Speaker of the evening was Prof. A. N. Tifford of Ohio State Univ., whose topic was "Escape from Earth," or "Getting Away from it All!"

AC ELECTRONICS DIVISION

NEEDS **HYDRAULIC RESEARCH ENGINEERS**

To Develop TEST FACILITIES for Jet Engine Fuel Control Systems and Components.

Working with: High Energy Fuels at Extremes of Temperatures and High Pressures



Test Stands

Environmental Test Cells

Remote Instrumentation

Servo Operated Afterburner Fuel Controls, Inlet Temperature and Turbine Speed Sensing Electro-Hydraulic Servo Controls.

Applicant should have B.S. Degree Plus 4-6 Years Experience Relative to Hydraulic Engineering, Valve Design, Hydraulic Servos, Instrumentation and Testing of Fluid Control Devices, or Other Associated Fields.—Write to Mr. J. Heffinger, Supervisor of Salaried Personnel

AC THE ELECTRONICS DIVISION

GENERAL MOTORS CORPORATION

MILWAUKEE 2, WISCONSIN also FLINT 2, MICHIGAN

ENGINEERS

***ARMA** announces*

INERTIAL NAVIGATION

development program for an advanced Air Force missile

Inertial Navigation offers the most advanced concept in guidance, requiring no terrestrial source of energy or information, no earth-bound direction once the ultimate destination is selected. It offers the most promising solution of the guidance problem for the long-range missile.

While the principles are simple, the realization involves advanced creative engineering. ARMA's many successes in the creation of precision instruments and systems for navigation and fire control, especially precision gyroscopic reference systems for all applications, fit it uniquely for a major role in this advanced area.

The height of imaginative resourcefulness and engineering skill are required to create the degree of precision—hitherto unattained—in the components essential to the guidance of advanced missile systems—the gyros, accelerometers, and computer elements. Miniaturization must be coupled with extraordinary ability to provide utmost accuracy under conditions of extreme velocities, temperatures, and accelerations.

There's significant scientific progress to be achieved at this leadership company and individual renown to be won, by engineers associated with ARMA's Inertial Navigation Program. Many supplementary benefits make a career here doubly attractive. ARMA engineers are currently working a 48 hour week at premium rates to meet a critical demand in the Defense Dept's missile program. Moving allowances arranged.

Salary — up to $15,000
(Commensurate with experience)

Send resume in confidence to:
Manager of Technical Personnel, Dept. 674

Immediate openings for Supervisory and Staff positions as well as for Senior Engineers, Engineers, and Associate Engineers, experienced in:

Systems Evaluation
Gyroscopics
Digital Computers
Accelerometers
Telemetry
Guidance Systems
Reliability
Stabilizing Devices
Servomechanisms
Automatic Controls
Thermodynamics
Environmental Research
Weight Control
Transformers
Production Test Equipment

ARMA

Division of American Bosch Arma Corporation
Roosevelt Field, Garden City, Long Island, N. Y.

Do you think about Angular Acceleration?

***BOEING** does*

...and uses Statham Angular Accelerometers to test...

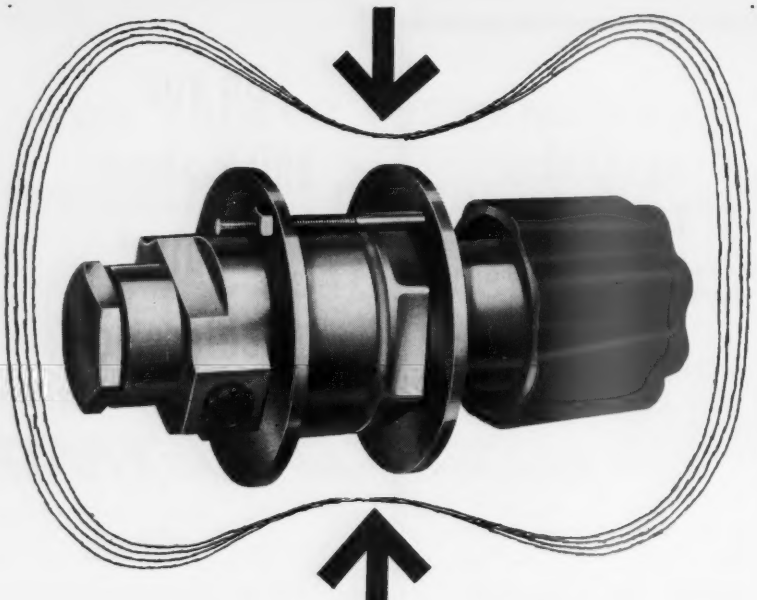


Statham unbonded strain gage liquid rotor angular accelerometers offer a simple, reliable means for the study of the rotary motion of a test body under conditions where a fixed mechanical reference is not available. For static and dynamic measurements in ranges from ± 1.5 to $\pm 3{,}000$ rad/sec^2, four standard models are offered.

Please request Bulletin AA2

Statham

LABORATORIES
LOS ANGELES 64, CALIFORNIA



REVOLUTIONARY, NEW HIGH PRESSURE REGULATOR

Look at these outstanding new developments:

- Widest adjustment range available for manual regulation due to greater sensitivity created by a new engineering innovation!
- ¼" tube straight thread gasket seal bosses per AND10050!
- Maximum inlet pressure of 4500 psi!
- Internal relief valve and filter!
- Internal valve and filter are removable without disturbing spring, diaphragm structure!

Catalog Number	Adjustable Range Outlet Pressure PSI
110100-2	5/150
110100-4	15/300
110100-6	30/750
110100-8	150/1500
110100-10	400/3000

Write today for new engineering data sheet and catalog covering our complete range of regulators.

APCO **ACCESSORY PRODUCTS CORP.**
Dept.–J-6 616 W. Whittier Blvd.
Whittier, Calif. • Phone: OXford 3-3747



James J. Mazzoni, President
St. Louis Section

Mazzoni to Head St. Louis

FORTY ARS members met in St. Louis at the Congress Hotel to elect new officers and directors on Feb. 29. Guest Speaker James J. Harford, Executive Secretary of the ARS, outlined the relation of the local section to the other sections and its purpose and direction. After Mr. Harford's talk, the recommendations of the nominating committee were accepted, as follows: president, James J. Mazzoni (McDonnell Aircraft Corp.); vice-president, Robert A. Cooley (Olin-Mathieson Chemical Corp.); secretary-treasurer, P. W. Godfrey (McDonnell); board of directors: B. G. Bromberg and S. C. McDonnell (McDonnell); Joseph A. Volk (Greenleaf Mfg. Co.); Charles C. Durham (White-Rodgers Electric Co.); Dale Anderson (Parks Air College); Julian H. Miller (*Prom Magazine*); and Commander B. V. Turner (Navy Engineering Officer at McDonnell).

Student Chapter News

Academy of Aeronautics. Charles J. Marsel, president of the New York Section, presented the charter to the Chapter at an assembly on May 17. Recipient was the Chapter president, Alex Havriliak.

Michigan. H. Muhrlein, Jr., has replaced Clifford Robinette as treasurer.

Polytechnic Institute of Brooklyn. On May 9 the charter was presented to Chapter president Mario Cardullo by James J. Harford, executive secretary. Mr. Harford was introduced by Professor T. P. Torda, faculty advisor. Cardullo has succeeded to the presidency upon the resignation of Donald Morin, due to illness.

ARS Meetings Calendar

June 18–20—ARS-ASME Semi-Annual Meeting, Hotel Statler, Cleveland. Liquid rockets, solid rockets, ramjets, satellites. ARS Banquet on June 18.

Sept. 17–21—Seventh International Astronautical Congress, Palazzo dei Congressi, Rome. Space flight.

Sept. 17–21—Annual Meeting and Exhibition, Instrument Society of America, Coliseum, New York (see page 509).

Sept. 24–26—ARS Fall Meeting. Hotel Statler, Buffalo. Combustion, instrumentation, education, liquid propellants.

Nov. 25–30—ARS-ASME Annual Meeting, New York. General subjects. (Abstracts due June 15, manuscripts August 27; to Andrew G. Haley, 1735 DeSales St., Washington 6, D. C.)

what helps an engineer grow?

Answers by 3 outstanding Avco scientists reveal both the thinking and opportunity at Avco Research and Advanced Development Division.

"Technical support"

says Dr. J. P. Silvers, specializing in thermodynamics, hydrodynamics in reactor design; formerly with Navy Nuclear Power Division; now with Avco Research and Advanced Development.

"An engineer should be given plentiful technical assistance. His potential cannot be fully realized when his energies are consumed by routine duties."

"An atmosphere of inquiry"

says Eaton H. Draper, noted nuclear weapons systems expert and Engineering Manager of Avco Research and Advanced Development Division.

"Provide a climate which encourages a healthy questioning of the known, as well as the unknown, and an engineer will perform at his peak . . . and even beyond."

"Top-level associates"

says Dr. J. A. Kyger, noted authority on nuclear engineering; formerly Chief Scientist for Nuclear Power Division, U. S. Navy Bureau of Ships; now Project Director of Avco Research and Advanced Development Division.

"An engineer's development depends on mental stimulation provided by able associates. It's important at all levels and it is essential to a young engineer."







Helping talented engineers and scientists—at all levels—become more effective is the best way we, at Avco Advanced Development, know of helping our own growth. For outstanding men, Avco's long-range expansion—in missiles and in all the physical sciences—offers unprecedented opportunity. Write Dr. E. R. Piore, Vice-President in Charge of Research, Room 403 F, Avco Research and Advanced Development Division, Stratford, Conn., or Phone Bridgeport, Conn., DRexel 8-0431.

WANTED:
Leaders in the exploitation of new areas of Science

Physical Scientists
Advanced degree preferred in—Physics · Aerodynamics
Electronics · Metallurgy · Physical Chemistry · Mathematics

Engineers
Electronic · Mechanical · Aeronautical
Chemical



avco Research and Advanced Development division

avco defense and industrial products

combine the scientific skills, and production facilities of 3 great divisions of Avco Manufacturing Corp.: Research and Advanced Development; Crosley; Lycoming — which currently produce power plants, electronics, airframe components, and precision parts.

ENGINEERING TIMETABLE



3:35 P.M. "Soft Words and Hard Arguments"

That, says the *Handbook of Proverbs*, is the key to success. When you apply the adage to group discussion, such as that pictured above, you have a sound rule for making fast progress on difficult problems.

At Fairchild Guided Missiles Division talented and inventive engineers work together on projects, following them through from start to finish *as a team*. The concept of group brainpower puts more thinking to work solving problems in such fields as inertial guidance, passive guidance and radar, and entire new missile systems.

Where do you fit into this dynamic engineering picture? Take a look at the listings on the right and see. Arrange an interview. You'll like what you see when you investigate the excellent working climate at Fairchild Guided Missiles Division.

Send your resume to R. B. Gulliver.

Senior Electronics Engineers:
Missile systems

Senior Electronics Engineers:
Servo and Analog Computer experience

Project Engineers:
Electronics or Electromechanical background

Senior Aerodynamicists:
Supersonic Aerodynamics, includes performance, stability and control analysis

...WHERE THE FUTURE IS MEASURED IN LIGHT-YEARS!

FAIRCHILD

GUIDED MISSILES DIVISION • WYANDANCH, LONG ISLAND, N.Y.

A Division of Fairchild Engine and Airplane Corporation

ARS SECTIONS AND PRESIDENTS

Alabama
Conrad Swanson, *Redstone Arsenal*

Antelope Valley
Richard A. Schmidt, *Edwards AFB*

Arizona
Charles J. Green, *Hughes Aircraft Co.*

Central Texas
Elton Rush (acting), *Phillips Petroleum Co.*

Chicago
Gerald M. Platz, *Armour Research Foundation*

Cleveland-Akron
A. O. Tischler, *Lewis Flight Propulsion Laboratory, NACA*

Connecticut Valley
Charles H. King, Jr., *United Aircraft Corp.*

Detroit
C. W. Williams, *Chrysler Corp.*

Florida
Verl O. Smith, *Northrop Aircraft, Inc.*

Fort Wayne
Lloyd Wadekamper, *Indiana Tech. College*

Holloman-Alamogordo Group
John P. Stapp, *Holloman Air Development Center*

Indiana
James A. Bottorff, *Purdue University*

Maryland
William A. Webb, *Aircraft Armaments, Inc.*

National Capital
J. D. Gilchrist, *Aerojet-General Corp.*

New England
Lawrence Levy, *Allied Research Assoc., Inc.*

Niagara Frontier
W. M. Smith, *Bell Aircraft Corp.*

New Mexico-West Texas
Russell K. Sherburne, *New Mexico College of A.&M.A.*

New York
Charles J. Marsel, *New York University*

North Texas
George Craig, *Convair*

Northeastern New York
A. H. Fox, *Union College*

Northern California
A. J. Eggers, *Ames Aero. Lab., NACA*

Pacific Northwest
Jim C. Drury, *Boeing Airplane Co.*

Princeton Group
Jerry Grey, *Princeton Univ.*

San Diego
Krafft Ehricke, *Convair*

St. Louis
J. J. Mazzoni, *McDonnell Aircraft Corp.*

Southern California
Richard D. Geckler, *Aerojet-General Corp.*

Southern Ohio
W. C. Cooley, *General Electric (ANP Dept.)*

Twin Cities
C. C. Chang (acting), *University of Minnesota*

Wichita
J. F. Reagan, *Beech Aircraft Corp.*

New Patents

George F. McLaughlin, *Contributor*

Jet engine control (2,737,015). Alexander M. Wright, W. Hartford, Conn., assignor to Pratt & Whitney Co., Inc.

Engines mounted so they are movable relative to the aircraft in proportion to the reaction thrust of their jets. The propulsion power output is automatically regulated by varying the air supply in proportion to engine movement.

Afterburner controls (2,737,016). Robert E. Day, San Diego, Calif., assignor to Solar Aircraft Co.

Means responsive solely to temperature variations in the outlet of the primary jet engine actuating a motor-driven valve to regulate fuel flow.

Variable area convergent-divergent diffuser (2,737,019). Louis S. Billman, Portland, Conn., assignor to the U. S. Navy.

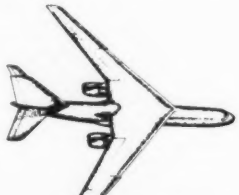
Diffuser for a reactive propulsion engine for supersonic speeds. A pressure regulator within a duct has a longitudinal ram air passage for varying the contour of a valve member, in response to pressure differentials induced by engine speed.

Radio controlled projectiles (2,737,356). Russell H. Varian and Wm. W. Hansen, Garden City, N. Y., assignors to Sperry Rand Corp.

System for controlling the direction of flight of a guided missile launched from an aircraft. A universally mounted antenna radiates modulated energy to provide highly directional beams with their relative positions in space determined, and overlapping to define an equi-signal zone. The flight control means is actuated so the missile automatically seeks and follows the equi-signal zone.

Hydraulic jet catapult with automatic jet control (2,737,357). Friedrich O. Ringleb, Woodbury Heights, N. J., assignor to the U. S. Navy.

System for accelerating a shuttle on which the buckets are curved to direct exhausted fluid to open a valve. The valve, between the high pressure fluid source and the nozzle, controls time of operation.

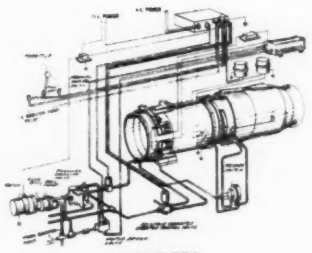


177,029

Aeroplane (design) 177,029. Eugene C. Frost and Albert J. Lechner, North Hollywood, Calif., assignors to Lockheed Aircraft Corp.

Torque responsive control for an emergency fuel system (2,737,776). Robert I. Strough, E. Hartford, Conn., assignor to United Aircraft Corp.

Aircraft gas turbine power plant, including main and emergency fuel systems. Means responsive to a substantial decrease in torque resulting from failure of the main fuel system for automatically rendering operative the emergency system.



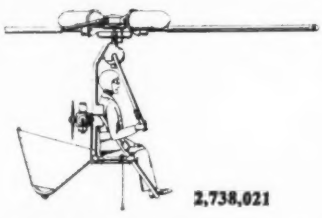
2,737,775

Afterburner electric controls (2,737,775). Philip M. Klauber, San Diego, Calif., assignor to Solar Aircraft Co.

Two relays with multiple sets of contacts cause fuel to be pumped into (and ignited in) the afterburner. A third relay, responsive to pressure variations in the afterburner, actuates controls which adjust a variable area nozzle to accommodate fuel combustion.

Combustion equipment for gas-turbine engines with anticarbon wall portion (2,741,090). Francis M. Johnson, London, England, assignor to Rolls-Royce, Ltd.

Flame tube having an imperforate inlet wall curved away from the combustion space and bounding a duct through which air flows into the tube. Air entering the combustion space passes along the surface of the inlet wall, substantially reducing carbon formation.



2,738,021

Jet driven helicopter rotor system (2,738,021). Bruno Nagler, Boston, Mass., assignor to Nagler Helicopter Co., Inc.

Series of solid-fuel rocket units mounted on a rotor assembly and means for igniting and expending the charges in sequences through passages in the rotor blades. The charges are directed to at least one jet orifice along the trailing edge of each blade.

Protective devices (2,738,029). Norman Battle and Philip B. Smith, Mickleover, England, assignors to Rolls-Royce, Ltd.

Debris guard hinged within an intake duct. In operative position it lies across the duct, and in retracted position it is substantially out of the path of fluid flowing in the duct.

Surge control for axial flow compressors (2,738,644). Joseph S. Alford, Nahant, Mass., assignor to General Electric Co.

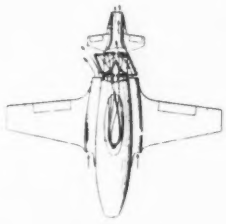
Controls for supplying fuel at a variable rate and in accordance with a preselected schedule of operating conditions of a gas turbine power plant.

Multistage turbojet engine having auxiliary nozzles located in an intermediate state (2,738,645). Pierre Destival, Paris, France, assignor to Compagnie Electro-Mecanique.

Fixed section jet behind a turbine provided with reheating to increase gas pressure. Engine power is increased by raising the gas temperature at the inlet above the limit at which surging normally occurs in the compressor.

Flow control means for intermittent impulse ducts (2,738,646). Marcel Kadosch, F. G. Paris, J. H. Bertin, and R. H. Marchal, Paris, France, assignors to Société Nationale d'Étude et de Construction de Moteurs d'Aviation.

Open frontal inlet passage for the downstream flow of air but through which an upstream flow of combustion gases is produced. The flow guiding means includes a wall extending outward a part of the periphery of the passage with means for laterally deflecting the upstream flow.



2,738,147

Means for turning and braking jet propelled aircraft (2,738,147). Verne L. Leech, Minneapolis, Minn.

Deflector plates hinged and mounted on each side of the aircraft, and arranged to be moved into the flow of the jet blast. To change the direction of flight or deflect the flow to both sides for braking. For turning, the deflector plate on one side or the other is moved into the flow; for braking, both plates are moved into the flow.

Gas turbine engine frame structure (2,738,647). Henry C. Hill, Seattle, Wash., assignor to Boeing Airplane Co.

Power output and gas producing sections in axial alignment and at opposite ends of a turbine housing. A tubular frame constitutes a passage sustaining fluid flow between the sections.

Safety device, including fusible member for rocket engine starting control (2,741,085). Spencer S. Prentiss, Bartlesville, Okla., assignor to Phillips Petroleum Co.

Fusible member mounted within the combustion chamber. When subjected to the combustion temperature of the fuel, the member melts and interrupts operation of valves in the fuel and oxygen conduits communicating with the chamber.

Controlling fuel supply for an aircraft turbine engine during acceleration at different altitudes (2,741,089). James H. Jagger, Coventry, England, assignor to Armstrong Siddeley Motors, Ltd.

Air/fuel ratio device for regulating the fuel supply at both steady and fluctuating speeds. A flow control depends upon atmospheric pressure changes with varying altitudes for its operation. A barometric means responsive to inlet pressure acts upon a choke in the delivery passage to vary its effective size.

EDITOR'S NOTE: The patents listed above were selected from recent issues of the Official Gazette of the U. S. Patent Office. Printed copies of patents may be obtained at a cost of 25 cents each, from the Commissioner of Patents, Washington 25, D. C.

New Equipment and Processes

Equipment

Electrical, Electronic

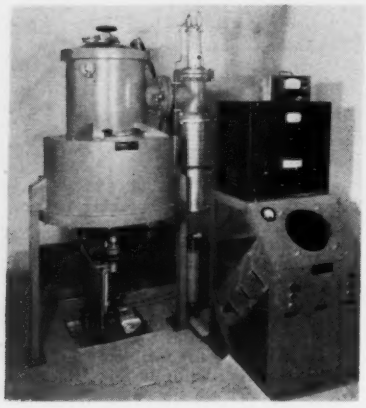
Transistor Battery. Mercury cell delivers 4 v for transistors and tubes. Tube Div., Radio Corp. of America, Harrison, N. J.

All Metal Heaters. Chromalox Metaray Lamp core with standard screw base. Figure 8 heating element is fully enclosed. 375–1200 w at 120–600 v. Edwin L. Wiegand Co., 7500 Thomas Blvd., Pittsburgh 8, Pa.

Pressure Transducer. Range of −1000 ft to +20,000 ft at 205–590 knots air speed. Components Div., Fairchild Controls Corp., 225 Park Ave., Hicksville, N. Y.

Waveguide Detector. For KU band, uses crystal bolometer or thermistor elements. Narda Corp., Mineola, N. Y.

Purge Type Thermocouple. Platinum-rhodium couple used for temperatures to 2900 F. Trinity Equipment Corp., 472 Westfield Ave., Roselle Park, N. J.



High Vacuum High Temp Furnace. Water cooled, graphite electrode for 2250–2700 C sintering or degassing at pressures below 1 micron Hg absolute. Vacuum Specialties Co., 77 Prospect St., Somerville 43, Mass.

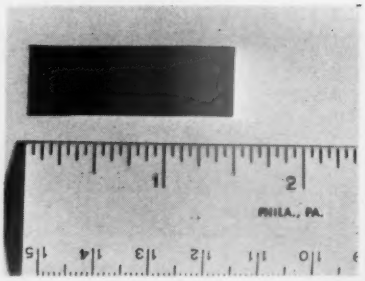
High Temperature Connector. For missile use, GHR1F-H withstands 2000 F. Electronic Div., Gorn Electric Co., Stamford, Conn.

Insulators. Kelon-T (Teflon), compression type, subminiature and miniature for high-frequency, high temp (−110 to +500 F), high voltage service. Shambam Engineering Co., 11617 W. Jefferson Blvd., Culver City, Calif.

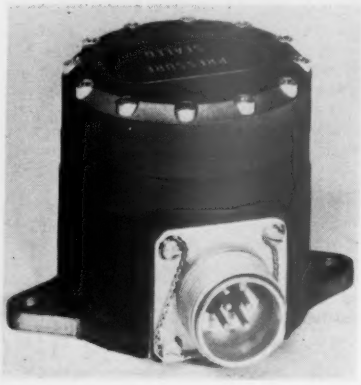
Silicon Diode. High sensitivity 1N23D as X-band mixer. Normal and reversed polarity. Discriminator Cavity, x-band TE 112 made of invar. Adjustable frequency splitting from 0 to 5 megacycles. Bomac Labs, Beverly, Mass.

Tandem Transistor. MT-1 features two dc-coupled transistors to form two-stage cascade. Marvelco Electronic Div., National Aircraft Corp., 3411 Tulare Ave., Burbank, Calif.

Precision Potentiometer. Series C-200, BC-200 ball bearing with sine-cosine function for servo and guided missile control. Dissipates 4 w, 2 in. high. DeJur Amsco Corp., 45-01 Northern Blvd., Long Island City 1, N. Y.



Strain Gages. Made of 0.0005-in. copper-nickel foil for use at normal temperatures. Baldwin-Lima-Hamilton Corp., Philadelphia 42, Pa.



Linear Accelerometer. For missile use, G22 series available in ranges from less than ±0.5 g full scale to more than 50 g's. Linearity is ±2% max. Power is 28 v dc at 1/2 w. Wide band d-c amplifier. Plug-in Type C23125 for scanning thermocouples or magnetic tape recording. Doelcam, Minneapolis-Honeywell, 1400 Soldier's Field Rd., Boston 35, Mass.



Miniature Load Cell. SR-4 for force up to 10,000-lb compression. Calibration accuracy is within ±0.25% full range at any load at 70 F. Resistance across power terminals is 120 ohms. Baldwin-Lima-Hamilton Corp., Philadelphia 42, Pa.

General Purpose Computer. LGP-30 is low cost, desk size. Memory unit stores 4096 words, 31 bits in length. Electric typewriter serves as input-output. Librascope, Inc., 808 Western Ave., Glendale, Calif.

Analog Computer. GEDA A14 has linear and nonlinear computing capabilities. Single or multiconsole configurations. Goodyear Aircraft Corp., Akron 15, Ohio.

Circuit Analyzer. Model 80 is automatic and tests 200 circuits in 20 sec. Checks connections, shorts, insulation. Functional Tester. Model 250F is designed for testing multiple relay systems. DIT-MCO, Inc., 505 W. 9th St., Kansas City, Mo.

Silcad Battery. Silver-cadmium battery cell, 6 amp-hr has a filled weight of 4.95 oz, volume of 5.05 cu in., delivers 1.25 v max, working voltage of 1.1. Yardney Electric Corp., 44 Leonard St., New York 13, N. Y.



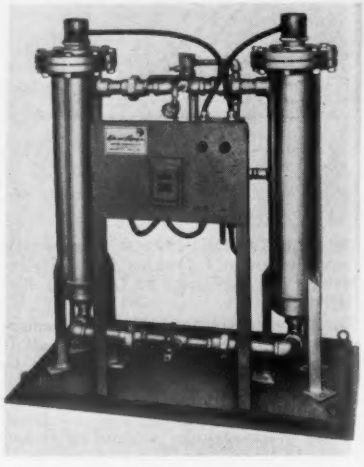
Low Cost Digital Computer. ALWAC III-E is medium speed, high capacity. Operates with punched cards, magnetic tape and automatic typewriter. Logistics Research, Inc., Redondo Beach, Calif.

Mechanical

Explosive Valve. Squib operated at 1/2 amp. Operating pressure 5000 psi, proof pressure 10,000 psi, 5 oz, 3 1/2 in. long. Explosive Products Div., Conax Corp., 7811 Sheridan Dr., Buffalo 21, N. Y.

Miniature Pressure Switch. Can be set within 2% at 2000–50,000 ft altitude. Rating is 10 amp ac or dc. Absolute or differential pressures. Aero Mechanisms, Dept. AW-6, Los Angeles, Calif.

Solenoid Operated Valves. Model 40 series for tube size of 1/4–1/2 in., 0–5000 psi, −65 to +275 F, flow rates up to 10 gpm. Explosion proof, stainless steel models for peroxide and acid. Mar Vista Engineering Co., 5420 W. 104th St., Los Angeles 45, Calif.



Compressed Gas Dehydrator. Twin adsorption towers can lower dew point to −50 F or lower. Six models, including high pressure, are available. Kahn & Co., 543 Windsor St., Hartford 1, Conn.

SCIENCE AND ENGINEERING

AT LOCKHEED MISSILE SYSTEMS DIVISION



THE OPERATIONAL APPROACH TO RELIABILITY

Scientists and engineers at Lockheed Missile Systems Division apply an operational approach to Reliability in all phases of missile systems research, development and operation.

Under the Lockheed philosophy of Reliability, scientists and engineers combine their talents to study: human factors; training; design and operational safety; ground support and maintenance systems; airborne systems reliability; statistical methods; components application, including electronic, electrical, electromechanical and mechanical systems and environmental conditions.

Those possessing keen interest in these and related fields are invited to write. Please address inquiries to the Research and Engineering Staff at Van Nuys.

Dr. Richard R. Carhart, Carl D. Lindberg, Reliability Staff Dept. Engineer, and Dr. O. B. Moan evaluate the functional and operational reliability effects of proposed revisions in the electrical power supply of a missile.

Lockheed

MISSILE SYSTEMS DIVISION

LOCKHEED AIRCRAFT CORPORATION

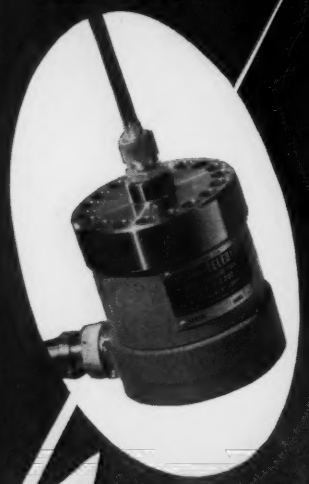
VAN NUYS • PALO ALTO • SUNNYVALE

CALIFORNIA

SUPERSONIC AGE

PRESSURE

Telemetering



Teledyne

BONDED STRAIN GAGE

ELECTRICAL PRESSURE TRANSMITTER

For research and testing on rockets, guided missiles and jets. Fifteen ranges, up to 10,000 P.S.I.

The Teledyne now enjoys an enviable reputation with aircraft research and test personnel for many reasons. This rugged instrument transmits high pressures for telemetering from hazardous to protected locations. Bonded strain gage construction makes the Teledyne insensitive to vibration or shock with extreme durability and high resolution. It is easily disassembled for clean-out and repairs. High frequency response, linear output over full pressure range. Temperature compensated for zero shift and sensitivity change. High overload ratings on standard instruments.

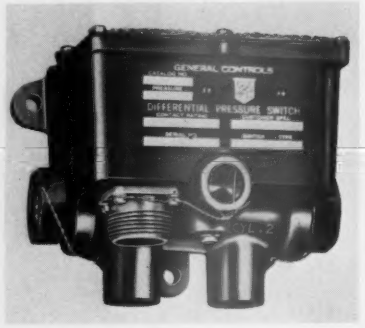
Write for Illustrated Literature

Taber

TABER INSTRUMENT CORPORATION
SECTION 00
211 Goundry St., N. Tonawanda, N.Y.

Oil-Hydraulic Selector Valve. Solenoid operated, pressure up to 4500 psi, temp to 300 F. Four-way closed center. Vickers, Inc., 1400 Oakman Blvd., Detroit 32, Mich.





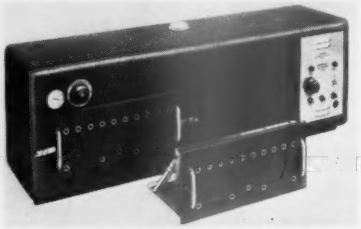
Pressure Switch. AL-58D weighs less than 8 oz, 3.5-in. overall for pressure limit control operation of pumps, systems. Piston reacts to 25–10,000 psi with 10% differential. Handles corrosives. Two-System Pressure Switch. AL-58N is adjusted at neutral. In unbalance at either line, switch detects, determines deviation, and actuates corrective feedback. General Controls, Glendale, Calif.

Test

Wind Tunnel Support. Hydraulically operated carriage. Oilgear Co., 15820 W. Pierce St., Milwaukee 4, Wis.

Pulse Timer. Supplies 1, 2, 4, 5, 8, or 10 pulses/sec for ballistic testing. Accuracy is 0.5%. Operates at −50 F to +150 F. Photographic Products Inc., 1000 N. Olive St., Anaheim, Calif.

Magnetic Recorder. Type PD-12 multichannel and amplifier for mobile use. Model 800 in 2–14 channels. Ampex Corp., 934 Charter St., Redwood City, Calif.



Portable Test Chamber. Model TC-2A is self-contained and low in cost. For temperature testing of instruments, electronic components, mechanical devices. Statham Development Corp., 12411 W. Olympic Blvd., Los Angeles 64, Calif.

AERODYNAMICISTS

Honeywell's Aeronautical Division, the largest manufacturer of automatic pilots and associated flight control equipment, is continuing its program of expansion and diversification.

■ Our aerodynamic analysis group currently has openings for qualified aeronautical engineers with background and interest in aerodynamic analysis of closed loop systems and their relation to boundary layer control, flutter, buffeting and inlet geometry control.

■ These positions provide a variety of unusually interesting opportunities as our equipment is already scheduled for a number of supersonic aircraft and missiles, offering exceptional diversification in the aerodynamic field.

CONSIDER THESE ADVANTAGES

■ Minneapolis, the city of lakes and parks, offers you metropolitan living in a suburban atmosphere. No commuting.

■ Your travel and family moving expenses paid.

■ Salaries, insurance-pension programs, plant and technical facilities are all first-rate.

WRITE TO US

If you are interested in a permanent position with a sound, diversified growth company, call collect or send your resume to Bruce Wood, Dept. JP-6-100, 2600 Ridgway Road, Minneapolis 13.

MINNEAPOLIS Honeywell

First in Controls

This "Big Stick" stops trouble before it starts

So powerful that it revises infantry strategy, the Douglas *Honest John* is an artillery rocket of tremendous destructive force and deadly accuracy.

Designed and built by Douglas Aircraft, Honest John moves into position on its own launching truck. This free-flight missile can carry the heaviest high explosive charge, or an atomic warhead in weather that grounds tactical air cover. Its very existence deters an enemy from massing for effective ground attack.



HONEST JOHN puts a mobile atomic weapon up front with the infantry

Development of Honest John by Douglas engineers fills a vital infantry need and provides new muscle for our armed forces. But the basic strength of any defense depends on the people manning it. Find out what an important future there is for *you* in U. S. Army service.

Depend on *DOUGLAS* **First in Aviation**

Openings in Florida . . . Instrumentation Engineers . . . up to $9,500

Electrical Engineers with experience in Radar, Telemetry, Timing or Communications.

•

Challenging problems associated with the precision instrumentation for tracking of high velocity missiles being tested over a course that extends thousands of miles.

•

Pleasant family living on Florida's Central East Coast. Unprecedented opportunities with world leader in electronics.

•

To arrange confidential interview, send resume to Box J, AMERICAN ROCKET SOCIETY, 500 Fifth Ave., New York 36, New York





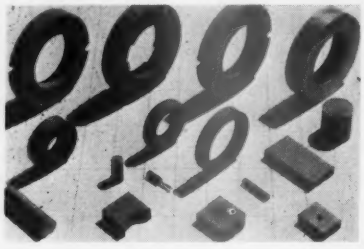
Evaporgraph. Infrared radiation is focused onto an oil film. Oil evaporates at a rate proportional to radiation received at each point, producing a thermal image which can be photographed in color. Temperature range of several thousand degrees F and sensitivity to about 0.2 F. Baird Associates, 33 University Rd., Cambridge 38, Mass.

Explosion Resisting Oven. For interior or exterior conditions which contain explosive or flammable vapors. Electric Hotpack Co., 5099 Cottman St., Philadelphia, Pa.

Materials

Copper Clad Steel. Available in 1, 2, or 3 ply. Copper cladding on low carbon, stainless, or invar. Joseph Kinney Co., Carnegie, Pa.

Hard Facing. Colmony no. 70 is a nickel, chromium, boron metal with high tungsten content for high temperature service. Wall Colmony Corp., 19345 John R St., Detroit 3, Mich.



Ceramic Magnets. Almost 100% electrical resistivity. Linear to 400 C. Made of barium and iron oxides. Specific gravity is 4.85. Can be machined after magnetizing. Electronics Components Div., Stackpole Carbon Co., St. Mary's Pa.

engineer, *ME, EE or AE*

CONTROLS DESIGN NUCLEAR AIRCRAFT ENGINES

First came the propeller, followed by the jet engine—and now, aircraft nuclear propulsion with its tremendous power potential. General Electric's ANP Department has a career opening for the qualified engineer who desires to achieve the professional stature his talents deserve.

The present position requires 1 to 3 years' experience in aircraft control or accessory systems design and application, and involves the design of turbine type engine controls. Both creative and analytical ability are desirable

Openings in Cincinnati, Ohio and Idaho Falls, Idaho

Address Replies stating salary requirements to location you prefer

W. J. Kelly
P.O. Box 132
Cincinnati, Ohio

L. A. Munther
P.O. Box 535
Idaho Falls, Idaho

GENERAL ELECTRIC

THE APPLIED PHYSICS LABORATORY of the JOHNS HOPKINS UNIVERSITY

offers an exceptional opportunity to qualified men who want to advance themselves professionally in the GUIDED-MISSILE field. The Laboratory has a reputation for the recognition and encouragement of individual responsibility and self-direction.

Our program of

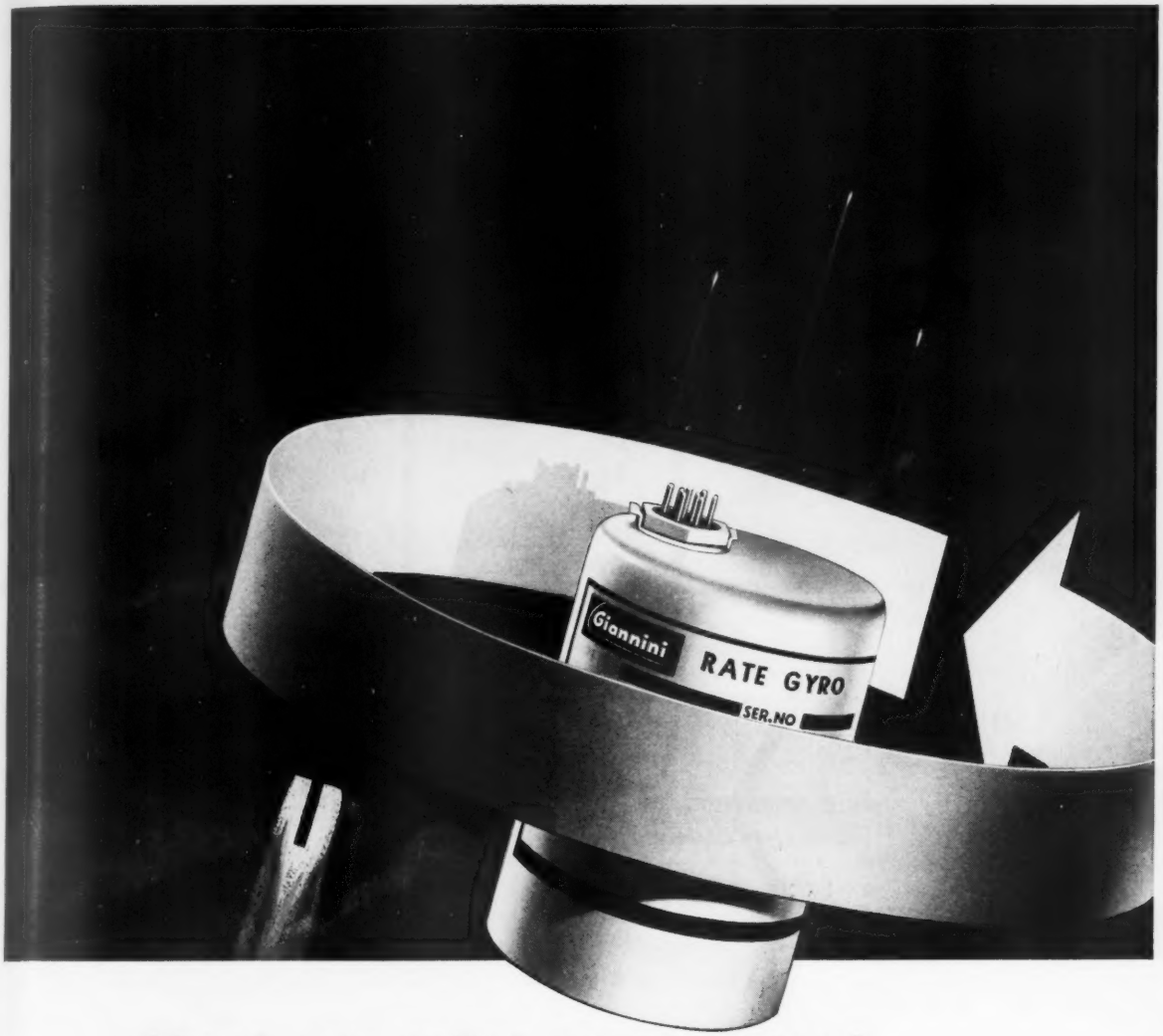
GUIDED MISSILE RESEARCH and DEVELOPMENT

provides such an opportunity for men in:

SUPERSONIC MISSILE DESIGN
WIND TUNNEL TESTS AND DATA ANALYSIS
RAMJET DESIGN AND ANALYSIS
CIRCUIT DESIGN AND ANALYSIS
ELECTRONIC PACKAGING
DESIGN, TEST, AND EVALUATION OF MISSILE SYSTEMS
FIELD TESTING OF RADARS AND GROUND SYSTEMS

Please send your resume to Professional Staff Appointments

APPLIED PHYSICS LABORATORY
THE JOHNS HOPKINS UNIVERSITY
8617 Georgia Avenue
Silver Spring, Maryland



NOW-30 DAY DELIVERY!

Thirty day delivery for the precision Giannini Model 36128 Rate Gyro is Real News!

This is the instrument that made Giannini *First Source* for rate gyros on the Navy's newest and fastest supersonic day fighter, and is standard equipment on many other high performance aircraft and missiles. A carefully planned production schedule based on confidence in the future of this proven instrument permits the unusually short lead time of only *one month* for delivery of the complex Model 36128.

This rugged (40g shock!) instrument is available in standard ranges from ±15°/sec to ±200°/sec. Electrical output proportional to rate is provided by a precision potentiometer which can supply high level output up to 70v requiring no amplification for most applications, and no demodulation where a dc signal is desired. Linearity is 1.5% or better. This small, 2-inch gyro can be obtained in a special, ruggedized version capable of withstanding shock up to 100g! Complete specifications and quotations are available at Giannini Sales Offices. Write for Bulletin 36128.

Giannini
Standard Model 36128

RATE GYRO

Application:
Flight Telemetering & Control,
Guided Missile & Aircraft

Features:
Ranges from ±15°/sec to ±200°/sec
Precision potentiometer output to 70V!
Linearity 1.5% or better
115V or 200V 3-phase 400 cps rotor
Oil filled and viscous damped
Thermostatically controlled heater
40g shock (up to 100g available)

Giannini **Gyro** DIVISION

NEW YORK 1, N.Y., Empire State Bldg., CHickering 4-4700
CHICAGO, Ill., 8 So. Michigan Ave., ANdover 3-5272
PASADENA, Calif., 918 E. Green St., RYan 1-7152

Engineering positions are open at several Giannini locations for career-minded young men—write for details.

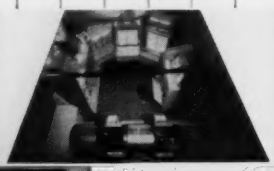
G. M. GIANNINI & CO., INC. 918 EAST GREEN STREET • PASADENA, CALIFORNIA

● Manufacturing ●● Manufacturing and product development ●●● Manufacturing, product development and research □●● Pilot manufacturing, product development and research

I	II	III	IV	V	VI	VII	VIII	IX	X	XI	XII	XIII	GPE CAPACITIES
●●●	●●	●●	□●●	●●	●●●		●●	●●●	●●	●●	●●	●●●	Precision Mechanics, Optical Devices, Ceramics
●●●	●	●			●●●		●●●	●●	●	●●	●	●●●	Electrical Equipment and Components
●●●	●●	●●●	●●●		●●●		●	●●		●●●	●●	●●●	Electronics
	●●			●●●		●●●				●●●			Hydraulics, Liquids Processing, Heat Exchange
●	●		●●●		●					●			Television: Studio, Theatre, Business, Institutional, Industrial
●●●	●	●●	□●●		●●●	●●●	●●	●●		●●●	●	●●●	Instruments, Servos, Controls: Hydraulic, Pneumatic, Magnetic, Electronic
●●●	●		●●●		●●●		●			●●	●	●●●	Aircraft and Missile Guidance, Control, Simulation
●●●	●	●	□●●		●●●					●●●		●●●	Automatic Computers and Components
●●●	●	●●	●●●		●●			●		●			Radar, Microwave, Ultrasonics
	●●●		□●●				●●	●●●	●●●		●●●		Motion Picture and Audio Equipment
●●●				●●						●●		●●●	Nuclear Power Components and Controls
●●●			●●●	●●●	●●●	●●●				●●●		●●●	SYSTEMS ENGINEERING



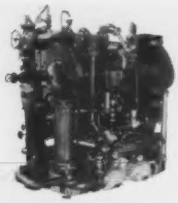
Librascope Desk-Size Computer



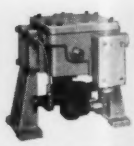
Link Aviation F-89D Jet Simulator



GPL Industrial-Institutional TV System



Griscom-Russell Shipboard Distilling Plant



Askania Electro-Jet Power Package

GPE → SYSTEMS ENGINEERING

The GPE Companies are leaders in that small, select group in American industry which is broadly qualified to develop and produce the systems needed today for defense and industry. GPE leadership accounts for some of the most advanced systems in use in business, television, aviation, marine, steel, oil, and other industrial fields.

In Systems Engineering, highly advanced capacities and resources are prerequisite. Yet, no matter how highly advanced, they are of little use if limited to a few areas. Finding optimum solutions to complex systems problems calls for *balanced competences*. And beyond that, success calls for the consistent application of such competences *at every stage* — beginning with research, and extending all the way through development, production and final testing.

No GPE company is limited by the boundaries of its own specialties. The basic GPE operating policy, GPE Coordinated Precision Technology, places at the command of each company in the group all GPE research, development and production facilities, and the skills and experience of the more than 2500 GPE technical men working in depth in the wide range of advanced capacities indicated in the chart above.

Behind each group working on a specific problem in one GPE company stands the whole group of GPE scientists, engineers and technicians with the answers — or the knowledge that will find the answers — to questions underlying and related to that problem. To the customers of GPE Companies this means that the concept and development of equipment, components and systems are not restricted or distorted by traditional allegiance to specific competences.

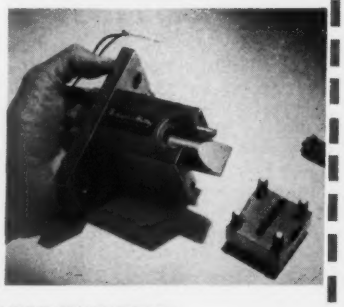
The five systems illustrated, while products of different GPE companies, are all examples of the consistent application of balanced competences, achieved through GPE coordination. For brochure describing GPE Coordinated Precision Technology and the work of the GPE Companies, or help on a specific problem, write: General Precision Equipment Corporation, 92 Gold Street, New York 38, N. Y.

GENERAL PRECISION EQUIPMENT CORPORATION

THE GPE PRODUCING COMPANIES

(I) KEARFOTT COMPANY, INC. (II) INTERNATIONAL PROJECTOR CORPORATION (III) BLUDWORTH MARINE
(IV) GENERAL PRECISION LABORATORY INCORPORATED (V) THE GRISCOM-RUSSELL COMPANY (VI) LINK AVIATION, INC.
(VII) SHAND AND JURS CO. (VIII) THE HERTNER ELECTRIC COMPANY (IX) THE STRONG ELECTRIC CORPORATION
(X) J. E. McAULEY MFG. CO. (XI) ASKANIA REGULATOR COMPANY (XII) AMPRO CORPORATION (XIII) LIBRASCOPE, INCORPORATED

PRE-PACKAGED
POWER
explosive-actuated devices



CABLE CHOPPER

Severs cable up to 1⅛ inches diameter, initiated over a simple electrical circuit requiring a minimum of 5000 ergs. One of several types used in missiles and aircraft for separating structural and electrical cables, oil lines, etc.



DISCONNECT

Combined into the body of an AN standard electrical plug and receptacle, this unit gives instantaneous opening of as many as 100 circuits on a non-shorting basis. Controlled time delay can be included.

Used in nearly all major missiles, Beckman & Whitley Explosive-Actuated Devices include standard items for many applications. A well-rounded organization of personnel and facilities provides for rapid modifications and adaptations to cover the needs of your special applications.
Completely integrated, pre-loaded packages are supplied ready for immediate use. Besides the Cable Chopper and Explosive Disconnect shown, the Beckman & Whitley line includes Explosive Bolts and Safety and Security Destructors.
Your special inquiries are invited for actuation problems involving large punch in a small package.

Beckman & Whitley INC.
SAN CARLOS 12, CALIFORNIA

expand metal
shrink metal
roll-form metal

Shown:

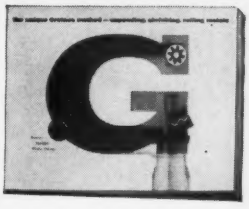
A jet engine ring as produced on GROTNES machines (except for welding).

G

GROTNES machines have been or can be designed to:

coil
trim
form
size

jet engine, missile and rocket parts.

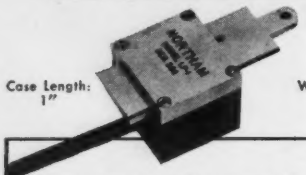


GET THIS FACT BOOK
explaining the GROTNES method of cold-forming metals.

GROTNES
MACHINE WORKS, INC.
5454 N. Wolcott Ave., Chicago 40, Ill., U.S.A.

NORTHAM

LINEAR POSITION TRANSDUCER



Case Length: 1"

Weight: 4 oz.

For conversion of linear motion or position into an electrical output for remote indication, recording, and control. The instrument is of the variable inductance type and provides precise measurements under extremes of acceleration as well as under static conditions. All electrical components are rigidly embedded in the case, permitting operation under shock and vibration conditions.

MODEL LP-1 SPECIFICATIONS:

Range of Motion:.....± ½ in. to ± 2 ins.
Accuracy:.....± 1% full scale
Excitation Frequency: From 60 to 20,000 cps

WRITE FOR BULLETIN NO. JP-1

Northam Engineering Facilities Are Available To Assist You With Any Application Problems.

NORTHAM PRODUCTS INCLUDE . . .
Transducers for pressure, acceleration and displacement measurement and auxiliary electronic equipment for complete systems.

NORTH AMERICAN INSTRUMENTS, INC.
2420 North Lake Avenue • Altadena, Calif.

ENGINEER

JET ENGINE EVALUATION AND FLIGHT TESTING

This position calls for a rare combination of leadership and technical knowledge. You'll be the liaison between advanced jet engine test and design teams at the Aircraft Gas Turbine Division of General Electric—the world's largest privately-owned aircraft propulsion center.

In addition to planning and participating in the flight testing of advanced jet engines, you will authorize expenditures of funds and recommend design and installation changes.

This is a stepping-off spot for enhancing your professional stature. Stimulating creative associates. Wide-ranging company benefits. High starting salary.

Please send resume to

Mr. Mark Peters
Technical Recruiting Building 100
Aircraft Gas Turbine Division

GENERAL ELECTRIC
Cincinnati 15, Ohio

Book Reviews

Ali Bulent Cambel, Northwestern University, *Associate Editor*

Fifth Symposium (International) on Combustion. Combustion in Engines and Combustion Kinetics, published for the Combustion Institute under the auspices of the Standing Committee on Combustion Symposia; Reinhold, New York; Chapman Hall, London, 1955, 802 pp., illus. $15.

Reviewed by GEORGE G. LAMB
Northwestern University

This publication of the 42 foreign and 59 USA papers presented at the Fifth Symposium held at the University of Pittsburgh in August 1954 offers a most authoritative and up-to-date body of knowledge on the combustion problems involved in the operation of all types of internal combustion reciprocating, turbojet, ramjet, and liquid and solid propellant rocket engines. Six invited papers on the unsolved problems of engine combustion point out that knock, smoke, odor, combustion instability, low efficiencies, and carbon formation are primarily still treated empirically; and much more theoretical and experimental work is needed to understand, to predict, and to improve performance of engines to meet the requirements being set by modern advances in propulsion systems. Five invited papers on the kinetics of combustion processes outline progress and problems of kinetics in high temperature reaction systems, chemical kinetics of hydrocarbon combustion, and very high space heat release rates.

The text and discussions of the remaining ninety papers presented at the Symposium outline clearly the current status and progress in theoretical and experimental investigations of the many interlocking facets involved in our understanding of combustion problems. Six papers deal with the preheating, vaporization, and combustion of droplets as affected by fuel droplet sizes, turbulence effects, ignition lags, and flame stability limits. Nine papers discuss ignition lags, burning rates, and temperature distributions of mono- and bipropellant systems. Six papers deal with the combustion or thermal decomposition of solids such as carbon, coal, and inorganic pyrotechnic materials. Physical and chemical mixing and reaction rates and the formation of carbon or smoke in diffusion flames are discussed in five papers. Eight papers report on combustion in engines: three on theoretical analyses of turbojet or ramjet combustors, and five on cool flames, autoignition and knock in reciprocating piston internal combustion engines. Special experimental techniques, using a shock tube, Langmuir probe, polarographic analysis, microwaves, and iodine absorption spectra for studying high temperature gas phase reactions, are described in five papers.

Forty-five contributions discuss many detailed experimental factors in the very complex field of the chemical kinetics of combustion of hydrocarbons and of non-hydrocarbon fuels. Reaction mechanisms involving radical chains, energy chains, chemical intermediates as activated complexes or chain breakers, the processes of energy transfer among the bonds within a complex fuel molecule, the effects of non-equilibrium distribution of molecular energies, and effects of atomic radiation on combustion reactions are considered. One of the review papers outlines the possibility that chemical reactions at high temperatures, as in flames, may be treated by simpler, generalized methods or mechanisms in contrast to the very detailed and complex mechanisms considered in most laboratory chemical kinetic studies at lower temperatures and pressures. The last five papers on flame spectra and dissociation energies discuss the use of spectroscopic investigations to identify the transient intermediate products and processes involved in combustion phenomena. Panel discussions on heterogeneous burning and on the status of the theory of the kinetics of combustion reactions conclude the Symposium.

Scientists and engineers interested in any aspect of combustion research or in very rapid chemical reactions should find this book a very stimulating and valuable source of up-to-date information. The authors and discussers point out many experimental and theoretical problems that need further study, and the Combustion Institute should be congratulated for the excellent, stimulating program of papers which they have published. This collection of papers in easily available form should aid workers interested in the field of combustion in selecting problems to provide answers for the incomplete portions of the field. By providing a better insight and broader perspective of the interlocking disciplines, this book should stimulate progress in the interpretation of accumulated facts to provide sound theories that will permit the greater utilization of deductive thinking in solving the many problems of combustion in engines, where research and applications are expanding at an exponential rate.

Theory of Aeroelasticity, by Y. C. Fung, John Wiley and Sons, Inc., New York, 1955, 490 pp. $10.50.

Reviewed by R. L. BISPLINGHOFF
Massachusetts Institute of Technology

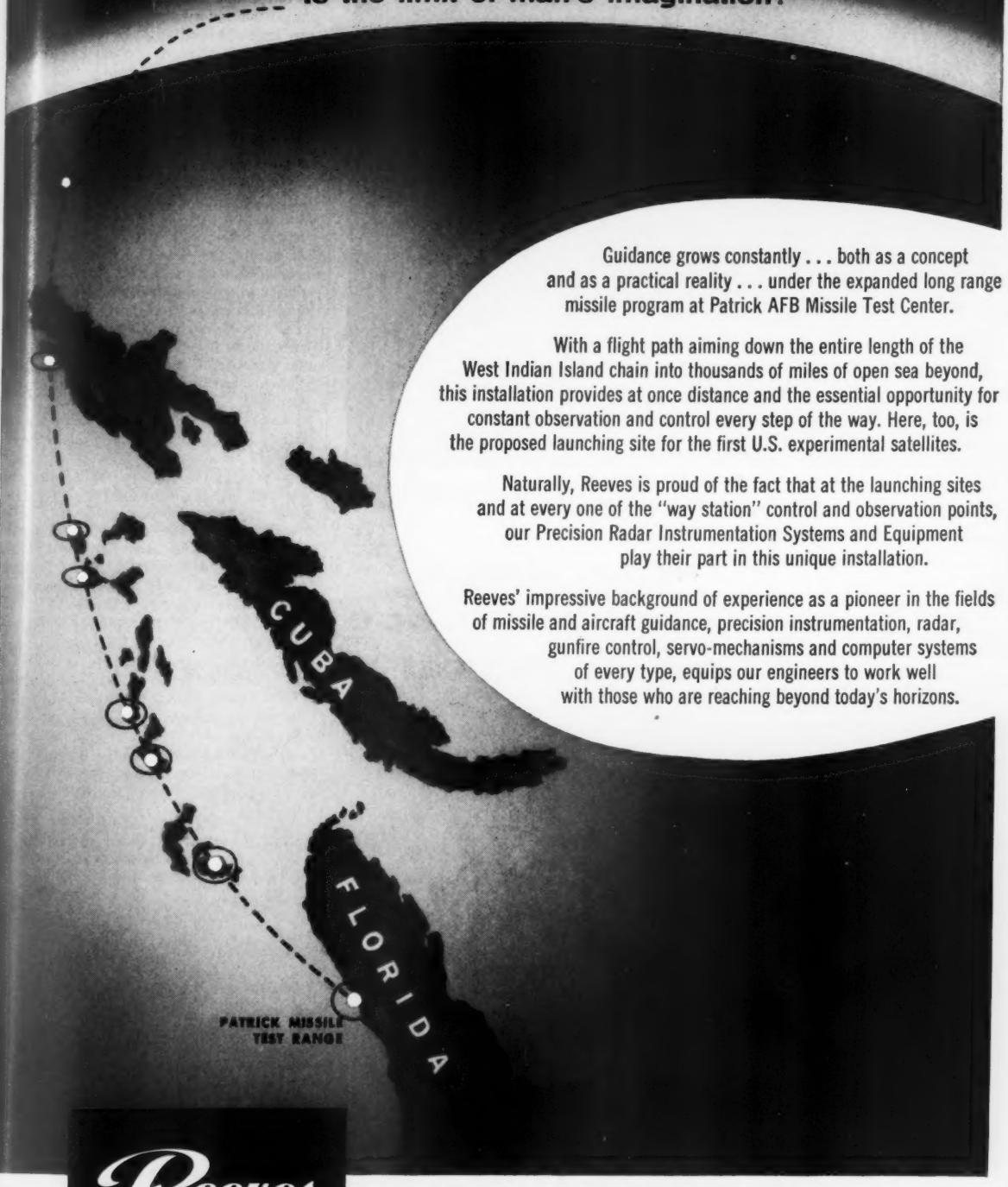
Dr. Fung can be congratulated for providing a clear introductory textbook on a rather complicated subject. His purpose has been to produce an introductory textbook on fundamental principles and not a book which is a compendium of information for practicing engineers. By restricting his aims in this way, Dr. Fung has succeeded admirably well in producing a relatively concise (490 pages) book which should find much use among students and engineers grappling with the subject for the first time.

After an introduction which emphasizes the stability aspects of aeroelastic problems, the first chapter covers certain preliminary information which must be established before any discussion of aeroelasticity can be commenced. This information

at PATRICK AFB Missile Test Range . . .

INSTRUMENTATION RADAR and GUIDANCE by Reeves INSTRUMENT CORPORATION

to the limit of man's imagination!



Guidance grows constantly . . . both as a concept and as a practical reality . . . under the expanded long range missile program at Patrick AFB Missile Test Center.

With a flight path aiming down the entire length of the West Indian Island chain into thousands of miles of open sea beyond, this installation provides at once distance and the essential opportunity for constant observation and control every step of the way. Here, too, is the proposed launching site for the first U.S. experimental satellites.

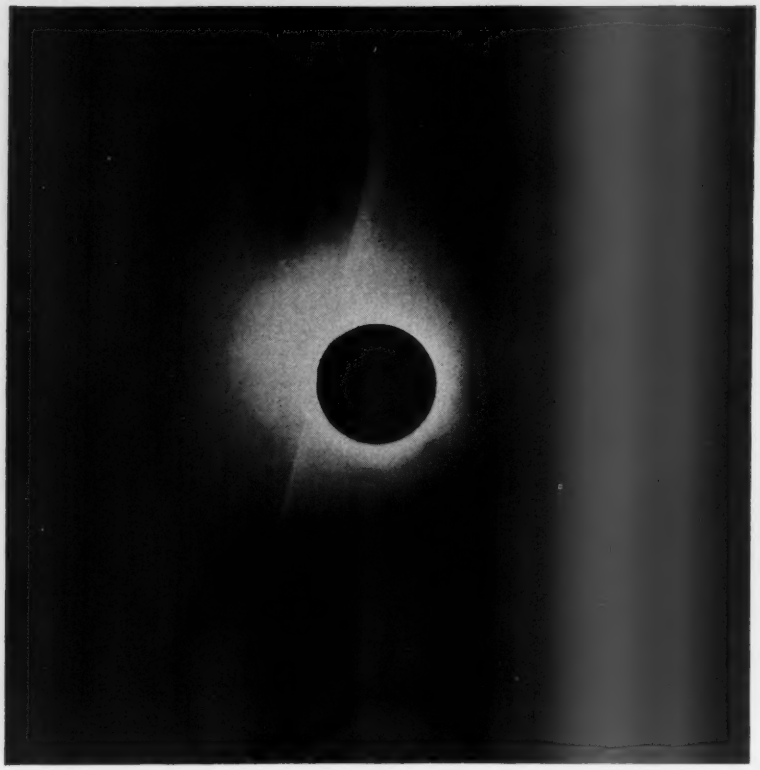
Naturally, Reeves is proud of the fact that at the launching sites and at every one of the "way station" control and observation points, our Precision Radar Instrumentation Systems and Equipment play their part in this unique installation.

Reeves' impressive background of experience as a pioneer in the fields of missile and aircraft guidance, precision instrumentation, radar, gunfire control, servo-mechanisms and computer systems of every type, equips our engineers to work well with those who are reaching beyond today's horizons.

Reeves INSTRUMENT CORPORATION

6RV56AR

REEVES INSTRUMENT CORPORATION
A Subsidiary of Dynamics Corporation of America
215 East 91st St., New York 28, N. Y.



what does
outer space
mean to you?

Because of an unmatched record of scientific experience in upper-air research as builders of the Viking Rocket series for the Navy, Martin was awarded the prime contract on the project known as ESV VANGUARD—the Earth Satellite Vehicle that will take its place in history as man's first exploratory step in the conquest of the final frontier, space itself.

What does space mean to you as an engineer?

Today, no other aircraft company in the world can give you more penetrating answers to that question. And tomorrow...

If you are interested in the greatest engineering adventure of our time, contact J. M. Hollyday, Dept. JP-06, The Martin Company, Baltimore 3, Maryland.

MARTIN

relates to elasticity, aerodynamics and mechanical vibrations. Since this chapter is relatively short (55 pages) these matters cannot, of course, be discussed in great detail. The balance of the book, following Chap. 1, is divided into two parts. Chaps. 2 through 11 contain a survey of aeroelastic problems, their historical background, basic physical concepts, and the principles of analysis. Chaps. 12 to 15 contain the fundamentals of oscillating airfoil theory and a brief summary of experimental results.

Chap. 2 is of interest to those not in the aeronautical engineering field in that it discusses problems of aeroelasticity in civil and mechanical engineering. The principal problems of aeronautical interest are developed in Chaps. 3 to 11. These include unusually clear and comprehensive discussions of static aeroelastic problems, flutter, dynamic loading, buffeting, and stall flutter. In the latter problems, statistical concepts and techniques are emphasized. The theory of aeroelasticity is concluded in Chap. 11 with a general formulation and a brief discussion of the basic mathematical characteristics. This is one of the most valuable chapters in the book since the author manages to skillfully focus the attention of the reader on the mathematical character of the equations of aeroelasticity.

Any engineer who has grappled with the intricacies of unsteady aerodynamics will welcome the discussion of aerodynamics of oscillating airfoils given in Chaps. 12 through 15. This is a subject which, for some strange reason, is given very little attention in textbooks on aerodynamics. The aeroelastician has heretofore been forced to use various technical reports as a source of fundamental information. Textbook coverage, even though it is of a brief and introductory nature, will form a valuable addition to the literature.

It should be of interest to those in the jet propulsion field engaged in turbine blade design that the subject of stall flutter is treated rather thoroughly in Chap. 9.

The author has included selected references which are readily accessible to the general reader.

Solid Propellant Rockets, by Alfred J. Zaehringer, American Rocket Co., Box 1112, Wyandotte, Mich., 1955, 162 pp. $4.

Reviewed by G. M. Platz
Armour Research Foundation

This book presents a comprehensive fundamental introduction and a historical review of the evolution of solid propellant rockets. It provides the newcomer with an over-all general description of the formulation, testing, ballistic, and application problems, both past and present, in the field of solid propellants.

Should the reader so desire, the numerous references cited in this paper-bound book will permit a more detailed investigation of the intricacies of the specific problem in question. The author has included a glossary and a list of symbols which will provide the reader with a general definition of the terms and equations cited in this book.

AERONAUTICAL ENGINEERS

Aerodynamicists

Research engineers are needed to formulate and carry out complex research in aerodynamic, aerothermodynamic and gas dynamic theory.

Typical problems relate to hypersonic missile aerodynamics and aerodynamic heating; high energy gas dynamics equipment such as shock tubes and rotating wave machines, and fundamental fluid dynamics.

Write for our new brochure "A DECADE OF RESEARCH."

CORNELL AERONAUTICAL Laboratory, Inc.
4354 GENESEE ST. BUFFALO 21, N. Y.

ENGINEER

HIGH LEVEL SPECIALIST IN STRESS ANALYSIS

The Aircraft Gas Turbine Division of General Electric is looking for a high level specialist who can serve as a recognized authority in design initiation and review.

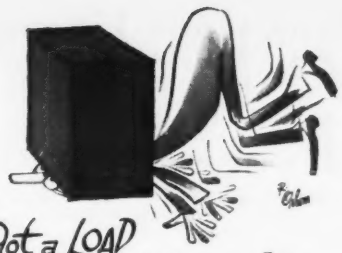
You should be familiar with advanced practice and theory in thin gauge sheet design—stress resulting from gas loading—high temperature and high rotational speed—all areas of which call for new materials application and creative design (NOT BOARD WORK, of course).

The professional environment is excellent. Wide-ranging company benefits. High starting salary.

Please send resume to:

Mr. Mark Peters
Technical Recruiting Building 100
Aircraft Gas Turbine Division

GENERAL ELECTRIC
Cincinnati 15, Ohio



Got a LOAD on Your mind?

Burdened down with a problem in design diminution, weight reduction, power capsulation? lighten the load on your mind; send for the amazing story of how MPB's*



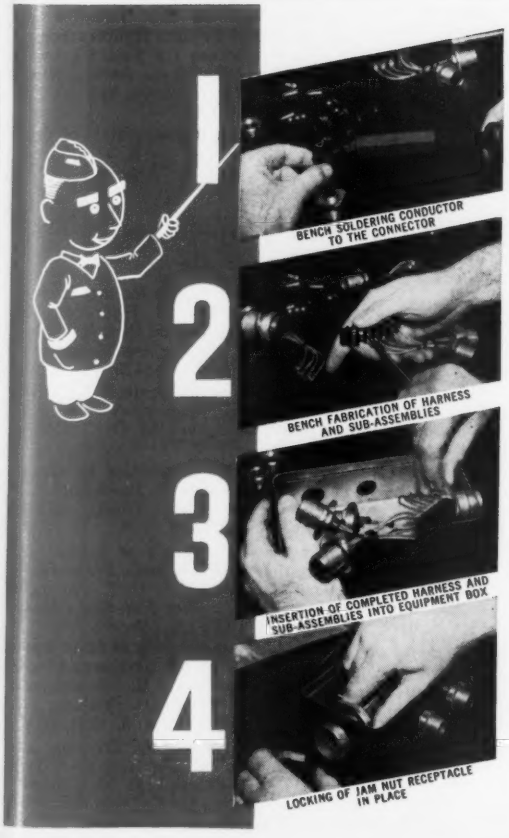
such as these BALL BEARINGS ACTUAL SIZE

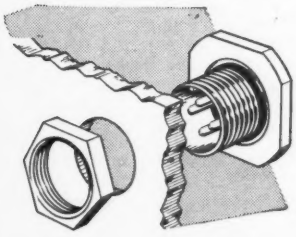
make designing a breeze.

*MINIATURE PRECISION BEARINGS, INC.
20 Precision Park, Keene, N. H.

Please send MPB's new Catalog to

Name.....Title.....
Company.....
Street.....
City.....Zone.....State.....





Bendix

JAM NUT RECEPTACLES

Easy to install, to service, to replace

Jam nut receptacles offer such positive savings in assembly time that it will pay you to check into their application on your product. These receptacles permit bench wiring of harness and sub-assemblies prior to final installation with proven savings in assembly labor.

Just consider these design advantages—only one mounting hole required per receptacle—no extra gasket required—no user problem of sealing around screw holes—no extra hardware necessary such as screws, washers or nuts.

Write for complete detailed specifications

Bendix SCINTILLA DIVISION Bendix AVIATION CORPORATION
SIDNEY, NEW YORK

Export Sales and Service: Bendix International Division, 205 East 42nd St., New York 17, N. Y.

Technical Literature Digest

M. H. Smith, *Associate Editor*, and M. H. Fisher, *Contributor*
The James Forrestal Research Center, Princeton University

Jet Propulsion Engines

Performance Characteristics of Cylindrical Target-Type Thrust Reversers, by Fred W. Steffen and Jack G. McArdle, *NACA RM* E55I29, Jan. 1956, 40 pp.

Velocity Tests of NRL Valve Pulsejet and Whirling Loss Evaluation, by C. D. Porter and M. A. Persechino, *Naval Res. Lab. Rep.* 4621, Nov. 1955, 17 pp.

The Armstrong-Siddeley Sapphire, *Flight*, vol. 69, Jan. 6, 1956, pp. 17–22.

Influence of Diffuser and Afterburner Total Pressure Drops on Theoretical Turbojet Thrust, by J. C. McAtee, *Wright Air Dev. Center, Power Plant Lab.*, TN-55-568, Sept. 1955, 22 pp.

Evaluation Testing of a Gas Turbine, by R. A. Harmon and J. H. Bonin, *Ill. Inst. Tech., Armour Res. Found, Final Rep.*, March 1955, 1 vol.

Analytical Investigation of Turbines With Adjustable Stator Blades and Effect of These Turbines on Jet Engine Performance, by David H. Silvern and William R. Slivka, *NACA RM* E50E05, July 1950, 51 pp. (Declassified from Restricted, 1954.)

Preliminary Correlation of Efficiency of Aircraft Gas Turbine Combustors for Different Operating Conditions, by J. Howard Childs, *NACA RM* E50F15, Sept. 1950, 40 pp. (Declassified from Confidential, Feb. 10, 1956.)

Some Effects of Blade Trailing-Edge Thickness on Performance of a Single-Stage Axial-Flow Compressor, by J. J. Moses and G. K. Serovy, *NACA RM* E51F28, Oct. 1951, 14 pp. (Declassified from Confidential, Feb. 10, 1956.)

Turbo Powerplants in Pressure-Jet Convertiplanes, by Charles J. Fletcher, *Aero Digest*, vol. 72, Feb. 1956, pp. 40–42, 44, 45.

How to Match Ramjet Inlets and Performance, by A. N. Thomas, *Aviation Age*, vol. 25, Feb. 1956, pp. 24–31.

Microjet . . . Pneumatically Controls Jet Engines, by W. E. Reed, *SAE J.*, vol. 64, Feb. 1956, pp. 21–22.

Allison T56 Turboprop Features Flexibility, by John B. Wheatley, D. G. Zimmerman, and R. W. Hicks, *SAE J.*, vol. 64, Feb. 1956, pp. 23–26.

High Temperature Problems Featured at Turbojet Engine Symposium (Turbojet Engine Hydraulic Symposium, Detroit, Feb. 1956), *Appl. Hydraulics*, vol. 9, Mar. 1956, pp. 118–120, 122, 124.

Planning Pays in Turbine Maintenance, by H. A. McGill and J. H. Zylko, *Petrol. Refiner*, vol. 35, Jan. 1956, pp. 140–143.

How to Reduce Compressor Downtime, by J. J. Julian and R. A. Schaefer, *Petrol. Refiner*, vol. 35, Jan. 1956, pp. 129–132.

Jet Engines—What Price Power?, by V. L. Schatz, A. L. Wynn, and R. W. Remke, *SAE Prepr.* 669, Jan. 1956, 5 pp.

Compressor and Turbine Matching Considerations in Turboprop Engines, by Elmer H. Davidson, *SAE Prepr.* 695, Jan. 1956, 4 pp.

Foreign Object Ingestion in Turbojet Engines, by H. E. Card and R. L. Mathias, *SAE Prepr.* 702, Jan. 1956, 4 pp.

Fuel Control and Burning in Aero-Gas-Turbine Engines, by E. A. Watson, *Chartered Mech. Engr.*, vol. 3, Feb. 1956, pp. 91–127.

Heat Transfer and Fluid Flow

Experimental and Calculated Temperature and Mass Histories of Vaporizing Drops, by M. M. El Wakil, R. J. Priem, H. J. Brikowski, P. S. Myers, and O. A. Uyehara, *NACA TN* 3490, Jan. 1956, 82 pp.

Investigation of the Far Noise Field of Jets. I. Effect of Nozzle Shape, by Edmund E. Callaghan and Willard E. Coles. **II. Comparison of Air Jets and Jet Engines,** by Willard D. Coles and Edmund E. Callaghan, *NACA TN* 3590 and 3591, Jan. 1956, 44 and 19 pp.

The Thermal Conductivity of Liquid and Gaseous Oxygen, by H. Ziebland and J. T. A. Burton, *Brit. J. Appl. Phys.*, vol. 6, Dec. 1955, pp. 416–421.

Radiant Heat Transfer Between Infinite Parallel Plates, *Nat. Bur. Standards, Rep.* 4239 (Progress Rep.), Aug. 1, 1955, 19 pp.

A Note on the Cooling of Turbine Rotor Blades by Water Jets, by K. R. F. Kenworthy, *Gt. Brit. Nat. Gas Turbine Estab. Mem.* M.227, Oct. 1954, 6 pp.

Flow Equations for Multicomponent Fluid Systems. I. General Equations. II. Binary Boundary Layer Equations, by N. A. Hall, *Minnesota Univ. Inst. of Tech. TR* 2 on Theoretical and Experimental Investigations on Mass Transfer Cooling, Aug. 22, 1955, 33 pp.

Analytical Design of a Family of Supersonic Nozzles by the Friedrichs Method Including Computation Tables and a Summary of Calibration Data, by J. R. Baron, *Wright Air Dev. Center*, TR 54-279, June 1954, 425 pp.

Analysis of Turbulent Heat Transfer, Mass Transfer and Friction in Smooth Tubes at High Prandtl and Schmidt Numbers, by Robert G. Deissler, *NACA Rep.* 1210, 1955, 14 pp.

Dynamics of Vapor Bubbles and Boiling Heat Transfer, by H. K. Forster, *Amer. Inst. Chem. Engrs. J.*, vol. 1, Dec. 1955, pp. 531–535.

Combustion

Theories of Detonation and Burning, by Carl V. Bertsch, *Picatinny Arsenal, Samuel Feltman Ammunition Labs., Tech. Rep.* 2268, Jan. 1956, 12 pp.

Characteristics of Turbulent Combustion by Flame Space and Space Heating Rates, by D. M. Simon and P. Wagner, *Indust. Engng. Chem.*, vol. 48, Jan. 1956, pp. 129–133.

Combustion Oscillations in Ducted Burners, by J. C. Truman and R. T. Newton, *Gen. Electric Co., Tech. Rep.* R55SE48, Aug. 1, 1955, 33 pp.

Combustion with Ozone-Modification of Flame Speeds; C_2 Hydrocarbon-Air Mixtures, by M. E. Gluckstein, R. B. Morrison, and others, *Univ. of Mich., Engng. Res. Inst., Rep.* 2279-1-T; *Off. Sci. Res. TN* 55-227, Aug. 1, 1955, 16 pp.

Investigation of Jet Flameholders. Quarterly Progress Report no. 1, April 1–July 1, 1955, *Stanford Res. Inst.*, July 12, 1955, 12 pp.

Solution of Thermochemical Propellant Calculations on a High Speed Digital Computer, by Arthur J. Donegan and Milton Farber, *Calif. Inst. Technology, Jet Propulsion Lab., Mem.* 20-114, Sept. 1955, 20 pp.

New Instrumentation for Engine Combustion Studies, by J. A. Warren and J. B. Hinkamp, *SAE Prepr.* 682, Jan. 1956, 12 pp.

Effect of Inlet Oxygen Concentration on Combustion Efficiency of J33 Single Combustor Operating With Gaseous Propane, by Charles C. Graves, *NACA RM* E53A27, March 1953, 22 pp. (Declassified from Confidential, Feb. 10, 1956.)

Effect of Oxygen Concentration of the Inlet Oxygen-Nitrogen Mixture on the Combustion Efficiency of a Single J33 Turbojet Combustor, by Charles C. Graves, *NACA RM* E52F13, Aug. 1952, 45 pp. (Declassified from Confidential, Feb. 10, 1956.)

Preliminary Correlation of Efficiency of Aircraft Gas Turbine Combustors for Different Operating Conditions, by J. Howard Childs, *NACA RM* E50F15, Sept. 1950, 40 pp. (Declassified from Confidential, Feb. 10, 1956.)

Effect of Spark Repetition Rate on the Ignition Limits of a Single Tubular Combustor, by Hampton H. Foster, *NACA RM* E51J18, Dec. 1951, 12 pp. (Declassified from Confidential, Feb. 10, 1956.)

Artificial Ignition at Low Pressures, by H. Guenoche, E. Freling, and P. Dugleux (in French), *Inst. Francais du Petrole, Rev. et Ann. Combustibles Liquides*, vol. 10, Oct 1955, pp 1209–1223

Investigations on the Oxidation and Auto-Ignition of Paraffin Hydrocarbons in the Gaseous Phase (in French), by E. Freling, *Inst. Francais du Petrole, Rev. et Ann. Combustibles Liquides*, vol. 10, Oct. 1955, pp. 1224–1279.

A Study of the Fundamentals of Combustion, by S. A. Weil and R. T. Ellington, *Inst. Gas Technology, Rep.* no. 1, Feb. 1956.

Fuels, Propellants, and Materials

Recommended Values for the Thermodynamic Properties of Hydrogen and Deuterium Peroxides, by Paul A. Giguere and I. D. Liu, *J. Amer. Chem. Soc.*, vol. 77, Dec. 20, 1955, pp. 6477–6479.

The Reactivity and Structure of Nitrogen Dioxide, by Peter Gray and A. D. Yoffe, *Chem. Revs,*, vol. 55, Dec. 1955, pp. 1069–1154.

Nitrogen Oxide Impurities in Ozone, by B. E. Saltzman, D. H. Byers, and F. L. Hylsop, *Indust. Engng. Chem.*, vol. 48, Jan. 1956, pp. 115–118.

Heat Capacity, Heats of Fusion and Vaporization, and Vapor Pressure of Decaborane ($B_{10}H_{14}$), by G. T. Furukawa and R. P. Park, *J. Res. Nat. Bur. Stands.*, vol. 55, Nov. 1955, pp. 255–260.

Volatility Characteristics of Eight Types of Turbine Fuel at Temperatures to 450° F, by A. J. Rothenberg, H. Edwards, and E. W. Woodell, *Thompson Products, Inc. Rep.* ING. ER-176, June 15, 1954, 66 pp.

Solubility of Nitrogen, Oxygen, and Carbon Dioxide in JP-4 and JP-5 Type Fuels, by A. R. Polishuk, R. M. Kennedy, and J. L. Jezl, *Sun Oil Co. Rep.* RD-2166, May 9, 1955, 138 pp.

ACTUATORS

By... NEWBROOK MACHINE CORP

SILVER CREEK, NEW YORK.



An effective combination of design, know how and precise workmanship have made available this linear actuator. This rugged, compact, dependable unit has proven able to perform under the most adverse conditions and temperature changes.

In this particular design, overloads on the drive tube, in both directions of the stroke, actuate a short stub shaft, compressing the spring and operating a limit switch which is connected to the power source.

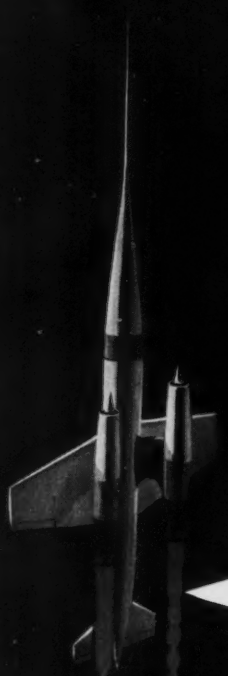
New heights of performance demand new standards of precision and dependability. Bring your next actuator design problem to us.

Call or phone:

NEWBROOK MACHINE CORP.

SILVER CREEK, NEW YORK

PHONE: 44



INDIVIDUAL PROFESSIONAL DEVELOPMENT

for engineers in supersonic propulsion

Marquardt, the leader in supersonic propulsion, has inaugurated a program of Individual Professional Development for its engineers. You can help us maintain this leadership for the future of supersonic propulsion.

I.P.D. gives our engineers a chance to advance to their maximum potential in their present fields... and those beyond... in a climate of continuing professional growth from in-plant courses and more than fifty current courses in Southern California's leading universities. New courses are constantly being added.

I.P.D. differs in its concept and objectives from ordinary company training programs in that it gives each engineer an opportunity to grow and plan his development toward his own goal and at his own pace rather than having to follow a rigid predetermined pattern.

I.P.D. is a part of an overall expansion program which anticipates a two-fold increase in personnel during the current year. This increase represents many additional engineering opportunities. You can become a leader in supersonic propulsion. Write for details.

marquardt AIRCRAFT CO.

Attention: Professional Personnel
Industrial Relations Department • 16556 Saticoy St., Van Nuys, California
MARQUARDT BUILDS THE POWERPLANT FOR THE BOMARC IM-99 INTERCEPTOR MISSILE

Summary Report on Work Accomplished on Contract AF 33(600)-18875 (Development of a White Fuming Nitric Acid Combination Shipping, Storage and Jettison Tank), *Wright Air Dev. Center, Power Plant Lab. TN*-55-162, June 8, 1955, 18 pp.

Explosive Classification Tests for CPN Propellant. *Phillips Petrol. Co., Rep.* 703-1-55RF, 1955, 188 pp.

Hydrides and Borohydrides of Light Weight Elements and Related Compounds, by H. I. Schlesinger and G. Urry, *Chicago Univ., Annual Tech. Rep.*, Aug. 1, 1954–July 31, 1955, 48 pp.

Jet and Rocket Applications of the New Metals, Part II, by G. D. Johnson, *J. Space Flight*, vol. 8, Jan. 1956, pp. 1–6.

Using Turbine Fuels at Low Temperatures, by H. Strawson, *Shell Aviation News*, No. 210, Dec. 1955, pp. 8–12.

Research on the Safety Characteristics of Normal Propyl Nitrate, *Bur. Mines, Div. Explosives Tech., Prog. Rep.* 2, Nov.-Dec. 1955, 6 pp.

High Temperature Resistant Ceramic Coatings, Ceramic and Metal Ceramic Bodies, by C. L. Hoenig, B. D. Roesch, and others, *Illinois Univ., Quart. Prog. Rep.* 4, March 26, 1955, 16 pp.

A Study of the Effects of Porosity-Hole Erosion in Cast-Steel Rocket Chamber Parts, by A. Kitzmiller and J. Hodges, *Hercules Powder Co., Allegany Ballist. Lab., Rep.* ABL/X-3, Jan. 1955, 9 pp.

Future of Synthetic Liquid and Gaseous Fuels, by Howard R. Batchelder and Harlan W. Nelson, *Mech. Engng.*, vol. 78, Jan. 1956, pp. 11–14.

Space Flight, Astrophysics, Aerophysics

The Surface Temperature Climate of Mars, by Frank Gifford, Jr., *Astrophys. J.*, vol. 123, Jan. 1956, pp. 154–161.

Electrical Conductivity of the Lower Chromosphere of the Sun, by S. Magasawa, *Pub. Japan Astron. Soc.*, vol. 7, no. 9, 1955. (Abstract in *Rep. Ionosphere Res. in Japan*, vol. 9, no. 4, 1955, p. 222.)

Measurement of Temperature at Elevations of 30 to 80 Kilometers by the Rocket Grenade Method, by M. Ference, W. G. Stroud, J. R. Walsh, and A. G. Weiser, *J. Meteorol.*, vol. 13, Feb. 1956, pp. 5–12.

The Face of the Sun, by H. W. Newton, *London Times Rev. Sci.*, No. 19, Spring 1956, pp. 6–9.

Young Stars, by Adrian Blauw, *Sci. Amer.*, vol. 194, Feb. 1956, pp. 36–41.

The Earth Satellite Program, by Joseph Kaplan and Hugh Odishaw, *News Rep. Nat. Acad. Sci.*, vol. 6, Jan.-Feb. 1956, pp. 1–3.

A Rocket Measurement of Upper Atmosphere Density by Paschen's Law, by H. L. Smith, H. C. Early, and N. W. Spencer, *Mich. Univ., Engng. Res. Inst., Sci. Rep.* CS-3, May 1955, 41 pp.

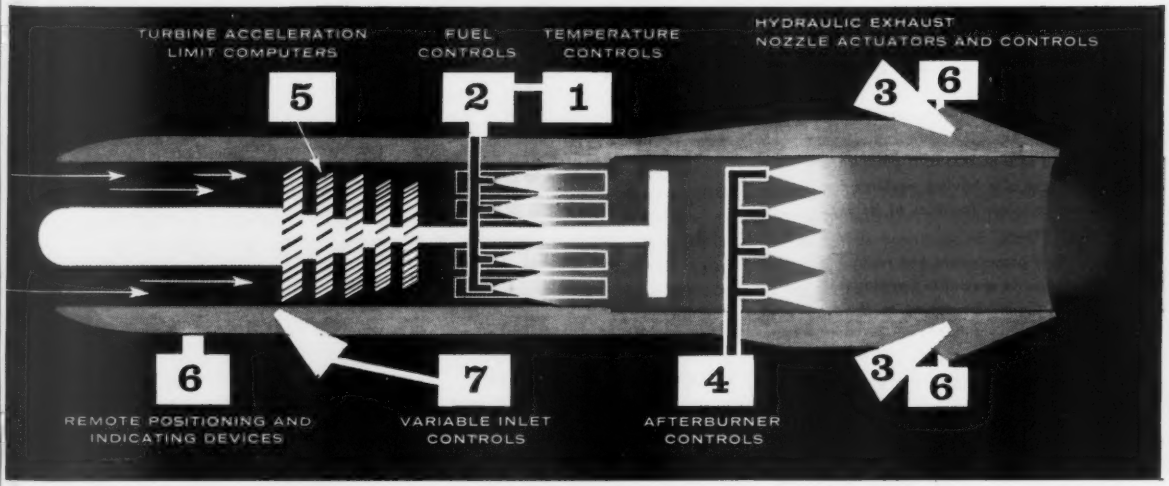
Near Infrared Transmission Through Synthetic Atmospheres, by John Nelson Howard, Darrell L. Burch, and Dudley Williams, *AF Cambridge Res. Center, Geophysics Res. Papers* no. 40, Nov. 1955, 244 pp.

Conference on Atmosphere Elasticity, May 1954, Proceedings, *AF Cambridge Res. Center, Geophysics Res. Papers* no. 42, Nov. 1955, 244 pp.

Observations on Stars and Heavy Primaries Recorded in Emulsions Flow in Viking Rocket No. 9, by Herman Yagoda, *Can. J. Phys.*, vol. 34, Jan. 1956, pp. 122–146.



CONTROL SYSTEMS FOR ADVANCED JET ENGINES



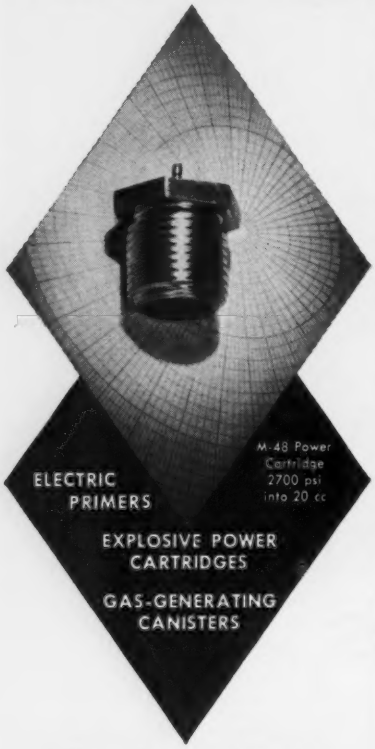
With the increasing speed of aircraft it has become more important to integrate power plant controls with the airplane and its mission. For over 10 years Sperry engineers have been actively engaged in developing complete control systems for turboprop, turbojet and ramjet engines. Our Aeronautical Equipment Division will be happy to help solve your engine control problems.

Engineers are required to man various exciting programs in engine control development. Write J. W. Dwyer, 1B5.

SPERRY GYROSCOPE COMPANY
Great Neck, New York
DIVISION OF SPERRY RAND CORPORATION

CLEVELAND • NEW ORLEANS • BROOKLYN
LOS ANGELES • SAN FRANCISCO • SEATTLE
IN CANADA: SPERRY GYROSCOPE COMPANY OF CANADA, LIMITED, MONTREAL, QUEBEC

SQUIB SPECIALISTS



An organization specializing in the design, development, and manufacture of explosive ordnance, McCormick Selph places first emphasis on dependability. The entire group is located in a 60,000-sq-ft plant on a 200-acre site having perhaps the most complete facilities of its kind in existence.

Your procurement and reliability problems in specialized explosives* can probably be solved at McCormick Selph — either with standard items, tried and proved, or with units produced to meet your specific need.

Send for data or submit your problems to:

* Ignition
Actuation
Ejection
Fracturing

McCORMICK SELPH ASSOCIATES
HOLLISTER 2, CALIFORNIA

A Quicker Method for the Conquest of Space, Part I, by Theodore B. Dufur, *J. Space Flight*, vol. 8, Feb. 1956, pp. 1–6.

Measurement of Winds at Elevations of 30 to 80 Kilometers by the Rocket Grenade Experiment, by Allen G. Weisner, *J. Meteorol.*, vol. 13, Feb. 1956, pp. 30–39.

The Geomagnetic Latitude Effect on the Nucleon and Meson Component of Cosmic Rays at Sea Level, by D. C. Rose and J. Katzman, *Can. J. Phys.*, vol. 34, Jan. 1956, pp. 1–19.

Meteor Echo Durations and Visual Magnitudes, by Peter M. Millman and D. W. R. McKinley, *Can. J. Phys.*, vol. 34, Jan. 1956, pp. 50–61.

Atomic Energy

Nuclear Energy Power-Plants, *Aeroplane*, vol. 90, Jan. 13, 1956, pp. 48–49.

More About Nuclear-Powered Aircraft, *Aeroplane*, vol. 90, Jan. 20, 1956, pp. 92–93.

Evaluation of the Nonlinear Kinetic Behavior of a Nuclear Power Reactor, by R. C. Howard, *Trans. ASME*, vol. 78, Jan. 1956, pp. 163–169.

Testing of a Reactor to Destruction: Inherent Safety of Nuclear Power Plants, by Joseph R. Dietrich, *Engng.*, vol. 181, Jan. 13, 1956, pp. 36–37.

Heat Transfer in Reactors Cooled and Moderated by Water, by M. Altman, *Nucleonics*, vol. 14, Feb. 1956, pp. 66–73.

Pyroprocessing for Nuclear Fuels, by Robert C. Reid, Dick Duffey, and J. Edward Vivian, *Nucleonics*, vol. 14, Feb. 1956, pp. 22–25.

Reactor Transfer Functions, by F. E. O'Meara, *Atomics*, vol. 7, Feb. 1956, pp. 49–51.

Engineer, Design

NUCLEAR AIRCRAFT ENGINES, MECHANICAL COMPONENTS AND SYSTEMS

From all indications the jet age will be dwarfed by the age of the application of atomic power to aircraft. An opportunity to enter this unusual field in its early stages is now offered the qualified engineer by General Electric's Aircraft Nuclear Propulsion Department.

Assignments will involve the designs of mechanical components and systems for use with aircraft nuclear power plants. For this work an ME degree or equivalent is needed, plus 3 to 5 years' experience in design of mechanical devices, structures or systems analysis. Though not essential, work in aircraft power plant field is especially desirable.

Publication of research results in the appropriate classified or open literature is encouraged.

OPENINGS IN CINCINNATI, OHIO AND IDAHO FALLS, IDAHO

Address Replies stating salary requirements to location you prefer

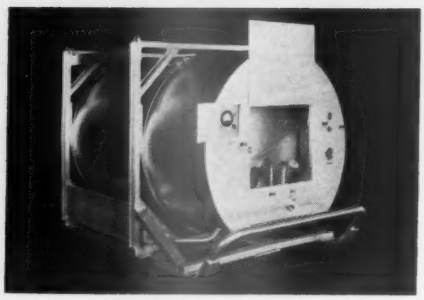
W. J. Kelly
P.O. Box 132
Cincinnati, O.

L. A. Munther
P.O. Box 535
Idaho Falls, Idaho

GENERAL ELECTRIC

Solve Your Liquid Oxygen Handling Problems

USE VACUUM INSULATED STORAGE AND TRANSPORT CONTAINERS FOR LIQUEFIED OXYGEN OR NITROGEN



IN 50 TO 4000 GALLON CAPACITIES

STATIONARY UNITS
•
ROADABLE TRAILERS
•
SEMI-TRAILERS

MODEL LOX 150 SHOWN

produced by

CRYOGENIC DIVISION
RONAN AND KUNZL, INC.

MARSHALL, MICHIGAN — 1620 WILSHIRE BLVD., SANTA MONICA, CALIF.

ILLUSTRATED LITERATURE IS AVAILABLE. WE INVITE YOUR INQUIRY.

ENGINEER

CREATIVELY-FLEXIBLE ENGINEER
ROCKET DESIGN & TESTING

The Aircraft Gas Turbine Division of General Electric has an opening for a "creatively-flexible" engineer who is familiar with comprehensive test requirements and procedures, and knows design criteria, based on cycle analysis and high temperature applications in the crucial fields of stress and heat transfer.

You'll be at home in this professional environment—because it makes for the kind of thinking that goes with recognition and promotion. You will associate with the many respected specialists in General Electric's Rocket Development program. High starting salary for positions in Cincinnati, Ohio and Malta, Ballston Spa, New York.

Please send resume to:

Mr. Bruce Mathews
Technical Recruiting Bldg. 100
Aircraft Gas Turbine Division

GENERAL ELECTRIC

Cincinnati 15, Ohio

STURTEVANT TORQUE TESTING FIXTURE



FOR TESTING Screws, thread-cutting and thread-forming screws—all types of threaded fasteners; threaded parts and threaded connections.

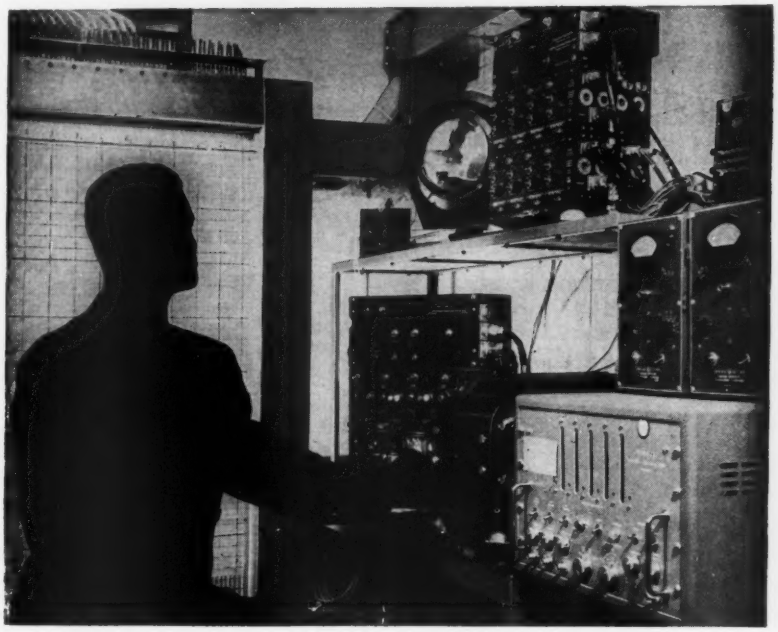
FOR MANUFACTURERS
DESIGNERS
INSPECTORS
TOOL ENGINEERS
LABORATORIES and for **PRODUCT CONTROL** in assembly.

Capacities: (0-200 in. lbs.) or (0-150 ft. lbs.)

Write for Bulletin TTF

P. A. STURTEVANT CO.
ADDISON (QUALITY) ILLINOIS

TO THE FINE ENGINEERING MIND SEEKING THE CHALLENGING PROJECTS IN



ROCKET PROPULSION ENGINEERING

ROCKET PROPULSION ENGINEERS are offered unusual career opportunities now at Convair in beautiful, San Diego, California, including: *Design Engineers* for design and analysis of advanced high performance rocket engine systems and components including propellant systems, lubrication systems, control systems, mounting structure, and auxiliary power plants; *Development Engineers* for liaison with Engineering Test Laboratories and Test Stations in the planning, analysis, and coordination of rocket engine system and component tests; *Development Engineers* for coordination with Rocket Engine Manufacturers in the installation design, performance analysis, and development tests in conjunction with Convair missile programs. Professional engineering experience in rocket missiles and aircraft propulsion system development will qualify you for an exceptional opportunity.

CONVAIR offers you an imaginative, explorative, energetic engineering department... truly the "engineer's" engineering department to challenge your mind, your skills, your abilities in solving the complex problems of vital, new, long-range programs. You will find salaries, facilities, engineering policies, educational opportunities and personal advantages excellent.

Generous travel allowances to engineers who are accepted. Write at once enclosing full resume to:

H. T. Brooks, Engineering Personnel, Dept. 1418

CONVAIR

A Division of General Dynamics Corporation

3302 PACIFIC HIGHWAY **SAN DIEGO, CALIFORNIA**

SMOG-FREE SAN DIEGO, lovely, sunny city on the coast of Southern California, offers you and your family a wonderful, new way of life... a way of life judged by most as the Nation's finest for climate, natural beauty and easy (indoor-outdoor) living. Housing is plentiful and reasonable.

SANBORN *Recording Permapaper*

ALL SANBORN 150 SERIES OSCILLOGRAPHIC RECORDERS PROVIDE THESE

SPECIFIC ADVANTAGES

The three foremost operating advantages of a Sanborn "150" are evident in the record, and are given at the right. Equally popular with industrial users is the *wide versatility* of these systems. Each one comprises a basic assembly to which the user adds his choice of an interchangeable, plug-in type preamplifier for each channel. Presently available different preamplifiers now number *eleven*.

Rectangular Coordinate Recording

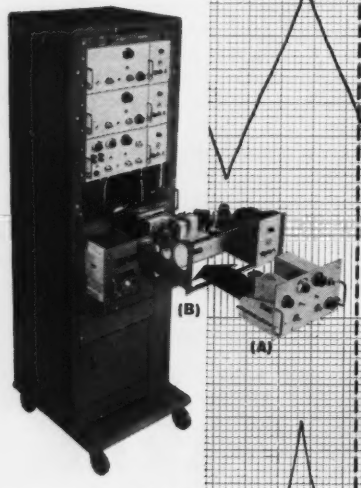
is a Sanborn feature that is especially valuable in multi-channel recording. The user of a 2-, 4-, 6- or 8-channel "150" system can record interrelated events simultaneously on one strip of record paper, and then correlate them against time quickly and accurately, even during the recording.

Clear, Sharp, Inkless Tracings

The nichrome ribbon tip "150" heated stylus removes the white opaque surface of Sanborn recording paper (Permapaper) permitting the black undercoating to show. Tracings are permanent, will not fade or smudge.

Improved Over-all Linearity

resulting from current feedback design of Driver Amplifiers and new shorted coil frame, high torque (200,000 dyne cm.) galvanometers. Maximum error over middle 4 cm. of chart: 0.25 mm . . . over entire 5 cm. chart width: 0.5 mm.



Preamplifier (A) shown in position to plug into a Driver Amplifier with Power Supply (B) which are normally already in place in the Basic Cabinet Assembly



INDUSTRIAL DIVISION
SANBORN CO.
195 Massachusetts Ave., Cambridge Mass.

A new "150" Catalog provides complete descriptive data, specifications and prices on all 150 Systems, Accessories and Cabinets. A copy will be sent on request.

Something About Nothing

No matter what we do, most of us are interrupted from time to time by the request for a document euphemistically entitled a progress report. Because of their tacit assumptions, they are often a source of chagrin to otherwise phlegmatic scientists; for it is difficult indeed to write something about nothing.

Balm for the writhings and groans of the hapless individuals who must regularly wrestle with a progress report is now here. This valuable contribution to the progress of science is known as the standard progress report —it can be used anytime, anywhere. It is the result of long and arduous study by William Cohen, China Lake, Calif. As freely translated below, it is expressly for unfortunates who otherwise face extinction. Cohen says he never uses it himself. Type in batches of 100 and then date and sign a year's supply. Be sure the secretary omits the translations.

Standard Progress Report for Those with No Progress to Report

During the report period which ends —(fill in appropriate date) considerable progress has been made in the preliminary work directed toward the establishment of the initial activities. (We are getting ready to start, but we haven't done anything yet.) The background information has been surveyed and the functional structure of the component parts of the cognizant organization has been clarified. (We looked at the assignment and decided that George would do it.)

Considerable difficulty has been encountered in the selection of optimum materials and experimental methods, but this problem is being attacked vigorously and we expect that the development phase will proceed at a satisfactory rate. (George is looking through the handbook.) In order to prevent unnecessary duplication of previous efforts in the same field, it was necessary to establish a survey team which has conducted a rather extensive tour through various facilities in the immediate vicinity of manufacturers. (George and Harry had a nice time in New York.)

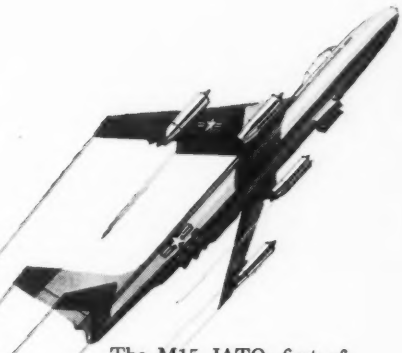
The Steering Committee held its regular meeting and considered rather important policy matters pertaining to the over-all organizational levels of the line and staff responsibilities that devolve on the personnel associated with the specific assignments resulting from the broad functional specifications. (Untranslatable—sorry.) It is believed that the rate of progress will continue to accelerate as necessary personnel are recruited to fill vacant billets. (We'll get some work done as soon as we find someone who knows something.)

Reprinted with permission of Chemical and Engineering News.

OPPORTUNITIES FOR
SCIENTISTS AND ENGINEERS



Largest thrust rocket ever fired, based on available information, used a propellant developed and manufactured by Rocket Fuels Division of Phillips Petroleum Company.



The M15 JATO, first of its kind to meet the most stringent Air Force performance tests, was developed by Phillips scientists and engineers.

THERE'S A FUTURE WITH PHILLIPS IN ROCKETS

Phillips Petroleum Company has a number of key positions for scientists and engineers with experience and proved ability in the rapidly expanding rocket field. There are challenging opportunities for recent graduates also. Write our technical personnel office. Confidential interviews arranged for qualified applicants.

Rocket Fuels Division
PHILLIPS PETROLEUM COMPANY
McGregor, Texas

Phillips 66

Index to Advertisers

AC Spark Plug Division, General Motors Corporation 513
E. H. Brown Advertising Agency, Chicago, Ill.

Accessory Products Corporation 514
Anderson-McConnell Advertising Agency, Hollywood, Calif.

Admiral Corporation 504
Cruttenden & Eger Associates, Chicago, Ill.

Aerojet-General Corporation ..... Back Cover
D'Arcy Advertising Co., Los Angeles, Calif.

Aero Research Instrument Company 502
Brandt Advertising Company, Chicago, Ill.

Air Products, Incorporated 440
Thoma & Gill, East Orange, New Jersey

Applied Physics Laboratory
The Johns Hopkins University 522
Equity Advertising Agency, New York, N.Y.

Arma Division, American Bosch Arma Corporation 513
Deutsch & Shea, New York, N.Y.

Avco Manufacturing Corporation
Advanced Development Division 515
Benton & Bowles, Inc., New York, N.Y.

Baldwin-Lima-Hamilton Corporation 512
Ketchum, MacLeod & Grove, Inc., Pittsburgh, Pa.

Beckman & Whitley, Incorporated 525
Sturges and Associates, San Carlos, Calif.

Bendix Aviation Corporation
Pacific Division 433
The Shaw Company, Los Angeles, Calif.

Scintilla Division 529
MacManus, John & Adams, Inc., Bloomfield Hills, Mich.

California Institute of Technology, Jet Propulsion Laboratory 503
Frank Barrett Cole Advertising, Pasadena, Calif.

Carborundum Company 426
G. M. Basford Co., New York, N. Y.

Convair, A Division of General Dynamics Corporation ..... Third Cover, 535
Buchanan & Company, Inc., Los Angeles, Calif.
Barnes Chase Company, San Diego, California

Cornell Aeronautical Laboratory, Incorporated 529
Melvin F. Hall, Buffalo, N.Y.

Douglas Aircraft Company, Incorporated 428, 521
J. Walter Thompson Company, Los Angeles, Calif.

Du Pont de Nemours, E.I., and Company 432
Batten, Barton, Durstine and Osborn, New York, N.Y.

Eastern Industries, Incorporated 427
Remsen Advertising Agency, Inc., New Haven, Conn.

Fairchild Engine and Airplane Corporation, Guided Missile Division 516
Gaynor Colman Prentis & Varley, Inc., New York, N.Y.

Ford Instrument Company, A Division of Sperry Rand Corporation 438
G. M. Basford Company, New York, N.Y.

General Electric Company, AGT Development Division 436, 526, 529, 535
Deutsch & Shea, Inc., New York, N.Y.

Aircraft Nuclear Propulsion Department 522, 534
Deutsch & Shea, Inc., New York, N.Y.

General Mills Incorporated 430, 431
Knox Reeves Advertising, Inc., Minneapolis, Minn.

General Precision Equipment Corporation 524
Geer, DuBois & Company, Inc., New York, N. Y.

Giannini, G. M., and Company, Incorporated 523
Western Advertising Agency, Inc., Los Angeles, Calif.

Grotnes Machine Works 525
The Gerstel Agency, Inc., Chicago, Ill.

Lockheed Aircraft Corporation, Missile Systems Division 519
Hal Stebbins, Inc., Los Angeles, Calif.

Marquardt Aircraft Company 532, 540
Heintz & Co., Inc., Los Angeles, Calif.
Doyle, Kitchen & McCormick, Inc., New York, N.Y.

Martin, The Glenn L., Company 511, 528
Vansant, Dugdale & Company, Baltimore, Maryland

McCormick-Selph Associates 534
Gerth-Pacinc Advertising Agency, San Francisco, Calif.

Miniature Precision Bearings, Incorporated 529
Henry A. Louden, Advertising, Inc., Boston, Mass.

Minneapolis-Honeywell Regulator Company 520
Foote, Cone & Belding, Chicago, Ill.

New York Air Brake Company 437
Humbert & Jones, New York, N.Y.

Newbrook Machine Corporation 531

North American Instruments, Incorporated 526
Heintz & Co., Inc., Los Angeles, Calif.

Northrop Aircraft, Incorporated 510
West-Marquis, Incorporated, Los Angeles, Calif.

Norton Company 441
James Thomas Chirurg Company, Boston, Mass.

Olin Mathieson Chemical Corporation 540
Doyle, Kitchen & McCormick, Inc., New York, N.Y.

Explosives Division 429
D'Arcy Advertising Company, Saint Louis, Mo.

Parsons, The Ralph M., Company 442
Dozier Eastman & Company, Los Angeles, Calif.

Pennsylvania Salt Manufacturing Company 439
Geare-Marston, Philadelphia, Pa.

Phillips Petroleum Company 537
Lambert & Feasley, Inc., New York, N.Y.

Reaction Motors, Incorporated ..... Second Cover, 540
J. Wheelock Associates, New York, N.Y.
Doyle, Kitchen & McCormick, Inc., New York, N.Y.

Reeves Instrument Corporation 527
The Edward W. Robotham Company, Hartford, Conn.

Rocketdyne, A Division of North American Aviation, Incorporated 434
Batten, Barton, Durstine & Osborn, Los Angeles, Calif.

Ronan and Kunzl, Incorporated 534

Sanborn Company 536
Meissner & Culver, Inc., Boston, Mass.

Solar Aircraft Company 539
Phillips Ramsey Company, San Diego, Calif.

Sperry Gyroscope Company, A Division of Sperry Rand Corporation 533
Reach, Yates & Mattoon, Newark, N.J.

Statham Laboratories, Incorporated 513
Western Advertising Agency, Inc., Los Angeles, Calif.

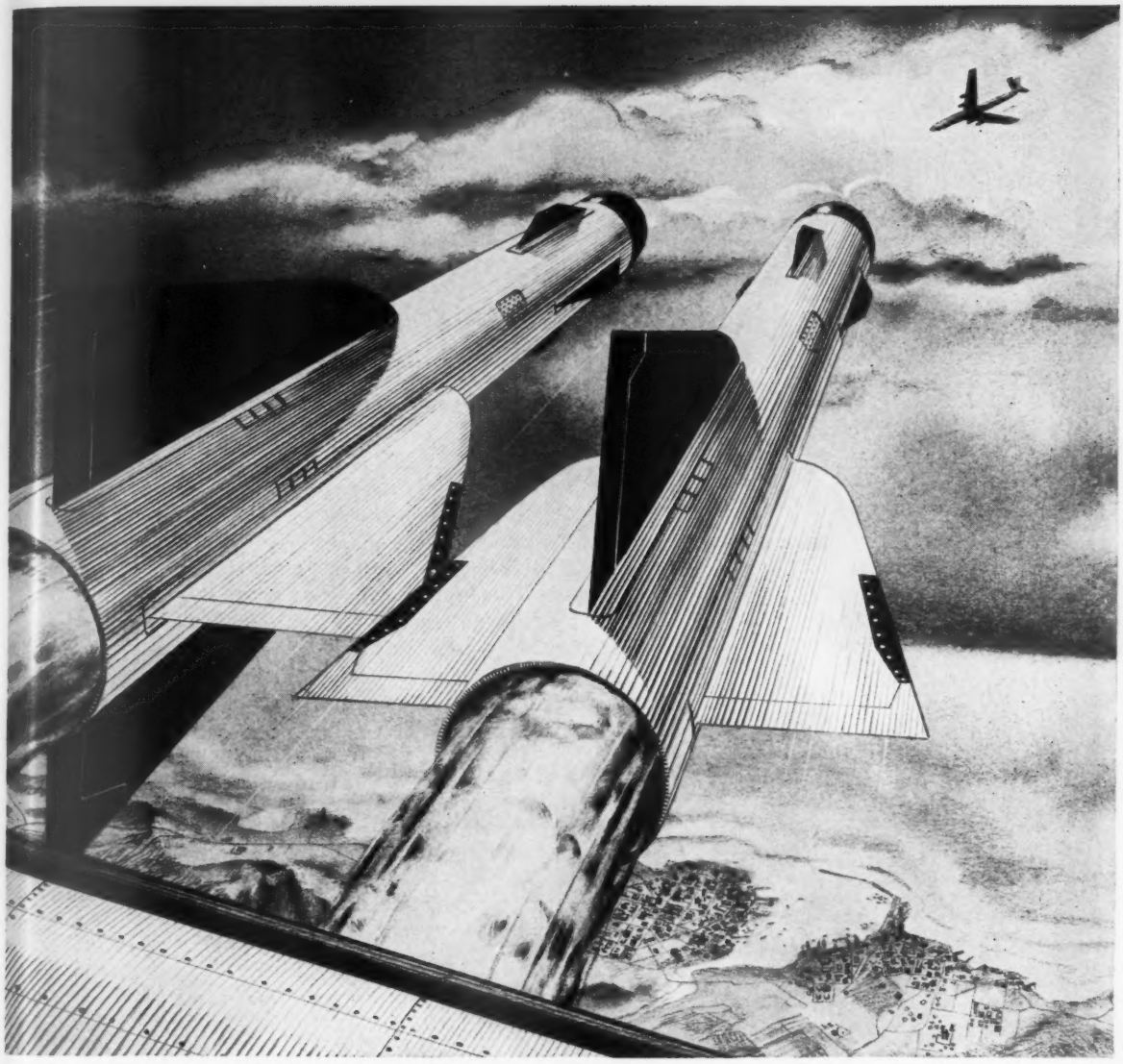
Stauffer Chemical Company 495
John Mather Lupton Company, New York, N.Y.

Sturtevant, P. A., Company 535
Ross Llewellyn, Inc., Chicago, Ill.

Taber Instrument Corporation 520
The Pursell Company, Buffalo, N.Y.

Watertown Division, The New York Air Brake Company 437
Humbert & Jones, New York, N.Y.

Westvaco Chlor-Alkali Division, Food Machinery and Chemical Corporation 435
James J. McMahon, New York, N.Y.



Solar skills help produce guided missiles in quantity



INFORMATION BOOKLET

New brochure on Solar missile production capabilities—write for a copy today.

GUIDED MISSILES REQUIRE imaginative engineering and precision fabrication with unending emphasis on quality. Solar has stressed these attributes for decades in designing and building aircraft components of tough alloys for use under stringent service conditions. In addition, Solar's direct activity in missile programs extends from research and development work through to volume manufacture of components—such as current fabrication of fuselages for the air-to-air Hughes Falcon. For more information on Solar's missile production capabilities, write Dept. C-27, Solar Aircraft Company, San Diego 12, Calif.

SOLAR
AIRCRAFT COMPANY
SOLAR
SAN DIEGO DES MOINES

Designers, developers and manufacturers of gas turbines—aircraft and missile components—bellows—controls—high temperature coatings—metal alloy products



rockets give helicopters extra lift

Reaction Motors, developer and producer of rocket engines and powerplant systems for guided missiles, aircraft, and ordnance-type rockets, is an important participant in the OMAR program. With Marquardt Aircraft, the West's largest jet engine research and development center, and Olin Mathieson Chemical, RMI contributes to a continuous joint technical effort to advance the science and technology of supersonic powerplants and fuels.

The OMAR program illustrates the integration of effort by a well-coordinated industrial team . . . the weapons systems concept in action. This combination of technical and production skills, products, services, and corporate strength has the capacity to provide an effective assist to those responsible for the common defense.

Engineers, chemists, physicists, production and tool specialists . . . a wide variety of fascinating careers await you on this weapons systems team. For information write OMAR Employment Officer at the company nearest you.

Tiny rotor-tip rocket engines increase the payload of the Sikorsky HRS-2 helicopter up to 100 per cent. Having started their vertical take-offs at same instant, equally heavily loaded Marine helicopters demonstrate relative hovering capabilities. Standard HRS-2 (background) hovers only as high as ground effect will permit. ROR (rocket-on-rotor) helicopter climbed straight up through ground effect and was still climbing when this photo was taken. Developed by Reaction Motors, Inc., for the Navy, ROR provides auxiliary power for take-off or emergency situations.

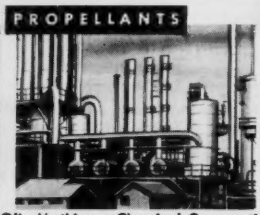


RAMJETS



Marquardt Aircraft Company
Van Nuys, California

PROPELLANTS



Olin Mathieson Chemical Corporation
New York, New York

ROCKETS



Reaction Motors, Inc.
Denville, New Jersey

MARQUARDT AIRCRAFT
OLIN MATHIESON CHEMICAL
REACTION MOTORS

OMAR